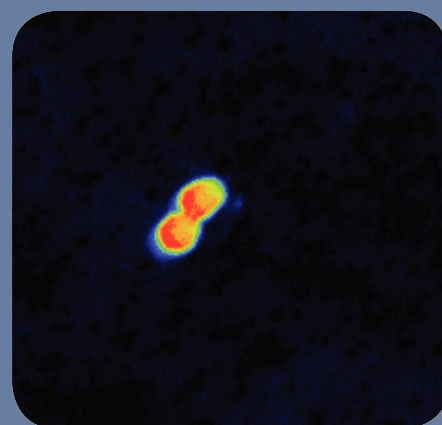
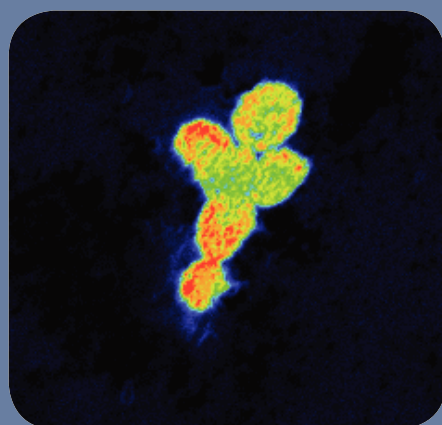
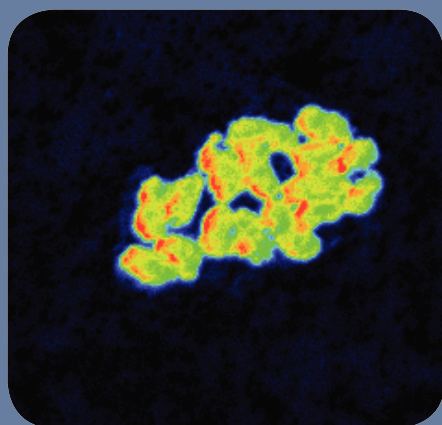


Hydrocarbon-degrading sulfate-reducing bacteria in marine hydrocarbon seep sediments



Sara Kleindienst

Cover: ^{13}C -mass images of alkane-degrading SRB from Amon Mud Volcano or Guaymas Basin marine seep sediments as determined by NanoSIMS analysis.

**Hydrocarbon-degrading
sulfate-reducing bacteria
in marine hydrocarbon seep sediments**

Dissertation zur Erlangung
des Grades eines
Doktors der Naturwissenschaften
- Dr. rer. nat. -

Dem Fachbereich Biologie/Chemie der
Universität Bremen
vorgelegt von

Sara Kleindienst

Bremen
April 2012

Die vorliegende Arbeit wurde in der Zeit von September 2008 bis April 2012 im Rahmen der „International Max Planck Research School of Marine Microbiology (MarMic)“ in der Abteilung Molekulare Ökologie am Max-Planck-Institut für marine Mikrobiologie in Bremen angefertigt.

1. Gutachter: Prof. Dr. Rudolf Amann
2. Gutachter: Prof. Dr. Heribert Cypionka

Tag des Promotionskolloquiums: 24. Mai 2012

Table of Contents

Summary	III
Zusammenfassung	IV
List of Abbreviations	V
Chapter I	1
General Introduction	1
1. Hydrocarbons	1
2. Hot spots of hydrocarbon sources in the ocean.....	3
2.1. Hydrothermal vents	3
2.2. Cold seeps	4
2.3. Anthropogenic oil spills	8
3. Benthic communities at hydrocarbon seeps	9
3.1. Chemosynthetic communities	9
3.2. Microbial communities	9
4. Microbial non-methane hydrocarbon-degradation in anoxic seep sediments.....	11
4.1. Cultured non-methane hydrocarbon degrading SRB	13
4.2. Metabolic pathways for anaerobic hydrocarbon degradation by SRB.....	14
5. Stable-isotope probing techniques in microbial ecology	17
Objectives of this thesis	20
Contribution to manuscripts	22
Chapter II	24
Distribution and in situ abundance of sulfate-reducing bacteria in diverse marine hydrocarbon seep sediments	24
Chapter III	59
Specialists instead of generalists oxidize alkanes in anoxic marine hydrocarbon seep sediments	59
Chapter IV	90
Activity and in situ abundance of alkane-degrading sulfate-reducing bacteria at marine hydrocarbon seeps	90
Chapter V	127
Impact of natural oil and higher hydrocarbons on microbial diversity, distribution and activity in Gulf of Mexico cold seep sediments	127
Chapter VI	129
Synopsis of Results, General Discussion and Conclusions	129
1. DSS hydrocarbon degraders at marine seeps	129
1.1. SCA-SRB1 are global key players involved in short-chain alkane degradation.....	131
1.2. SCA-SRB2 are Guaymas Basin-endemic short-chain alkane degraders	135
1.3. LCA-SRB1 are long-chain alkane degraders	136
1.4. SEEP-SRB1 are globally abundant candidates for hydrocarbon degradation	136
2. Non-DSS hydrocarbon degraders at marine seeps.....	137
2.1. SEEP-SRB2 are novel ANME-partners involved in AOM	137
2.2. SEEP-SRB3 and SEEP-SRB4 are candidates for hydrocarbon degradation .	140
2.3. LCA-SRB2 are global key players involved in long-chain alkane degradation.....	140
2.4. <i>Desulfobacterium anilini</i> and relatives are involved in oil degradation	141
3. Unexplored groups involved in hydrocarbon degradation at marine seeps	142
4. Environmental impact of hydrocarbon-degrading SRB.....	144
4.1. Cellular activities of alkane-degrading SRB.....	144
4.2. SR rates coupled to alkane oxidation at hydrocarbon seeps	145

5. Future Perspectives	146
References	148
Acknowledgements.....	159
Appendix	161
Curriculum Vitae	182

Summary

Microorganisms are key players in our biosphere because of their ability to degrade various organic compounds including a wide range of hydrocarbons. At marine hydrocarbon seeps, more than 90% of sulfate reduction (SR) is potentially coupled to non-methane hydrocarbon oxidation. Several hydrocarbon-degrading sulfate-reducing bacteria (SRB) were enriched or isolated from marine sediments. However, in situ active SRB remained largely unknown.

In the present thesis, the global distribution and abundance of SRB at diverse gas and hydrocarbon seeps was investigated by catalyzed-reporter deposition fluorescence in situ hybridization (CARD-FISH). The majority of *Deltaproteobacteria* was assigned to specific SRB groups, for instance on average 83% and 61% at gas and hydrocarbon seeps. Members of the *Desulfosarcina/Desulfococcus* (DSS) clade significantly dominated all sites, suggesting their important role in hydrocarbon degradation processes. Furthermore, butane- and dodecane-degrading SRB were identified from two contrasting marine hydrocarbon seeps using ^{13}C -stable-isotope probing techniques. The identified key players affiliated with four distinct groups, of which three belonged to the DSS clade. Specific groups were, according to their ability to oxidize short-chain alkanes (SCA) or long-chain alkanes (LCA), denoted as “SCA-SRB1” and “SCA-SRB2” as well as “LCA-SRB1” and “LCA-SRB2”.

Based on the obtained data it is assumed that diverse and highly specialized DSS organisms are involved in hydrocarbon degradation at marine seeps rather than generalists of one dominant subgroup. At marine hydrocarbon seeps, groups SCA-SRB1 and SCA-SRB2 constituted up to 31 and 9% of all *Deltaproteobacteria*, respectively. In addition, LCA-SRB2 comprised up to 6% of all detected *Deltaproteobacteria*. Furthermore, activities for these groups were analyzed on the cellular level by Nanometer-scale Secondary Ion Mass Spectrometry (NanoSIMS). Alkane oxidation rates for specific groups were determined to be on average between 45 and 58 amol butane and 1 amol dodecane per cell and per day. Extrapolated data indicate that specific alkane-degrading SRB groups have the potential to contribute up to 100% of the total SR rates at seeps from the Gulf of Mexico. Therefore, alkane-degrading SRB groups may significantly impact sulfur and carbon cycles at marine hydrocarbon seeps.

In addition, based on the obtained data, members of the uncultured group SEEP-SRB2 are hypothesized to be involved in hydrocarbon degradation. SEEP-SRB2 were visualized for the first time using CARD-FISH and were detected either in association with methanotrophic archaea (ANME-2/SEEP2 and ANME-1/SEEP2 consortia) or as single cells. Furthermore, the high abundance of SEEP-SRB2 indicates their important ecological role at marine hydrocarbon seeps.

Zusammenfassung

Mikroorganismen sind wichtige Komponenten in unserer Biosphäre, weil sie viele organische Verbindungen, wie z.B. verschiedene Kohlenwasserstoffe abbauen können. An marinen Kohlenwasserstoffquellen sind vermutlich mehr als 90% der Sulfatreduktion (SR) an methanunabhängige Kohlenwasserstoffoxidation gekoppelt. Mehrere kohlenwasserstoffabbauende, sulfatreduzierende Bakterien (SRB) wurden bereits aus marinen Sedimenten angereichert oder isoliert. Die in situ aktiven SRB sind jedoch noch größtenteils unerforscht.

Im Rahmen der vorliegenden Arbeit wurde die globale Verbreitung und Abundanz von SRB mittels Fluoreszenz-in-situ-Hybridsierung mit enzymmarkierten Oligonukleotidsonden und Tyramid-Signalverstärkung (CARD-FISH) an verschiedenen Gas- und Kohlenwasserstoffquellen untersucht. Der Großteil der Deltaproteobakterien, z.B. 83% an Gas- bzw. 61% an Kohlenwasserstoffquellen, wurde spezifischen SRB-Gruppen zugeordnet. Hierbei dominierte die *Desulfosarcina/Desulfococcus* (DSS) Gruppe alle Standorte, woraus ihre wichtige Rolle am Kohlenwasserstoffabbau geschlussfolgert wurde. Darüber hinaus wurden butan- und dodekanabbauende SRB von zwei Kohlenwasserstoffquellen mittels Markierung mit stabilen ^{13}C -Isotopen identifiziert. Die identifizierten Mikroorganismen wurden vier Gruppen zugeordnet, von denen drei zu den DSS gehören. Die Gruppen wurden als SCA-SRB1, SCA-SRB2, LCA-SRB1 und LCA-SRB2 bezeichnet, entsprechend ihrer Fähigkeit, kurzkettige oder langkettige Alkane abzubauen (engl. *Short-Chain Alkanes*, *Long-Chain Alkanes*).

Aus den Daten ergibt sich die Hypothese, dass eher Spezialisten als Generalisten der DSS-Gruppe am Abbau von Kohlenwasserstoffen beteiligt sind. Die Gruppen SCA-SRB1 und SCA-SRB2 hatten an den Kohlenwasserstoffquellen jeweils einen Anteil von bis zu 31% bzw. 9% aller detektierter Deltaproteobakterien. Der Anteil der LCA-SRB2-Gruppe umfasste bis zu 6% der Deltaproteobakterien. Darüber hinaus wurden mikrobielle Aktivitäten mittels Nanometer-Sekundärionen-Massenspektrometrie (NanoSIMS) auf Zellebene untersucht. Die ermittelten Alkanoxidationsraten für die spezifischen Gruppen betragen zwischen 45 und 58 amol Butan bzw. 1 amol Dodekan pro Zelle und pro Tag. Eine Extrapolation der Daten lässt vermuten, dass alkanabbauende SRB an bestimmten Kohlenwasserstoffquellen im Golf von Mexiko für die gesamte SR verantwortlich sein könnten. Daraus kann geschlossen werden, dass alkanabbauende SRB signifikant den Kohlenstoff- und Schwefelkreislauf an marinen Kohlenwasserstoffquellen beeinflussen.

Darüber hinaus deuten die erzielten Ergebnisse darauf hin, dass unkultivierte *Deltaproteobakterien* der Gruppe SEEP-SRB2 am Kohlenwasserstoffabbau beteiligt sein könnten. SEEP-SRB2 wurde zum ersten Mal mittels CARD-FISH untersucht und entweder in Assoziation mit methanotrophen Archaeen (ANME-2/SEEP2 und ANME-1/SEEP2 Konsortien) oder als Einzelzellen entdeckt. Die hohe Abundanz der SEEP-SRB2 ist ein Indiz für ihre wichtige ökologische Rolle an den marinen Kohlenwasserstoffquellen.

List of Abbreviations

ANME	Anaerobic methanotrophs
AOM	Anaerobic oxidation of methane
Ass	Alkylsuccinate synthase
AT%	Atomic percent
Bss	Benzylsuccinate synthase
BTEX	Benzene, toluene, ethylene and xylene
CARD-FISH	Catalyzed reporter deposition-fluorescence in situ hybridization
DNA-SIP	DNA-based stable isotope probing
DSS	<i>Desulfosarcina/Desulfococcus</i> branch of <i>Deltaproteobacteria</i>
GC-IRMS	Gas chromatography-isotope ratio mass spectrometry
Gt	Gigatonnes
HRP	Horseradish peroxidase
IPL	Intact polar lipid
LC-MS/MS	Liquid chromatography–mass spectrometry/mass spectrometry
Mas	(1-methyl)alkylsuccinate synthase
NanoSIMS	Nanometer scale secondary-ion mass spectrometry
Nms	(2-naphthylmethyl)succinate synthase
PLFA	Phospholipid fatty acid
Protein-SIP	Protein-based stable isotope probing
Pyro-SIP	Pyrosequencing in combination with stable isotope probing
RNA-SIP	RNA-based stable isotope probing
SIP	Stable isotope probing
SR	Sulfate reduction
SRB	Sulfate-reducing bacteria
UCM	Unresolved complex mixture

Chapter I

General Introduction

1. Hydrocarbons

Hydrocarbons are among the most abundant organic compounds in our biogeosphere. They consist exclusively of the elements carbon and hydrogen. Caused by a lack of functional groups they are largely apolar and show low chemical reactivity at room. Commonly, hydrocarbons are divided into four groups according to their bonding characteristics: alkanes, alkenes, alkynes and aromatic hydrocarbons. Aliphatic hydrocarbons are defined as hydrocarbons that are not aromatic and can further be classified as straight-chain (e.g. *n*-alkanes), branched-chain and cyclic (alicyclic) compounds. Aromatic hydrocarbons can be mono- or polycyclic and they often occur with aliphatic hydrocarbon chains as alkyl-substituted aromatic hydrocarbons.

Hydrocarbons are formed biogenically by living organisms as biosynthetic products (Birch & Bachofen, 1988) or abiogenically during geological transformations of organic matter (Went, 1960). The major fraction of hydrocarbons was formed by maturations and conversions of organic matter during diagenesis, catagenesis and metagenesis (Fig. I.1).

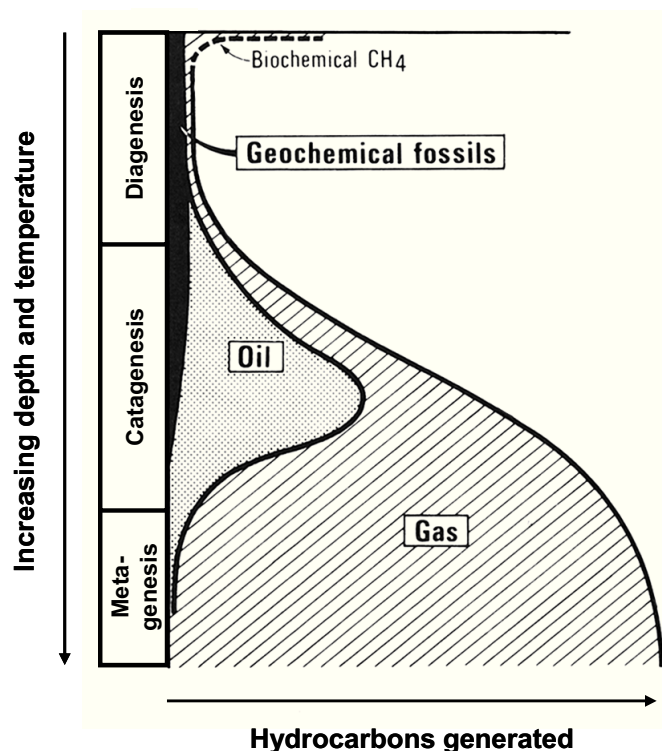


Fig. I.1: General scheme of hydrocarbon formation during diagenesis, catagenesis and metagenesis. Depth and temperature are only indicative and vary according to the particular geological conditions. Fig. modified from Tissot & Welte (1984).

Diagenesis is characterized by early defunctionalization and condensation reactions of sedimented and buried biomass at moderate temperatures, resulting in the formation of highly complex polymeric organic material termed as kerogen. Subsequently, under higher temperature and pressure in a process called catagenesis, kerogen is broken down to hydrocarbons. Finally, under high temperature and pressure within the metagenesis, methane and other gases (e.g. CO₂, H₂S and N₂) are produced. The amount and the composition of hydrocarbons as well as the depth of gas and hydrocarbon generation differ between various sediment types. The temperature threshold for petroleum formation ranges from 50°C to 115°C and the time for oil formation varies from a few million to 300 million years (Tissot & Welte, 1984). However, within certain areas of the deep-sea, hydrocarbon formation processes have rather short time frames. A well investigated example is located in the Gulf of California at Guaymas Basin. Here, oil generation, expulsion and migration processes were estimated being shorter than 5000 years (Didyk & Simoneit, 1989).

Hydrocarbons occur in gaseous, liquid or solid phases. In the environment, gaseous hydrocarbons are considered to comprise C₁ to C₄ compounds, while liquid hydrocarbons are assumed to contain compounds \geq C₅. However, gases can naturally include varying amounts of dissolved hydrocarbons, which would normally occur in a liquid phase and also vice versa; oils contain varying amounts of dissolved gases.

Gaseous hydrocarbons are often dominated by methane, while crude oils (often referred to as petroleum) are more diverse in their hydrocarbon composition. Commonly, main constituents of crude oils are saturated aliphatic hydrocarbons and aromatic hydrocarbons, which on the average account for 86% (Tissot & Welte, 1984). In crude oils, an average of 33% of the total hydrocarbons consists of alkanes. In addition, cycloalkanes such as cyclopentane and cyclohexane as well as their low molecular weight derivatives (e.g. methylcyclohexane) are important constituents of crude oil with an average of 32% of total hydrocarbons. Furthermore, aromatic hydrocarbons such as benzene, naphthalene and phenanthrene are often present in forms of alkylated derivatives and are on average 35% of total hydrocarbons in crude oils (Tissot & Welte, 1984). Alkenes are relatively unstable because of their unsaturated chains and they are therefore less common in crude oil. However, they can be found in lower concentrations as it was shown for *n*-hexene, *n*-heptene and *n*-octene (Putscher, 1952). Besides, crude oils contain a substantial but variable fraction of non-hydrocarbon compounds such as resins and asphaltenes, which are on average 14% by weight (Tissot & Welte, 1984). Resins and asphaltenes are high molecular weight (>500) polycyclic organic molecules that contain N, S, and O atoms.

2. Hot spots of hydrocarbon sources in the ocean

2.1. Hydrothermal vents

In 1977, hydrothermal vents were discovered in the oceans as the first seep systems (Peter, 1977; Corliss et al., 1979). This event fundamentally changed the understanding of life on the deep-sea seafloor, which was thought to be rather sparsely colonized by living organisms. Hydrothermal vents occur especially at convergent plate boundaries (Fig. I.2; Haymon et al., 1991). Here, highly reduced organic and inorganic compounds are produced abiotically by magmatic degassing and subsurface water-rock reactions at high pressures and high temperatures. Hydrothermal fluids that emit from black and white smokers are rich in electron donors potentially used by microorganisms (hydrogen, methane, hydrogen sulfide, ammonia, iron (II) and manganese (II); Jannasch & Mottl, 1985) and mix with seawater that contains different electron acceptors (carbon dioxide, sulfate, sulfur, iron (III), nitrate or oxygen). These electron donors and acceptors are used by various aerobic, anaerobic and symbiotic microorganisms (Jannasch, 1985; Miroshnichenko & Bonch-Osmolovskaya, 2006). In the present thesis, hydrothermal vent sites from Guaymas Basin were investigated, which will be introduced in the following.

Guaymas Basin. At Guaymas Basin in the Gulf of California (Table I.1, Fig. I.2) a thick sediment layer overlies a transitional oceanic-continental rift system (Simoneit et al., 1990). Therefore, hydrothermal vents and cold seeps are mixed in the same geotectonic region. Diffusive fluids with temperatures of up to 200°C rise through chimneys and the porous sediment (Lonsdale & Becker, 1985) and release crude oil components (Simoneit & Lonsdale, 1982; Kawka & Simoneit, 1987; Bazyliniski et al., 1988). In addition to crude oil compounds, vents at Guaymas Basin include short-chain organic acids and ammonia (Von Damm et al., 1985; Martens, 1990), which are released by pyrolysis of organic material in the sediments. Hydrothermal vents at Guaymas Basin are often associated with chemosynthetic communities such as thick bacterial mats on the sediment surface (Gundersen et al., 1992). Because of steep temperature gradients, the living environment of microbes is often limited to the upper sediment layers. Usually, the microbial community found at hydrothermal vents from Guaymas Basin is partly different from those detected at cold seeps (Teske et al., 2002). For example, the seep-endemic groups of sulfate-reducing bacteria (SRB) were found in lower frequency (e.g. Dhillon et al., 2003). The anaerobic oxidation of methane (AOM) is typically mediated by microbial consortia of anaerobic methanotrophic (ANME) archaea and SRB (Boetius et al., 2000). At Guaymas Basin, thermophilic AOM was shown to be mediated

by ANME-1 archaea and HotSEEP1 bacteria, a deep branching group of *Deltaproteobacteria* (Holler et al., 2011).

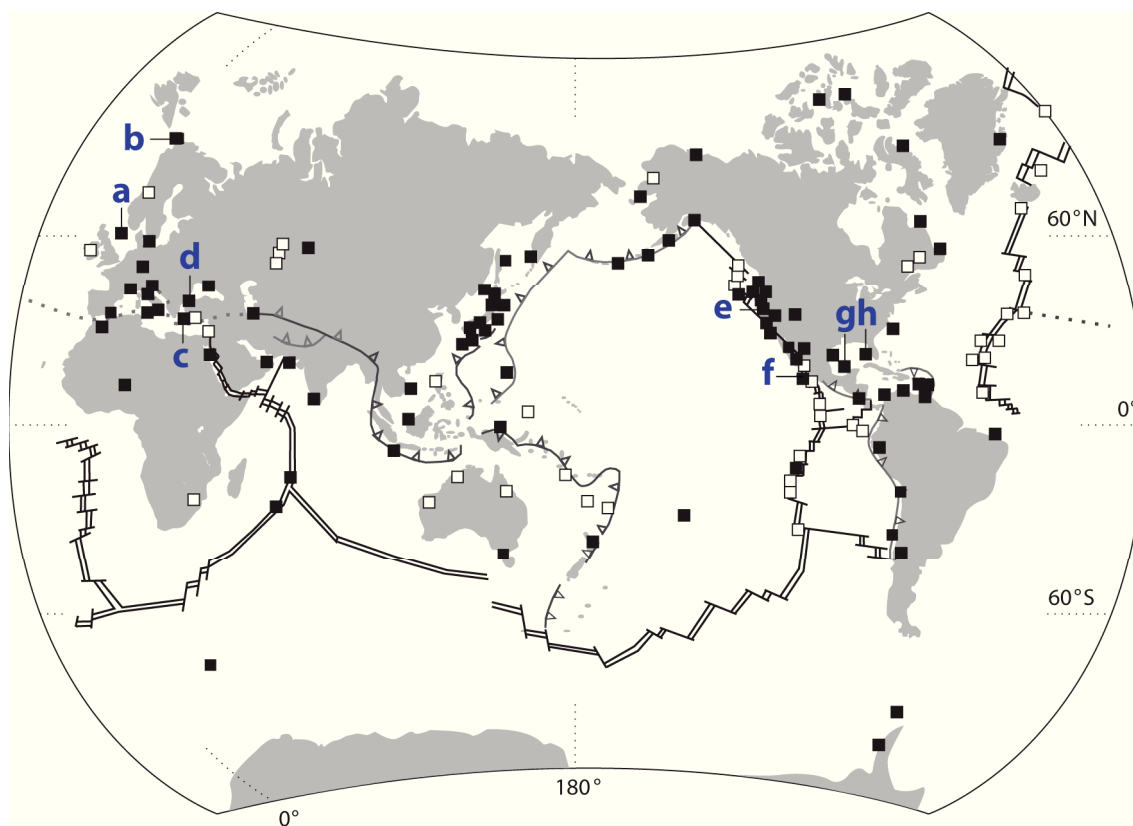


Fig. I.2: Distribution of hydrocarbon seeps (black squares) and hydrothermal vents (open squares). Particularly well-studied gas seepage sites include Tommeliten in the central North Sea (a), mud volcanoes in the Barents Sea (b) and the Mediterranean Sea (c), and microbial mats from Black Sea methanotrophic reefs (d). Additional well-known gas seeps are located at Hydrate Ridge off Oregon (e). Well-studied hydrocarbon seepage sites are located e.g. at Guaymas Basin in the Gulf of California (f), and at the Florida Escarpment in the Gulf of Mexico (g, h). Fig. modified from Campbell (2006).

2.2. Cold seeps

Cold seeps have been first discovered in the Gulf of Mexico (Kennicutt II et al., 1985) and the Cascadia subduction zone in the Pacific (Kulm et al., 1986). Up to now, a huge diversity of different cold seep systems was characterized such as pockmarks, gas chimneys, mud volcanoes, brine pools, and oil or asphalt seeps. Cold seeps occur especially at continental margins and divergent plate boundaries at water depth ranging from about 200 to 3,500 m. Here, hydrocarbon seepage is mainly driven by tectonic processes. Cold seeps are often associated with authigenic carbonate outcrops that result from AOM (e.g. Elvert et al., 1999; Hinrichs et al., 1999; Thiel et al., 1999; Boetius et al., 2000; Valentine, 2002; Treude et al., 2003). Also, gas hydrates are frequently found at cold seep systems. These hydrates form

under elevated pressure (>60 bar) and low temperatures (<4 °C) within the gas-hydrate stability zone. Besides structure I gas hydrates consisting of >99% methane and small amounts of ethane, carbon dioxide and hydrogen sulfide, structure II gas hydrates were described. Structure II gas hydrates were characterized by elevated concentrations of ethane, propane, iso-butane, butane and pentane compared to methane (e.g. Sassen et al., 1998; Orcutt et al., 2004). While the gas composition of structure I gas hydrates was discussed to be mainly of biogenic origin, hydrocarbons of structure II gas hydrates are of thermogenic origin (Brooks et al., 1986). The biogenic versus thermogenic origin of the gaseous hydrocarbons is usually reflected by their stable carbon isotopic signatures, often indicated as ratio of ^{13}C to ^{12}C ($\delta^{13}\text{C}$; Hayes, 2001). Structure II gas hydrates were for instance frequently found at cold seeps where gas migrated from deeper hydrocarbon reservoirs e.g. at the Gulf of Mexico (Sassen et al., 1999; MacDonald et al., 2004; Sassen et al., 2004).

In the following, an overview is provided about the geology, biogeochemistry and microbiology of cold seeps which were investigated in the present thesis (Fig. I.2). Hydrocarbon seeps with emission of gaseous hydrocarbons are hereafter termed as gas seeps. An introduction to benthic communities is given in section 3.

Hydrate Ridge. At Hydrate Ridge on the Cascadia convergent margin in the Northeastern Pacific Ocean (Table I.1, Fig. I.2), fluids and methane ascend along faults from deep sediments to the surface caused by tectonic activities (Whiticar et al., 1995; Suess et al., 1999). Structure I gas hydrates are abundant in the surface sediments at water depths between 600 and 800 m and dominated by methane (>95%; Suess et al., 1999), resulting in a benthic microbial community that is dominated by AOM-mediating consortia, which harbor >90% of total cells. Surface communities are either dominated by sulfur-oxidizing bacteria, clams or mussels (Treude et al., 2003). Only small amounts of short-chain alkanes were detected in addition to methane (Bohrmann et al., 1998).

Amon Mud Volcano. The Amon Mud Volcano is located between the Central and Eastern province on the Central Nile deep-sea fan in the Mediterranean Sea (Table I.1, Fig. I.2) (Masclé et al., 2001; Dupré et al., 2007; Dupré et al., 2008). The dome shaped structure was formed by the upward transport of gases, fluids and mud from the deep subsurface. Distinct provinces were described for the Amon Mud Volcano. The central dome emits highest gas and fluid flows, while the flow is significantly reduced in the surrounding area, which is covered by patches of bacterial mats (Felden, 2009). Here, dominant communities are either involved in AOM or in non-methane hydrocarbon sulfate-reduction (SR). These communities are responsible for high-sulfide production, which supports the formation of microbial mats

on the sediment surface. Next to this area, a relatively flat slope is covered by biogenic mounds (Dupré et al., 2008) formed by deep-sea mud shrimps causing bioturbation (Felden, 2009). At the base of the mud volcano lateral outflow was described which contains blackish, highly reduced mud and brines (Dupré et al., 2008). The seepage activity of the Amon Mud Volcano is mainly derived from thermally-derived gaseous hydrocarbons including methane, propane and butane (Stadnitskaia et al., 2006; Hensen et al., 2007; Mastalerz et al., 2009).

Table I.1: Gas and hydrocarbon seeps investigated in this thesis.

Feature	Gas seeps					Hydrocarbon seeps		
	Hydrate Ridge	Amon Mud Volcano	Haakon Mosby Mud Volcano	Tommeli-ten	Black Sea	Gulf of Mexico	Chapopote Asphalt Volcano	Guaymas Basin
Location	NE Pacific Ocean	Mediterranean Sea	Barents Sea	North Sea	NW shelf of the Black Sea	Northern Gulf of Mexico	Southern Gulf of Mexico	Gulf of California
Sample type	Hydrate bearing sediment	Sediment	Sediment	Sediment	Microbial mat from reef-like structure	Sediment	Sediment with tar deposits	Sediment
Dominant hydrocarbon compounds	Methane (>95%)	Mainly C ₁ ; C ₂ -C ₄	Methane (>99%)	Methane (>99%)	Methane (>95%)	Methane and/or crude oil dominated	Crude oil dominated	Crude oil-like hydrocarbons
Water depth [m]	780	1100	1300	75	190	400-1400	2900	2000
Temperature [°C]	2-4	14	-1	4	8	4	4	3 to 50 ^a
Dominant chemo-synthetic community	Bacterial mats, clams or mussels	Bacterial mats or mud shrimps	Bacterial mats or tube worms	Bacterial mats	None	Bacterial mats, clams, mussels or tube worms	Bacterial mats, clams, mussels or tube worms	Bacterial mats
Dominant AOM-mediating population	ANME-2/DSS	ANME-2/DSS	ANME-3/DBB	ANME-2/DSS	ANME-1, ANME-2/DSS	ANME-1, ANME-2/DSS	NA	NA
References	Suess et al. 1999, Treude et al. 2003, Knittel et al. 2005	Omeregje et al. 2009, Grünke et al. 2011	Ginsburg et al. 1999, Niemann et al. 2006b, Lösekann et al. 2007	Hovland et al. 2002, Niemann et al. 2005, Wegener et al. 2008	Michaelis et al. 2002, Treude et al. 2005, Rossel et al. 2008	Joye et al. 2004, Orcutt et al. 2005	MacDonald et al. 2004, Schubotz et al. 2011	Bazylinski et al. 1988, Teske et al. 2002

^a Typical temperature gradient from 0 to 20 cm sediment depth (McKay; pers. communication). NA, not analyzed.

Haakon Mosby Mud Volcano. The Haakon Mosby Mud Volcano is a submarine mud volcano located in the Barents Sea (Table I.1, Fig. I.2). The thermal center is colonized by aerobic methanotrophic bacteria (Niemann et al., 2006b; Lösekann et al., 2007), while the surrounding area is covered by patches of microbial mats. The benthic community was described to be dominated by AOM consortia. The rim of the crater is populated by siboglinid tube worms, harboring symbiotic bacteria (Niemann et al., 2006b; Lösekann et al., 2007). In contrast to the Amon Mud Volcano, the up streaming gas in the center of the mud volcano consists of 99% methane, which was discussed to be a mixture of biogenic and thermogenic derived gas (Ginsburg et al., 1999; Niemann et al., 2006b). Short-chain alkanes from ethane to butane were only measured in concentrations below 1% (Ginsburg et al., 1999).

Tommeliten. The Tommeliten seepage area is located in the central North Sea at shallow water depth (Table I.1, Fig. I.2). Thermogenically derived methane was produced in deeper sediments (Hovland et al., 1993; Niemann et al., 2005) and migrates through cracks in a buried marl horizon into overlying sediments (Hovland & Judd, 1988). Single bubbles of methane, small patches covered with microbial mats and methane-derived authigenic carbonate outcrops, which are features of active seeps, were described (Hovland & Sommerville, 1985; Hovland & Judd, 1988). For sites investigated in this study, the community resembled those of deep sea ecosystems. However, AOM mediating communities were detected in lower abundances. Aggregates with ANME-2 archaea were found up to $2 \times 10^6 \text{ cm}^{-3}$ (Wegener et al., 2008), while at Hydrate Ridge 35× higher aggregate numbers were reported (cf. Boetius et al., 2000).

Black Sea. The Black Sea is the largest anoxic marine basin on Earth. At the northwestern shelf (Table I.1, Fig. I.2), numerous gas seeps occur. Above the seafloor, giant accumulations of methanotrophic microorganisms form microbial mats that build tall reef-like structures (Fig. I.4a) composed of microbial biomass and carbonate (Michaelis et al., 2002; Treude et al., 2005). The microbial communities of the reef-like structures are dominated by AOM-mediating communities (e.g. Michaelis et al., 2002; Reitner et al., 2005a; Reitner et al., 2005b). The main hydrocarbon source at these seeps is methane with about 95% of total gas content (Pimenov et al., 1997; Michaelis et al., 2002).

Gulf of Mexico. At hydrocarbon seepage sites non-methane hydrocarbons account for a substantial fraction. Along the continental slope in the Gulf of Mexico (Table I.1, Fig. I.2), salt tectonics generate faults that act as natural migration pathways for gas, crude oil and brine fluid from deep reservoirs to surface sediments (Behrens, 1988; Kennicutt II et al., 1988b; Aharon, 1994). Generally, within sediments at water depths of 400-3500 m, natural gas and

hydrocarbon seepage occurs, differing in hydrocarbon compositions (Anderson et al., 1983; Kennicutt II et al., 1988a; Kennicutt II et al., 1988b). If temperature and pressure conditions are suitable, gas hydrates are formed (Fig. I.4f; Kvenvolden, 1993), including structure II gas hydrates, comprising up to 30% C₂-C₅ alkanes (Brooks et al., 1984; Brooks et al., 1986; Klapp et al., 2010). In addition to the northern seeps, sites in the southern Gulf of Mexico were investigated (Table I.1; Fig. I.2). In the Campeche Knolls region, the Chapopote Asphalt Volcano is a unique hydrocarbon seep with tar deposits (MacDonald et al., 2004). The Campeche Knolls area is characterized by salt diapirs rising from an evaporate deposit that underlies the entire slope region. Besides hydrates, seeps from the Gulf of Mexico are often associated with chemosynthetic communities and carbonate outcrops. Gulf of Mexico sites investigated in this study, differed in hydrocarbon compositions, which influenced the benthic microbial community (Orcutt et al., 2010).

2.3. Anthropogenic oil spills

Hydrocarbons enter the marine environment through natural gas and hydrocarbon seepages but also through human activities such as oil spillage and gasoline leakage (Fig. I.3). Recently, the Deepwater Horizon blowout at the northern Gulf of Mexico led within 84 days to a largely uncontrolled gas and oil discharge at 1,480 m water depth. This pollution event from April 22nd to July 14th, 2010, resulted in $2.6-3.6 \times 10^5$ t gas and $5.9-8.4 \times 10^5$ t oil release (Joye et al., 2011) and was reported as the largest offshore oil spill in history (Camilli et al., 2010). The amount of carbon through the oil spill accounts for 5,000-10,000 t carbon per day from the BP wellhead compared to natural seepage of 220-550 t carbon per day within the entire Gulf of Mexico system (National Research Council, 2003; Joye et al., 2011) and therefore impacts life e.g. in the surrounding water column and sediments. It was for instance discussed that the oxidation of hydrocarbons in the oceanic deep waters could lead to anoxic zones (Joye et al., 2011), which may be toxic for resident aerobic organisms such as fishes.

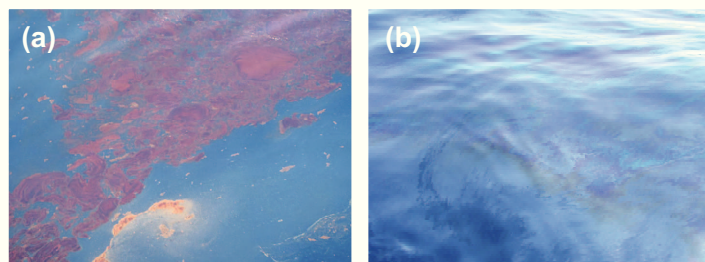


Fig. I.3: Oil on the water surface in the Gulf of Mexico as effects of (a) the oil spill and (b) natural hydrocarbon seepage. Images: Samantha Joye (University of Georgia, USA; a) and Ian MacDonald (A&M University, Texas, USA; b).

In contrast to the toxic effects of such an enormous oil spill are natural hydrocarbon seeps, which largely fuel a huge diversity of animals and microorganisms in these ecosystems, described as deep-sea oases of life.

3. Benthic communities at hydrocarbon seeps

3.1. Chemosynthetic communities

At marine hydrocarbon seeps a huge diversity was described for microorganisms and fauna. Its presence is a widely used criterion to identify these ecosystems. Sulfide-oxidizing bacterial mats consisting of filamentous bacteria of the taxa *Beggiatoa*, *Thioploca* and *Thiothrix* (Larkin & Strohl, 1983) or giant vacuolated bacteria of the genus *Thiomargarita* (Schulz & Schulz, 2005) often form on the sediment surface. Such bacteria use oxygen or internally stored nitrate to oxidize sulfur and fix carbon dioxide for growth (e.g. Schulz & de Beer, 2002). Furthermore, megafauna such as tube worms, mussels, and clams (Fig. I.4) form a major part of the biomass at hydrocarbon seeps. They host either, sulfide-oxidizing symbionts (Fiala-Médioni et al., 1993), methanotrophic symbionts (Childress et al., 1986) or both (Fisher et al., 1993). Very recently, hydrogen-oxidizing symbionts were discovered (Petersen et al., 2011). Tube worms found at seeps, often belong to the genera *Lamellibrachia* and *Escarpia* (Black et al., 1997). Seep mussels belong mostly to the genus *Bathymodiolus* (e.g. Kenk & Wilson, 1985) and form extensive mussel beds. Also seep clams can occur in high densities and are usually members of the family *Vesicomysidae* (Kennicutt II et al., 1985).

3.2. Microbial communities

In marine sediments organic matter is mineralized by microorganisms using a variety of metabolic pathways. Thereby, the electron acceptors are depleted successively according to their redox and free energy potentials. Electron acceptors are usually reduced in the order of oxygen, nitrate, oxidized manganese and iron metals, sulfate and finally bicarbonate (Froelich et al., 1979). At marine seeps oxygen is generally depleted within the upper cm sediment depth (e.g. Jørgensen & Revsbech, 1985; de Beer et al., 2006; Felden, 2009). Typical community members of anoxic marine sediments are SRB of the family *Desulfobacteraceae* including the DSS clade, which comprises the genera *Desulfosarcina*, *Desulfococcus*, *Desulfonema* and some additional cultured and uncultured microorganisms (e.g. Cravo-Laureau et al., 2004; Schreiber et al., 2010). Also SRB of the family *Desulfobulbaceae* including the genus *Desulfobulbus* are often present in marine sediments. Besides

Deltaproteobacteria, *Gammaproteobacteria* including sulfur-oxidizing bacteria and *Epsilonproteobacteria* were frequently detected in marine sediments. In addition, 16S rRNA gene sequence analysis revealed numerous so-called candidate divisions (reviewed in Rappé & Giovannoni, 2003), which comprise not a single cultured representative yet. These candidate divisions carry prefixes (such as OP, WS, JS, TM) according to their original discoveries. For instance, sequences of OP3, OP9, OP11 and WS3 were frequently retrieved from seep sediments (e.g. Orphan et al., 2001; Teske et al., 2002; Reed et al., 2006).

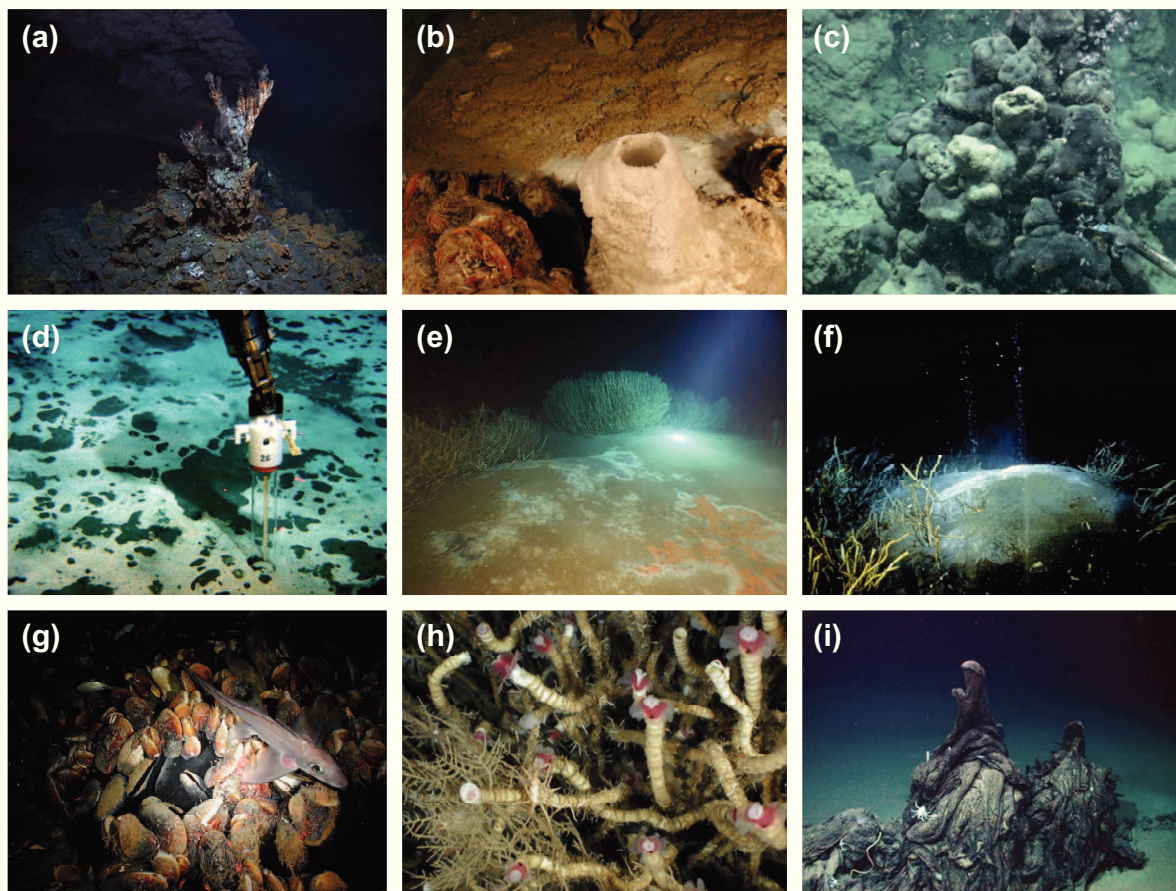


Fig. 1.4: Features found at hydrothermal vents and cold seeps: (a) black smoker from the Atlantic Ocean, (b) mineral chimney and microbial mats on the sea floor in the Gulf of Mexico, (c) methanotrophic microbial reef of the Black Sea, (d) patches of microbial mats at Haakon Mosby Mud Volcano, (e) Large tubeworm aggregations and mats of sulfide-oxidizing bacteria from the Gulf of Mexico, (f) gas hydrate from the Gulf of Mexico, (g) black, oxygen-depleted brine water and a mussel bed, (h) *Lamellibrachia* tube worms from the Gulf of Mexico, (i) asphalt from the Chapopote Asphalt Volcano. Images: MARUM (Research Centre Ocean Margin; Germany; a, c, i), IFREMER (French Research Institute for Exploitation of the Sea; France; d) and Ian MacDonald (A&M University, Texas, USA; b, e-h).

Communities involved in AOM. The dominant process at methane seeps is AOM, mediated by a syntrophic consortium of methanotrophic ANME archaea and SRB (Hinrichs et al., 1999; Boetius et al., 2000; Knittel & Boetius, 2009). This process was described to be one

of the major global sinks for methane (Krüger et al., 2005; Reeburgh, 2007). While the biochemical pathway of AOM still remains largely unknown, the responsible community has been identified: methanotrophic euryarchaeotal groups ANME-1, ANME-2 and ANME-3 are phylogenetically related to the orders *Methanosarcinales* and *Methanomicrobiales*. Sulfate-reducing bacterial partners of ANME archaea are mostly associated with members of the *Desulfosarcina/Desulfococcus* (DSS) clade (Boetius et al., 2000; Orphan et al., 2001; Michaelis et al., 2002; Orphan et al., 2002; Knittel et al., 2003; Knittel et al., 2005). These DSS were recently further assigned to the group SEEP-SRB1a (Schreiber et al., 2010). However, ANME-2c archaea have also been found with *Desulfobulbaceae* as bacterial partner (Pernthaler et al., 2008) and ANME-3 archaea were mostly found to be associated with members of uncultured *Desulfobulbaceae* (Lösekann et al., 2007).

Seep-endemic SRB groups. Besides SEEP-SRB1a, additional phylogenetic clusters of seep endemic SRB were identified from various seep sediments by 16S rRNA gene sequence analysis. These uncultivated groups, named SEEP-SRB (Knittel et al., 2003), were discussed to be involved in hydrocarbon-degradation. The group SEEP-SRB1 was later divided into six subgroups named SEEP-SRB1a-f (Schreiber et al., 2010). While SEEP-SRB1a were identified as dominant bacterial partners of ANME-2 archaea at marine seeps, the abundance, distribution, and ecological function of the subgroups SEEP-SRB1b-f as well as of groups SEEP-SRB2 to SEEP-SRB4 remain largely unknown. The main reason for this uncertainty is that the SEEP-SRB groups comprise only uncultured members.

4. Microbial non-methane hydrocarbon-degradation in anoxic seep sediments

First in situ biogeochemical indications for microbial non-methane hydrocarbon oxidation at cold seeps from the Gulf of Mexico came from isotopic data of gaseous hydrocarbons (Sassen et al., 1999; Sassen et al., 2004). Molecular and isotopic compositions of gas samples from gas hydrate bearing sediments below chemosynthetic communities at the Gulf of Mexico gave evidence, that C₂-C₅ hydrocarbons were altered by microbial oxidation (Sassen et al., 1999). Furthermore, based on isotopic compositions it was proposed that ethane, isobutane and isopentane are least affected, while propane, butane and pentane were most affected by microbial oxidation (Sassen et al., 2004). In addition, the analysis of carbon isotope compositions of authigenic carbonates demonstrated that methane is a contributor but not the dominant source of metabolic energy at sites of active venting. Instead, oxidation of non-

methane hydrocarbons was discussed to be the primary source of carbonate alkalinity (Formolo et al., 2004).

At methane seeps, SR was discussed to be mainly fueled by AOM, leading to a 1:1 coupling of these two processes (Treude et al., 2003). However, at hydrocarbon seeps from the Gulf of Mexico methane-dependent SR rates dropped to less than 10% of total SR rates (Joye et al., 2004). This loose coupling between AOM and SR rates indicated that other seep-related compounds such as non-methane hydrocarbons were oxidized by SRB. The same phenomena were detected when AOM rates and SR rates were measured in hydrothermal vent sediments from Guaymas Basin under different pressure and temperature conditions. Here, AOM rates contributed only 1 to 5% to SR rates (Kallmeyer & Boetius, 2004).

Later on, more biogeochemical evidence for anaerobic sulfate-dependent non-methane hydrocarbon degradation came from mud volcanoes from the Gulf of Cadiz as well as mud volcanoes from the Central Nile deep-sea fan. The decrease of C₂-C₄ compounds together with the detection of a strong unresolved complex mixture (UCM) of hydrocarbons in the SR zone indicated that SR fueled by higher hydrocarbons could be an important microbial process in mud volcano sediments in the Gulf of Cadiz (Niemann et al., 2006a). UCM appears during gas chromatographic analysis typically as a hump in chromatograms and becomes more apparent when oils are biodegraded resulting in a depletion of *n*-alkanes. Another study, which investigated molecular and isotopic composition of gaseous hydrocarbons, revealed that the seepage activity of Isis and Amon Mud Volcano was mainly derived from SR of thermogenic derived methane, propane and butane (Mastalerz et al., 2009). Ethane and isobutane were also found but were proposed to be the second substrate choice for microorganisms. In addition, the presence of distinct sulfate-hydrocarbon interfaces was shown e.g. between 20 and 50 cm below seafloor at the Amon Mud Volcano.

Recently, analysis of intact polar membrane lipids (IPLs), petroleum hydrocarbons and stable carbon isotopic compositions of hydrocarbon gases from the Chapopote Asphalt Volcano in the southern Gulf of Mexico showed additional evidence for anaerobic hydrocarbon oxidation. Crude oil was found to be biodegraded by lacking e.g. *n*-alkanes, while diagnostic IPLs indicated that, besides other community members, SRB are present and may play an important role in petroleum degradation (Schubotz et al., 2011).

Lately, a compiled global survey indicated that SR rates are enhanced by the presence of aliphatic hydrocarbons or gaseous alkanes (Bowles et al., 2011). It was shown that SR rates exceeded those of AOM in various (even) methane dominated seeps and the estimated average integrated global AOM rate was determined to be only 5% (Bowles et al., 2011) of

the ones previously reported (Hinrichs & Boetius, 2002). Another contemporary study estimated rates for anaerobic oxidation of propane in marine environments, and demonstrated the potential importance of this process as a potential sink for propane (Quistad & Valentine, 2011). Therefore, SRB may have a greater impact on non-methane hydrocarbon concentrations in the ocean and the atmosphere as previously recognized.

4.1. Cultured non-methane hydrocarbon degrading SRB

The mineralization of hydrocarbons has been long considered to be feasible only under oxic conditions. The main reason behind this dogma was based on the argument, that oxygen is required for the enzymatic activation of hydrocarbons, which are mostly chemically inert (cf. Wilkes & Schwarzbauer, 2010). Nevertheless, microorganisms were found to be capable of hydrocarbon degradation under anoxic conditions. Anaerobic microbial hydrocarbon degradation was described for microorganisms using nitrate (Gilewicz et al., 1997), iron(III) (Lovley et al., 1993) or sulfate (Aeckersberg et al., 1991) as electron acceptor as well as under methanogenic conditions (Zengler et al., 1999b) or by anoxygenic photosynthesis (Zengler et al., 1999a). Generally, hydrocarbon-oxidizing bacteria belong to the phyla *Actinobacteria*, *Bacteroidetes*, *Cyanobacteria*, *Deinococcus-Thermus*, *Firmicutes* and *Proteobacteria*. The latter phylum comprises most of the known hydrocarbon-degrading SRB, which in the following will be introduced in more detail.

SRB possess numerous oxidative capabilities with respect to electron donors such as hydrogen, fatty acids and alcohols (reviewed by Muyzer & Stams, 2008). Furthermore, only 20 years ago SRB were shown to degrade hydrocarbons.

Hydrocarbon-degrading SRB are highly diverse with respect to substrate usage and their phylogeny. So far, cultured SRB mainly belong to *Deltaproteobacteria* with the exception of *Desulfosporosinus* sp. strain Y5 (Liu et al., 2004) and *Desulfotomaculum* sp. strain OX39 (Morasch et al., 2004) within the *Clostridia*. Most deltaproteobacterial isolates were phylogenetically affiliated with the *Desulfosarcina/Desulfococcus* (DSS) clade (Fig. I.5) (Aeckersberg et al., 1991; Aeckersberg et al., 1998; Harms et al., 1999; So & Young, 1999; Meckenstock et al., 2000; Cravo-Laureau et al., 2004; Kniemeyer et al., 2007; Higashioka et al., 2009). Additional isolates affiliated with *Desulfobacterium* spp. (Rabus et al., 1993; Ommedal & Torsvik, 2007) or with *Desulfobacterium anilini* (Galushko et al., 1999; Harms et al., 1999; Kniemeyer et al., 2003; Musat et al., 2009), a strain for which the phylogenetic reclassification is still pending (Kniemeyer et al., 2003).

The range of hydrocarbons, used anaerobically by microorganisms, is restricted to a narrow range of chain lengths or even only a single compound, such as toluene. Up to now, isolated SRB were described to degrade C₃-C₂₀ *n*-alkanes, C₇-C₂₃ *n*-alkenes or aromatic hydrocarbons such as benzene, toluene or naphthalene (Fig. I.5; see Widdel et al., 2010 and references therein). The capability of microorganisms to degrade both aliphatic and aromatic hydrocarbons was not observed. Also, compounds from crude oils, mainly alkanes and aromatic hydrocarbons, have been shown to be oxidized by SRB (e.g. Rueter et al., 1994).

Several SRB with the ability to oxidize hydrocarbons are of marine origin. Short-chain alkane degraders were enriched and isolated from marine seeps e.g. the strain BuS5, which was isolated from Guaymas Basin (Kniemeyer et al., 2007) or the enrichment culture Butane-GMe12 from Gulf of Mexico (Kniemeyer et al., 2007; Jaekel, 2011). Also aromatic hydrocarbon-degrading SRB include isolates from marine environments: strain EbS7, which oxidizes ethylbenzene, was isolated from Guaymas Basin (Kniemeyer et al., 2003). Furthermore, strains NaphS2, NaphS3 and NaphS6 oxidize e.g. naphthalene originated from North Sea and Mediterranean sediments (Galushko et al., 1999; Musat et al., 2009).

4.2. Metabolic pathways for anaerobic hydrocarbon degradation by SRB

Current knowledge about possible hydrocarbon degradation pathways of SRB is mainly based on analogies to denitrifying bacteria (see Johann, 2007 and references therein). The most common activation mechanism under anoxic conditions for non-methane alkanes and alkyl-substituted aromatic hydrocarbons is fumarate activation (cf. Widdel & Grundmann, 2010). It starts with a C-H bond cleavage by a protein-hosted radical followed by the addition of the radical product to fumarate, which finally results in substituted alkylsuccinates (Fig. I.6). This activation mechanism resembles that for toluene and some other alkylbenzenes in anaerobic bacteria, whereas the subsequent reactions of the alkylsuccinates differ. Glycyl radical enzymes that were proposed for the anaerobic hydrocarbon-activation are the benzylsuccinate synthase (Bss; Biegert et al., 1996; Beller & Spormann, 1997), the (1-methyl)alkylsuccinate synthase (Mas or Ass; Callaghan et al., 2008; Grundmann et al., 2008) and (2-naphthylmethyl)succinate synthase (Nms; Musat et al., 2009).

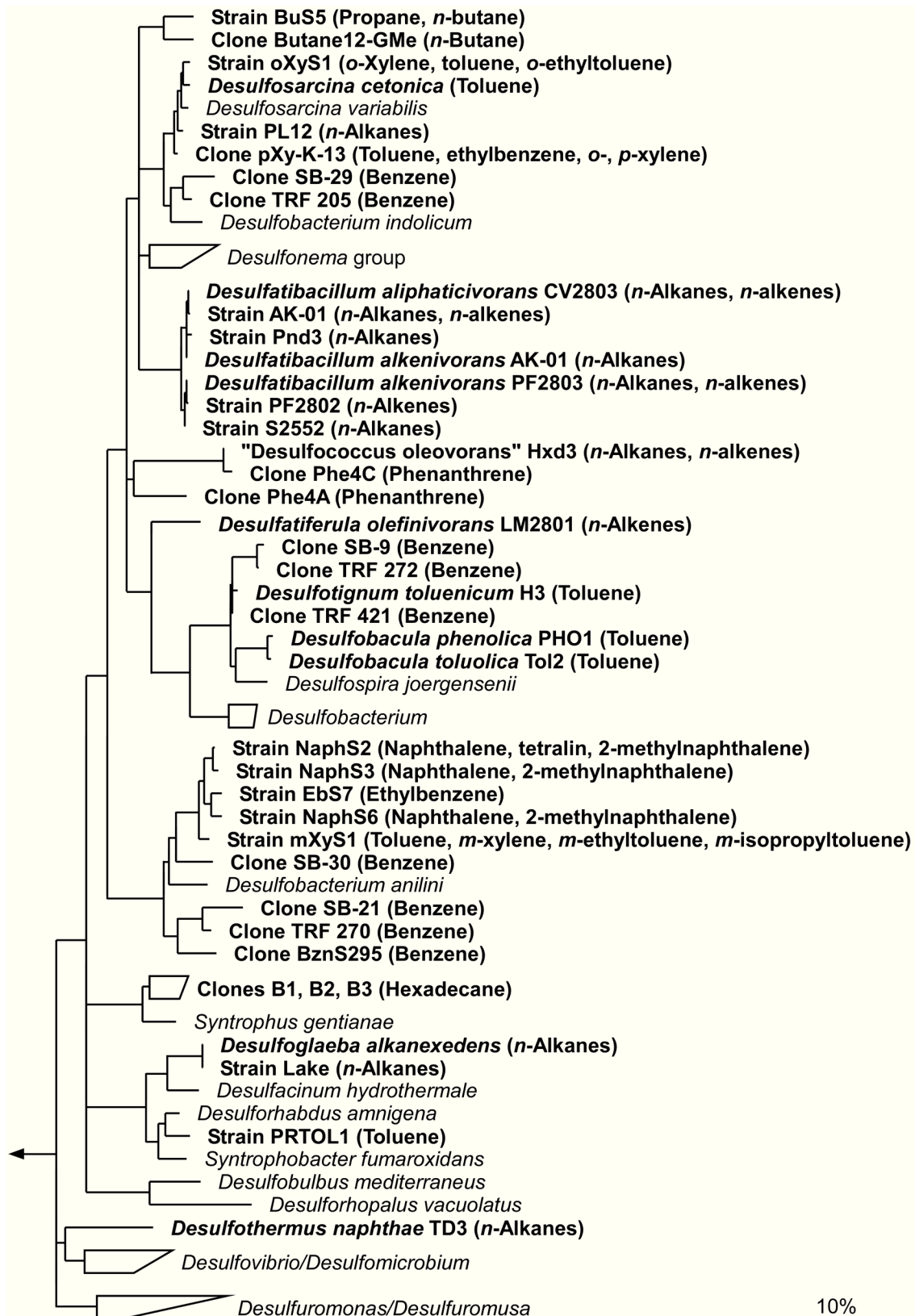


Fig. I.5: The majority of the so far known SRB able to anaerobically utilize non-methane hydrocarbons (bold) are *Deltaproteobacteria* as indicated in the 16S rRNA-based phylogenetic tree shown here. The majority is further assigned to the DSS clade or affiliates with *Desulfobacterium anilini*. The bar indicates 10% sequence diversity. Fig. modified from Widdel et al. (2010).

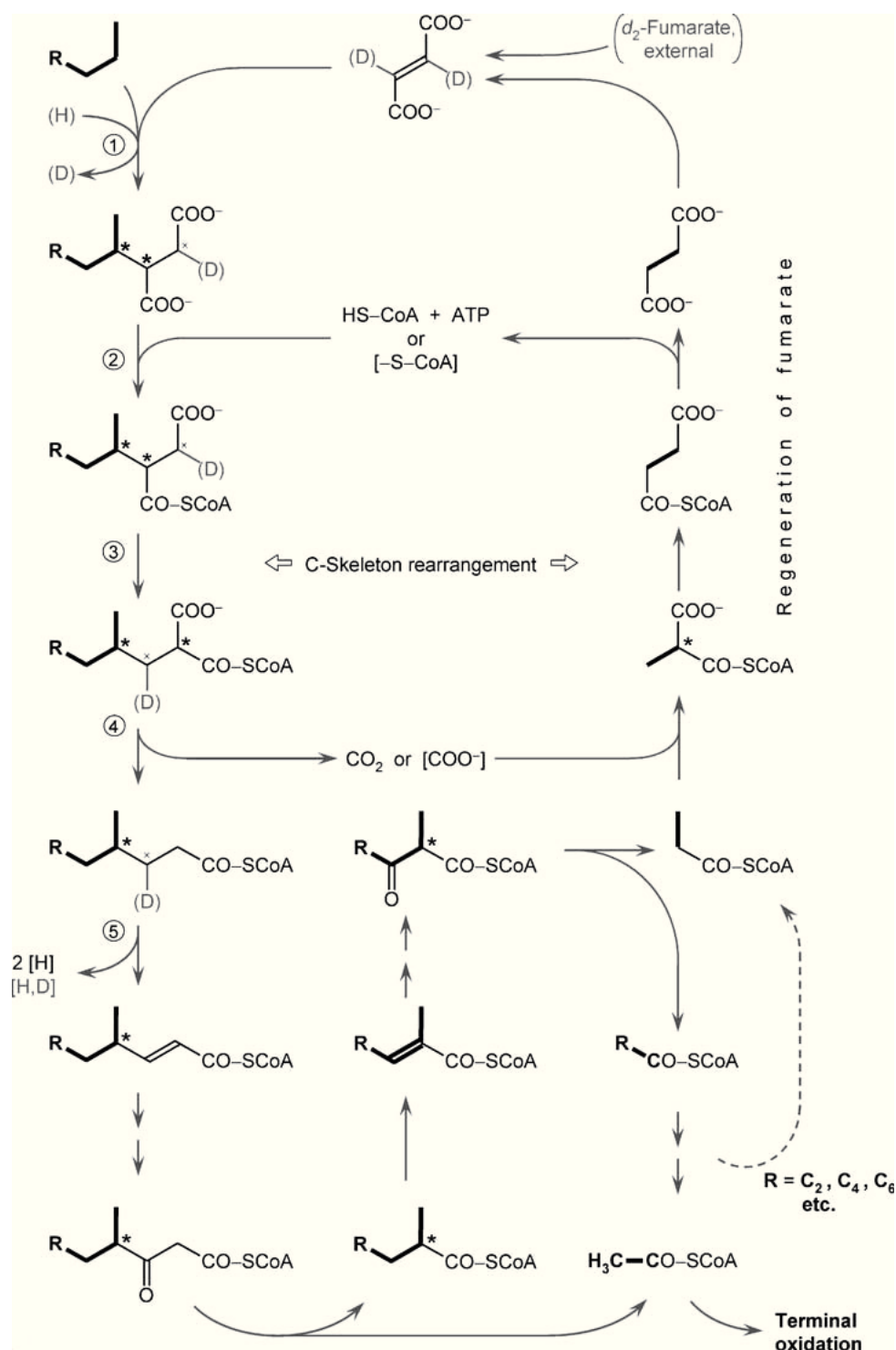


Fig. 1.6: Proposed pathway for the anaerobic degradation of *n*-alkanes. Initial fumarate activation reaction (1): an H-atom (H^\bullet) is abstracted yielding a secondary alkyl radical ($R-CH_2-\bullet CH-CH_3$) that adds to fumarate. Then, the (1-methylalkyl)succinyl radical is saturated with the H-atom to yield the first stable intermediate, which is (1-methylalkyl)succinate. Afterwards one deuterium exchanges with hydrogen from water by an unknown mechanism. After an assumed activation to the thioester with free CoA or via a CoA-transferase (2), the C-skeleton is rearranged (3) to allow decarboxylation or transcarboxylation (4). Dehydrogenation of (1-methylalkyl)succinyl-CoA (5) specifically removes the remaining deuterium. The stereogenic centers are indicated by asterisks. Fig. taken from Widdel & Grundmann (2010).

5. Stable-isotope probing techniques in microbial ecology

The elements C, N, S, H and O occur naturally with more than one isotope. Isotopes of elements are characterized by the same numbers of protons but different numbers of neutrons in their atomic nuclei (Peterson & Fry, 1987). The majority of carbon, for example, appears as ^{12}C -isotope, while the ^{13}C stable-isotope of carbon has a natural abundance of only 1.1%. In general, biological reactions discriminate against the heavier ^{13}C stable-isotope resulting in an enrichment of the lighter ^{12}C -isotope (Peterson & Fry, 1987). These so called isotopic fractionations can subsequently be determined by gas chromatography-isotope ratio mass spectrometry GC-IRMS (Hayes, 2001) and be used to draw conclusions about biogenic or thermogenic origin of an organic compound (Killips & Killips, 2004). Isotopic fractionations were analyzed to identify active methanotrophic organisms (Hinrichs et al., 1999) and to determine rates of nitrogen fixation (McNeill et al., 1994).

Stable-isotope probing (SIP) techniques allow the identification of active organisms that are involved in the degradation of a certain compound, when offering substrates labeled with a stable isotope. Within SIP-incubations usually environmental samples are amended with ^{13}C -, ^{15}N , or ^{18}O -labeled substrates (Fig. I.7a). Active organisms metabolize this substrate and use it for biomass synthesis (Radajewski et al., 2000). First SIP-experiments were carried out based on the analysis of phospholipid fatty acids (PLFA; Boschker et al., 1998), while later on DNA-, rRNA-, and protein-based SIP-techniques were developed (Radajewski et al., 2000; Manefield et al., 2002; Jehmlich et al., 2010).

PLFA-based SIP is the most sensitive technique (required incorporation <0.1 atomic percent; AT%). Low amounts of ^{13}C -incorporation into the fatty acids are measured with a combination of gas chromatography and isotope mass spectrometry (GC-IRMS, Fig. I.7b; Boschker et al., 1998). However, a drawback of this method is that the taxonomic identification of active organisms based on PLFA (Zelles, 1999) is restricted to the family or genus level and dependent on cultured representatives (Boschker & Middelburg, 2002).

Another sensitive method is protein-based SIP (Protein-SIP), which determines the amount of label incorporation into proteins (required incorporation ~ 2 AT%). Within Protein-SIP studies the amount of incorporation provides an estimation of substrate assimilation and the sequence information from peptide analysis obtained by mass spectrometry delivers phylogenetic information (Fig. I.7d; Jehmlich et al., 2008b; Jehmlich et al., 2010). However, the phylogenetic information obtained is dependent on sequenced representatives and identification can be conducted down to strain level only when sequenced strains are

investigated (Jehmlich et al., 2008a). For environmental samples, genetic information is usually sparse and protein identification can be obtained at the genus level at best.

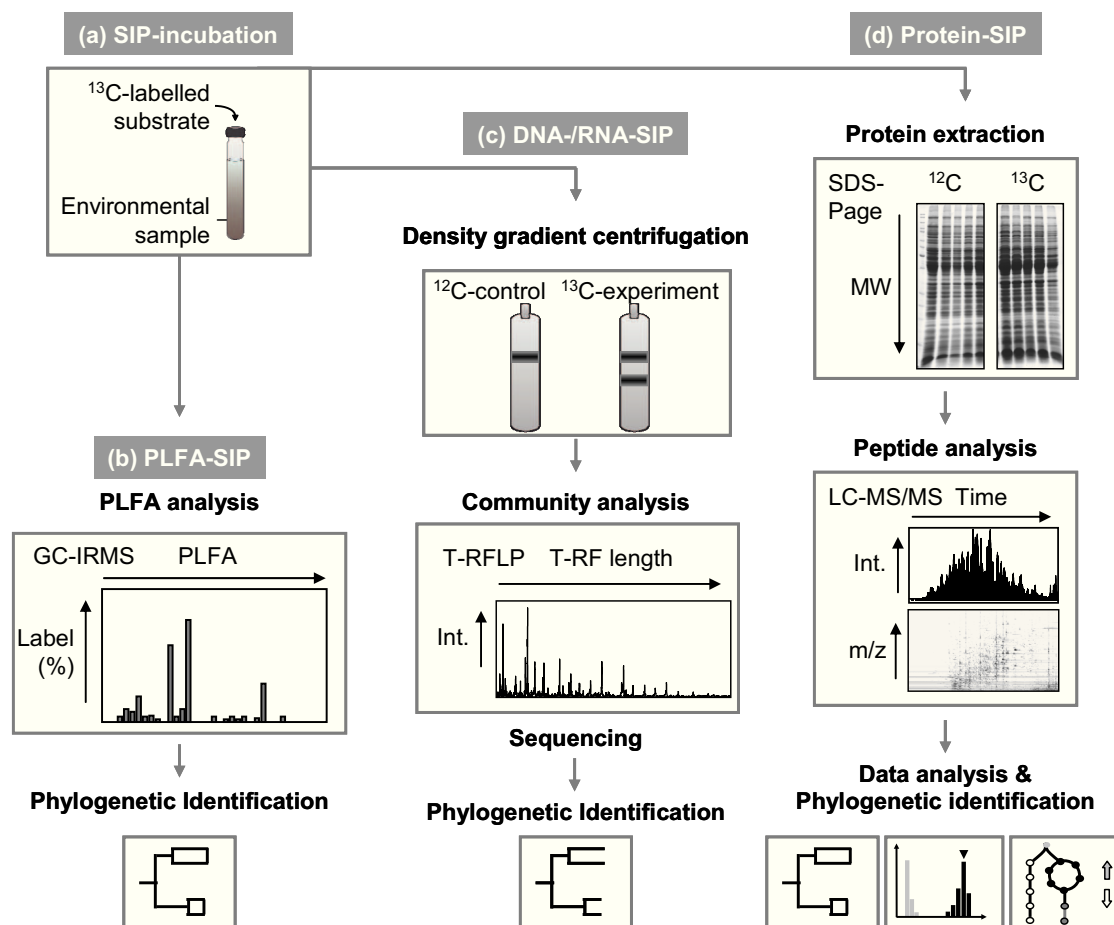


Fig. I.7: Overview of typical workflows for (b) PLFA-SIP, (c) DNA-/RNA-SIP, and (d) Protein-SIP. (a) ^{13}C -labelled substrate is added to an environmental sample. Within incubation the labeled substrate is incorporated into the biomass of active microorganisms. (b) PLFA are extracted and analyzed by GC-IRMS to reveal active microorganisms that grew on the ^{13}C -labeled substrate. (c) RNA/DNA of active organisms is separated from the community RNA/DNA by density gradient centrifugation. Community analysis (e.g. T-RFLP) is used to detect labeled organisms, which are later on identified by 16S rRNA sequencing. (d) Proteins are purified e.g. via SDS-Page. Proteolytically digested proteins are characterized by mass spectrometry e.g. liquid chromatography–mass spectrometry/mass spectrometry (LC-MS/MS). For this, peptides are detected by a high-resolution and high-sensitivity survey scan (single-stage MS spectrum) and then isolated (ion trap) and further fragmented (fragmentation scan, MS/MS spectrum) to obtain sequence information. Data analyses reveal e.g. ^{13}C -incorporation into certain proteins and the phylogenetic affiliation of active microorganisms. The Protein-SIP workflow of this Fig. was modified from Jehmlich et al. (2010).

DNA- and rRNA-based SIP techniques, that target the 16S rRNA, enable taxonomic identification on the genus or species level (Radajewski et al., 2000; Manefield et al., 2002). For these methods labeled and unlabeled nucleic acids are separated within density gradient centrifugation (Fig. I.7c). These separations based on isopycnic centrifugation are possible due to mass differences caused by additional neutrons within the ^{13}C -atoms. SIP based on

rRNA is more sensitive (required incorporation 15-20 AT%) than DNA-based SIP (required incorporation 25-30 AT%) because rRNA synthesis is dependent on activity (Molin & Givskov, 1999) while DNA synthesis is directly coupled to cell replication. Recently, a combination of high-throughput pyrosequencing and SIP techniques (Pyro-SIP) was developed (Pilloni et al., 2011).

For SIP-experiments longer incubation times are especially needed, when applying techniques that require higher label incorporation such as DNA-SIP. However, long incubation time causes the risk of cross-feeding. Cross feeding occurs for example when organisms (secondary consumers) that can feed on degradation products of other organisms (primary consumers) may become labeled during SIP-incubation. Cross feeding was often discussed as one of the disadvantages, but it is advantageous when the flow of e.g. carbon through an ecosystem has to be determined. Therefore, cross feeding and other dynamics within SIP-incubations are ideally monitored by several sampling points and their analysis. Up to now, SIP-studies coupled diverse substrates and environments to target various metabolic pathways. SIP-studies using labeled hydrocarbons included for instance ^{13}C -labeled benzene in groundwater enrichment cultures (Kasai et al., 2006; Kunapuli et al., 2007), benzoate in enrichments from marine sediments (Gallagher et al., 2005), biphenyl in pine root soil (Leigh et al., 2007), naphthalene in soils and a soil bioreactor (Jeon et al., 2003; Singleton et al., 2005; Yu & Chu, 2005), pentachlorophenol in grassland soil (Mahmood et al., 2005), phenantrene in a soil bioreactor (Singleton et al., 2005; Singleton et al., 2007), phenol in bioreactor sludge and soils (Manefield et al., 2002; Padmanabhan et al., 2003; DeRito et al., 2005; Manefield et al., 2005) and toluene in aquifer sediments (Winderl et al., 2010). Furthermore, SIP applications have to date not always been restricted to the laboratory as they also have been applied in situ in the field (e.g. Jeon et al., 2003; Takano et al., 2010).

Lately, a method was developed, which allows the measurement of the isotopic compositions on the single cell level by nanometer scale secondary-ion mass spectrometry (NanoSIMS; Li et al., 2008; Musat et al., 2008). Within NanoSIMS-analysis the sample is sputtered by a small beam of primary ions (500 nm Cs^+ , 200 nm O^-), followed by the ionization of secondary ions. These secondary ions are then analyzed by mass spectrometry, which allows the parallel detection of up to seven masses. NanoSIMS is currently the most sensitive method and is often used in combination with horseradish-peroxidase (HRP)-labeled oligonucleotide probes and fluorine-containing tyramides to identify active microorganisms from SIP-experiments (Musat et al., 2008). Furthermore, based on single cells isotopic ratios metabolic activities of single cells can be quantified.

Objectives of this thesis

SRB are key players in marine sediments responsible for up to 50% of organic matter mineralization (Jørgensen, 1982). At marine hydrocarbon seeps, anaerobic non-methane hydrocarbon degradation by SRB was discussed to be an important ecological process (e.g. Joye et al., 2004; Kallmeyer & Boetius, 2004; Bowles et al., 2011). Numerous SRB able to degrade alkanes, alkenes and aromatic hydrocarbons were isolated from various habitats, including marine seep sediments (e.g. Kniermeyer et al., 2003; Kniermeyer et al., 2007). However, knowledge about the population catalyzing anaerobic hydrocarbon degradation at marine seep sediments is lacking behind. Therefore, in this doctoral thesis I targeted the following questions:

(1) Which groups of SRB dominate marine gas and hydrocarbon seep sediments?

The first aim of this study was to investigate the distribution and abundance of several groups of SRB in various marine gas and hydrocarbon seep sediments (Chapter II). Of particular interest were cultured and uncultured SRB groups, often retrieved from clone libraries. In addition, hydrocarbon-degrading SRB from enrichments or pure cultures were in focus. To address these questions, SRB from selected seep sediments, with known hydrocarbon compositions, were analyzed in situ using catalyzed reporter deposition-fluorescence in situ hybridization (CARD-FISH). To get more insights into active hydrocarbon-oxidizing SRB, RNA-based clone libraries were used to reveal the diversity of sulfate-reducing prokaryotes in oily hydrate-bearing sediments from the Gulf of Mexico. In addition, statistical analysis aimed to unravel distribution patterns of SRB.

(2) What are key players of hydrocarbon-oxidation processes in situ?

The second aim of this study was to identify key players for butane and dodecane degradation in selected marine seep sediments (Chapter III). Hereby, a link between biogeochemical processes and cultured representatives was intended by discovering in situ active SRB. Sediments from two contrasting hydrocarbon seeps were selected for SIP-incubations to identify short-chain (C_3 - C_4) and long chain alkane (C_6 - C_{20}) degraders. Various SIP-techniques (DNA-, rRNA-, and Protein-SIP) were applied to identify key players, track the ^{13}C -carbon flow and unravel possible pathways.

(3) How abundant and active is the alkane-degrading community?

The third aim of this study was to finally get information about the in situ abundance and cellular hydrocarbon-oxidation rates of SRB degrading short-chain and long chain alkanes (Chapter IV). Herewith, an estimation of the in situ turnover of alkanes by SRB at

marine seeps was intended. Specifically defined groups of SRB, actively oxidizing short-chain and long-chain alkanes within sediments from a gas and a hydrocarbon seep, were analyzed on the single-cell level using NanoSIMS. Measurements of ^{13}C -isotope ratios aimed to calculate rates for distinct phylogenetic groups of SRB. Finally, the extrapolation of SR rates fueled by non-methane hydrocarbons was aspired, to estimate the impact of alkane degradation on the marine carbon and sulfur cycles at hydrocarbon seeps.

Please note that references for Chapter I are provided after Chapter VI starting with page 148.

Contribution to manuscripts

Chapter II - full manuscript

Distribution and in situ abundance of sulfate-reducing bacteria in diverse marine hydrocarbon seep sediments

Sara Kleindienst, Alban Ramette, Rudolf Amann, and Katrin Knittel

S.K. and K.K. designed the project. S.K. tested probes, performed CARD-FISH experiments and analysis of 16S rRNA and *aprA* gene sequences. K.K. did the laser scanning microscopy, A.R. carried out statistical analysis. S.K. interpreted statistical data under supervision of A.R. S.K. and K.K. wrote the manuscript with input from A.R. and R.A.

Environmental Microbiology, in press.

Chapter III - full manuscript

Specialists instead of generalists oxidize alkanes in anoxic marine hydrocarbon seep sediments

Sara Kleindienst, Florian-Alexander Herbst, Frederick von Netzer, Rudolf Amann, Jörg Peplies, Martin von Bergen, Jana Seifert, Florin Musat, Tillmann Lueders, Katrin Knittel

S.K. designed the project under supervision of F.M. and K.K. S.K. accomplished SIP-experiments, performed sulfide, butane and DIC measurements. In addition, S.K. performed DNA- and rRNA-based SIP and conducted T-TFLP analysis as well as analysis of 454-pyrosequences and assembled amplicon contigs under supervision of T.L. Furthermore, S.K. designed the probes under supervision of K.K. and carried out CARD-FISH experiments. F.v.N. carried out T-REX analysis. J.P. performed NGS-pipeline analysis. F.A.H. carried out Protein-SIP analysis under supervision of J.S. and M.v.B. S.K. wrote the manuscript with input from F.A.H., R.A., J.S., F.M., T.L., and K.K.

In preparation

Chapter IV - full manuscript

Impact of alkane degrading sulfate-reducing bacteria on marine carbon cycling

Sara Kleindienst, Lubos Polerecky, Florin Musat, Katrin Knittel

S.K. designed the project under supervision of F.M. and K.K. S.K. carried out SIP-experiments, TOC measurements and CARD-FISH experiments. S.K. evaluated and performed sediment sample preparation for NanoSIMS analysis. S.K. conducted post processing of NanoSIMS data. L.P. developed the models for rate calculations. S.K. wrote the

manuscript with input from all co-authors.

In preparation

Chapter V

Abstract of a published manuscript to which I contributed as a co-author as part of my thesis

Impact of natural oil and higher hydrocarbons on microbial diversity, distribution and activity in Gulf of Mexico cold seep sediments

Beth Orcutt, Samantha Joye, Sara Kleindienst, Katrin Knittel, Alban Ramette, Anja Reitz, Vladimir Samarkin, Tina Treude, Antje Boetius

B.O., S.J. and A.B. designed the project. B.O. and T.T. collected the samples, and B.O., T.T., V.S., and A.R. carried out the geochemical analyses. S.K. carried out CARD-FISH experiments. K.K. designed probes and performed analysis of 16S rRNA gene sequences. A.R. carried out statistical analysis. B.O. wrote the manuscript with input from all co-authors.

Published in *Deep-Sea Research II*, vol. 57, pp. 2008-2021 (2010).

Chapter II

Distribution and in situ abundance of sulfate-reducing bacteria in diverse marine hydrocarbon seep sediments

Sara Kleindienst, Alban Ramette, Rudolf Amann, and Katrin Knittel*

Environmental Microbiology

In press

*Corresponding author: Katrin Knittel (Department of Molecular Ecology),
Phone: +49 421 2028 935, Fax: +49 421 2028 580, E-mail: kknittel@mpi-bremen.de
Max-Planck-Institute for Marine Microbiology, Celsiusstrasse 1, D-28359 Bremen, Germany

Summary

Marine gas and hydrocarbon seeps are hot spots of sulfate-reduction, which is fueled by methane, other short-chain alkanes or a complex mixture of hydrocarbons. In this study, we investigated the global distribution and abundance of sulfate-reducing bacteria (SRB) in eight gas and hydrocarbon seeps by catalyzed-reporter deposition fluorescence in situ hybridization (CARD-FISH). The majority of *Deltaproteobacteria* were assigned to specific SRB groups, i.e. $83\% \pm 14\%$ at gas seeps and $61\% \pm 35\%$ at hydrocarbon seeps, indicating that the probe set used was sufficient for classification of marine SRB. Statistical analysis showed that SRB abundance and distribution were significantly influenced by habitat type and sediment depth. Members of the *Desulfosarcina/Desulfococcus* (DSS) clade strongly dominated all sites. Data suggested rather the presence of numerous diverse and specialized but low abundant DSS species than the presence of one dominant subgroup. In addition, SEEP-SRB2, an uncultured deep-branching deltaproteobacterial group, was ubiquitously found in high abundances at all sites. SEEP-SRB2 members occurred either in a novel association with methanotrophic archaea in shell-type ANME-2/SEEP-SRB2 consortia, in association with ANME-1 archaea in Black Sea microbial mats or as single cells. Two other uncultured groups, SEEP-SRB3 and SEEP-SRB4, were preferentially detected in surface sediments from mud volcanoes.

Introduction

Sediments of marine hydrocarbon seeps are hot spots of microbial sulfate reduction (SR). Many hydrocarbon seeps are dominated by methane seepage and only minor concentrations of other hydrocarbon gases (ethane through butane) that are present as trace gases (Claypool & Kvenvolden, 1983). In contrast, seeps in the Gulf of Mexico (Paull et al., 1984; Orcutt et al., 2004; Schubotz et al., 2011) and in the hydrothermally active Guaymas Basin (Simoneit & Lonsdale, 1982) are characterized by the emission of a complex mixture of hydrocarbons including alkanes, cycloalkanes and aromatics.

SR rates are several orders of magnitude higher in seep sediments than in non-seepage sediments ($>1 \mu\text{mol cm}^{-3} \text{d}^{-1}$ versus low $\text{nmol cm}^{-3} \text{d}^{-1}$; Aharon & Fu, 2000; Boetius et al., 2000; Michaelis et al., 2002; Treude et al., 2003; Joye et al., 2004). At methane seeps, SR is mainly fueled by the anaerobic oxidation of methane (AOM) which is mediated by a consortium of methanotrophic archaea (ANME) and sulfate-reducing bacteria (SRB), leading to a ~1:1 coupling of these two processes (Nauhaus et al., 2002). Three ANME groups have been identified so far: ANME-1, ANME-2, and ANME-3 (Hinrichs et al., 1999; Boetius et al., 2000; Niemann et al., 2006b). All groups have been shown to live in consortia with SRB of the *Desulfosarcina/Desulfococcus* (DSS) clade, more specifically with the subgroup SEEP-SRB1a (Schreiber et al., 2010), or with *Desulfobulbus* relatives (ANME-2, and ANME-3) but have also repeatedly found without any partner (Orphan et al., 2002; Knittel et al., 2005; Lösekann et al., 2007; Pernthaler et al., 2008).

In sediments with seepage of higher hydrocarbons in addition to methane, SR gets decoupled from AOM. Methane-dependent SR drops to less than 10% of total SR rates, e.g. at the Gulf of Mexico (Joye et al., 2004; Orcutt et al., 2010), Guaymas Basin (Kallmeyer & Boetius, 2004), and some mud volcanoes in the Mediterranean Sea (Omorigie et al., 2009) suggesting other hydrocarbons than methane as electron donors for SRB. Chemical analyses of anoxic hydrocarbon-rich sediments confirmed biodegradation of short-chain hydrocarbons (Sassen et al., 2004; Niemann et al., 2006a; Mastalerz et al., 2009). What fraction of this microbial oxidation in situ is attributable to SR is still unclear.

Kniemeyer et al. (2007) provided the first direct microbiological evidence for the biological oxidation of propane and butane by SRB. BuS5, a mesophilic strain which uses propane and butane, was isolated from marine sediment of Guaymas Basin. Prior to that study, several organisms have been isolated which degrade longer alkanes, alkenes, and aromatic hydrocarbons (Aeckersberg et al., 1991; Rabus et al., 1993; Rueter et al., 1994; Aeckersberg et al., 1998). Most of the SRB isolates degrading hydrocarbons are *Deltaproteobacteria* and

only few belong to the gram-positive *Firmicutes*. The 16S rRNA gene sequences of several clades of yet uncultivated SRB (SEEP-SRB1 to SEEP-SRB4; Knittel et al., 2003) are commonly and exclusively found at seeps, especially when short-chain alkanes are present. However, which of these microorganisms are environmentally relevant and responsible for sulfate-dependent hydrocarbon oxidation in situ remains unknown.

In this study we investigated the abundance and distribution of specific groups of SRB in eight marine seep habitats differing in hydrocarbon composition, concentration, sulfate fluxes, or temperature. We provide a comprehensive dataset for SRB composition and their spatial distribution at marine seeps as determined by catalyzed-reporter deposition fluorescence in situ hybridization (CARD-FISH). In addition, we investigated the in situ abundance of cultured hydrocarbon-degrading SRB. A special focus was on the four unclassified groups SEEP-SRB1 to SEEP-SRB4. CARD-FISH data were analyzed by statistical methods to identify significant factors influencing SRB community structure. Furthermore, cDNA-clone libraries for 16S rRNA and adenosine-5'-phosphosulfate reductase subunit A (*aprA*) were constructed and allowed the identification of active SRB in an oily sediment from the Gulf of Mexico.

Results

Design and evaluation of new probe SEEP2-658

An oligonucleotide probe was developed for the specific detection of the deltaproteobacterial group SEEP-SRB2, which had been frequently found in 16S rRNA gene libraries from marine seep sediments. The new probe SEEP2-658 has currently a perfect coverage of 100% of the target group and only 11 non-target hits in ARB SILVA Ref108 database containing 618,442 sequences (release date 01 Sept 2011). The probe was evaluated by Clone-FISH and showed bright fluorescence signals under specific hybridization conditions of 45% formamide.

Cross-hybridization of probes DSS658 and SEEP2-658

Parallel hybridizations with the new probe SEEP2-658 and probe DSS658, specific for the not-overlapping DSS clade, on pure cultures as well as on environmental samples indicated cross-hybridization. We retrieved bright signals of DSS as well as SEEP-SRB2 cells at hybridization conditions assumed to be specific for both probes. The probe target regions on the 16S rRNA are identical, but the two probes differ in 2 out of 18 bases (second and third last position of probe sequence). This newly discovered cross-hybridization of probes

DSS658 and SEEP2-658 should be kept in mind for the interpretation of published DSS abundance data. Cross-hybridization could be avoided by adding DSS658 as an unlabeled competitor to probe SEEP2-658 and vice versa (adding an unlabeled SEEP2-658 competitor to probe DSS658), a strategy originally suggested by Manz et al. (1992). Thereby, we were able to discriminate the DSS clade from the SEEP-SRB2 group in this study.

Estimating total SRB in marine hydrocarbon seep sediments

Since most marine SRB belong to *Deltaproteobacteria*, a general deltaproteobacterial probe together with a probe for *Desulfotomaculum*, a widely distributed genus of SRB within the *Firmicutes*, was used for estimation of total SRB. This might slightly overestimate the real numbers of SRB since not all *Deltaproteobacteria* are SRB. Depth distribution was analyzed in a 1 to 2 cm-resolution from the sediment surface down to 15-25 cm depth. SRB of the genus *Desulfotomaculum* were investigated for seeps at Guaymas Basin but were only found in low abundance at the oily site 4487-6 at Guaymas Basin (<1% of total cells, data not shown).

Deltaproteobacteria were found in high numbers at all seep sites investigated either as ‘free-living’ single cells or aggregated with ANME archaea in AOM-mediating consortia (Table II.1 and Table II.2). The fraction of *Deltaproteobacteria* was large at all sites with highest relative values close to the sediment surface: *Deltaproteobacteria* accounted for 57-65% of total cells at Hydrate Ridge (up to 2.6×10^{10} cells cm^{-3}), 14-59% at Amon mud volcano (Amon MV; up to 2.2×10^9 cells cm^{-3}), 1-15% at Haakon Mosby mud volcano (Haakon Mosby MV; up to 7.9×10^8 cells cm^{-3}), 8-22% at Tommeliten seep sites (up to 1.1×10^9 cells cm^{-3}), 7-40% at Gulf of Mexico seeps (up to 1.4×10^9 cells cm^{-3}), and 1-16% at Guaymas Basin (up to 1.9×10^9 cells cm^{-3}). The large differences in deltaproteobacterial cell numbers, of almost two orders of magnitude, can be explained by the huge microbial biomass of ANME-2/DSS consortia at Hydrate Ridge, which harbor >90% of total cells. All known SRB capable of non-methane hydrocarbon degradation are free-living organisms and thus likely contribute remarkably to the fraction of single *Deltaproteobacteria* at hydrocarbon seeps. In general, single *Deltaproteobacteria* accounted for a relatively large fraction of the free-living microbial community between 5% and 20% and always more than 10^8 cells cm^{-3} . Highest numbers of single deltaproteobacterial cells were detected at sites with a complex mixture of hydrocarbons such as the Guaymas Basin site GB4489-1 with 1.9×10^9 cells cm^{-3} and at Tommeliten site 1274-K3 with 1.1×10^9 cells cm^{-3} . *Deltaproteobacteria* made up a remarkably high fraction in sediments from the main “fresh” asphalt field (10625-9) as well

as in pure asphalt (10625-16) from Chapopote asphalt volcano in the Gulf of Mexico with 10-17% of total cells.

When we calculated depth-integrated deltaproteobacterial cell numbers for the top 10 cm of the sediment (Table II.1), all were in the narrow range of 1.8 to 8.8×10^{13} cells m^{-2} , with the exception of Hydrate Ridge sediments where numbers were two orders of magnitude higher.

SRB community structure

With a set of group- and genus-specific SRB probes (Table II.S1), $83\% \pm 14\%$ of *Deltaproteobacteria* could be assigned to particular subgroups in sediments dominated by gaseous hydrocarbons and $63\% \pm 31\%$ of *Deltaproteobacteria* were further assigned in sediments with complex hydrocarbon composition.

Members of the DSS clade turned out to be the overall dominant fraction of SRB in most samples investigated (Fig. II.1, Table II.2) with numbers of 7-94% of *Deltaproteobacteria* at Haakon Mosby MV, 55-94% at Amon MV, 19-88% at Tommeliten seep sites, 15-92% at Gulf of Mexico seeps, and 15-100% at Guaymas Basin.

Table II.1: Geochemical characteristics of investigated sampling sites and abundance of AOM aggregates

	Tommeliten, North Sea	Gulf of Mexico		Chapopote Asphalt Volcano (Campeche Knolls, southern Gulf of Mexico)				Guaymas Basin	
Station	1274-K1-3	156	161	140	GeoB10619-6	GeoB10619-13	GeoB10625-9	GeoB10625-16	Marker2-4489
Device, device #, dive #	PUC	TV-MUC	TV-MUC	TV-Grab	Dive82-PUC9	Dive82-PUC36	Dive84-PUC32	Dive84	Dive4489-PUC1
Cruise	AL 267	SO174	SO174	SO174	M67/2	M67/2	M67/2	M67/2	AT 15-40
Date	38596	Oct/Nov 2003	Oct/Nov 2003	Oct/Nov 2003	Apr 2006	Apr 2006	Apr 2006	Apr 2006	Dec 2008
Longitude	02°59.800E	91°30.47W	90°58.86W	93°26.4W	93°26.1828W	93°26.1828W	93°26.2049W	93°26.252W	111°24.537W
Latitude	56°29.900N	27°46.95N	27°33.48N	21°54.00N	21°53.9910N	21°53.9910N	21°53.907N	21°53.957N	27°0.468N
Sample type	Sediment	Very gassy, near oily sediment	Oily sediment, hydrate	Oily sediment near Chapopote asphalt volcano	Oily sediments	Mat on brittle asphalt	Oily sediments close to main asphalt field	Asphalt with white precipitate	Hydrocarbon-rich sediment
Chemosynthetic community	Bacterial mat	Sulfide-oxidizing bacteria, tubeworms	White sulfide-oxidizing bacteria	Tubeworms	Bacterial mat	Bacterial mat	Bacterial mat	Bacterial mat	Bacterial mat
Water depth [m]	75	550	950	2900	2908	2908	2922	2922	2000
Temp. [°C]	4	NA	NA	NA	4	4	4	4	Gradient: 3 to 50 ^d
Gaseous hydrocarbon composition	>99% C ₁ , <1% other gaseous alkanes	84% C ₁ , 16% C ₂	69% C ₁ , 8% C ₂ , 16% C ₃ , 5% <i>iso</i> -C ₄ , 3% <i>n</i> -C ₄	87% C ₁ , 4% C ₂ , 7% C ₃ , 2% <i>iso</i> -C ₄ , <1% <i>n</i> -C ₄	95% C ₁ , 5% C ₂	NA	95% C ₁ , 3% C ₂ , 2% 2Me-C ₅	72% C ₁ , 8% C ₂ , 7% C ₃ , 6% C ₄ , 5% C ₅ , 2% C ₆	96% C ₁ , 3% C ₂ , 2% C ₃ , 1% C ₄ , 1% C ₅ , 1% C ₆ ^e
Other hydrocarbons	NA	hexadecane, isoprenoids, aromatics (naphthalene, phenanthrene, toluene) and crude oil	hexadecane, isoprenoids, aromatics (naphthalene, phenanthrene, toluene) and crude oil	<i>n</i> -alkanes (peak at C ₃₀) and few C ₂₉ -C ₃₂ hopanes	mainly steranes and hopanes, few paraffins, alkylbenzenes, cycloalkanes	mainly steranes and hopanes, few paraffins, alkylbenzenes, cycloalkanes	mainly paraffins (<i>n</i> -alkanes, branched alkanes and isoprenoids C ₁₄ to C ₄₀), alkylcycloalkanes, alkylbenzenes, polyaromatics, few steranes and hopanes	mainly paraffins (<i>n</i> -alkanes, branched alkanes and isoprenoids C ₁₄ to C ₄₀), alkylcycloalkanes, alkylbenzenes, polyaromatics, few steranes and hopanes	C ₁₂ -C ₃₈ alkanes, cycloalkanes, diverse aromatics
Depth-integrated SRR [mmol m⁻² d⁻¹]^b	NA	5.6	27.9	0.2	27.1 ± 31.9	NA	36.7 ± 25.9	NA	NA
Depth-integrated SRB abundance [10¹³ m²]^a	7.11	8.80	3.58	2.44	1.81	NA	3.26	NA	3.55
Depth-integrated AOM rate [mmol m⁻² d⁻¹]^b	NA	21.2 ± 0.1	NA	0.1 ± 0	0.3 ± 0.3	NA	NA	NA	NA
Dominant AOM consortia	ANME2/ SEEP2	ANME2/SEEP2, ANME2/DSS	ANME2/DSS	ANME2/DSS	ANME-2/SEEP2 ANME-2/DSS	NA	ANME-2/SEEP2 ANME-2/DSS	NA	NA
Aggregate no. [cm⁻³]	up to 1 x 10 ⁶	up to 1 x 10 ⁷	NA	NA	NA	NA	NA	NA	NA
References	Niemann et al. 2005; Kennicutt II et al., 1988; Orcutt et al. Hovland et al. 1993; 2005, 2010; Schreiber et al. 2010 Wegener et al. 2008			MacDonald et al., 2004; Orcutt et al., 2010	Brüning et al., 2010; Schubotz et al 2011; Wegener et al., unpubl.				Bazylnski et al., 1988

Table continued on next page

Table II.1: continued

	Haakon Mosby Mud Volcano, Barents Sea		Amon Mud Volcano, Mediterranean Sea		Hydrate Ridge, Cascadia Margin		Black Sea		
Station	19	22	760	825	19-2	38	822	795	268
Device, device #, dive #	Dive4-PUC-27	MUC	PUC-40	PUC-9	TV-MUC	TV-MUC			Dive146-1
Cruise	AWI	AWI	M70/2	M70/2	SO-148/1	SO-148/1	P317/3	P317/3	M72-2
Date	Aug 2001	Aug 2001	Oct/Nov 2006	Oct/Nov 2006	July 2000	July 2000	Oct 2004	Oct 2004	Feb 2007
Longitude	14°43.67E	14°43.39E	31°42.6623E	31°42.6679E	125° 08.807W	125° 08.847W	31°58.978E	31°59.164E	31°59.539E
Latitude	72°00.19N	72°00.08N	32°22.1299N	32°22.1283N	44°34.186N	44°34.104N	44°46.542N	44°46.775N	44°46.501N
Sample type	Sediment	Sediment	Sediment	Sediment	Sediment	Sediment	Methano- trophic microbial mat	Methano- trophic microbial mat	Methano- trophic microbial mat
Chemosynthetic community	<i>Beggiatoa</i> mat	<i>Pogonophora</i> field	<i>Beggiatoa</i> mat	Bacterial mat	<i>Beggiatoa</i> mats	<i>Calyptogena</i> field	none	none	none
Water depth [m]	1260	1264	1122	1122	777	787	190	189	221
Temp. [°C]	- 1	- 1	14	14	2-4	2-4	8*	8*	8*
Hydrocarbon composition	>99% C ₁ , <1% others	>99% C ₁ , <1% others	mainly C ₁ ; C ₂ - C ₄	mainly C ₁ ; C ₂ - C ₄	>99% C ₁ , other gaseous alkanes	>99% C ₁ , <1% other gaseous alkanes	95% C ₁	95% C ₁	95% C ₁
Depth-integrated SRR [mmol m⁻² d⁻¹]^c	12 ± 5.4	0.3 ± 0.1	23.9 ± NA	80.5 ± NA	32 ± 34	65 ± 58	NA	NA	NA
Depth-integrated SRB abundance [10¹³ m⁻²]^a	1.49	2.24	5.42	9.51	122.03	154.00	NA	NA	NA
Depth-integrated AOM rate [mmol m⁻² d⁻¹]^c	8.5 ± 2.9	0.6 ± 0.1	NA	14.9 ± NA	5.1 ± 4.4	56 ± 54	NA	NA	NA
Dominant AOM consortia	ANME3/DBB	ANME3/DBB	ANME2/DSS	ANME2/DSS	ANME2/DSS	ANME2/DSS	ANME-1; ANME-2/DSS	ANME2/DSS, ANME-1/ SEEP2	ANME2/DSS, ANME-1/ SEEP2
Aggregate no. [cm⁻³]	up to 2 x 10 ⁷	up to 1 x 10 ⁶	up to 3 x 10 ⁶	up to 1 x 10 ⁷	up to 1 x 10 ⁸	up to 1 x 10 ⁸	NA	NA	NA
References	Niemann et al. 2006, de Beer et al. 2006, Lösekann et al. 2007		Felden 2009, Gruenke et al. 2011, Mastalerz et al., 2009		Knittel et al. 2005, Treude et al. 2003		Rossel et al., 2008		

^a: Total Deltaproteobacteria per m² integrated over a depth of 10 cm as determined by CARD-FISH

^b: Depth integrated rates over 10 cm

^c: μmol gdw⁻¹ d⁻¹

^d: Typical temperature gradient from 0 to 20 cm depth from sediments with overlying orange bacterial mats at Guaymas Basin (McKay; pers. communication)

^e: Kellermann; pers. communication

* Shipboard measurements

The dominance of DSS was independent of numerous aggregated cells present in ANME-2/DSS consortia, which were particularly abundant at Hydrate Ridge methane seeps where they caused extremely large DSS fractions of 84-99% of total *Deltaproteobacteria*.

Single cells of DSS were in the range of 1×10^7 to 3.6×10^8 cm^{-3} . There was no clear correlation with depth at all gas and hydrocarbon seep sites (Table II.2). At most sites (e.g. Gulf of Mexico stations 156 and 161, Haakon Mosby MV station ATL19 or Hydrate Ridge station 19) abundance was highest between 2 and 5 cm depth whereas at Amon MV, Guaymas Basin or Chapopote asphalt volcano the abundance was highest at sediment surface. Highest abundances of DSS single cell were found at the *Pogonophora* site at Haakon Mosby MV at 3.5 cm depth with 3.6×10^8 cells cm^{-3} , at Chapopote brittle asphalt sediments at site 10619-6 with 3.7×10^8 cells cm^{-3} and at three Tommeliten gas seep sites with $1-3 \times 10^8$ cells cm^{-3} . The morphology of detected DSS cells was quite diverse and included small and large cocci (0.5-1.5 μm) as well as filaments and rods of largely different cell diameters (Fig. II.2A).

To further resolve the dominant DSS group, several subgroup probes were used. The probes DSS138 and DSS449 targeting two subgroups of uncultivated DSS (Mußmann et al., 2005) did not show signals in any seep sediment. Confirming the data of Schreiber and colleagues (2010), SEEP-SRB1a could be identified as the partner of ANME2. Abundances for most other SEEP-SRB1 subgroups were below 0.5% except for SEEP-SRB1e at gas seep sites (Table II.2, Fig. II.2B): SEEP-SRB1e was detected in all layers along the vertical profile, however, strongly increased with depth. In Tommeliten sediments at site 1274-K3 SEEP-SRB1e made up 6% of total cells (1.8×10^8 cells cm^{-3}) in a depth of 8 cm, at Amon MV site 825 3% at 13 cm depth, and at Haakon Mosby MV sites ATL19 and ATL22 2% and 4% (2×10^6 and 2×10^7 cells cm^{-3}) at 12.5 and 14.5 cm depth, respectively. In contrast, at hydrocarbon seeps all SEEP-SRB1 subgroups were below 0.5% of total single cells.

Cells of SEEP-SRB2 were found to be abundant at several seep sites (Fig. II.1, Table II.2). Numbers were high at all Tommeliten gas seep sites with 1.9 to 4.8×10^8 cells cm^{-3} . In hydrocarbon-rich sediments SEEP-SRB2 abundances were always high, in particular at Gulf of Mexico (sites 156 and 161; 0.7×10^8 cells cm^{-3}), Chapopote asphalt fields (10625-9; 2.0×10^8 cells cm^{-3}), and at Guaymas Basin station 4489-1 (1.8×10^8 cells cm^{-3}). This corresponded to 1-5% of total single cells. A vertical zonation of SEEP-SRB2 was not observed. Detected cells were short, thin rod-shaped or vibrio-like of 1 μm to 2 μm in length (Fig. II.2C).

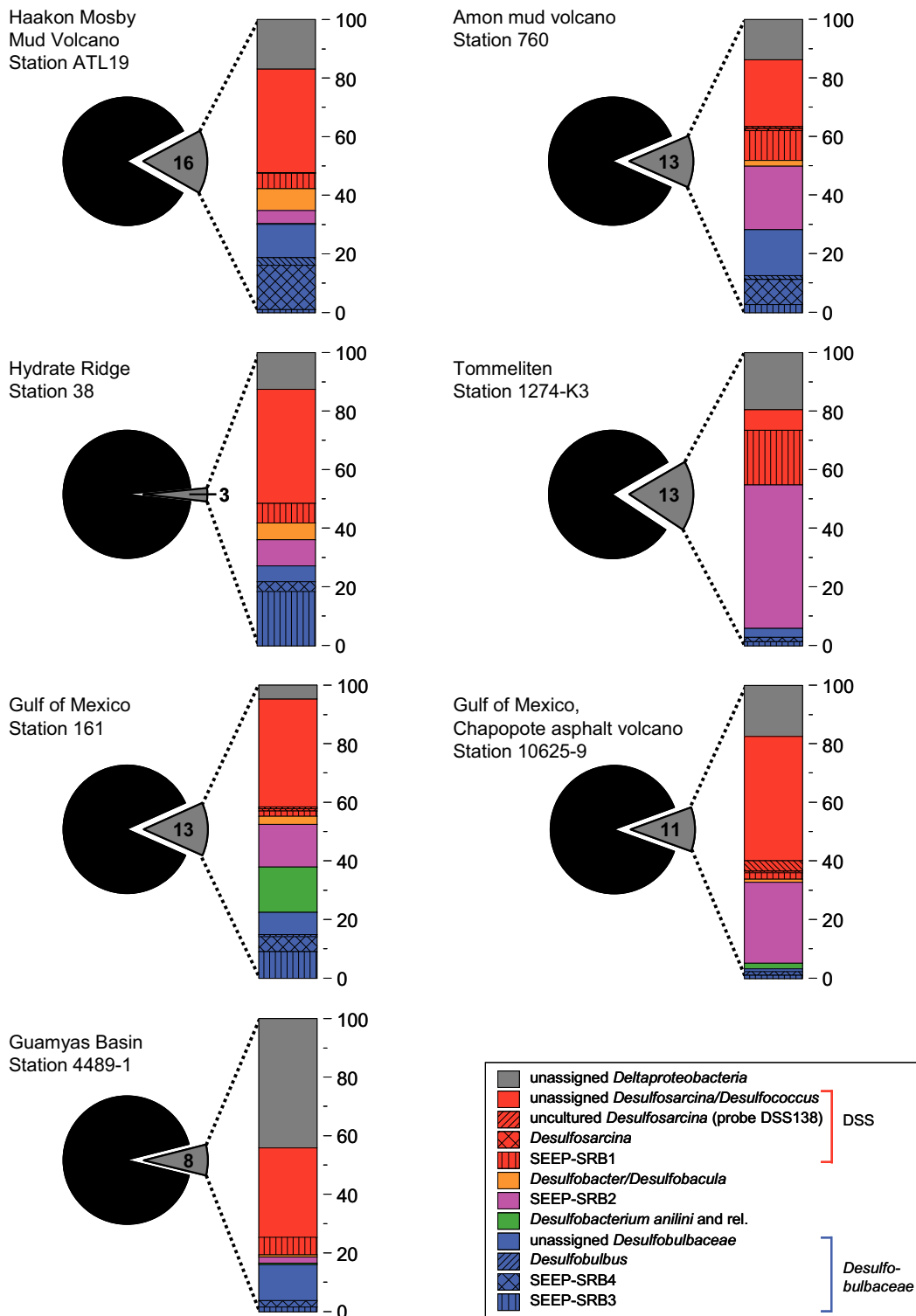


Fig. II.1: Relative fractions of different groups of ‘free-living’ single SRB in seep sediments. Fractions were calculated based on depth-integrated SRB single cell numbers for the individual groups in 0-10 cm sediment as determined by CARD-FISH. The pie chart represents the fraction of single *Deltaproteobacteria* compared to total cells. The bar chart shows the relative percentage of SRB subgroup fractions of single *Deltaproteobacteria*.

Desulfobulbaceae were identified to constitute a remarkable fraction of SRB in most seep sediments. All *Desulfobulbaceae* as detected by probe DSB706 were single cells except for bacteria in ANME-3/DBB consortia present in *Beggiatoa*-covered sediments from Haakon Mosby MV ATL19 (Lösekann et al., 2007). Single *Desulfobulbaceae* were, in contrast to DSS cells, rather present in hot spots than ubiquitous and were most abundant at the sediment surface. Hot spots at hydrocarbon seeps were surface layers at Gulf of Mexico GoM161, Guaymas Basin GB 4489-1, and in asphalts from Chapopote asphalt volcano sites 10625-16 and 10619-13, in which they accounted for 1.5×10^8 , 8.6×10^8 , and $1.1\text{-}1.9 \times 10^8 \text{ cm}^{-3}$, respectively (Table II.2). These numbers corresponded to 2%, 6%, and 5% of total cells (21%, 45%, and 35% of the deltaproteobacterial community). Subgroups SEEP-SRB3 and SEEP-SRB4, both frequently found in clone libraries from seep sediments, were detected at all hydrocarbon seep sites investigated but, in general, in low relative abundance of <1% of total cells (Fig. II.2D, E). Exceptions were the surface layer at Guaymas Basin in which SEEP-SRB3 accounted for 7% and SEEP-SRB4 for 9% of *Deltaproteobacteria*.

At gas seeps, *Desulfobulbaceae* were abundant at all sites investigated, in particular at mud volcanoes. At Haakon Mosby MV *Beggiatoa* site ATL19, *Desulfobulbaceae* made up 3% of total cells (73% of total Deltaproteobacteria, $3.0 \times 10^8 \text{ cells cm}^{-3}$) in surface sediments, more than a half were further assigned to SEEP-SRB4. In surface layers from Amon MV sites AMV760 and AMV825, *Desulfobulbaceae* were almost as abundant as in Haakon Mosby MV sediments with 6% of total cells (41% of *Deltaproteobacteria*, $2.7 \times 10^8 \text{ cells cm}^{-3}$) and 2% of total cells (6% of *Deltaproteobacteria*, $0.7 \times 10^8 \text{ cells cm}^{-3}$). Of these, 40% belonged to SEEP-SRB4 at Amon MV site 760 (2% of total cells).

SRB affiliated with *Desulfobacterium anilini* and relatives were detected in all hydrocarbon seep sediments but in none from gas seeps. Abundance was highest in surface layers of Gulf of Mexico site 161 with $1.1 \times 10^8 \text{ cells cm}^{-3}$ (2% of total cells, 15% of *Deltaproteobacteria*; Fig. II.2F).

Table II.2: Quantification of *Deltaproteobacteria* in gas and hydrocarbon seep sediments as determined by CARD-FISH.

Station	Depth [cm]	Sulfate reduction rates [▼] [nmol cm ⁻³ d ⁻¹]	Cell counts [▲]		<i>Deltaproteobacteria</i>			DSS			SEEP1a, c-f		<i>Desulfobacula / Desulfobacter</i> probe	<i>Desulfobacterium anilini</i> probe	SEEP2		SEEP3*	SEEP4*	<i>Desulfobulbaceae</i> probe	<i>Desulfobulbus</i> probe		
			total cells [10 ⁸ cm ⁻³]	single cells [10 ⁸ cm ⁻³]	single cells [10 ⁸ cm ⁻³]	total cells [10 ⁸ cm ⁻³]	assigned to specific groups % <i>Deltaprot.</i>	single cells [10 ⁸ cm ⁻³]	total cells [10 ⁸ cm ⁻³]	% <i>Deltaprot.</i>	single cells [10 ⁸ cm ⁻³]	total cells [10 ⁸ cm ⁻³]	single cells [10 ⁸ cm ⁻³]	total cells [10 ⁸ cm ⁻³]	single cells [10 ⁸ cm ⁻³]	total cells [10 ⁸ cm ⁻³]	single cells [10 ⁸ cm ⁻³]	total cells [10 ⁸ cm ⁻³]	single cells [10 ⁸ cm ⁻³]	total cells [10 ⁸ cm ⁻³]		
Northern Gulf of Mexico (GoM)	156	1	48.3	43.9	30.7	4.9	13.8	76	0.9	9.5	69	0.1	6.9	0.1	0.1	0.7	2.8	<0.08	0.1	0.3	0.1	
		3	95.1	35.0	20.9	2.3	11.6	92	1.6	9.8	85	0.2	6.2	0	0.1	0.6	3.9	<0.05	0.1	0.8	0	
		5	118.2	27.5	20.0	2.7	7.7	68	1.1	4.6	60	0.1	3.4	0.05	0	0.5	2.2	<0.05	0	0.1	0	
		7	16.9	28.4	14.3	1.1	11.2	94	0.4	10.3	92	0.04	5.4	0	0	0.2	5.0	0	0.04	0.04	0	
		9	0.9	13.1	9.8	1.0	2.2	36	0.5	1.0	27	0.02	0.6	0	0.02	0.1	1.2	<0.02	0.1	0	0	
		11	1.5	15.4	11.2	0.9	4.0	49	0.8	2.2	47	0	0	0	0	0.1	1.8	0	0	0	0	
	15	NA	19.0	13.9	1.6	5.1	64	0.9	2.7	53	0.03	1.8	0	0.03	0.5	2.3	0	0	0.03	0		
	161	1	558.8	64.3	64.3	7.4	7.4 [§]	62	1.1	1.1	15	0.2	0.2	0.5	1.1	1.1	2.3	<0.5	0.2	1.5	0.2	
		5	NA	25.5	25.5	3.2	4.2 [§]	100	2.5	2.5	78	0.1	0.1	0	0.1	0.2	0.2	0.3	0.1	0.2	0	
		7	1.2	2.9	2.9	0.4	0.4 [§]	101	0.1	0.1	27	0.01	0.01	0.01	0.1	0.1	0.1	0.1	0.04	0.2	0	
	13	675.8	57.1	57.1	4.2	4.2 [§]	77	1.3	1.3	31	0.1	0.1	0	0	1.5	1.5	0.4	0.01	0.4	0		
	Chapopote Asphalt Volcano (GoM-AV)	140	1	0.9	8.6	8.6	0.3	0.3	101	0.3	0.3	95	0	0	0	0.02	0	0	0	0	n.d.	0
			3	0.9	11.6	11.6	0.5	0.5	45	0.1	0.1	26	0.03	0.03	0	0.03	0.03	0.03	0	0.03	n.d.	0
5			0.2	10.6	10.6	0.2	0.2	30	0.03	0.03	15	0.03	0.03	0	0	0	0	<0.03	0	0.03	0	
7			0.1	9.9	9.9	0.2	0.2	75	0.1	0.1	62	0	0	0	0	0	0	0	0.02	0.02	0	
9			0.0	11.8	11.8	0.1	0.1	100	0.0	0.0	0.00	0	0	0	0	0	0	0	0	0.1	0	
11			0.0	8.6	8.6	0.2	0.2	126	0.2	0.2	115	0	0	0	0	0	0	0	0.02	0.1	0	
13		0.4	9.9	9.9	0.02	0.02	NA	NA	NA	NA	0	0	0	0	0	0	0	NA	NA	0		
15		0.0	11.1	11.1	0.4	0.4	14	0.03	0.03	7	0	0	0	0	0	0	0	0.03	0.1	0		
17		0.1	9.5	9.5	0.1	0.1	100	0	0	0	0	0	0	0	0	0	0	0	0.1	0.1	0	
19		0.1	10.0	10.0	0.1	0.1	33	0	0	0	0	0	0	0	0	0	0	0.03	0.1	0		
0		NA	NA	249.2	11.9	NA	NA	11.1	NA	NA	0.6	NA	<0.6	<0.6	0.6	0.6	<0.6	1.9	1.9	0		
10619-13 10619-6		1.25	38.4	NA	56.3	6.2	NA	NA	3.7	NA	NA	0.1	NA	0	0	0.1	0.1	<0.1	0.1	0.4	0	
		3.75	79.1	NA	24.1	1.2	NA	NA	1.0	NA	NA	0.1	NA	0	0	0.2	0.2	<0.1	0	n.d.	0	
		6.25	149.4	NA	21.6	0.7	NA	NA	0.2	NA	NA	0.1	NA	0	0	0.5	0.5	0	0	0.1	0	
		8.75	177.7	NA	29.8	0.7	NA	NA	0.4	NA	NA	0.1	NA	0	0	1.0	1.0	0	0	0.1	0	
		11.25	96.8	NA	22.0	0.8	NA	NA	0.1	NA	NA	0.1	NA	0	0	0.5	0.5	0	0	0.1	0	
		13.75	593.8	NA	34.9	1.2	NA	NA	0.5	NA	NA	0.1	NA	0	0	1.1	1.1	0	0	0.1	0	
		16.25	589.0	NA	19.7	0.8	NA	NA	0.05	NA	NA	0.05	NA	0	0	0.5	0.5	0	0	0.05	0	
		0	NA	NA	19.0	3.1	NA	NA	0.7	NA	NA	0.1	NA	0.05	0.05	0.3	0.3	<0.05	0.4	1.1	0.6	
		1.25	124.5	NA	40.7	4.6	NA	NA	2.1	NA	NA	0.1	NA	0.1	0.1	1.1	1.1	<0.1	0.1	0.3	0	
		3.75	404.4	NA	38.8	4.9	NA	NA	2.5	NA	NA	0.1	NA	0.1	0	2.0	2.0	0	0	0.1	0	
6.25	686.3	NA	21.6	2.2	NA	NA	1.1	NA	NA	0.1	NA	0	0.1	0.6	0.6	0	0	0.1	0			
8.75	264.5	NA	16.9	1.7	NA	NA	0.8	NA	NA	0.04	NA	0	0.04	0.3	0.3	<0.04	0.04	0.04	0			
11.25	16.6	NA	23.4	3.1	NA	NA	0.8	NA	NA	0.2	NA	0	0.1	1.1	1.1	0	0.1	0	0			
13.75	7.4	NA	24.5	4.2	NA	NA	2.0	NA	NA	0.1	NA	0	n.d.	1.2	1.2	0	0	0.1	0			
Hydrothermal vents at Guaymas Basin (GB)	4489-1	0.5	NA	175.9	175.9	19.2	19.2	45	2.9	2.9	15	0.4	0.4	<0.4	<0.4	1.8	1.8	<1.3	1.8	8.6	0	
		2.5	NA	20.1	20.1	3.2	3.2	38	1.0	1.0	31	0	0	0.1	0	0.1	0.1	<0.05	0.1	0.2	0	
	4.5	NA	2.1	2.1	0.1	0.1	19	0.03	0.03	19	0.01	0.01	0	0	0	0	0	0	0.02	0		
	6.5	NA	0.7	0.7	0.02	0.02	100	0.02	0.02	100	0	0	0	0	0	0	0	0	0	0		
	8.5	NA	2.2	2.2	0.03	0.03	0	0	0	0	0	0	0	0	0	0	0	0	0.01	0		
	10.5	NA	2.3	2.3	0.02	0.02	33	0	0	0	0	0	0.01	0	0	0	0	0	0.01	0		
	12.5	NA	0.9	0.9	0	0	NA	0	0	NA	0	0	0	0	0	0	0	0	0.002	0		
	14.5	NA	0.7	0.7	0	0	NA	0	0	NA	0	0	0.002	0	0	0	0	0	0	0		
	16.5	NA	1.5	1.5	0	0	NA	0	0	NA	0	0	0	0	0	0	0	0	0	0		
	18.5	NA	1.2	1.2	0.01	0.01	33	0	0	0	0	0	0	0	0.003	0	0	0	0	0		
	20.5	NA	0.3	0.3	0.002	0.002	0	0	0	0	0	0	0	0	0	0	0	0	0	0		
	22.5	NA	0.2	0.2	0	0	NA	0	0	NA	0	0	0	0	0	0	0	0	0	0		
	24.5	NA	0.3	0.3	0	0	NA	0	0	NA	0	0	0	0	0	0	0	0	0.002	0		

Table continued on next page

Sulfate-reducing bacteria at marine hydrocarbon seeps

SEEP-SRB2 in methanotrophic microbial mats

SEEP-SRB2 cells were not only found as single cells but also aggregated or in ‘mat-type’ consortia as described before for ANME-1/DSS associations (Knittel et al., 2005). Methanotrophic mats from the Black Sea seemed to be a special habitat for SEEP-SRB2 cells in which they accounted for 7% of total cells (7.7×10^8 cells g^{-1}) in the interior and oldest part of p822 mats and for 12% (1.4×10^9 cells g^{-1}) in the exterior part. Both parts of the reef are dominated by ANME-1 archaea (20-26% of total cells) while ANME-2 cells were rare ($\ll 1\%$; Arnds, pers. communication). In contrast, SEEP-SRB2 constituted only a small fraction of total cells ($<1\%$) at the top of the reef, which is the youngest part and dominated by ANME-2 archaea (15-24% of total cells) and SRB of the DSS group. Spatial distribution of SEEP-SRB2 and possible physical interactions with ANME archaea were studied on thin sections of mat 268 since no intact mats were available from p822. Mat 268 was quite heterogeneous with parts dominated by ANME-1 and others by ANME-2. We observed diverse types of SEEP-SRB2 physical interactions with ANME-1 and ANME-2 in these mats: i) clusters of SEEP-SRB2 surrounded by ANME-1 (Fig. II.2G), ii) single SEEP-SRB2 homogeneously mixed with ANME-1 (Fig. II.2H), iii) single SEEP-SRB2 without close ANME-1 or ANME-2 cells (Fig. II.2I), iv) single SEEP-SRB2 at the flank of ‘pure’ ANME-2/DSS regions (Fig. II.2J), and v) SEEP-SRB2 surrounding ANME-2/DSS consortia (Fig. II.2K).

ANME-2/SEEP-SRB2 consortia in gas and hydrocarbon seep sediments

In some sediments investigated, SEEP-SRB2 cells occurred aggregated with ANME-2 in ‘shell-type’ consortia (Fig. II.2B). These novel consortia were particularly abundant in sediments from the Gulf of Mexico site 156, but were also detected in all Tommeliten and both Chapopote asphalt volcano sediments, sites 10619-6 and 10625-9. The archaea within the ANME-2/SEEP-SRB2 consortia could be further assigned to subgroup ANME-2c. In addition, SEEP-SRB2 cells were rarely observed in ‘mixed-type’ consortia.

The vertical distribution of ANME-2/DSS versus ANME-2/SEEP-SRB2 consortia was studied in detail in Gulf of Mexico sediments from site 156 (Fig. II.3). In $\sim 90\%$ of the consortia the bacterial partner of ANME-2 could be assigned to either DSS or SEEP-SRB2; in $\sim 10\%$ of the consortia the bacterial partners were unknown.

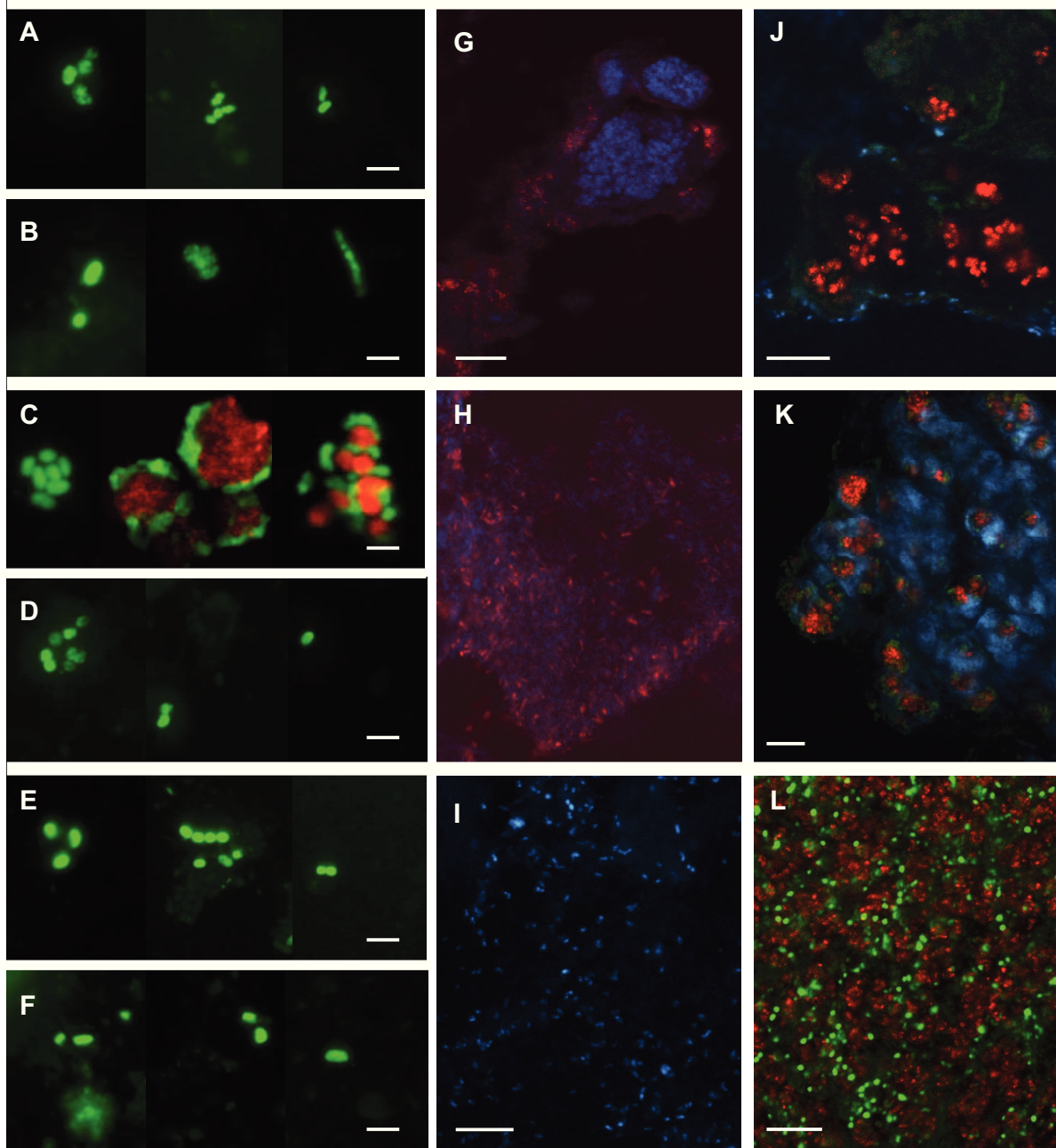


Fig. II.2: Single cells of sulfate-reducing bacteria and cell aggregates of ANME-1 and ANME-2 archaea with SEEP-SRB2 in diverse hydrocarbon seep sediments and thin sections of Black Sea microbial mats, visualized by CARD-FISH. Panels A to F are regular epifluorescence micrographs, panels G to L are confocal laser scanning micrographs. Scale bars = 2 μm (panel A to F) and 10 μm (panels G to L). (A) Single DSS cells (probe DSS658). (B) SEEP-SRB1a (probes SEEP1a-473, SEEP1a-1441), SEEP-SRB1d (probe SEEP1d-1420), and SEEP-SRB1f cells (from left to right, probe SEEP1f-153). (C) Single SEEP-SRB-2 cells (probe SEEP2-658) and ANME-2/SEEP-SRB2 aggregates (probe SEEP2-658 (green), probe ANME2-538 (red)). (D) SEEP-SRB3 cells (probe SEEP3-652). (E) SEEP-SRB4 cells (probe SEEP4-583). (F) *Desulfobacterium anilini* related cells (probe DBA818). (G to L) SEEP-SRB2 distribution and associations with ANME archaea in Black Sea microbial mats from station 268: (G) ANME-1 (red) surrounding a cluster of sarcina-like SEEP-SRB2 (blue). (H) Homogeneous mixture of SEEP-SRB2 (blue) and ANME-1 archaea (red). (I) Single vibrio-shaped SEEP-SRB2 without any associations with ANME archaea. (J) SEEP-SRB2 cells flanking an ANME-2 (red)/DSS (green) dominated mat region. (K) SEEP-SRB2 (blue) surrounding shell-type ANME-2/DSS consortia (ANME-2: red; DSS: green). (L) Typical region within mats dominated by ANME-2 (red) and DSS (green).

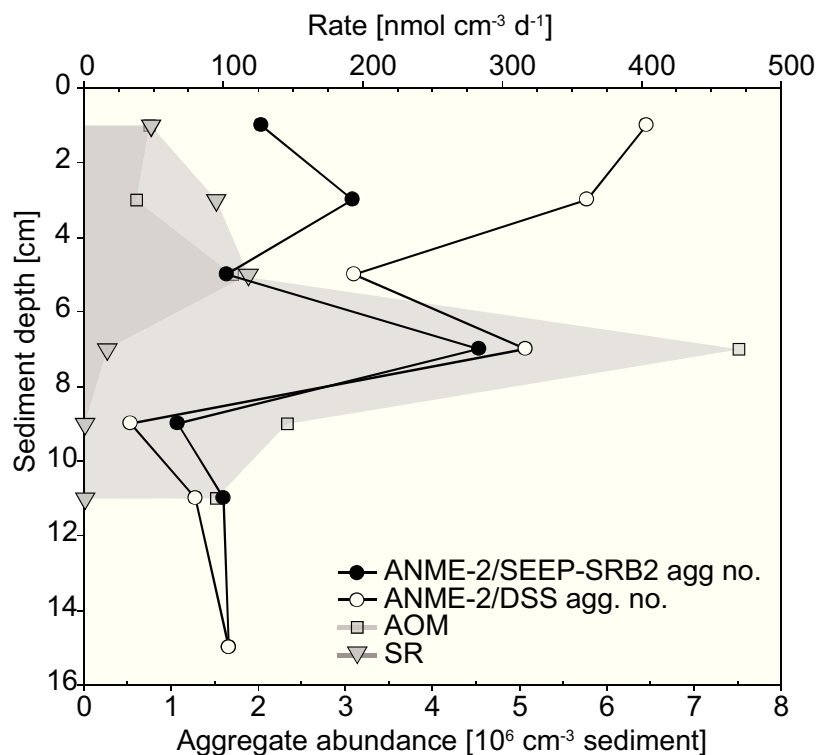


Fig. II.3: Vertical distribution of ANME-2/SEEP-SRB2 (●) and ANME-2/DSS (○) consortia in Gulf of Mexico sediments (station 156; 0-15 cm). Depth profiles of SR rates and AOM rates (taken from Orcutt et al., 2010) are indicated by grey-colored areas.

The ratios of ANME-2/DSS and ANME-2/SEEP-SRB2 changed with depth: DSS was the main partner of ANME-2 at 0-5 cm depth (62% ANME-2/DSS vs. 28% ANME-2/SEEP-SRB-2); at 7 cm depth, which is the layer with the highest AOM rates, and below ratios were equal or slightly shifted towards a dominance of ANME-2/SEEP-SRB-2 consortia. Average consortia sizes differed only slightly with depth (3.4 μm at 1-3 cm depth to 4.8 μm at 15 cm depth).

Global and spatial patterns of SRB abundance and distribution

Simple and partial Redundancy Analysis (RDA) models showed that SRB abundance and distribution were significantly affected by the specific effects of habitat type (p-value = 0.024; habitat types correspond to samples with short-chain alkanes, hydrocarbons, asphalt, hydrate, bacterial mats, clams, tube worms, carbonate outcrops) and sediment depth (p-value = 0.034), when geographic distances and water depth were taken into account as co-variables (Table II.3). Correlations of SRB abundance with sediment depth was tested for specific habitat types and could be shown to be significant for sediments with hydrocarbons, bacterial mats and clams (supplementary Fig. II.S1). At hydrocarbon-rich sediments, the abundance of

Deltaproteobacteria, unassigned *Deltaproteobacteria*, unassigned DSS and SEEP-SRB4 significantly decreased with depth. At sediments under bacterial mats the abundance of *Deltaproteobacteria*, unassigned *Deltaproteobacteria*, *Desulfobulbaceae*, SEEP-SRB4 and *Desulfobacter*, *Desulfobacula/Desulfobacter* species linearly decreased with sediment depth, while at clam sites only *Deltaproteobacteria* showed this trend.

Table II.3: Specific influence of environmental and spatial factors on variations in SRB abundance and distribution.

Factors ^a	Degrees of Freedom	F-ratio	P value
HT + SP + SD + WD	11	2.22	< 2.22e-16
HT controlling for SP + SD + WD	7	1.65	0.020
SPA controlling for HT + SD + WD	2	1.60	0.130
SD controlling for HT + SP + WD	1	2.50	0.034
WD controlling for HT + SP + SD	1	2.19	0.063

^aThe respective effects of Habitat type (HT), space (SP), sediment depth (SD) and water depth (WD) on the abundance and distribution of SRB (Hellinger-transformed CARD-FISH data) were determined by simple and partial RDA models. Significance of the models was tested with 1000 permutations.

Correspondence analysis of SRB groups and sediment samples was used to unravel associations of SRB groups with certain samples (Fig. II.4). Although samples from different geographic origins were generally associated with similar patterns of SRB group abundance (i.e. sample groupings overlapped between geographic regions), some specific associations could be identified. For instance, *Desulfobacterium anilini* and related species showed a very specific association with samples from the oily Gulf of Mexico station 161 (Fig. II.4). Furthermore, SEEP-SRB3 and *Desulfobacula/Desulfobacter* showed highest abundances in subsurface samples from various sites (Haakon Mosby MV, Guaymas Basin, Gulf of Mexico, Hydrate Ridge). SEEP-SRB4 was mostly associated with mud volcanoes and Hydrate Ridge. For other SRB groups no significant preference to habitat or depth was detected.

Different hypotheses for spatial and vertical distribution as well as abundance (% of single cells) of specific SRB groups were tested based on our CARD-FISH data, and overall the following conclusions were reached: i) SEEP-SRB1 showed higher abundances at gas seeps (n = 40, average abundance = 1.2) than at hydrocarbon seeps (n = 45, average abundance = 0.13) as determined by significant Welch Two Sample t-test (t = 4.6748, df = 42.949, p-value = 2.921×10^{-5}); ii) SEEP-SRB1 abundance was higher at Tommeliten, Haakon Mosby MV and Amon MV (n = 31, average abundance = 1.55, sd = 1.48) than at other seeps (n = 54, average abundance = 0.13; sd = 0.34; Student's t-test t = -6.7709,

$p < 0.0001$ based on 10,000 permutations), iii) SEEP-SRB2 abundance was not significantly higher at gas seeps ($n = 40$, average abundance = 1.28) than at hydrocarbon seeps ($n = 45$, average abundance = 1.44; $t = -0.3532$, $df = 62.92$, p -value = 0.7251), iv) relative SEEP-SRB2 cell numbers were higher at Tommeliten, Amon MV, Gulf of Mexico and Chapopote AV ($n = 45$, average abundance = 2.33, $sd = 2.51$) than at other seeps investigated ($n = 40$, average abundance = 0.28; $sd = 0.64$; Student's t -test $t = -5.033$, $p < 0.0001$ based on 10,000 permutations), and v) members of the DSS group were more abundant at gas seeps ($n = 40$, average abundance = 5.6) than at hydrocarbon seeps ($n = 45$, average abundance = 3.49; Welch Two Sample t -test, $t = 2.9654$, $df = 74.177$, p -value = 0.0041).

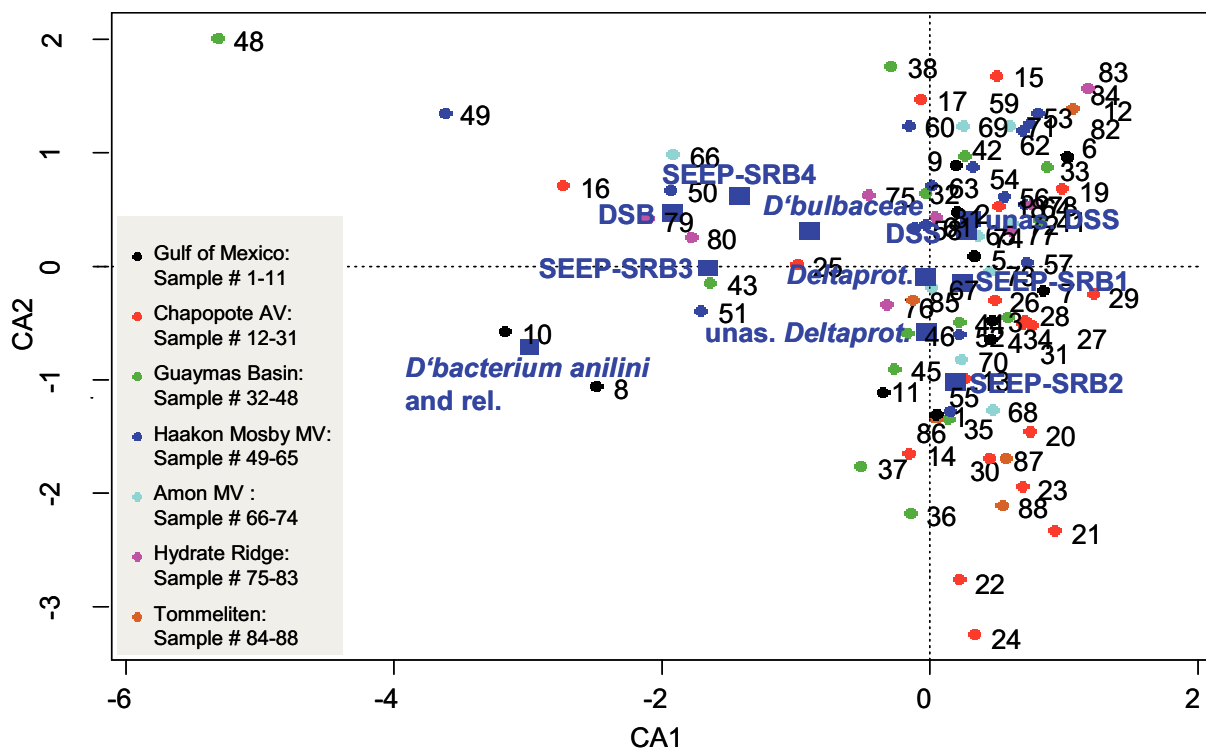


Fig. II.4: Correspondence analysis joint plot of SRB groups and samples explaining 47.7% of the data variation on two axes. Samples (colored circles) that are close to a probe name (blue squares) have more chance to have high relative abundance values with that probe. Probes targeted *Deltaproteobacteria* (*Deltaprot.*), the DSS clade, *Desulfobulbaceae* (*D'bulbaceae*), *Desulfobacterium* (*D'bacterium*) *anilini* and related spp., *Desulfobacter*, *Desulfobacula/ Desulfobacter* (DSB), SEEP-SRB1, SEEP-SRB2, SEEP-SRB3 and SEEP-SRB4. Also, unassigned fractions of *Deltaproteobacteria* and DSS, which were not further assigned to subgroups, are illustrated.

16S rRNA and aprA cDNA clone libraries

Only a minor fraction of detected DSS could be identified by subgroup probes. For example, less than 10% of DSS could be assigned to subgroups in GoM161 sediments. Thus, we used this sediment to construct cDNA-based clone libraries for 16S rRNA and adenosine-5'-phosphosulfate reductase subunit A (*aprA*), a functional gene of SRB which catalyzed the

Using the specific primer set for DSS, most of the 134 sequences belonged to DSS (70 sequences), others were affiliated with close relatives such as *Desulfobacterium anilini* and other *Desulfobacteraceae* (27 sequences), SEEP-SRB2 (16 sequences) and *Syntrophobacteraceae* (11 sequences). The major fraction of DSS was affiliated with SEEP-SRB1 subgroups a-f, in particular with SEEP-SRB1c (1 mm to DSS658; 15 sequences) and SEEP-SRB1f (27 sequences). Other DSS sequences were found to be closely related to the propane- and butane-degrading organisms BuS5 and Butane-GMe12 (16 sequences). Amplification of SEEP-SRB2 with primer DSS658 (identical with the probe) was not surprising since we showed cross-hybridization of DSS and SEEP-SRB2 in CARD-FISH.

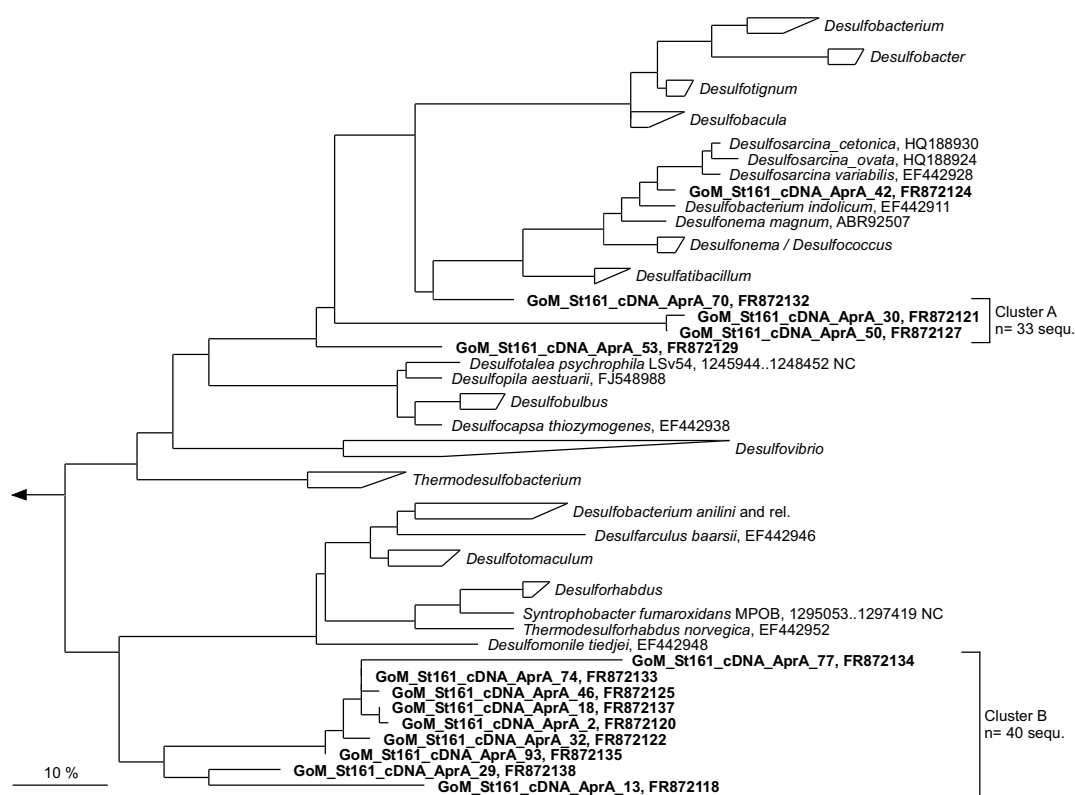


Fig. II.6: Phylogenetic tree showing the affiliation of Gulf of Mexico (site 161) cDNA sequences coding for the alpha subunit of adenosine-5'-phosphosulfate reductase subunit A (*aprA*) to selected reference sequences. The tree was generated from deduced amino acid sequences (>104 amino acids) by Maximum Likelihood analysis (PhyML) with a 30% amino acid frequency filter. Clone sequences from site 161 sediments are in boldface type. The bar represents 10% estimated sequence divergence.

In total, 86 sequences were retrieved from the *aprA* cDNA library. Most of the sequences clustered into two distinct clusters: 38% (33 sequences) belonged to cluster A and 47% (40 sequences) to cluster B (Fig. II.6). No close relative could be found in the public databases; both clusters comprise exclusively only sequences from our library. Cluster A is distantly related to *aprA* sequences from *Desulfobacteraceae*. It is represented by 5 OTUs

(based on 97% identity level) and has a 92% intragroup identity. Cluster B is deep-branching and related to a cluster with *aprA* from *Desulfotomaculum*, *Desulfobacterium anilini* and *Desulfomonile*. It is represented by 11 OTUs and has 71% intragroup identity. The high frequency of cluster B *aprA* sequences co-occurred with a high frequency of 16S rRNA sequences from SEEP-SRB2, a deep-branching cluster based on their 16S rRNA phylogeny. Thus, one can speculate that cluster B might be derived from SEEP-SRB2.

Discussion

Environmental factors structuring the SRB community at marine seeps

Habitat type and sediment depth were most crucial for structuring the SRB community, while geographic distance and water depth most likely did not have a significant impact: Identical or highly similar SRB groups dominated seep sediments with similar environmental conditions, independent of the geographical location.

Cell numbers for *Deltaproteobacteria* were used as an estimate for total SRB. Our results (excluding data from Hydrate Ridge) clearly showed that total SRB cell numbers depth-integrated over the first 10 cm of the sediments did not vary significantly between gas seeps ($1.5\text{--}9.5 \times 10^{13}$ cells m^{-2}) and hydrocarbon seeps ($1.8\text{--}8.8 \times 10^{13}$ cells m^{-2}). Interestingly, there was no correlation of total SRB with SR rates (Table II.1) indicating the presence of differently active SRB communities. Two orders of magnitude higher SRB numbers were detected at Hydrate Ridge with 122×10^{13} and 154×10^{13} cells m^{-2} for station 19-2 and 38, respectively, although SR rates were in the same range as measured at Amon MV (Knittel et al., 2003; Felden, 2009).

Dominance of DSS

In this study we showed DSS to be globally distributed and dominant at all seep sites investigated independent of hydrocarbon content, temperature and depth. The overall dominance of the DSS species is obvious and supported by findings from previous studies (Orphan et al., 2001; Knittel et al., 2003; Boetius & Suess, 2004; Wegener et al., 2008). Furthermore, DSS has been reported to be dominant in marine non-seep coastal sediments as well (e.g. Ravensschlag et al., 2000; Mußmann et al., 2005; Musat et al., 2006). This broad distribution is reflected in a large DSS intragroup diversity with 16S rRNA gene similarity values as low as 80%. Although isolates were taxonomically classified as *Desulfobacteraceae* this is far below the proposed cut-off of $87.7\% \pm 2.5$ minimum level for family boundaries

and the DSS clade should rather be regarded a novel order proposed by Yarza and colleagues (2010). It is likely that this evolutionary diversity is also reflected in a high degree of metabolic diversity which is most probably caused by a long-term supply of hydrocarbon substrates to the natural communities. Cultivated DSS species are capable of degradation of a wide range of hydrocarbon such as (C₃-C₂₀) *n*-alkanes, (C₇-C₂₃) *n*-alkenes or even aromatic hydrocarbons, e.g. benzene and toluene (for review see Widdel et al., 2010). The high abundance suggests DSS as key players at marine gas and hydrocarbon seeps involved in methane as well as non-methane hydrocarbon degradation. We assume the presence of diverse and numerous ecological niches and high substrate specialization of the species for two reasons: At first, abundance of individual subgroups was relatively low compared to the high total abundance of DSS and at second, cDNA-based clone libraries showed a high diversity within the DSS group.

SEEP-SRB1 was found to be widely distributed at seeps investigated but occurred in highly different percentages and cell numbers. Intragroup diversity of SEEP-SRB1 is as low as 83%. This evolutionary distance is reflected in a rather wide habitat range. Our results confirmed previous findings from Schreiber and colleagues (2010) who assigned the sulfate-reducing bacterial partners in ANME-2/DSS consortia to SEEP-SRB1a. In accordance, we detected SEEP-SRB1a as ANME-2 partner at Hydrate Ridge, Gulf of Mexico, and Amon MV and as ANME-3 partner at the *Beggiatoa* site of Haakon Mosby MV ATL19 where they occurred in mini-consortia of single bacterial cells attached to a single archaeon, most likely ANME-3. Single SEEP-SRB1a cells were present but quite rare at all sites suggesting a restriction of SEEP-SRB1a to syntrophic life with ANME archaea.

Subgroups SEEP-SRB1c, SEEP-SRB1e and SEEP-SRB1f are more likely involved in non-methane hydrocarbon degradation suggested by an in situ dominance at the gas seeps Amon MV, Haakon Mosby MV and Tommeliten or by frequent retrieval of corresponding 16S rRNA sequences from our cDNA clone library from Gulf of Mexico site 161.

Role of uncultured groups SEEP-SRB2, SEEP-SRB3, and SEEP-SRB4 in AOM and non-methane hydrocarbon oxidation

Sequences of SEEP-SRB2, a deep-branching deltaproteobacterial group, were repeatedly retrieved from diverse marine seep sediments (Niemann et al., 2005; Wegener et al., 2008; Joye et al., 2009; Orcutt et al., 2010). Here, we report a strong in situ dominance of SEEP-SRB2 in all seep habitats investigated. Thus, we hypothesize that carbon sources for SEEP-SRB2 might include short-chain alkanes as well as higher hydrocarbons or aromatic

compounds. SEEP-SRB2 cells were particularly abundant in sediments from Tommeliten gas seeps in which they accounted for up to 17% of total cells which refers to more than three-quarters of detected *Deltaproteobacteria*. The Tommeliten site is the only shallow water seep investigated in this study and differed from the other seeps, for example, by a reduced availability of dissolved methane due to a decreased solubility of methane at low hydrostatic pressure or a high bottom water current causing relocations of particles and sporadic influx of oxygen into the sediments (Wegener et al., 2008).

SEEP-SRB2 species were not only detected as single cells, but also associated with ANME archaea: Together with ANME-2 archaea they form ANME-2/SEEP-SRB2 consortia at Gulf of Mexico, Tommeliten and Chapopote asphalt volcano. In Gulf of Mexico sediments, station 156, we found ANME-2/SEEP-SRB2 consortia in a 1:1 ratio mixed with ANME-2/DSS consortia in the layer with highest AOM rates (Orcutt et al., 2010). These findings expand the spectrum of ‘available’ SRB partners for ANME-2 to four groups, i.e. SEEP-SRB1a of the DSS (Boetius et al., 2000; Schreiber et al., 2010), two groups of *Desulfobulbus*-related organisms (Lösekan et al., 2007; Pernthaler et al., 2008) and SEEP-SRB2.

Furthermore, SEEP-SRB2 has also been detected in different association types with ANME-1 archaea in Black Sea microbial mats. We found SEEP-SRB2 relative abundance positively correlated with ANME-1, but negatively correlated with ANME-2 abundance within different parts of two Black Sea microbial mats. Associations between ANME-1 archaea and SEEP-SRB2 could be described as ‘mat-type’ consortia as reported before for ANME-1/DSS associations from other Black Sea mats (Knittel et al., 2005). Thus, these groups most likely do not only co-exist but mediate AOM in a syntrophic partnership.

Groups SEEP-SRB3, closely related to the genus *Desulfobulbus*, and SEEP-SRB4, distantly related to *Desulforhopalus*, have been found in low abundance at all gas seeps investigated but only sporadically at hydrocarbon seeps. Both groups were predominantly detected in surface sediment layers covered by bacterial mats (Amon MV site 760, Haakon Mosby MV site ATL19) or clams (Hydrate Ridge site 38). Chemotrophic bacterial mats and faunal communities are characteristic for hot spots of SR rates, hydrogen sulfide concentration, AOM, and methane and fluid fluxes (Otte et al., 1999; Boetius et al., 2000; Weber & Jørgensen, 2002; Joye et al., 2004). SEEP-SRB4 was highly abundant with 4% and 3% of single cells in surface sediments at the two mud volcanoes investigated, Haakon Mosby MV and Amon MV, respectively. These findings are in agreement with frequent retrieval of SEEP-SRB4 16S rRNA gene sequences from these mud volcanoes (Lösekan et al., 2007;

Omeregje et al., 2009). As mud volcanoes are characterized by a high alkane gas-flow (Niemann et al., 2005; Mastalerz et al., 2009), SEEP-SRB4 is likely involved in short-chain alkane degradation either directly by oxidation of non-methane alkanes or indirectly by thriving on AOM intermediates or biomass produced therein. Their restriction to surface sediments was most likely because of the limited sulfate penetration into the sediments due to high fluid fluxes at mud volcanoes (de Beer et al., 2006).

For SEEP-SRB3 distribution a positively correlation with *Desulfobacterium anilini* relatives (correlation coefficient 0.64) was found suggesting a possible similar substrate spectrum, i.e. mainly aromatic compounds.

Environmental relevance of cultured hydrocarbon-degrading SRB

Many cultivated SRB known to degrade alkanes, alkenes and aromatics are distributed within the DSS group (for reference see Widdel et al., 2010). Use of highly specific probes for butane-degrading organisms Butane12-GMe and BuS5 (Kniemeyer et al., 2007), resulted in the detection of very few target cells (<<0.5% of total single cells at Gulf of Mexico, Guaymas Basin and Hydrate Ridge) or detection even failed. Nevertheless, based on the high diversity of DSS 16S rRNA gene sequences from the literature (Teske et al., 2002; Knittel et al., 2003; Lösekann et al., 2007; Wegener et al., 2008; Orcutt et al., 2010) as well as on 16S rRNA sequences from our cDNA library, we expect that BuS5, Butane-GMe12 and relatives are important for short-chain alkane degradation at marine seeps. SRB affiliated with *Desulfobacterium anilini* have been shown to be capable of naphthalene, 2-methylnaphthalene, toluene, and (ethyl)benzene degradation (Galushko et al., 1999; Harms et al., 1999; Kniemeyer et al., 2003; Musat et al., 2009). In agreement with their carbon sources, we could identify this group only at hydrocarbon seeps (GoM, Chapopote, Guaymas Basin), but not at gas seeps. Other cultivated benzene- and toluene-degrading SRB of the genera *Desulfobacula* and *Desulfotignum* (Rabus et al., 1993; Ommedal & Torsvik, 2007) or of *Firmicutes* (Liu et al., 2004; Morasch et al., 2004; Kniemeyer et al., 2007) were found to be rather of local than of global environmental relevance since we detected them at only one site. However, with respect to *Firmicutes*, spores might have been present as shown before for Arctic marine sediments (Hubert et al., 2009).

Conclusion

Deltaproteobacteria have been quantified as a proxy for SRB living in marine sediments, which could be capable of hydrocarbon degradation. The vast majority of the

Deltaproteobacteria could be assigned to a specific SRB group, i.e. $83\% \pm 14$ at gas seeps and $61\% \pm 35$ at hydrocarbon seeps, thus indicating most key players were detected. However, a finer resolution of the most dominant DSS group turned out to be rather difficult by in situ quantification since the intragroup 16S rRNA diversity as well as metabolic diversity of cultured representatives is extremely high. Our data indicate rather the presence of many highly specialized hydrocarbon-degrading SRB than an abundant single subgroup. The wide distribution and high numbers of uncultivated SEEP-SRB1 to SEEP-SRB4 cells suggests a much larger hydrocarbon-degrading SRB community as expected based on cultivation attempts. Also the AOM mediating community might be more diverse than currently known as we detected SEEP-SRB2 in novel association with methanotrophic archaea. Stable isotope probing experiments with different types of sediments and different hydrocarbons as energy source should be the next step and will allow proving our hypotheses suggested in this paper.

Experimental procedures

Sampling and site description

Eight hydrocarbon seep habitats were chosen for quantification of SRB on the basis of available biogeochemical and microbial diversity data. Five of these habitats (Haakon Mosby mud volcano, Amon mud volcano, Hydrate Ridge, Black Sea, Tommeliten) are characterized by gaseous hydrocarbons and are referred to as gas seeps; the three other habitats (Gulf of Mexico, Guaymas Basin, Chapopote asphalt volcano) are characterized by a seepage of complex hydrocarbon composition and are referred to as hydrocarbon seeps. Detailed site description is given in Table II.1.

Catalyzed reporter deposition fluorescence in situ hybridization (CARD-FISH)

Sediment samples have been fixed in 3% paraformaldehyde or formaldehyde, washed with $1\times$ PBS and stored in ethanol-PBS (1:1) at -20°C . In situ hybridizations with horseradish peroxidase (HRP)-labeled probes followed by fluorescently-labeled-tyramide signal amplification (catalyzed reporter deposition) were carried out as described previously (Pernthaler et al., 2002). Lysozyme treatment (10 mg ml^{-1}) was turned out to be the best permeabilization for bacterial groups of interest (30-60 min, 37°C). Hybridized samples were analyzed with an epifluorescence microscope (Axioplan 2; Carl Zeiss, Jena, Germany). For each probe and sample, 1000 DAPI-stained single cells and their corresponding FISH signals or alternatively, if very low cell numbers were present, at least 100 independent microscopic

fields were counted. Relative abundances close to the detection limit are given as <0.5% and <1%, respectively. *Desulfosarcina/Desulfococcus* (DSS658) subgroup probes (DSS138 and DSS449) were used for samples with >5% *Desulfosarcina/Desulfococcus* species. To differentiate between DSS658 and SEEP2-658-target organisms dual CARD-FISH hybridization was applied using two different tyramides (Alexa488, Alexa594) as described before (Kubo et al., 2011). Probes (ordered from biomers.net; Ulm, Germany), formamide concentrations and probe coverage are given in Table II.S1.

Total cell counts

Total counts of individual cells were done by epifluorescence microscopy after staining with acridine orange (AODC) according to the method of Meyer-Reil (1983). For each sample, two replicate filters and at least 30 grids per filter were randomly counted. Total cell counts were defined as the sum of single cells and estimated numbers of aggregated cells present in AOM consortia. Aggregates cells were calculated according to Lösekann et al. (2007) using average cell diameter of DSS cells of 0.65 μm , SEEP-SRB2 cells of 0.65 μm , ANME-2a of 0.55 μm , ANME-2c of 0.6 μm and ANME-3 of 0.7 μm .

Construction of cDNA-based clone libraries and phylogenetic analysis

Total RNA was directly extracted from 2 g of frozen sediment (stored at -80°C) following previously described methods (Chomczynski & Sacchi, 2006). Residual DNA was degraded with DNase I (Invitrogen). Total RNA was purified with the RNeasy Protect Mini Kit (Qiagen). cDNA synthesis was performed with the M-MLV Reverse Transcriptase, RNase H Minus, Point Mutant (Promega, Madison, WI, USA) according to manufacturer's recommendation. A general bacterial 16S rRNA gene library was constructed following polymerase chain reaction (PCR) using the primer set GM1F/GM2R (58°C annealing temperature, 30 cycles) (Muyzer et al., 1993). Two libraries were constructed using GM3F/DSS658 (Muyzer et al., 1995; Manz et al., 1998) and DSS658/GM4R (Muyzer et al., 1995; Manz et al., 1998). Another library was set up for the functional *apr* gene using 31 cycles and the primer set APRA1FW/ APRA5RV (annealing temperature 58°C decreased 0.5°C per cycle for 18 cycles then annealing temperature 48°C for 13 cycles; (Meyer & Kuever, 2007). Clone libraries were constructed in pGEM-T-Easy (Promega, Madison, WI, USA) and transformed into *E. coli* TOP10 cells according to the manufacturer's recommendations. Sequencing was performed by Taq cycle sequencing with a model ABI377 sequencer (Applied Biosystems). Sequence data were analyzed with the ARB software

package (Ludwig et al., 2004) using databases from ARB SILVA resources (Pruesse et al., 2007). Phylogenetic trees of 16S rRNA gene sequences were calculated by neighbor-joining and maximum-likelihood analysis with different sets of filters. For tree calculation, only nearly full-length sequences (>1300 bp) were considered. Partial sequences were inserted into the reconstructed tree by parsimony criteria without allowing changes in the overall tree topology. The *aprA* tree was calculated from amino acid sequences by Maximum Likelihood analysis (PhyML) using a 30% amino acid frequency filter.

Nucleotide sequence accession numbers

Sequence data reported here are available in the EMBL, GenBank and DDBJ nucleotide sequence databases under the accession numbers FR871945 - FR872100 (16S rRNA) and FR872101 - FR872138 (*aprA*).

Statistical analyses

Correspondence analysis was used to identify and visualize the putative associations between samples and SRB abundance profiles. The technique is particularly suited when the data table contains many zeros and when less weight needs to be given for the problematic cases of double absence (double-zeros) when assessing sample similarity (reviewed in Ramette, 2007). When determining the effects of factors structuring SRB abundance and distribution, CARD-FISH data were Hellinger-transformed prior to applying linear multivariate statistical procedures such as Redundancy Analyses, as recommended (Legendre & Gallagher, 2001) and the qualitative factor “Habitat type” was recoded into a set of dummy variables. To evaluate the respective effects of different factors, the total variance, also called inertia, of the count table was partitioned into the specific contribution of each factor while taking the other factor into consideration, using the variation partitioning method (Borcard et al., 1992). The overall and partial redundancy analysis (RDA) models were then tested for significance based on 1000 permutations of the multivariate models. All statistical procedures were implemented with the R statistical platform using the package *vegan* for multivariate analyses, *gmt* for spatial conversion of geographic coordinates to metric distances, and *stats* for simple linear modeling, and mean comparisons (Student’s t and Welch tests).

Acknowledgements

We greatly acknowledge Antje Boetius for fruitful discussions and for providing samples from expeditions with the research vessels SONNE, POLARSTERN, L'ATALANTE, METEOR, and ALKOR; Tina Treude for samples from POSEIDON, and Andreas Teske as well as Marc Mußmann for samples from ATLANTIS. Samples were taken in the framework of the GEOTECHNOLOGIEN programs MUMM I and II (grants 03G0554A and 03G0608A) funded by the German Ministry of Education and Research (BMBF) and the German Research foundation as well as by the EU 6th FP HERMES. Sampling in Guaymas Basin was supported by NSF-OCE (grant 0647633). We also thank Gunter Wegener for sharing unpublished data. Special thanks go to Wiebke Rentzsch, Nicole Rödiger, Stephanie Bodden, Anita Ritz and Anne-Mareike Jarzak for assistance regarding hybridizations, probe evaluations and AODC total cell counts. This study is part of the DFG Priority Program SPP1319 "Transformation of hydrocarbons under anoxic conditions: from molecular to global scale" within the Deutsche Forschungsgemeinschaft. Further support was provided by the Max Planck Society, Germany.

References

- Aeckersberg F, Bak F, and Widdel F. (1991). Anaerobic oxidation of saturated-hydrocarbons to CO₂ by a new type of sulfate-reducing bacterium. *Arch Microbiol* **156**: 5-14.
- Aeckersberg F, Rainey FA, and Widdel F. (1998). Growth, natural relationships, cellular fatty acids and metabolic adaptation of sulfate-reducing bacteria that utilize long-chain alkanes under anoxic conditions. *Arch Microbiol* **170**: 361-369.
- Aharon P and Fu B. (2000). Microbial sulfate reduction rates and sulfur and oxygen isotope fractionations at oil and gas seeps in deepwater Gulf of Mexico. *Geochim Cosmochim Acta* **64**: 233-246.
- de Beer D, Sauter E, Niemann H, Kaul N, Foucher JP, Witte U, Schlüter M, and Boetius A. (2006). In situ fluxes and zonation of microbial activity in surface sediments of the Haakon Mosby Mud Volcano. *Limnol Oceanogr* **51**: 1315-1331.
- Boetius A, Ravensschlag K, Schubert CJ, Rickert D, Widdel F, Gieseke A, Amann R, Jørgensen BB, Witte U, and Pfannkuche O. (2000). A marine microbial consortium apparently mediating anaerobic oxidation of methane. *Nature* **407**: 623-626.
- Boetius A and Suess E. (2004). Hydrate Ridge: a natural laboratory for the study of microbial life fueled by methane from near-surface gas hydrates. *Chem Geol* **205**: 291-310.
- Borcard D, Legendre P, and Drapeau P. (1992). Partialling out the spatial component of ecological variation. *Ecology* **73**: 1045-1055.
- Chomczynski P and Sacchi N. (2006). The single-step method of RNA isolation by acid guanidinium thiocyanate-phenol-chloroform extraction: twenty-something years on. *Nature Prot* **1**: 581-585.
- Claypool GE and Kvenvolden KA. (1983). Methane and other hydrocarbon gases in marine sediment. *Ann Rev Earth Planet Sci* **11**: 299-327.
- Felden J. (2009). Methane fluxes and associated biogeochemical processes in cold seep ecosystems. Doctoral dissertation, Jacobs University Bremen.
- Galushko A, Minz D, Schink B, and Widdel F. (1999). Anaerobic degradation of naphthalene by a pure culture of a novel type of marine sulphate-reducing bacterium. *Environ Microbiol* **1**: 415-420.
- Harms G, Zengler K, Rabus R, Aeckersberg F, Minz D, Rosselló-Móra R, and Widdel F. (1999). Anaerobic oxidation of o-xylene, m-xylene, and homologous alkylbenzenes by new types of sulfate-reducing bacteria. *Appl Environ Microbiol* **65**: 999-1004.
- Hinrichs K-U, Hayes JM, Sylva SP, Brewer PG, and DeLong EF. (1999). Methane-consuming archaeobacteria in marine sediments. *Nature* **398**: 802-805.
- Hubert C, Loy A, Nickel M, Arnosti C, Baranyi C, Brüchert V, Ferdelman T, Finster K, Christensen FM, Rosa de Rezende J, Vandieken V, and Jørgensen B, B. (2009). A constant flux of diverse thermophilic bacteria into the cold arctic seabed. *Science* **325**: 1541-1544.
- Joye SB, Boetius A, Orcutt BN, Montoya JP, Schulz HN, Erickson MJ, and Lugo SK. (2004). The anaerobic oxidation of methane and sulfate reduction in sediments from Gulf of Mexico cold seeps. *Chem Geol* **205**: 219-238.
- Joye SB, Samarkin VA, Orcutt BN, MacDonald IR, Hinrichs K-U, Elvert M, Teske AP, Lloyd KG, Lever MA, Montoya JP, and Meile CD. (2009). Metabolic variability in seafloor brines revealed by carbon and sulphur dynamics. *Nature Geosci* **2**: 349-354.
- Kallmeyer J and Boetius A. (2004). Effects of temperature and pressure on sulfate reduction and anaerobic oxidation of methane in hydrothermal sediments of Guaymas Basin. *Appl Environ Microbiol* **70**: 1231-1233.
- Kniemeyer O, Fischer T, Wilkes H, Glöckner FO, and Widdel F. (2003). Anaerobic degradation of ethylbenzene by a new type of marine sulfate-reducing bacterium. *Appl Environ Microbiol* **69**: 760-768.

- Kniemeyer O, Musat F, Sievert SM, Knittel K, Wilkes H, Blumenberg M, Michaelis W, Classen A, Bolm C, Joye SB, and Widdel F. (2007). Anaerobic oxidation of short-chain hydrocarbons by marine sulphate-reducing bacteria. *Nature* **449**: 898-910.
- Knittel K, Boetius A, Lemke A, Eilers H, Lochte K, Pfannkuche O, Linke P, and Amann R. (2003). Activity, distribution, and diversity of sulfate reducers and other bacteria in sediments above gas hydrate (Cascadia margin, Oregon). *Geomicrobiol J* **20**: 269-294.
- Knittel K, Lösekann T, Boetius A, Kort R, and Amann R. (2005). Diversity and distribution of methanotrophic archaea at cold seeps. *Appl Environ Microbiol* **71**: 467-479.
- Kubo K, Knittel K, Amann R, Fukui M, and Matsuura K. (2011). Sulfur-metabolizing bacterial populations in microbial mats of the Nakabusa hot spring, Japan. *Syst Appl Microbiol* **34**: 293-302.
- Legendre P and Gallagher E. (2001). Ecologically meaningful transformations for ordination of species data. *Oecologia* **129**: 271-280.
- Liu A, Garcia-Dominguez E, Rhine ED, and Young LY. (2004). A novel arsenate respiring isolate that can utilize aromatic substrates. *FEMS Microbiol Ecol* **48**: 323-332.
- Lösekann T, Knittel K, Nadalig T, Fuchs B, Niemann H, Boetius A, and Amann R. (2007). Diversity and abundance of aerobic and anaerobic methane oxidizers at the Haakon Mosby Mud Volcano, Barents Sea. *Appl Environ Microbiol* **73**: 3348-3362.
- Manz W, Amann R, Ludwig W, Wagner M, and Schleifer K-H. (1992). Phylogenetic oligodeoxynucleotide probes for the major subclasses of *Proteobacteria*: problems and solutions. *Syst Appl Microbiol* **15**: 593-600.
- Manz W, Eisenbrecher M, Neu TR, and Szewzyk U. (1998). Abundance and spatial organization of gram-negative sulfate-reducing bacteria in activated sludge investigated by in situ probing with specific 16S rRNA targeted oligonucleotides. *FEMS Microbiol Ecol* **25**: 43-61.
- Mastalerz V, de Lange GJ, and Dählmann A. (2009). Differential aerobic and anaerobic oxidation of hydrocarbon gases discharged at mud volcanoes in the Nile deep-sea fan. *Geochim Cosmochim Acta* **73**: 3849-3863.
- Meyer-Reil LA. (1983). Benthic response to sedimentation events during autumn to spring at a shallow-water station in the western Kiel bight. *Mar Biol* **77**: 247-256.
- Meyer B and Kuever J. (2007). Phylogeny of the alpha and beta subunits of the dissimilatory adenosine-5'-phosphosulfate (APS) reductase from sulfate-reducing prokaryotes - origin and evolution of the dissimilatory sulfate-reduction pathway. *Microbiol* **153**: 2026-2044.
- Michaelis W, Seifert R, Nauhaus K, Treude T, Thiel V, Blumenberg M, Knittel K, Gieseke A, Peterknecht K, Pape T, Boetius A, Amann R, Jørgensen B, B., Widdel F, Peckmann J, Pimenov NV, and Gulin MB. (2002). Microbial reefs in the Black Sea fueled by anaerobic oxidation of methane. *Science* **297**: 1013-1015.
- Morasch B, Schink B, Tebbe CC, and Meckenstock RU. (2004). Degradation of o-xylene and m-xylene by a novel sulfate-reducer belonging to the genus *Desulfotomaculum*. *Arch Microbiol* **181**: 407-417.
- Musat F, Galushko A, Jacob J, Widdel F, Kube M, Reinhardt R, Wilkes H, Schink B, and Rabus R. (2009). Anaerobic degradation of naphthalene and 2-methylnaphthalene by strains of marine sulfate-reducing bacteria. *Environ Microbiol* **11**: 209-219.
- Musat N, Werner U, Knittel K, Kolb S, Dodenhof T, van Beusekom JEE, de Beer D, Dubilier N, and Amann R. (2006). Microbial community structure of sandy intertidal sediments in the North Sea, Sylt-Rømø Basin, Wadden Sea. *Syst. Appl. Microbiol.* **29**: 333-348.
- Mußmann M, Ishii K, Rabus R, and Amann R. (2005). Diversity and vertical distribution of cultured and uncultured *Deltaproteobacteria* in an intertidal mud flat of the Wadden Sea. *Environ Microbiol* **7**: 405-418.

- Muyzer G, Dewaal EC, and Uitterlinden AG. (1993). Profiling of complex microbial-populations by denaturing gradient gel-electrophoresis analysis of polymerase chain reaction-amplified genes-coding for 16S ribosomal-RNA. *Appl Environ Microbiol* **59**: 695-700.
- Muyzer G, Teske A, Wirsén CO, and Jannasch HW. (1995). Phylogenetic-relationships of *Thiomicrospira* species and their identification in deep-sea hydrothermal vent samples by denaturing gradient gel-electrophoresis of 16s rDNA fragments. *Arch Microbiol* **164**: 165-172.
- Nauhaus K, Boetius A, Krüger M, and Widdel F. (2002). *In vitro* demonstration of anaerobic oxidation of methane coupled to sulphate reduction in sediment from a marine gas hydrate area. *Environ Microbiol* **4**: 296-305.
- Niemann H, Duarte J, Hensen C, Omeregíe E, Magalhães VH, Elvert M, Pinheiro LM, Kopf A, and Boetius A. (2006a). Microbial methane turnover at mud volcanoes of the Gulf of Cadiz. *Geochim Cosmochim Acta* **70**: 5336-5355.
- Niemann H, Elvert M, Hovland M, Orcutt B, Judd A, Suck I, Gutt J, Joye SB, Damm E, Finster K, and Boetius A. (2005). Methane emission and consumption at a North Sea gas seep (Tommeliten area). *Biogeosciences* **2**: 335-351.
- Niemann H, Lösekann T, de Beer D, Elvert M, Nadalig T, Knittel K, Amann R, Sauter EJ, Schlüter M, Klages M, Foucher JP, and Boetius A. (2006b). Novel microbial communities of the Haakon Mosby mud volcano and their role as a methane sink. *Nature* **443**: 854-858.
- Ommedal H and Torsvik T. (2007). *Desulfotignum toluenicum* sp. nov., a novel toluene-degrading, sulphate-reducing bacterium isolated from an oil-reservoir model column. *Int J Syst Evol Microbiol* **57**: 2865-2869.
- Omeregíe EO, Niemann H, Mastalerz V, de Lange GJ, Stadnitskaia A, Mascle J, Foucher JP, and Boetius A. (2009). Microbial methane oxidation and sulfate reduction at cold seeps of the deep Eastern Mediterranean Sea. *Mar Geology* **261**: 114-127.
- Orcutt BN, Boetius A, Lugo SK, MacDonald IR, Samarkin VA, and Joye SB. (2004). Life at the edge of methane ice: microbial cycling of carbon and sulfur in Gulf of Mexico gas hydrates. *Chem Geol* **205**: 239-251.
- Orcutt BN, Joye SB, Kleindienst S, Knittel K, Ramette A, Reitz A, Samarkin V, Treude T, and Boetius A. (2010). Impact of natural oil and higher hydrocarbons on microbial diversity, distribution, and activity in Gulf of Mexico cold-seep sediments. *Deep-Sea Res Pt II* **57**: 2008-2021.
- Orphan VJ, Hinrichs K-U, Ussler W, Paull CK, Taylor LT, Sylva SP, Hayes JM, and DeLong EF. (2001). Comparative analysis of methane-oxidizing archaea and sulfate-reducing bacteria in anoxic marine sediments. *Appl Environ Microbiol* **67**: 1922-1934.
- Orphan VJ, House CH, Hinrichs K-U, McKeegan KD, and DeLong EF. (2002). Multiple archaeal groups mediate methane oxidation in anoxic cold seep sediments. *Proc Natl Acad Sci USA* **99**: 7663-7668.
- Otte S, Kuenen JG, Nielsen LP, Paerl HW, Zopfi J, Schulz HN, Teske A, Strotmann B, Gallardo VA, and Jørgensen B, B. (1999). Nitrogen, carbon, and sulfur metabolism in natural *Thioploca* samples. *Appl Environ Microbiol* **65**: 3148-3157.
- Paull CK, Hecker B, Commeau R, Freeman-Lynde RP, Neumann C, Corso WP, Golubic S, Hook JE, Sikes E, and Curaray J. (1984). Biological communities at the Florida escarpment resemble hydrothermal vent taxa. *Science* **226**: 965-967.
- Pernthaler A, Dekas AE, Brown CT, Goffredi SK, Embaye T, and Orphan VJ. (2008). Diverse syntrophic partnerships from deep-sea methane vents revealed by direct cell capture and metagenomics. *Proc Natl Acad Sci USA* **105**: 7052-7057.

- Pernthaler A, Pernthaler J, and Amann R. (2002). Fluorescence in situ hybridization and catalyzed reporter deposition for the identification of marine bacteria. *Appl Environ Microbiol* **68**: 3094-3101.
- Pruesse E, Quast C, Knittel K, Fuchs BM, Ludwig W, Peplies J, and Glöckner FO. (2007). SILVA: a comprehensive online resource for quality checked and aligned ribosomal RNA sequence data compatible with ARB. *Nucl Acids Res* **35**: 7188-7196.
- Rabus R, Nordhaus R, Ludwig W, and Widdel F. (1993). Complete oxidation of toluene under strictly anoxic conditions by a new sulfate-reducing bacterium. *Appl Environ Microbiol* **59**: 1444-1451.
- Ramette A. (2007). Multivariate analyses in microbial ecology. *FEMS Microbiol Ecol* **62**: 142-160.
- Ravenschlag K, Sahn K, Knoblauch C, Jørgensen BB, and Amann R. (2000). Community structure, cellular rRNA content and activity of sulfate-reducing bacteria in marine Arctic sediments. *Appl Environ Microbiol* **66**: 3592-3602.
- Rueter P, Rabus R, Wilkes H, Aeckersberg F, Rainey FA, Jannasch HW, and Widdel F. (1994). Anaerobic oxidation of hydrocarbons in crude-oil by new types of sulfate-reducing bacteria. *Nature* **372**: 455-458.
- Sassen R, Roberts HH, Carney R, Milkov AV, DeFreitas DA, Lanoil B, and Zhang C. (2004). Free hydrocarbon gas, gas hydrate, and authigenic minerals in chemosynthetic communities of the northern Gulf of Mexico continental slope: relation to microbial processes. *Chem Geol* **205**: 195-217.
- Schreiber L, Holler T, Knittel K, Meyerdierks A, and Amann R. (2010). Identification of the dominant sulfate-reducing bacterial partner of anaerobic methanotrophs of the ANME-2 clade. *Environ Microbiol* **12**: 2327-2340.
- Schubotz F, Lipp JS, Elvert M, Kasten S, Mollar XP, Zabel M, Bohrmann G, and Hinrichs K-U. (2011). Petroleum degradation and associated microbial signatures at the Chapopote asphalt volcano, Southern Gulf of Mexico. *Geochim Cosmochim Acta* **75**: 4377-4398.
- Simoneit BRT and Lonsdale PF. (1982). Hydrothermal petroleum in mineralized mounds at the seabed of Guaymas Basin. *Nature* **295**: 198-202.
- Teske A, Hinrichs K-U, Edgcomb V, de Vera Gomez A, Kysela D, Sylva SP, Sogin ML, and Jannasch HW. (2002). Microbial diversity of hydrothermal sediments in the Guaymas Basin: evidence for anaerobic methanotrophic communities. *Appl Environ Microbiol* **68**: 1994-2007.
- Treude T, Boetius A, Knittel K, Wallmann K, and Jørgensen BB. (2003). Anaerobic oxidation of methane above gas hydrates at Hydrate Ridge, NE Pacific Ocean. *Mar Ecol Prog Ser* **264**: 1-14.
- Weber A and Jørgensen BB. (2002). Bacterial sulfate reduction in hydrothermal sediments of the Guaymas Basin, Gulf of California, Mexico. *Deep-Sea Res Pt I* **49**: 827-841.
- Wegener G, Shovitri M, Knittel K, Niemann H, Hovland M, and Boetius A. (2008). Biogeochemical processes and microbial diversity of the Gullfaks and Tommeliten methane seeps (Northern North Sea). *Biogeosciences* **5**: 1127-1144.
- Widdel F, Knittel K, and Galushko A. (2010) in *Handbook of hydrocarbon and lipid microbiology*, edited by K.N. Timmis, T. McGenity, J. R. van der Meer et al. (Springer Berlin Heidelberg), Vol. 3, pp. 1997-2021.
- Yarza P, Ludwig W, Euzéby J, Amann R, Schleifer K-H, Glöckner FO, and Rosselló-Móra R. (2010). Update of the all-species living tree project based on 16S and 23S rRNA sequence analyses. *Syst Appl Microbiol* **33**: 291-299.

Supplementary Information

Table SII.1: Oligonucleotide probes used in this study.

Probe name	Specificity	Form- amide [%]	Sequence (5' - 3')	Reference
Del495a-c*	Most <i>Deltaproteobacteria</i> and <i>Gemmatimonadetes</i>	30	AGT TAG CCG GTG CTT CCT AGT TAG CCG GCG CTT CCT AAT TAG CCG GTG CTT CCT	Loy et al., 2002; Macalady et al., 2006
DSS658	<i>Desulfosarcina/Desulfococcus</i> branch of <i>Deltaproteobacteria</i>	50	TCC ACT TCC CTC TCC CAT	Manz et al., 1998
cDSS658	Competitor against SEEP-SRB2	-	TCC ACT TCC CTC TCC GGT	This study
But5-620	Strain BuS5	50	AAA CGC CCT TCC GGG GTT	Kniemeyer et al., 2007
But12-1275	Butane-GMe12	20	CTGCTTTATGGGGTTAGC	Kniemeyer et al., 2007
SEEP1a-473*	SEEP-SRB1a	30	TTC AGT GAT ACC GTC AGT ATC CC	Schreiber et al., 2010
SEEP1a 1441*	SEEP-SRB1a	45	CCC CTT GCG GGT TGG TCC	Schreiber et al., 2010
SEEP1c-1309*	SEEP-SRB1c	30	ATG GAG TCG AAT TGC AGA CTC	Schreiber et al., 2010
SEEP1d-1420 [§]	SEEP-SRB1d	30	CAA CTT CTG GTA CAG CCA	Schreiber et al., 2010
SEEP1e-632 [§]	SEEP-SRB1e	45	CTC CCA TAC TCA AGC CCT TTA GT T	Schreiber et al., 2010
SEEP1f-153*	SEEP-SRB1f	35	AGC ATC GCT TTC GCG GTG	Schreiber et al., 2010
SEEP2-658	SEEP-SRB2	45	TCC ACT TCC CTC TCC GGT	This study
cSEEP2-658	Competitor against DSS	-	TCC ACT TCC CTC TCC CAT	This study
DSB985	<i>Desulfobacter</i> , <i>Desulfobacula</i> , <i>Desulfospira</i> , <i>Desulfotignum</i>	20	CAC AGG ATG TCA AAC CCA G	Manz et al., 1998
DBA818	<i>Desulfobacterium anilini</i> and relatives	35	RCT ACA CCT AGT TCT CAT	Orcutt et al., 2010
DSB706	Most <i>Desulfobulbaceae</i> and <i>Thermodesulforhabdus</i>	25	ACC GGT ATT CCT CCC GAT	Loy et al., 2002
660	Most <i>Desulfobulbus</i>	60	GAA TTC CAC TTT CCC CTC TG	Devereux et al., 1992
SEEP3-652	SEEP-SRB3	50	TAC CCC CTC TGG TAC TCA	Orcutt et al., 2010
SEEP4-583*	SEEP-SRB4	20	CTG ACA TAA CAR ACC ACC	Orcutt et al., 2010
DTM229	<i>Desulfotomaculum</i> cluster I and other <i>Firmicutes</i>	15	AAT GGG ACG CGG AXC CAT	Hristova et al., 2000

* Used with helper oligonucleotides

[§] Used with competitors

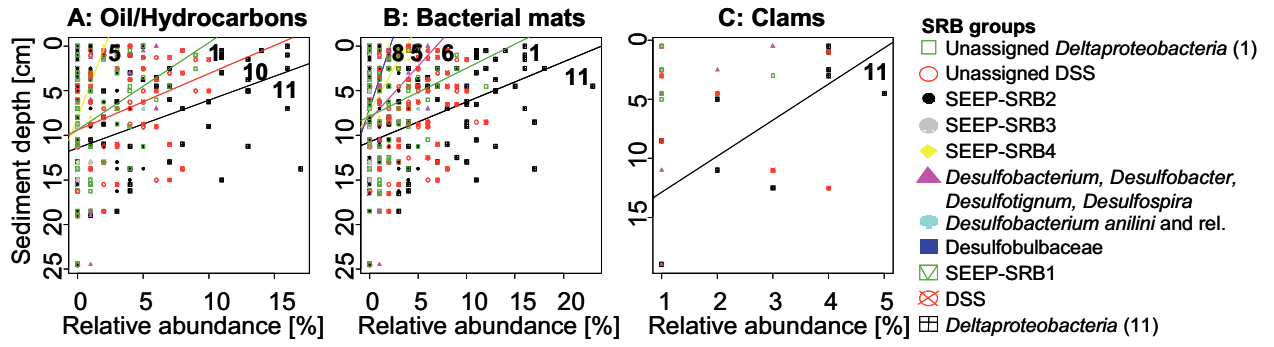


Fig. SII.1: Linear relationships between the relative abundance of SRB groups and sediment depth in particular habitat types that were defined according to the presence of oil/hydrocarbons (A), bacterial mats (B) and clams (C).

References for Supplementary Information

- Devereux R, Kane MD, Winfrey J, and Stahl DA. (1992). Genus- and group-specific hybridization probes for determinative and environmental studies of sulfate-reducing bacteria. *Syst Appl Microbiol* **15**: 601-609.
- Hristova KR, Mau M, Zheng D, Aminov RI, Mackie RI, Gaskins HR, and Raskin L. (2000). *Desulfotomaculum* genus- and subgenus-specific 16S rRNA hybridization probes for environmental studies. *Environ Microbiol* **2**: 143-159.
- Kniemeyer O, Musat F, Sievert SM, Knittel K, Wilkes H, Blumenberg M, Michaelis W, Classen A, Bolm C, Joye SB, and Widdel F. (2007). Anaerobic oxidation of short-chain hydrocarbons by marine sulphate-reducing bacteria. *Nature* **449**: 898-910.
- Loy A, Lehner A, Lee N, Adamczyk J, Meier H, Ernst J, Schleifer KH, and Wagner M. (2002). Oligonucleotide microarray for 16S rRNA gene-based detection of all recognized lineages of sulfate-reducing prokaryotes in the environment. *Appl Environ Microbiol* **68**: 5064-5081.
- Macalady JL, Lyon EH, Koffman B, Albertson LK, Meyer K, Galdenzi S, and Mariani S. (2006). Dominant microbial populations in limestone-corroding stream biofilms, Frasassi cave system, Italy. *Appl Environ Microbiol* **72**: 5596-5609.
- Manz W, Eisenbrecher M, Neu TR, and Szewzyk U. (1998). Abundance and spatial organization of gram-negative sulfate-reducing bacteria in activated sludge investigated by in situ probing with specific 16S rRNA targeted oligonucleotides. *FEMS Microbiol Ecol* **25**: 43-61.
- Orcutt BN, Joye SB, Kleindienst S, Knittel K, Ramette A, Reitz A, Samarkin V, Treude T, and Boetius A. (2010). Impact of natural oil and higher hydrocarbons on microbial diversity, distribution, and activity in Gulf of Mexico cold-seep sediments. *Deep-Sea Res Pt II* **57**: 2008-2021.
- Schreiber L, Holler T, Knittel K, Meyerdierks A, and Amann R. (2010). Identification of the dominant sulfate-reducing bacterial partner of anaerobic methanotrophs of the ANME-2 clade. *Environ Microbiol* **12**: 2327-2340.

Chapter III

Specialists instead of generalists oxidize alkanes in anoxic marine hydrocarbon seep sediments

Sara Kleindienst¹, Florian-Alexander Herbst², Frederick von Netzer³, Rudolf Amann¹,
Jörg Peplies¹, Martin von Bergen², Jana Seifert², Florin Musat¹,
Tillmann Lueders³, Katrin Knittel^{1*}

In preparation

*Corresponding author: Katrin Knittel (Department of Molecular Ecology),
Phone: +49 421 2028 935, Fax: +49 421 2028 580, E-mail: kknittel@mpi-bremen.de

¹Max-Planck-Institute for Marine Microbiology, Celsiusstrasse 1, D-28359 Bremen, Germany

²Helmholtz Centre for Environmental Research (UFZ), Permoserstrasse 15,
D-04318 Leipzig, Germany

³Helmholtz Zentrum München - German Research Center for Environmental Health, Institute
for Groundwater Ecology, Ingolstädter Landstrasse 1, D-85764 Neuherberg, Germany

Abstract

The anaerobic oxidation of non-methane hydrocarbons mediated by sulfate-reducing bacteria (SRB) is a major process of organic matter degradation at marine hydrocarbon seeps. Several SRB have been successfully cultured, however, knowledge about in situ active organisms is still very limited.

Here, we identified alkane-degrading key players from two contrasting seeps at the Mediterranean Amon Mud Volcano (Amon MV) and Guaymas Basin in the Gulf of California using complementary stable-isotope probing (SIP) techniques. Anoxic sediments were incubated with ^{13}C -labeled butane or dodecane under close to in situ conditions. DNA- and RNA-based SIP in combination with 454-pyrosequencing (PYRO-SIP) allowed the identification of four phylogenetically distinct deltaproteobacterial groups of alkane-oxidizing SRB within the family *Desulfobacteraceae*. We named the groups degrading short-chain alkanes ‘SCA-SRB1’ and ‘SCA-SRB2’ and those degrading long-chain alkanes ‘LCA-SRB1’ and ‘LCA-SRB2’. CARD-FISH with newly developed specific probes revealed a high relative in situ abundance of SCA-SRB1 and SCA-SRB2 with 2% of the total community, while groups LCA-SRB1 and LCA-SRB2 were below 1% of total cells. Protein-based SIP (Protein-SIP), which enables to trace stable isotopes from substrate to protein, confirmed alkane-degrading key players of the family *Desulfobacteraceae*. In addition, Protein-SIP indicated additional carbon sources for ^{13}C -biosynthesis besides alkanes, and gave insights into possible metabolic pathways: (1-methylalkyl)succinylation as initial step of butane degradation and the oxidative Wood–Ljungdahl pathway as terminal point of alkane degradation.

Introduction

Hydrocarbons are widespread on Earth and can be oxidized by a variety of aerobic and anaerobic microorganisms (reviewed by Widdel et al., 2010). Natural sources for hydrocarbons in marine systems are gas or crude oil seeps differing in hydrocarbon concentrations and composition. Several marine gas seeps show elevated concentrations of gaseous short-chain alkanes in addition to methane e.g. at gas seep sites at the Amon Mud Volcano (Amon MV) in the Mediterranean Sea (Mastalerz et al., 2007; Mastalerz et al., 2009). In contrast, other marine hydrocarbon seeps contain a broad range of alkanes, alkenes and aromatic hydrocarbons, e.g. hydrothermal vent sites from Guaymas Basin in the Gulf of California (Byrne & Emery, 1960; Simoneit & Lonsdale, 1982) or cold seeps in the Gulf of Mexico (Anderson et al., 1983; Kennicutt II et al., 1988a; Kennicutt II et al., 1988b). First in situ biogeochemical indications for microbial non-methane hydrocarbon oxidation at such sites were the detection of isotopic fractionation of gaseous hydrocarbons (Sassen et al., 2004) and the finding of high methane-independent sulfate-reduction (SR) rates (Joye et al., 2004; Kallmeyer & Boetius, 2004) in sediments from Gulf of Mexico and Guaymas Basin. These discoveries revolutionized our understanding of the energy sources that fuel high SR rates in these sediments and the impact of hydrocarbon biodegradation, which significantly affects the global hydrocarbon budget. However, knowledge about responsible communities has been lacking behind but is essential to close the gap between important biogeochemical processes and key players. Crucial research questions emerged: Are in situ active hydrocarbon degraders similar or distinct from the ones enriched or isolated using cultivation techniques? Is the different composition in hydrocarbons at various seep sites reflected in the ecophysiology of active organisms? Do marine sediments harbor generalistic hydrocarbon degraders?

Up to this point, cultured hydrocarbon-degrading SRB mainly belong to *Deltaproteobacteria* with the exception of *Desulfosporosinus* sp. strain Y5 (Liu et al., 2004) and *Desulfotomaculum* sp. strain OX39 (Morasch et al., 2004) within the *Clostridia*. To date, respective deltaproteobacterial isolates were phylogenetically affiliated with the *Desulfosarcina/Desulfococcus* (DSS) clade and can degrade C₃-C₂₀ *n*-alkanes, C₇-C₂₃ *n*-alkenes or aromatic hydrocarbons such as benzene, toluene or naphthalene (Aeckersberg et al., 1991; Aeckersberg et al., 1998; Harms et al., 1999; So & Young, 1999; Meckenstock et al., 2000; Cravo-Laureau et al., 2004; Kniemeyer et al., 2007; Higashioka et al., 2009). Additional isolates affiliated with *Desulfobacterium* spp. (Rabus et al., 1993; Ommedal & Torsvik, 2007), or with *Desulfobacterium anilini* (Galushko et al., 1999; Harms

et al., 1999; Kniemeyer et al., 2003; Musat et al., 2009), a strain for which phylogenetic reclassification is still pending (Kniemeyer et al., 2003). Several of these isolates and enrichments are of marine origin, e.g. the strain BuS5, which was isolated from Guaymas Basin (Kniemeyer et al., 2007) or the enrichment Butane-GMe12 from Gulf of Mexico (Kniemeyer et al., 2007; Jaekel, 2011). Furthermore, in situ analysis of SRB communities at marine gas and crude oil seeps showed that specific groups are highly abundant (Orcutt et al., 2010; Kleindienst et al., *submitted*). In particular, most seep sediments were dominated by members of the DSS clade. Also, the diversity of DSS species was shown to be high in complex hydrocarbon-rich sediments (Orcutt et al., 2010).

In this study, complementary stable-isotope probing (SIP) techniques were used to get novel insights into marine benthic organisms, degrading alkanes under close-to-in situ conditions. ^{13}C -labeled substrates were selected based on metabolic capabilities of isolated alkane degraders: butane was used as model substrate for organisms oxidizing short-chain alkanes ($\text{C}_3\text{-C}_4$) and dodecane was chosen as model substrate for candidates degrading longer alkanes (e.g. $\text{C}_6\text{-C}_{20}$; cf. Widdel et al., 2010). Furthermore, two seep types were selected in order to unravel potential differences of gas and hydrocarbon seep communities. The unique combination of various stable-isotope probing techniques enabled the identification of active microorganisms as well as the investigation of enzymes and therefore catabolic pathways involved in alkane oxidation. For this, pyrosequencing in combination with DNA- and rRNA based SIP (PYRO-SIP) as well as protein-based SIP (Protein-SIP) were carried out. In addition, the abundance of alkane-degrading SRB was monitored over the course of hydrocarbon degradation using catalyzed-reporter deposition fluorescence in situ hybridization (CARD-FISH).

Results and Discussion

Bacterial diversity of Amon MV and Guaymas Basin sediments

Two contrasting sediment types were investigated from a gas seep at the Amon MV emitting high fluxes of methane and other short-chain alkanes (Niemann et al., 2006; Mastalerz et al., 2007; Mastalerz et al., 2009) and a hydrocarbon seep from Guaymas Basin, characterized by a complex hydrocarbon composition similar to crude oil (*n*-alkanes and aromatic hydrocarbons) (Didyk & Simoneit, 1989). Insights into the bacterial diversity of both sediments was obtained by 454-pyrosequencing of a PCR-amplified ~500 bp-16S rRNA gene fragment (3000-6000 sequences per sample). In Amon MV gas seep sediments *Deltaproteobacteria* clearly dominated with 75% of all bacterial sequences (Table III.1) and were shown to be

highly diverse. 405 operational taxonomic units (OTUs) from overall 857 bacterial OTUs belonged to *Deltaproteobacteria* (Table III.1), which was determined based on a 97% sequence similarity criterion used as a cut-off for species level. Most sequences were affiliated with the highly diverse group SEEP-SRB-1 (155 OTUs) and additional uncultivated groups of the *Desulfobacteraceae* or *Desulfobulbaceae*, including novel defined groups (e.g. SCA-SRB1; 29 OTUs). Sequences found at lower frequency were affiliated with *Gammaproteobacteria*, *Epsilonproteobacteria* and few *Chloroflexi* as well as Candidate division OP9.

In Guaymas Basin sediments deltaproteobacterial sequences were also most frequently found (45%; Table III.1). However, other genera dominated as compared to the Amon MV gas seep sediments and they were less diverse as only 198 deltaproteobacterial from altogether 897 bacterial OTUs were formed. Most abundant was the deep-branching group Hot-Seep1 (17% of total bacterial sequences), which was shown to be involved in thermophilic anaerobic oxidation of methane (Holler et al., 2011). In addition, 12% of total bacterial sequences affiliated with *Epsilonproteobacteria* and 10% of sequences belonged to *Bacteroidetes* while a minor part of sequences clustered with uncultured *Chloroflexi* and *Spirochaetes*. According to our results, the same dominant taxa were previously detected in clone libraries and V6 taq-sequencing libraries constructed from Amon MV sediments (Omeregíe et al., 2009; Pachiadaki et al., 2011) and Guaymas Basin sediments (Teske et al., 2002; Dhillon et al., 2003; Biddle et al.). This accordance confirms that SIP-experiments were carried out with benthic communities that typically occur at these seeps.

Alkane-dependent activity in SIP-experiments with marine seep sediments

Sediments from two contrasting seeps at Amon MV and Guaymas Basin were amended with ^{13}C -labeled butane or ^{13}C -labeled dodecane and incubated for 29-309 days (Fig. III.1). Incubations with Amon MV sediments were performed at 20°C which is slightly higher compared to in situ temperature of 14°C (Grünke et al., 2011), for incubations with Guaymas Basin sediments 28°C was selected as a mean temperature of the naturally occurring steep temperature gradients for Guaymas Basin incubations (typical 3-50°C in situ temperature ranging from 0-20 cm sediment depth; McKay pers. communication).

Alkane-dependent microbial activity differed between the two sediments and supplied ^{13}C -alkanes. Fastest response was shown for the Amon MV sediment incubations with butane. Butane degradation started without lag phase, as determined by butane-dependent SR, decrease of butane concentrations and production of $^{13}\text{CO}_2$ (Fig. III.1). After 29 days, 6 mM

sulfide was produced while almost all added butane (2.1 mM) was consumed and resulting CO₂ showed a strong labeling of 15% ¹³C-DIC (Fig. III.1A). In contrast, in Guaymas Basin sediments butane-dependent SR started after a pronounced lag phase (20 days), and butane was consumed after 113 days leading to 21% ¹³C-DIC (Fig. III.1Bb). In both sediment types dodecane-dependent SR started later compared to the similar incubations amended with butane. Significant sulfide production started after 80 days of incubation (Fig. III.1C), and about 6 mM sulfide was produced after 232 (Guaymas Basin) and 309 (Amon MV) days of incubation, leading to an enrichment of 24% and 21% ¹³C-DIC, respectively (Fig. III.1C and D). Variation in microbial response times for different substrates are likely explained by different initial in situ abundances of alkane-oxidizing organisms and different generation times: for example, for the short-chain alkane degrader strain BuS5, doubling times of 4-5 d were reported (Kniemeyer et al., 2007), while longer doubling times of 9 d were estimated for decane degraders such as *Desulfococcus oleovorans* Hxd3 (Davidova et al., 2006). In our incubations initial in situ abundances of alkane degraders ranged from 1×10^5 ml⁻¹ to 7×10^6 ml⁻¹ as determined by CARD-FISH (Fig. III.1). These different abundances are potentially caused by previous exposure to different classes of naturally occurring alkanes. Lowest initial in situ cell numbers were detected for dodecane degraders (1×10^6 ml⁻¹ at Amon MV and 1×10^5 ml⁻¹ at Guaymas Basin; Fig. III.1C, D), which might be the reason for the longer response time to dodecane as compared to butane.

Identification of key players involved into alkane degradation by PYRO-SIP

Early (t₁) and late time points (t₃) of alkane-amended incubations were chosen for DNA and rRNA-based SIP. Terminal restriction fragment length polymorphism (T-RFLP) fingerprinting of gradient fractions with ‘light’ and ‘heavy’ nucleic acids were used to identify terminal restriction fragments (T-RFs) of microorganisms involved in ¹³C-butane and ¹³C-dodecane degradation, respectively. rRNA-SIP was used for Amon MV incubations, while DNA-SIP was performed for Guaymas Basin experiments, because these sediments did not yield sufficient amounts of high-quality rRNA needed for SIP. 16S rRNA (gene) pyrotag-sequencing of selected high-density fractions allowed the identification of labeled templates via linking to the respective density-resolved T-RFs (Pilloni et al., 2011) and phylogenetic analysis. We detected four distinct groups of alkane-degrading SRB as well as potential secondary metabolite consumers.

Tab III.1: Overview of 16S rRNA gene pyrosequences of *Bacteria* retrieved from sediments at gas seep Amon Mud Volcano and hydrocarbon seep Guaymas Basin. Sediments were stimulated with ¹³C-butane and -dodecane to investigate active alkane-degraders. Background community in untreated samples and active organisms in heavy fraction from density-resolved gradients from SIP-incubations were analyzed. OTUs were determined based on 97% sequence

^a Phylogenetic affiliation	Amon Mud Volcano (gas seep)								Guaymas Basin (hydrocarbon seep)							
	Untreated 0 days		Butane 29 days		Dodecane 309 days		^b TRF length	Reads per	Untreated 0 days		Butane 113 days		Dodecane 183 days		^b TRF length	Reads per
	Reads	OTUs	Reads	OTUs	Reads	OTUs	(bp)	contig	Reads	OTUs	Reads	OTUs	Reads	OTUs	(bp)	contig
<i>Bacteria</i>	5139	857	6181	405	4927	433	ND	ND	5244	897	5782	474	3145	189	ND	ND
<i>Acidobacteria</i>	9	3	11	5	43	13	ND	ND	23	1	24	5	3	1	ND	ND
<i>Bacteroidetes</i>	64	25	21	8	31	7	ND	ND	431	64	393	8	33	3	ND	ND
BD2-2	13	4	1	0	0	0	ND	ND	66	11	11	3	1	0	ND	ND
Uncult. <i>Marinilabiaceae</i>	5	3	5	2	3	1	ND	ND	63	8	<u>347</u>	2	27	1	<u>92</u>	343
VC2.1 Bac22	6	1	1	1	<u>5</u>	<u>1</u>	<u>89</u>	5	218	15	34	2	3	1	ND	ND
Candidate division OP3	2	2	0	0	173	5	ND	ND	13	4	248	7	<u>615</u>	5	<u>671</u>	558
Candidate division OP9	137	14	20	5	276	7	ND	ND	43	4	376	4	92	2	ND	ND
Candidate division WS3	15	9	2	2	23	10	ND	ND	77	20	67	12	4	0	ND	ND
<i>Chloroflexi</i>	84	27	47	17	250	56	ND	ND	263	60	400	52	131	32	ND	ND
Uncult. <i>Anaerolineaceae</i>	76	26	39	14	218	47	ND	ND	191	33	317	34	108	24	ND	ND
<i>Deferribacteres</i>	28	9	10	5	68	17	ND	ND	75	13	45	10	29	10	ND	ND
<i>Firmicutes</i>	10	6	1	0	7	4	ND	ND	93	13	4	1	1	1	ND	ND
<i>Fusobacteria</i>	55	10	13	5	99	8	ND	ND	78	12	260	8	51	6	ND	ND
<i>Proteobacteria</i>	4329	571	5894	297	3634	210	ND	ND	2514	284	2791	149	1870	68	ND	ND
<i>Deltaproteobacteria</i>	3646	405	5544	193	3443	159	ND	ND	1834	198	2494	125	1837	57	ND	ND
<i>Bacteriovoraceae</i>	1	0	0	0	1	1	ND	ND	<u>723</u>	24	272	9	56	5	<u>297</u>	296
<i>Desulfarculaceae</i>	44	18	23	9	54	13	ND	ND	222	34	418	32	74	13	ND	ND
<i>Desulfobacteraceae</i> spp.	3203	273	5333	141	2830	90	ND	ND	474	78	1432	44	378	19	ND	ND
LCA-SRB1 group	2	1	0	0	<u>984</u>	8	<u>163</u>	1057	0	0	1	1	0	0	ND	ND
<i>Desulfobacterium</i> spp.	7	3	4	4	2	2	ND	ND	19	7	37	4	2	0	ND	ND
<i>Desulfobacula</i> spp.	30	8	13	3	6	2	ND	ND	143	17	4	2	4	1	ND	ND
<i>Desulfococcus</i> spp.	48	11	216	6	78	5	ND	ND	18	4	6	2	4	1	ND	ND
LCA-SRB2 group	5	2	0	0	302	9	ND	ND	28	3	26	3	<u>328</u>	4	<u>164</u>	297
<i>Desulfosarcina</i> spp.	59	12	25	4	24	4	ND	ND	6	3	22	3	1	0	ND	ND
SEEP-SRB1 spp.	<u>2550</u>	155	614	37	1081	26	<u>511</u>	164	39	10	144	6	11	5	ND	ND
SCA-SRB1 group	209	29	<u>3246</u>	<u>62</u>	177	9	<u>132, 512</u>	138, 812	37	8	213	6	8	3	ND	ND
SCA-SRB2 group	<u>47</u>	4	65	4	88	5	ND	ND	14	3	<u>616</u>	8	6	2	<u>163</u>	584
<i>Desulfobulbaceae</i> spp.	181	53	59	20	280	18	ND	ND	93	14	120	9	1273	2	ND	ND
SEEP-SRB2 spp.	51	8	20	2	70	2	ND	ND	44	1	54	2	5	1	ND	ND
Uncult. <i>Desulfobulbaceae</i>	1	1	3	1	107	3	ND	ND	8	1	57	8	<u>1268</u>	1	<u>512</u>	1105
<i>Desulfuromonadales</i>	128	30	40	11	46	9	ND	ND	195	16	79	11	12	2	ND	ND
<i>Myxococcales</i>	19	12	1	1	77	8	ND	ND	22	8	8	4	4	0	ND	ND
Sva0485	50	10	57	3	81	6	ND	ND	60	10	18	4	10	3	ND	ND
<i>Syntrophobacterales</i>	8	5	24	5	15	4	ND	ND	10	4	108	6	1	1	ND	ND
<i>Epsilonproteobacteria</i>	235	41	105	20	79	15	ND	ND	585	51	66	16	17	8	ND	ND
<i>Gammaproteobacteria</i>	420	105	227	60	95	30	ND	ND	72	25	213	4	10	1	ND	ND
<i>Methylococcales</i>	136	26	92	16	10	4	ND	ND	7	2	1	0	0	0	ND	ND
<i>Spirochaetes</i>	7	4	8	3	16	7	ND	ND	110	19	31	9	3	1	ND	ND
<i>Thermodesulfobacteriales</i>	0	0	0	0	0	0	ND	ND	71	5	33	3	7	2	ND	ND
Other <i>Bacteria</i>	116	181	95	61	140	96	ND	ND	451	422	343	218	58	61	ND	ND

^aPhylum- or division-level read abundances (bold) include genus- or lineage-specific read abundances (non-bold).

^bCharacteristic T-RFs were predicted for important lineages via assembled amplicon contigs, but are given as T-RFs actually observed in the electropherograms in agreement to T-RFs verified for other, terrestrial sulfate-reducing hydrocarbon-degrading systems (Winderl et al., 2010; Pilloni et al., 2011). Commas separate more than one characteristic T-RF for a lineage. T-RFs and reads from respective samples are underlined; reads within contigs are given.

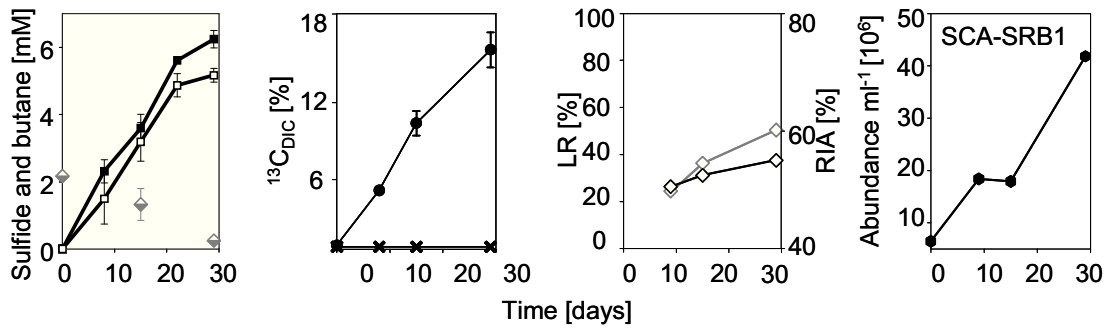
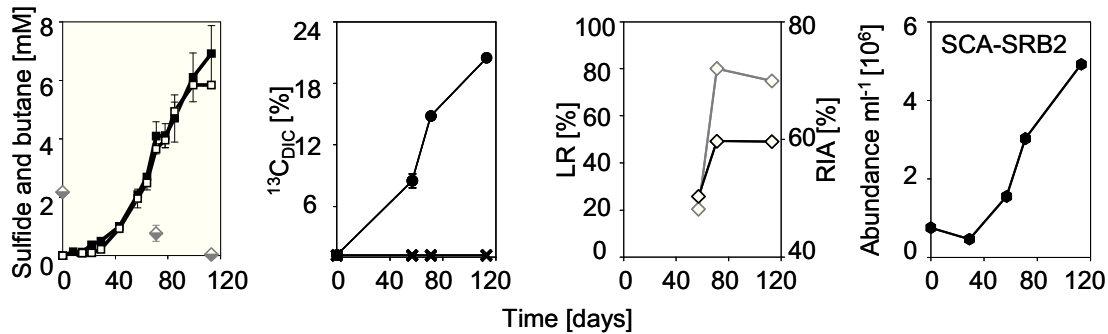
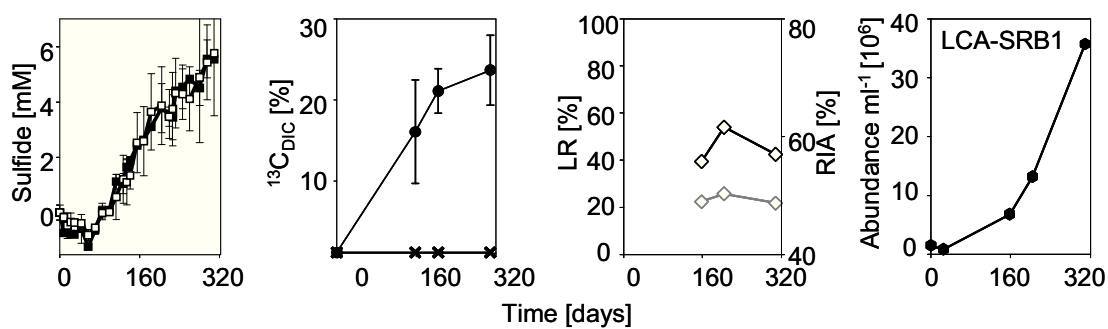
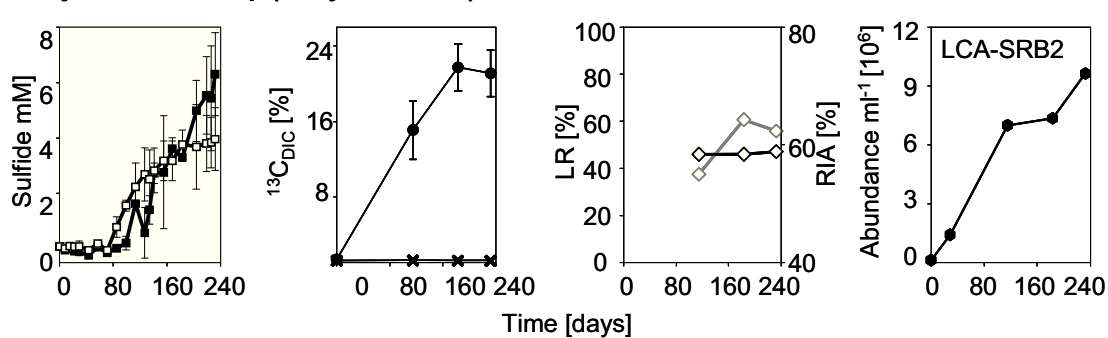
A: Gas seep (Amon Mud Volcano) incubations with butane**B: Hydrocarbon seep (Guaymas Basin) incubations with butane****C: Gas seep (Amon Mud Volcano) incubations with dodecane****D: Hydrocarbon seep (Guaymas Basin) incubations with dodecane**

Fig. III.1: Microbial butane- (panels A and B) and dodecane-dependent (panels C and D) sulfide production (■/□) in incubations with Amon Mud Volcano and Guaymas Basin seep sediments. Open symbols represent ^{12}C -incubations while filled symbols represent ^{13}C -incubations. In addition, consumption of butane (◇) as well as the ^{13}C -DIC abundance [%] of ^{13}C -incubations (●) and controls (×) were analyzed. Relative isotope abundance in peptides (RIA; ◇) and labelling ratio of labeled peptide to all peptide forms (LR; ◇) was determined. The absolute abundance of alkane degraders of groups SCA-SRB1, SCA-SRB2, LCA-SRB1, and LCA-SRB2 (●) were monitored at different time points using CARD-FISH.

Butane degraders. For butane-amended incubations of Amon MV gas seep sediments two T-RFs were identified to represent butane-degrading bacteria: i) after only 9 days a T-RF of 132 bp length became dominant in heavy RNA (Fig. III.2) and was identified to represent a close relative of strain BuS5 (Table III.1 and Fig. III.3; Kniemeyer et al., 2007). ii) After 29 days an additional OTU represented by a 512 bp-long T-RF was identified to be involved in butane degradation, representing microbes closely related to the dominant phylotype in the enrichment culture Butane-GMe12 from the DSS group. BuS5 and Butane-GMe12 were isolated and enriched from Guaymas Basin and Gulf of Mexico hydrocarbon seep sediments, respectively, and have been shown to degrade propane and butane under sulfate-reducing conditions (Kniemeyer et al., 2007). These species affiliated with other sequences from marine hydrocarbon seeps (Mills et al., 2004; Mills et al., 2005; Pachiadaki et al., 2011) and with phylotypes dominant in cultures enriched with propane or butane (Kniemeyer et al., 2007; Jaekel, 2011). They formed a distinct cluster within the DSS group, which we named “SCA-SRB1” (SCA; short-chain alkane). Based on the origin of sequences, known capabilities for certain species from the group SCA-SRB1 as well as on results from this study we propose that group members of SCA-SRB1 (intragroup similarity 93-97%) oxidize short-chain alkanes, in particular propane and butane, at marine hydrocarbon seeps (Fig. III.4).

In Guaymas Basin sediments, butane degradation was catalyzed by a different clade. T-RFs of two distinct candidates for butane degradation were shown to represent labeled DNA: i) after 57 days (t_1) a 163 bp T-RF (Fig. III.2) was detected that was phylogenetically assigned to an uncultivated group of the DSS which we named “SCA-SRB2” (Table III.1 and Fig. III.3). This group of organisms was identified to be the primary butane consumers in the Guaymas Basin incubation. Other sequences affiliating with the SCA-SRB2 group originated from hydrocarbon seep sediments at Gulf of Mexico (Martinez et al., 2006), the Mediterranean Kazan Mud Volcano (Pachiadaki et al., 2010), Santa Barbara (Orphan et al., 2001) and Eel River Basin (Pernthaler et al., 2008). All these sites are known for short-chain alkane seepage. The organism identified in this study is most likely a novel key player, which is involved into butane-degradation at marine seeps. ii) After 113 days (t_3) an additional labeled T-RF of 92 bp length became visible and was identified as uncultured *Marinilabiaceae* (*Bacteroidetes*). Members of *Marinilabiaceae* have been previously described as fermenting bacteria from an offshore mangrove sediment (Zhao et al., *in press*). We therefore assume that this organism might also have fermenting capabilities and likely is secondarily labeled by utilizing dead biomass of the primary consumer (Fig. III.4).

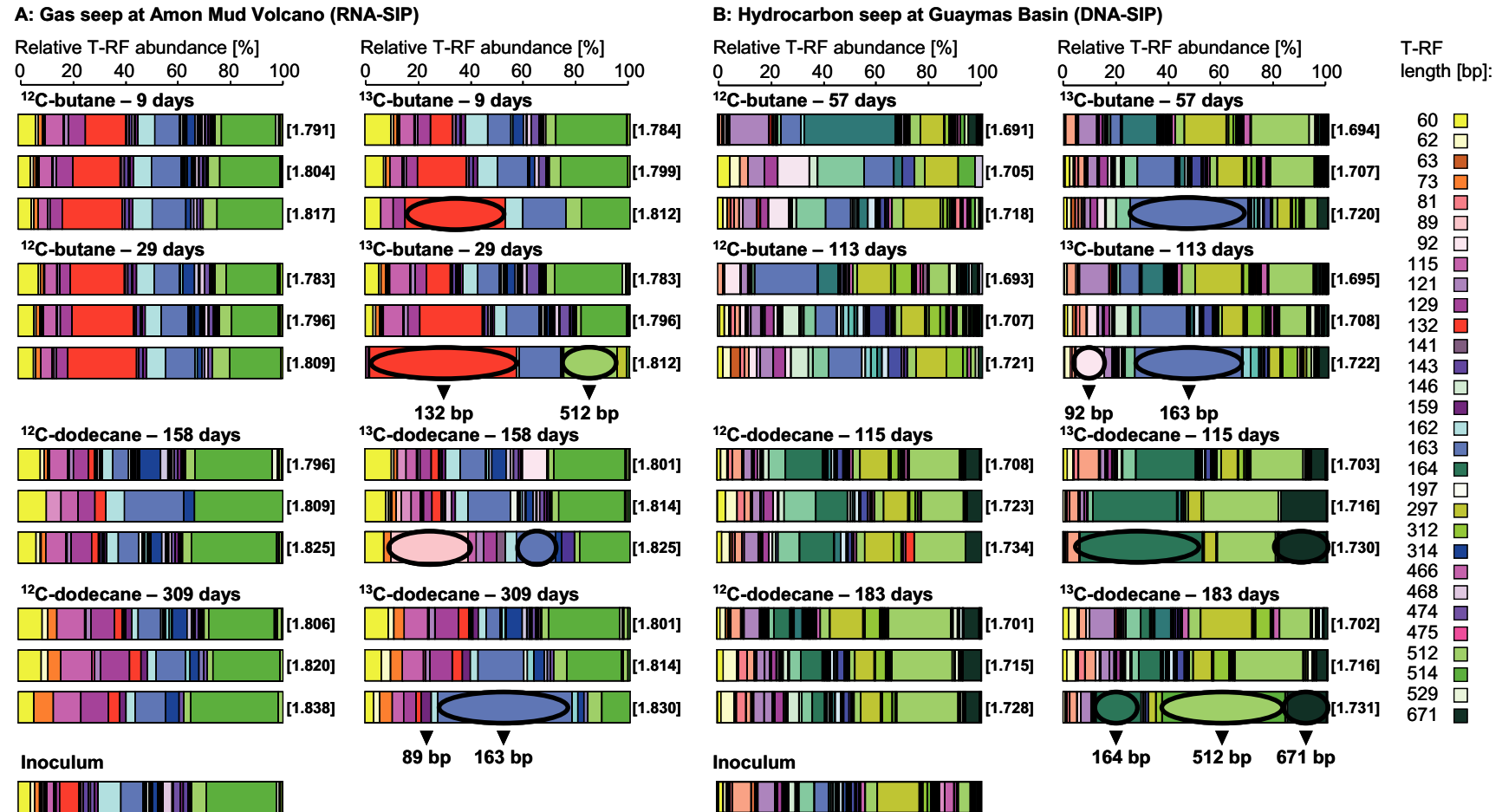


Fig III.2: Relative T-RF abundance within density-resolved gradient fractions. The first and the last sampling point of SIP-incubations are illustrated as indicated by time in days. T-RFs from labeled organisms are marked with black circles within the ¹³C-butane and -dodecane incubations. In addition, relative T-RF abundance of the ¹²C-incubations and inoculums are shown.

Dodecane degraders. Two T-RFs were detected in Amon MV sediments incubations to represent potential degraders of ^{13}C -dodecane: i) after 158 days (t_1) a 164 bp T-RF became apparent, originating from labeled organisms, which affiliated with a third group of uncultured species within the DSS (intragroup similarity >98%), which we named “LCA-SRB1” (LCA; long-chain alkane). This uncultured LCA-SRB1 group is clearly different from the uncultured SCA-SRB2 group (90%-85% intergroup similarity, Fig. III.3). The active dodecane consumer from Amon MV was next related to sequences from a marine hydrocarbon seep at New Zealand-Hikurangi Margin but also from South Atlantic Ocean Rio de la Plata river sediment (Alonso et al., 2010) and a meromictic lake (Halm et al., 2009) as well as from an oil field (Zhang et al., 2010). Hydrocarbon occurrence is not apparent but can also not be ruled out for the river and lake sites. Thus, it remains largely speculative, if members of the LCA-SRB1 group are physiologically more diverse than exclusively restricted to long-chain alkane degradation. ii) A second active organism was revealed by an 89 bp-long T-RF. This organism was identified as a *Bacteroidetes* species, but it was not detected any more after 204 (t_2) and 309 days (t_3). It is assumed that this organism was overgrown during the experiment (Fig. III.4).

The hydrocarbon seep sediments from Guaymas Basin supplemented with dodecane showed 3 T-RFs of key players within dodecane-degradation processes: i) after 115 days (t_1) a 164 bp T-RF was detected, which could be assigned to a fourth group of uncultured *Desulfobacteraceae* (“LCA-SRB2”; intragroup similarity >96%) again clearly different from the uncultured groups SCA-SRB2 and LCA-SRB1 (sequence similarity 90%-85% between groups SCA-SRB2 and LCA-SRB2 and 88%-87% between groups LCA-SRB1 and LCA-SRB2; Fig. III.3). This dodecane consumer was closely related to sequences from the seeps in the Gulf of Mexico (Orcutt et al., 2010), at Haakon Mosby Mud Volcano (Lösekann et al., 2007), polluted Bay of Cadiz (Köchling et al., 2011) and from an enrichment from Wadi Gaza, Palestine (Abed et al., 2011) grown on oil under sulfate-reducing conditions. This supports that members of the LCA-SRB2 group are involved in longer-chain alkane degradation. ii) a 671 bp T-RF (Fig. III.2) was identified from a second active species belonging to the candidate division OP3 (Table III.1). Previous studies identified OP3 species in propionate, butyrate and monoterpene enrichments (Uyttebroek et al., 2006; Tang et al., 2007; Rotarua et al., *in press*) and diverse anoxic environments (Hugenholtz et al., 1998; Alfreider et al., 2002; Chouari et al., 2003; Shigematsu et al., 2006).

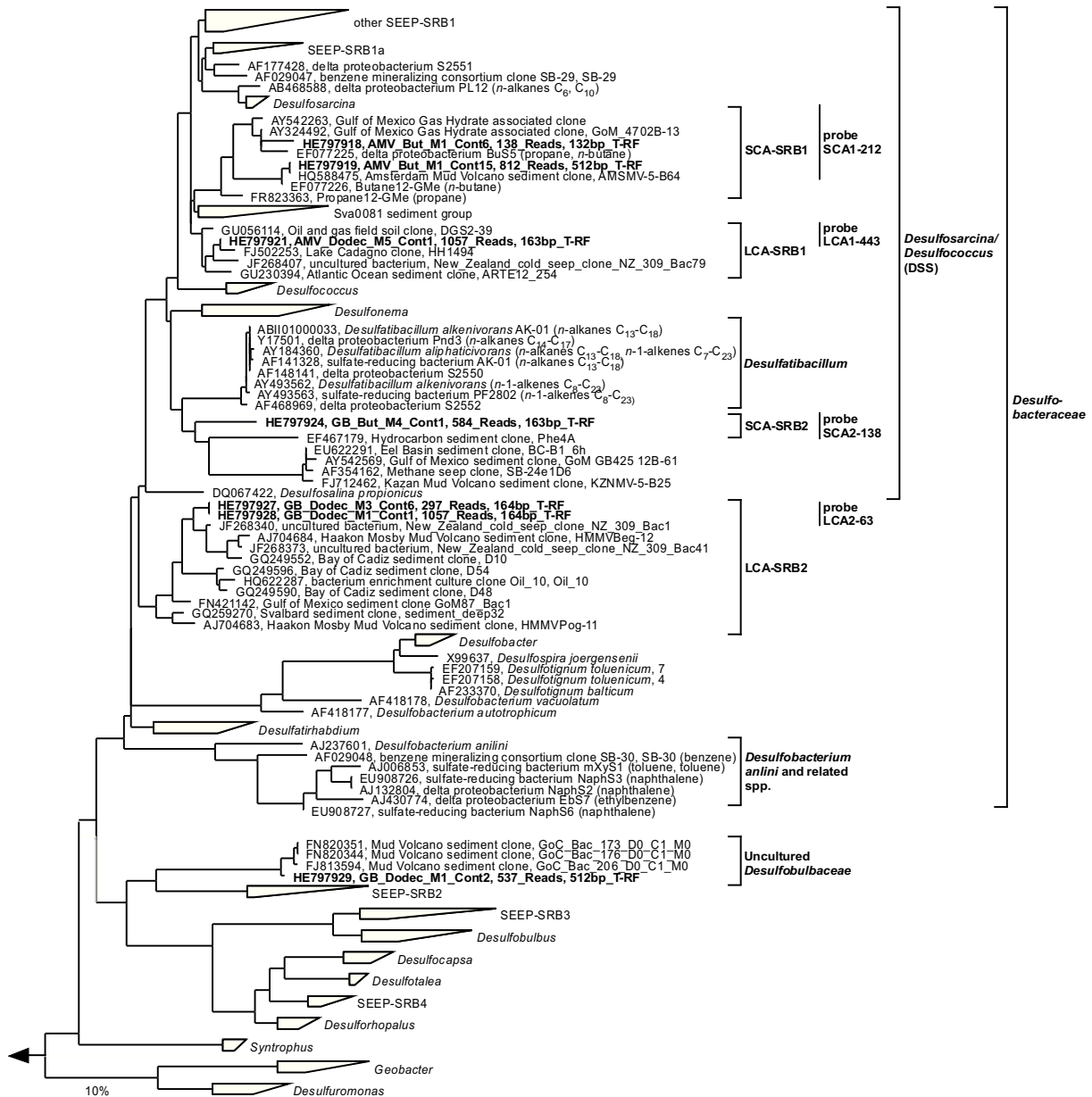


Fig. III.3: 16S rRNA-based phylogenetic tree of *Deltaproteobacteria* showing butane- and dodecane-degrading organisms in Amon MV and Guaymas Basin sediment as identified by stable isotope probing experiments. Assembled amplicon contigs for degraders identified by SIP-experiments are shown in bold and in comparison to related reference sequences. The spectrum of hydrocarbon usage by isolated SRB is indicated in brackets. Coverage of probes used for CARD-FISH is indicated by colored clamps. The bar represents 10% estimated sequence changes.

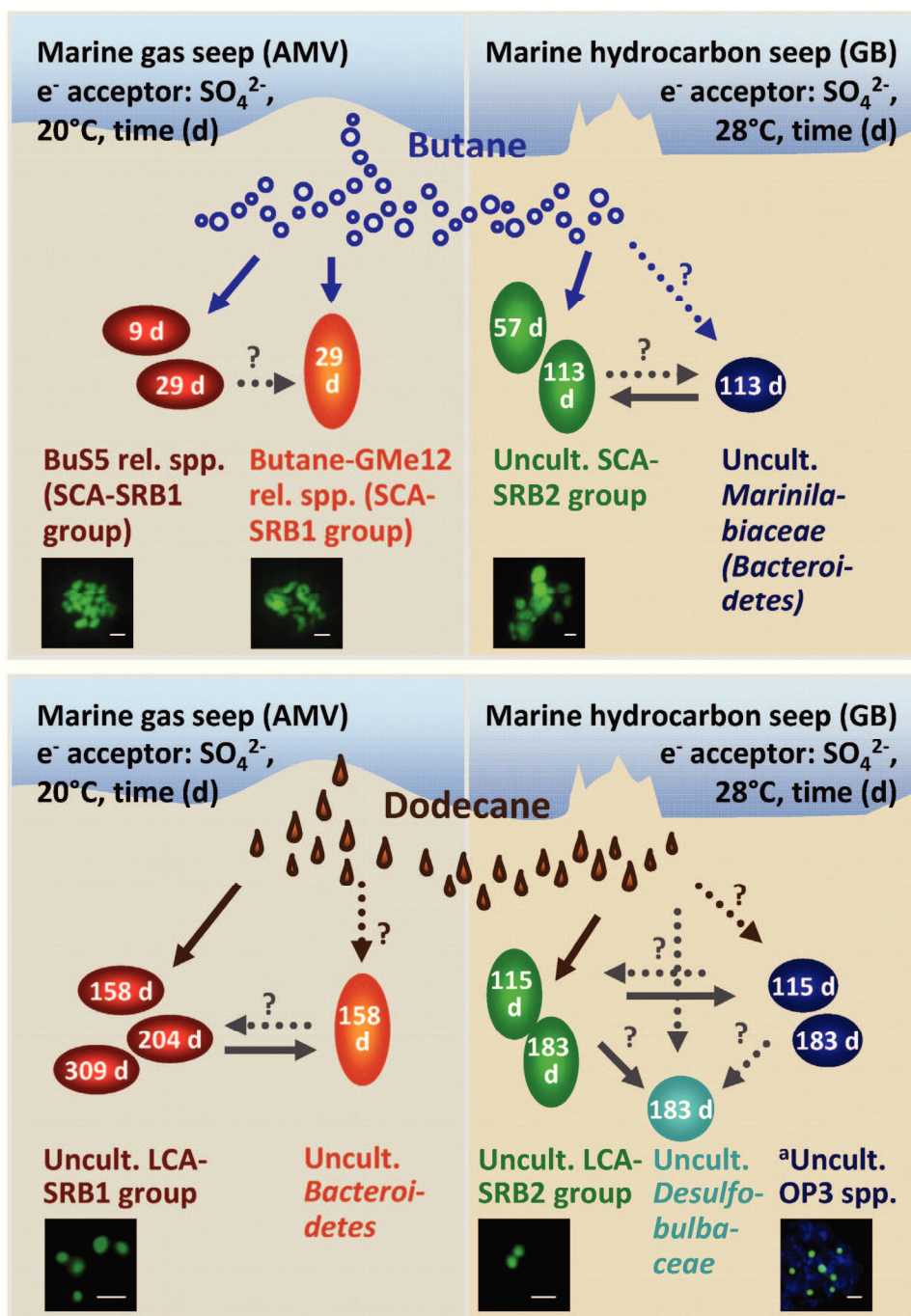


Fig III.4: Proposed ¹³C-carbon flow within hydrocarbon-degradation processes at Amon MV (AMV) and Guaymas Basin (GB) seep sediments. Identification of active community was done by rRNA- and DNA-SIP. First appearance of labeled organisms as determined by T-RFLP community analysis is given in days (d). Specific CARD-FISH probes were used to visualize the morphology of identified alkane degraders within samples from SIP-incubations. Bars within pictures represent 2 μm. ^aPicture showing OP3 coccoid cells (visualized with probe Pla46) attached to larger cells from butane-enrichment cultures with Amon MV sediments.

In our incubations, OP3 species are assumed to live in a syntrophy with the dodecane degraders or as beneficiaries because parallel enrichments showed small coccoid-shaped OP3 cells attached to SCA-SRB1 members (Fig. III.4). iii). In addition, after 183 days (t₂) a third 512 bp T-RF was identified within the incubation with dodecane and corresponded to

uncultured species of the *Desulfobulbaceae*. Cultured members of the *Desulfobulbaceae* use end products such as short-chain fatty acids (Widdel & Pfennig, 1982). However, next related sequences of the identified *Desulfobulbaceae* are SEEP-SRB2 members, which have been exclusively found at marine hydrocarbon-seeps and a direct involvement in dodecane consumption cannot be ruled out (Fig. III.4).

Proteins in active alkane-degrading SRB as identified by protein-SIP

In addition to the phylogenetic information of active microorganisms obtained by DNA- and rRNA-based SIP, protein-SIP has the potential to identify enzymes and therefore catabolic pathways involved in hydrocarbon oxidation. Stable-isotope labeled proteins can directly be linked to microorganisms involved in alkane degradation. Also, the turnover/biosynthesis of proteins (labeling ratio) and the dependence on particular carbon sources can exactly be calculated (relative isotope abundance). This functional metaproteomic approach identified between 18 and 117 proteins for the two habitats and substrates (Table III.2).

Table III.2: Overview of the numbers of identified proteins in each sample, classified after their phylogenetic origin or ^{13}C -incorporation.

	Guaymas Basin		Amon Mud Volcano	
	Butane	Dodecane	Butane	Dodecane
Identified proteins	63	18	96	117
Bacterial proteins	38	6	69	85
Archaeal proteins	25	12	27	32
Proteins with ^{13}C-incorporation	11	5	31	23

The phylogenetic affiliation has to be carefully interpreted for most of the proteins as no metagenome or strain-resolved sequences were available and the peptide sequence identifications were based on highly conserved regions from genome-sequenced strains. This drawback was already observable in the ^{13}C -labeling of peptides because often only part of the protein-associated peptides were either labeled or unlabeled (see supplementary Table SIII.4), pointing towards different organisms that synthesize a similar protein. The small number of labeled proteins identified via protein-SIP supports that key players belong to specialists of the family *Desulfobacteraceae*. A more in-depth taxonomic classification within the *Desulfobacteraceae* was not possible.

The labeling ratio (LR) of the proteins, which is a measure of protein synthesis (Seifert et al., 2012), remained constant after the second sampling point in all Guaymas Basin

incubations and the Amon MV dodecane-incubations (Fig. III.1, supplementary Table SIII.4). This suggests that the ^{13}C -labeled organisms may have stopped their protein synthesis and/or were replaced by other organisms, which were not distinguishable with the obtained data. Similar observations regarding T-RF abundance between different time points were made during the DNA/rRNA-based SIP-experiments. The rapid increase of the LR between the first and second sampling point in the Guaymas Basin butane experiments suggested that active organisms posed only a small portion of the original community and protein synthesis was heavily induced by the addition of butane.

Metabolic pathways involved in alkane degradation

Highest numbers of labeled proteins were found in the Amon MV samples and as expected comprised several proteins involved in dissimilatory sulfate reduction (Table III.2 and supplementary Table III.S3). Furthermore, labeled proteins of the Wood–Ljungdahl pathway were found in Amon MV and Guaymas Basin samples, including CO dehydrogenase, acetyl-CoA synthase and formate-tetrahydrofolate ligase (also named formyltetrahydrofolate synthetase). These findings suggest the importance of the Wood-Ljungdahl pathway for the terminal oxidation of reduced hydrocarbons as well as acetate and acetyl-CoA as central metabolites during alkane degradation.

The relative isotope abundance (RIA) in peptides which ranged from 50% to 60% is an evidence for additional carbon sources besides the ^{13}C -labeled alkanes for biomass synthesis, through processes such as heterotrophic carbon fixation. Those carbon sources may be unlabeled hydrocarbons that naturally occurred in the sediments or carbon dioxide, which was discussed in a previous study about anoxic toluene-degrading *Peptococcaceae* (Winderl et al., 2010). Winderl and colleagues pointed out that incomplete ^{13}C -labeled DNA in strict anaerobes can be explained by reductive carboxylation of acetyl-CoA for assimilation reactions.

Especially for the Amon MV butane sample a very good correlation between the increase of RIA and DIC was obtained (see supplementary Fig. III.S1). At the third time point, the mass spectrum peptide pattern was slightly left-skewed (Fig. supplementary III.S1), which was discussed as an indication of a carbon source with increasing ^{13}C -content, e.g. the enrichment of $^{13}\text{CO}_2$ by ^{13}C -alkane degradation (Seifert et al., 2012). An additional pyruvate-flavodoxin oxidoreductase with one labeled peptide, from overall two peptides, was identified, which supported the given explanation and the possibly underestimated role of *Proteobacteria* on carbon cycling (Swan et al., 2011). Additional identified and labeled

proteins from all samples were mainly highly conserved proteins like chaperones, ATP synthases and K^+ -insensitive pyrophosphate-energized proton pumps. As the identification of a protein is dependent on its abundance, pyrophosphate-energized proton pumps seem to be expressed at a high level in the key players, suggesting an important role for secondary transport of nutrients, osmoregulation (Maeshim, 2001) or ATP regeneration (Keister & Minton, 1971). The additional search against a database with catabolic proteins revealed two clearly labeled (1-methylalkyl)succinate synthases (Mas) in the Amon MV butane samples. These *mas* genes are likely involved in the initial step during butane degradation in Amon MV sediments (supplementary Table IIIS.2). In addition, identical *mas* genes were detected in the corresponding dodecane-incubated samples. However, *mas* genes were found to be unlabeled in these samples and were therefore likely not involved in dodecane degradation.

Conclusions and Perspectives

The microbial degradation of hydrocarbons by SRB at marine seeps has been described for various habitats and was repeatedly investigated (e.g. Joye et al., 2004; Kallmeyer & Boetius, 2004). However, so far, our understanding of SRB capable to degrade hydrocarbons was constrained to cultured and enriched representatives. The present study closes the gap between detected biogeochemical evidence and the responsible community for hydrocarbon degradation at marine seeps. The combination of complementary approaches, i.e. PYRO-SIP and Protein-SIP, linked the taxonomic identification of alkane degraders with function and responsible proteins.

Our results suggest that four distinct phylogenetic groups within the *Desulfobacteraceae* are novel key players of short-chain and long-chain hydrocarbon degradation in two contrasting types of anoxic seep sediments. Based on this study, we conclude that in situ active alkane-degrading microorganisms are rather specialists than being generalists, which may also be true for diverse seep types, reflecting differing hydrocarbon compositions. Furthermore, the fact that three out of five primary alkane-degraders affiliated with uncultured groups suggests that ecologically important microorganisms still await their detailed characterization. This study underlines the great ecological relevance of the highly abundant DSS group within anaerobic alkane-oxidizing processes at marine seeps. Furthermore, obtained results for Amon MV sediments indicated that the degradation of short-chain alkanes likely starts, in general, with (1-methylalkyl)succinylation and ends with terminal oxidation by a reverse Wood–Ljungdahl pathway. In addition, this study gave further

evidence for the importance of heterotrophic CO₂ fixation for alkane-degrading SRB at marine seeps.

These identified diverse anaerobic hydrocarbon-oxidizing SRB likely contribute significantly to the carbon flux in marine seep sediments and to overall SR rates. Further investigation of their in situ turnover, e.g. as determined by Nanometer scale Secondary Ion Mass Spectrometry (NanoSIMS) analysis, should be the next step to reveal the environmental impact of alkane degraders.

Material and methods

Sample collection

Anoxic sediments were collected from a cold seep at Amon Mud Volcano and a hydrothermal vent site at Guaymas Basin in 2009 during the cruises MSM13-3 (RV Maria S. Merian; ROVQUEST4000, MARUM) and AT 15-56 (RV Atlantis, submersible Alvin), respectively. Sediment samples from Amon Mud Volcano of the Nile Deep Sea Fan were collected from 2-20 cm below a microbial mat during dive 240, station 929 (PANGAEA EventLabel MSM13/3_929-1_PUC1; MSM13/3_929-1_PUC9, MSM13/3_929-1_PUC20; water depth 1122 m, 32°20.1321N, 31°42.6543E). A description of the sediment sampling site can be found elsewhere (Grünke et al., 2011). Guaymas Basin in the central Gulf of California harbors petroleum-rich hydrothermal sediments, covered with organic-rich layers of buried sedimentary organic matter. Hydrothermal fluids contain remarkable concentrations of hydrocarbons including alkanes and aromatic hydrocarbons (Didyk & Simoneit, 1989). Fine-grained sediment samples below a white *Beggiatoa* mat from 0-10 cm sediment depth (push cores 9 and 10, water depth 2010 m, 27°0.696N, 111°24.265W) with conspicuous hydrocarbon smell were collected during dive 4573 with the submersible Alvin.

Stable-isotope probing incubations

Sediments were stored for about 4 months at 4°C while pre-incubations were carried out with a subset of sediments, in order to select sediments with highest alkane-degrading microbial activities as determined by sulfide- and ¹³CO₂-production. For SIP-incubations, 15 mL sediment slurries (1:1 v/v with artificial anoxic seawater; Widdel & Bak., 1992) under anoxic atmosphere (N₂/CO₂ 90/10 v/v) were sacrificed per time point and method (rRNA- or DNA-SIP and Protein-SIP). Fully ¹³C-labeled butane or dodecane (Campro Scientific, Germany) were added to incubations, while unlabeled butane or dodecane were used for control

incubations. Hydrocarbon concentrations in our experiments (2.1 mM butane; 1.8 mM dodecane) exceeded the natural concentrations by >100× to prevent substrate-diffusion limitations for the bacteria. However, butane is a natural substrate at both seeps types (Amon MV station 929: 0.5-1.1 μM butane in 0-8 cm depth; Guaymas Basin at a site close by: 6-16 μM butane in 0-8 cm depth; M. Kellermann, pers. communication), while dodecane is often found at hydrocarbon seeps from Guaymas Basin (cf. Bazylnski et al., 1988). Sediments were incubated at 20°C and 28°C for Amon Mud Volcano and Guaymas Basin sites, respectively. Time points for sampling were chosen based on sulfide production: 9, 15 and 29 days for Amon Mud Volcano incubations with butane as well as 158, 204 and 309 days for dodecane-amended experiments, 57, 71 and 113 days for Guaymas Basin butane-experiments as well as at 115, 183 and 232 days for dodecane-incubations. Sediments were centrifuged (10 min, 4000× g) and pellets stored at -80°C. For FISH analysis 0.5 mL sediment slurries from SIP-incubations were fixed for 1 h at 4°C with a final concentration of 1% PFA, washed with PBS and stored in 1.5 mL 1:1 ethanol/PBS at -20°C.

Chemical analysis

Sulfide was quantified photometrically as colloidal CuS as described elsewhere (Cord-Ruwisch, 1985). Butane concentrations were measured by gas-chromatographic head-space analysis (oven 110°C, injector 150°C, detector 280°C, nitrogen carrier gas) as shown before (Musat & Widdel, 2008). The C-isotopic composition of dissolved inorganic carbon (DIC) from sediment slurries was analyzed using gas chromatography combustion isotope ratio mass spectrometry (GC-IRMS; Fisons VG Optima) as described before (Assayag et al., 2006). DIC-controls were killed with a final concentration of 4% paraformaldehyde at the beginning of the experiment.

CARD-FISH and Acridine Orange staining

In situ hybridizations with horseradish peroxidase (HRP)-labeled probes followed by fluorescently-labeled-tyramide signal amplification (catalyzed reporter deposition; CARD) were carried out as described previously (Pernthaler et al., 2002; Kleindienst et al., *submitted*). Probe sequences (probes ordered from biomers.net; Ulm, Germany) and formamide concentrations required for specific hybridization are given in supplementary Table III.S1. To determine the total number of single cells with Acridine Orange (AO), sediment sections were preserved and stored in artificial seawater with 2% formalin. Staining was performed according to previously described methods (Meyer-Reil, 1983; Boetius & Lochte, 1996).

Nucleic acid extractions, ultracentrifugation, real-time PCR and T-RFLP fingerprinting

Total RNA or DNA was directly extracted from 3-4 g of incubated sediments and stored at -80°C after SIP-sampling. RNA was extracted from Amon Mud Volcano sediments, while DNA extraction was chosen from Guaymas Basin sediments because RNA yielded in insufficient amounts for later on analysis. RNA was extracted with bead-beating in TCA-buffer (McIlroy et al., 2008), followed by phenol-chloroform extraction and two isopropanol precipitations for 12 h at -20°C. DNA was extracted with a method based on three different lyses mechanisms according to Zhou and colleagues (Zhou et al., 1996). A second isopropanol precipitation for 12 h at -20°C was applied. For ultracentrifugation 5 µg of DNA and 750 ng of RNA were loaded onto a gradient medium of CsCl (average density 1.71 g ml⁻¹, Calbiochem, Merck, Darmstadt, Germany) in gradient buffer (0.1 M Tris-HCl at pH 8, 0.1 M KCl, 1 mM EDTA) or CsTFA (average density 1.795 g ml⁻¹, Amersham Pharmacia Biotech) in gradient buffer as described elsewhere (Lueders, 2010). Fractionation of gradients, refractometric measurement of fraction buoyant density, and precipitation of nucleic acids was done as published before (Lueders, 2010). Distributions of DNA or RNA within the gradients was analyzed using bacterial 16S rRNA gene-targeted real-time PCR and real-time reverse-transcription PCR in an Mx3000P cycler (Stratagene, La Jolla, CA, USA) with the primers Ba519f/Ba907r (Lane, 1991) as described (Kunapuli et al., 2007; Glaubitz et al., 2009). Fractions containing notable amounts ‘light’ and ‘heavy’ nucleic acids were selected for bacterial 16S rRNA (gene)-targeted terminal restriction fragment length polymorphism (T-RFLP) fingerprinting as reported (Pilloni et al., 2011). Fingerprinting data was analyzed with T-REX (Culman et al., 2009). Background noise filtering (Abdo et al., 2006) was on the default factor 1.2, clustering threshold for aligning peaks across the samples was set to 1.5 bp using T-Align (Smith et al., 2005). Relative T-RF abundance was inferred from peak heights. For reduction of data complexity, T-RFs that occurred in less than 10% of the samples were excluded from further analysis.

Amplicon pyrosequencing, taxonomic classification and phylogenetic reconstruction

454-pyrosequencing was performed with untreated sediments samples as well as high density gradient fractions from ¹³C-labeled nucleic acids of active organisms. Amplicons for bidirectional pyrotag sequencing were prepared as reported (Pilloni et al., 2011). PCR conditions and forward-primer were the same as for T-RFLP. PCR-amplicons were purified and pooled in mixes of ~15 (1/8th FLX plate) or ~30 (for 1/4th FLX plate) and processed as recommended by the manufacturer. Emulsion PCR, emulsion breaking and sequencing were

performed applying the GS FLX Titanium chemistry and using a 454 GS FLX pyrosequencer (Roche), initial data processing and read quality trimming was done as reported (Pilloni et al., 2011). Taxonomic classification was done using a SILVA (SSURef-108) based NGS-pipeline. For T-RF prediction of sequenced amplicons forward- and reverse-reads were assembled into contigs as described (Pilloni et al., 2011). Subsequently, dominating amplicon contigs were again taxonomically classified using a SILVA (SSURef-108) based NGS-pipeline and imported into an ARB (Ludwig et al., 2004) database (version SSURef-108, Sep 2011). T-RFs of contigs were predicted using TRiFle (Junier et al., 2008) and ARB_EDIT4. Phylogenetic trees showing the affiliation of the assembled contigs were calculated by neighbor-joining and maximum-likelihood analysis with different sets of filters. For tree calculation, only nearly full-length sequences were considered. Partial sequences were integrated into the reconstructed tree by parsimony criteria by maintaining the overall tree topology. The selected amplicon contigs used for phylogenetic analysis are available in the EMBL, GenBank and DDBJ nucleotide sequence databases under the accession numbers HE797917 - HE797929.

Protein extraction and separation

For Protein-SIP all three sampling points, of each experiment, were analyzed. For direct protein extraction 2 g of incubated sediments were suspended in 5.4 mL extraction buffer (50 mM Tris/HCl, 1 mM PMSF, 0.1 mg ml⁻¹chloramphenicol). The slurry was subjected to 3 cycles of freeze (in liquid nitrogen) and thaw (water bath at 65°C) with the addition of 0.6 mL of SDS (10% w/v) before the last thaw. After Phenol extraction and acetate precipitation of the organic and aqueous phase, according to Benndorf et al. (Benndorf et al., 2009), pellets were resolved in SDS sample buffer and subjected to SDS-PAGE (Laemmli, 1970).

Mass Spectrometry

Five sections of each lane were excised from a SDS-PAGE, sections were de-stained and subsequently proteolytically digested overnight at 37°C by trypsin (Sigma, Munich, Germany) according to Jehmlich et al. (Jehmlich et al., 2008). Eluted peptides from the aqueous phase gel slices were combined and all peptide extracts were purified and concentrated using the 14 C18 Zip Tip columns (Millipore), resulting in 6 peptide samples per experimental sample. For LTQ-Orbitrap mass spectrometer analysis, peptides were reconstituted in 0.1% formic acid. Samples were injected by the autosampler and concentrated on a trapping column (nanoAcquity UPLC column, C18, 180 µm x 2 cm, 5 µm, Waters) with water containing 0.1%

formic acid at flow rates of $15 \mu\text{l}^{-1} \text{min}^{-1}$. After 6 min, the peptides were eluted into a separation column (nanoAcquity UPLC column, C18, $75 \mu\text{m} \times 15 \text{cm}$, $1.75 \mu\text{m}$, Waters). Chromatography was performed with 0.1% formic acid in solvent A (100% water) and B (100% acetonitrile). To elute the peptides the solvent B gradient was set in the first 54 min from 2 to 20% solvent B and subsequently 28 min from 20 to 85% solvent B using a nano-high pressure liquid chromatography system (nanoAcquity UPLC, Waters) coupled to an LTQ-Orbitrap mass spectrometer (Thermo Fisher Scientific). For an unbiased analysis continuous scanning of eluted peptide ions was carried out between 300-2000 m/z, automatically switching to MS/MS Collision-induced dissociation (CID) mode on ions exceeding an intensity of 3000. For MS/MS CID measurements a dynamic precursor exclusion of 3 min was enabled.

Peptide identification

First a survey search using Mascot (Perkins et al., 1999) against all entries of NCBI nr was performed. The main search utilized MaxQuant version 1.1.1.36 (Cox & Mann, 2008) and an artificial metagenome which was created according to 16S rRNA results and the prior survey search. This included all entries available from Uniprot database (www.uniprot.org) belonging to *Desulfobacterales*, *Syntrophobacterales*, *Thiomicrospira crunogena*, *Archaea* environmental samples and their associated sub-branches on April 5th 2011. Furthermore contaminants and reverse entries as decoys were added automatically by MaxQuant. Analysis of all fractions was done simultaneously, combining all corresponding gel slices per sample to one experiment. For peptide identification MaxQuant uses Andromeda (Cox et al., 2011). Cysteine carbamidomethylation was searched as a fixed modification, whereas methionine oxidation was searched as variable modification. The maximal false discovery rate was set to 1% for peptides. The offered first search was performed with a mass tolerance of 20 ppm against a smaller version of the database with proteins already identified in the survey search. Proteins were regarded as identified soundly if at least two peptides were found. Besides this the standard MaxQuant settings were used. A separate search against a database of published and unpublished sequences of catabolic genes of anaerobic alkane degradation was performed with the same settings.

Protein relative isotope-abundance and protein labeling-ratio

MS¹ spectra of identified peptides were extracted using the Qual Browser (v. 2.0.7 SP1, Thermo Fisher). The extracted mass spectrometric data were used to calculate the RIA and

LR using an in-house Excel (Microsoft) script. Information regarding the calculations and the script itself can be found elsewhere (Snijders et al., 2005; Seifert et al., 2012).

Acknowledgements

We would like to thank Antje Boetius, Janine Felden, Andreas Teske, Gunter Wegener and Thomas Holler (MPI Bremen) for sediment sampling. We acknowledge the officers, crews, and shipboard scientific parties of the cruises MSM13-3 and AT 15-56 in 2009. Samples were obtained via funding of the EU FP6 program HERMIONE (contract number 226354) and the DFG (METEOR/MERIAN SPP, MSM13-3 awarded to Antje Boetius) and the Max Planck Society. We especially acknowledge Gaute Lavik, Tim Kalvelage (MPI, Bremen), Katrin Hörmann, Giovanni Pilloni and Marion Engel (Helmholtz Zentrum, München) for analytical support as well as Marion Stagars (MPI, Bremen) and Matthias Kellermann (MARUM, Bremen) for sharing unpublished data. We would like to thank Barbara MacGregor for sharing RNA extraction protocols. This study is part of the DFG Priority Program SPP1319 “Transformation of hydrocarbons under anoxic conditions: from molecular to global scale” within the Deutsche Forschungsgemeinschaft. Further support was provided by the Max Planck Society, Germany and the EU-MAGICPAH project.

References

- Abdo Z, Schütte UME, Bent SJ, Williams CJ, Forney LJ, and Joyce P. (2006). Statistical methods for characterizing diversity of microbial communities by analysis of terminal restriction fragment length polymorphisms of 16S rRNA genes. *Environ Microbiol* **8**: 929 - 938.
- Abed RMM, Musat N, Musat F, and Mußmann M. (2011). Structure of microbial communities and hydrocarbon-dependent sulfate reduction in the anoxic layer of a polluted microbial mat. *Mar Pollut Bull* **62**: 539-546.
- Aeckersberg F, Bak F, and Widdel F. (1991). Anaerobic oxidation of saturated-hydrocarbons to CO₂ by a new type of sulfate-reducing bacterium. *Arch Microbiol* **156**: 5-14.
- Aeckersberg F, Rainey FA, and Widdel F. (1998). Growth, natural relationships, cellular fatty acids and metabolic adaptation of sulfate-reducing bacteria that utilize long-chain alkanes under anoxic conditions. *Arch Microbiol* **170**: 361-369.
- Alfreider A, Vogt C, and Babel W. (2002). Microbial diversity in an in situ reactor system treating monochlorobenzene contaminated groundwater as revealed by 16S ribosomal DNA analysis. *Syst Appl Microbiol* **25**: 232-240.
- Alonso C, Gómez-Pereira P, Ramette A, Ortega L, Fuchs BM, and Amann R. (2010). Multilevel analysis of the bacterial diversity along the environmental gradient Río de la Plata – South Atlantic Ocean. *Aquat Microb Ecol* **61**: 57-72.
- Anderson RK, Scalan RS, Parker PL, and Behrens EW. (1983). Seep oil and gas in Gulf of Mexico slope sediment. *Science* **222**: 619-621.
- Assayag N, Rivé K, Ader M, Jézéquel D, and Agrinier P. (2006). Improved method for isotopic and quantitative analysis of dissolved inorganic carbon in natural water samples. *Rapid Commun Mass Spectrom* **20**: 2243-2251.
- Bazylinski DA, Farrington JW, and Jannasch HW. (1988). Hydrocarbons in surface sediments from a Guaymas Basin hydrothermal vent site. *Org Geochem* **12**: 547-558.
- Benndorf D, Vogt C, Jehmlich N, Schmidt Y, Thomas H, Woffendin G, Shevchenko A, Richnow H-H, and von Bergen M. (2009). Improving protein extraction and separation methods for investigating the metaproteome of anaerobic benzene communities within sediments. *Biodegradation* **20**: 737-750.
- Biddle JF, Cardman Z, Mendlovitz H, Albert DB, Lloyd KG, Boetius A, and Teske A. (2011). Anaerobic oxidation of methane at different temperature regimes in Guaymas Basin hydrothermal sediments. *ISME J* **6**: 1018-1031.
- Boetius A and Lochte K. (1996). Effect of organic enrichments on hydrolytic potentials and growth of bacteria in deep-sea sediments. *Mar Ecol-Progr Ser* **140**: 239-250.
- Byrne JV and Emery KO. (1960). Sediments of the Gulf of California. *Geol Soc Am Bull* **71**: 983-1010.
- Chouari R, Le Paslier D, Daegelen P, Ginestet P, Weissenbach J, and Sghir A. (2003). Molecular evidence for novel planctomycete diversity in a municipal wastewater treatment plant. *Appl Environ Microbiol* **69**: 7354-7363.
- Cord-Ruwisch R. (1985). A quick method for the determination of dissolved and precipitated sulfides in cultures of sulfate-reducing bacteria. *J Microbiol Methods* **4**: 33-36.
- Cox J and Mann M. (2008). MaxQuant enables high peptide identification rates, individualized p.p.b.-range mass accuracies and proteome-wide protein quantification. *Nat Biotech* **26**: 1367-1372.
- Cox J, Neuhauser N, Michalski A, Scheltema RA, Olsen JV, and Mann M. (2011). Andromeda: A peptide search engine integrated into the MaxQuant environment. *J Proteome Res* **10**: 1794-1805.
- Cravo-Laureau C, Matheron R, Joulain C, Cayol JL, and Hirschler-Rea A. (2004). *Desulfatibacillum alkenivorans* sp nov., a novel *n*-alkene-degrading, sulfate-reducing

- bacterium, and emended description of the genus *Desulfatibacillum*. *Int J Syst Evol Microbiol* **54**: 1639-1642.
- Culman S, Bukowski R, Gauch H, Cadillo-Quiroz H, and Buckley D. (2009). T-REX: software for the processing and analysis of T-RFLP data. *BMC Bioinformatics* **10**: 171.
- Davidova IA, Duncan KE, Choi OK, and Suflita JM. (2006). *Desulfoglaeba alkanexedens* gen. nov., sp. nov., an *n*-alkane-degrading, sulfate-reducing bacterium. *Int J Syst Evol Microbiol* **56**: 2737-2742.
- Dhillon A, Teske A, Dillon J, Stahl DA, and Sogin ML. (2003). Molecular characterization of sulfate-reducing bacteria in the Guaymas Basin. *Appl Environ Microbiol* **69**: 2765-2772.
- Didyk BM and Simoneit BRT. (1989). Hydrothermal oil of Guaymas Basin and implications for petroleum formation mechanisms. *Nature* **342**: 65-69.
- Galushko A, Minz D, Schink B, and Widdel F. (1999). Anaerobic degradation of naphthalene by a pure culture of a novel type of marine sulphate-reducing bacterium. *Environ Microbiol* **1**: 415-420.
- Glaubitx S, Lueders T, Abraham WR, Jost G, Jürgens K, and Labrenz M. (2009). ¹³C-isotope analyses reveal that chemolithoautotrophic *Gamma*- and *Epsilon*proteobacteria feed a microbial food web in a pelagic redoxcline of the central Baltic Sea. *Environ Microbiol* **11**: 326-337.
- Grünke S, Felden J, Lichtschlag A, Girth AC, de Beer D, Wenzhöfer F, and Boetius A. (2011). Niche differentiation among mat-forming, sulfide-oxidizing bacteria at cold seeps of the Nile Deep Sea Fan (Eastern Mediterranean Sea). *Geobiology* **9**: 330-348.
- Halm H, Musat N, Lam P, Langlois R, Musat F, Peduzzi S, Lavik G, Schubert CJ, Singha B, LaRoche J, and Kuypers MMM. (2009). Co-occurrence of denitrification and nitrogen fixation in a meromictic lake, Lake Cadagno (Switzerland). *Environ Microbiol* **11**: 1945-1958.
- Harms G, Zengler K, Rabus R, Aeckersberg F, Minz D, Rosselló-Móra R, and Widdel F. (1999). Anaerobic oxidation of *o*-xylene, *m*-xylene, and homologous alkylbenzenes by new types of sulfate-reducing bacteria. *Appl Environ Microbiol* **65**: 999-1004.
- Higashioka Y, Kojima H, Nakagawa T, Sato S, and Fukui M. (2009). A novel *n*-alkane-degrading bacterium as a minor member of *p*-xylene-degrading sulfate-reducing consortium. *Biodegradation* **20**: 383-390.
- Holler T, Widdel F, Knittel K, Amann R, Kellermann MY, Hinrichs K-U, Teske A, Boetius A, and Wegener G. (2011). Thermophilic anaerobic oxidation of methane by marine microbial consortia. *ISME J* **5**: 1946-1956.
- Hugenholtz P, Pitulle C, Hershberger KL, and Pace NR. (1998). Novel division level bacterial diversity in a Yellowstone hot spring. *J Bacteriol* **180**: 366-376.
- Jaekel U. (2011). Anaerobic oxidation of short-chain and cyclic alkanes by sulfate-reducing bacteria. Doctoral dissertation, University Bremen.
- Jehmlich N, Schmidt F, Hartwich M, von Bergen M, Richnow H-H, and Vogt C. (2008). Incorporation of carbon and nitrogen atoms into proteins measured by protein-based stable isotope probing (Protein-SIP). *Rapid Commun Mass Spectrom* **22**: 2889-2897.
- Joye SB, Boetius A, Orcutt BN, Montoya JP, Schulz HN, Erickson MJ, and Lugo SK. (2004). The anaerobic oxidation of methane and sulfate reduction in sediments from Gulf of Mexico cold seeps. *Chem Geol* **205**: 219-238.
- Junier P, Junier T, and Witzel K-P. (2008). TRiFLe: a program for in silico T-RFLP analysis with user-defined sequences sets. *Appl Environ Microbiol* **74**: 6452-6456.
- Kallmeyer J and Boetius A. (2004). Effects of temperature and pressure on sulfate reduction and anaerobic oxidation of methane in hydrothermal sediments of Guaymas Basin. *Appl Environ Microbiol* **70**: 1231-1233.

- Keister DL and Minton NJ. (1971). ATP synthesis driven by inorganic pyrophosphate in *Rhodospirillum rubrum* chromatophores. *Biochem Biophys Res Commun* **42**: 932-939.
- Kennicutt II MC, Brooks JM, Bidigare RR, and Denoux GJ. (1988a). Gulf of Mexico hydrocarbon seep communities-I. Regional distribution of hydrocarbon seepage and associated fauna. *Deep-Sea Res* **35**: 1639-1651.
- Kennicutt II MC, Brooks JM, and Denoux GJ. (1988b). Leakage of deep, reservoired petroleum to the near-surface on the Gulf of Mexico continental-slope. *Mar Chem* **24**: 39-59.
- Kleindienst S, Ramette A, Amann R, and Knittel K. (*submitted*). Distribution and in situ abundance of sulfate-reducing bacteria in diverse marine hydrocarbon seep sediments. *Environ Microbiol*
- Kniemeyer O, Fischer T, Wilkes H, Glöckner FO, and Widdel F. (2003). Anaerobic degradation of ethylbenzene by a new type of marine sulfate-reducing bacterium. *Appl Environ Microbiol* **69**: 760-768.
- Kniemeyer O, Musat F, Sievert SM, Knittel K, Wilkes H, Blumenberg M, Michaelis W, Classen A, Bolm C, Joye SB, and Widdel F. (2007). Anaerobic oxidation of short-chain hydrocarbons by marine sulphate-reducing bacteria. *Nature* **449**: 898-910.
- Köchling T, Lara-Martín P, González-Mazo E, Amils R, and Sanz JL. (2011). Microbial community composition of anoxic marine sediments in the Bay of Cádiz (Spain). *Int Microbiol* **14**: 143-154.
- Kunapuli U, Lueders T, and Meckenstock RU. (2007). The use of stable isotope probing to identify key iron-reducing microorganisms involved in anaerobic benzene degradation. *ISME J* **1**: 643-653.
- Laemmli UK. (1970). Cleavage of structural proteins during the assembly of the head of bacteriophage T4. *Nature* **227**: 680-685.
- Lane DJ. (1991) in *Nucleic acid techniques in bacterial systematics*, edited by E Stackebrandt and M Goodfellow (John Wiley & Sons, New York, NY), Vol. 6, pp. 115–175.
- Liu A, Garcia-Dominguez E, Rhine ED, and Young LY. (2004). A novel arsenate respiring isolate that can utilize aromatic substrates. *FEMS Microbiol Ecol* **48**: 323-332.
- Lösekan T, Knittel K, Nadalig T, Fuchs B, Niemann H, Boetius A, and Amann R. (2007). Diversity and abundance of aerobic and anaerobic methane oxidizers at the Haakon Mosby Mud Volcano, Barents Sea. *Appl Environ Microbiol* **73**: 3348-3362.
- Ludwig W, Strunk O, Westram R, Richter L, Meier H, Yadhukumar, Buchner A, Lai T, Steppi S, Jobb G, Förster W, Brettske I, Gerber S, Ginhart AW, Gross O, Grumann S, Hermann S, Jost R, König A, Liss T, Lüßmann R, May M, Nonhoff B, Reichel B, Strehlow R, Stamatakis A, Stuckmann N, Vilbig A, Lenke M, Ludwig T, Bode A, and Schleifer KH. (2004). ARB: a software environment for sequence data. *Nucleic Acids Res* **32**: 1363-1371.
- Lueders T. (2010) in *Handbook of hydrocarbon and lipid microbiology*, edited by Kenneth N. Timmis (Springer, Berlin, Heidelberg), Vol. 5, pp. 4011-4026.
- Maeshim M. (2001). Tonoplast transporters: organization and function. *Annu Rev of Plant Phys* **52**: 469-497.
- Martinez RJ, Mills HJ, Story S, and Sobecky PA. (2006). Prokaryotic diversity and metabolically active microbial populations in sediments from an active mud volcano in the Gulf of Mexico. *Environ Microbiol* **8**: 1783-1796.
- Mastalerz V, de Lange GJ, and Dählmann A. (2009). Differential aerobic and anaerobic oxidation of hydrocarbon gases discharged at mud volcanoes in the Nile deep-sea fan. *Geochim Cosmochim Acta* **73**: 3849-3863.
- Mastalerz V, de Lange GJ, Dählmann A, and Feseker T. (2007). Active venting at the Isis mud volcano, offshore Egypt: Origin and migration of hydrocarbons. *Chem Geol* **246**: 87-106.

- McIlroy S, Porter K, Seviour RJ, and Tillett D. (2008). A simple and safe method for the simultaneous isolation of microbial RNA and DNA from problematic populations. *Appl Environ Microbiol* **74**: 6806-6807.
- Meckenstock RU, Annweiler E, Michaelis W, Richnow HH, and Schink B. (2000). Anaerobic naphthalene degradation by a sulfate-reducing enrichment culture. *Appl Environ Microbiol* **66**: 2743-2747.
- Meyer-Reil LA. (1983). Benthic response to sedimentation events during autumn to spring at a shallow-water station in the western Kiel bight. *Mar Biol* **77**: 247-256.
- Mills HJ, Martinez RJ, Story S, and Sobecky PA. (2004). Identification of members of the metabolically active microbial populations associated with *Beggiatoa* species mat communities from Gulf of Mexico cold-seep sediments. *Appl Environ Microbiol* **70**: 5447-5458.
- Mills HJ, Martinez RJ, Story S, and Sobecky PA. (2005). Characterization of microbial community structure in Gulf of Mexico gas hydrates: comparative analysis of DNA- and RNA-derived clone libraries. *Appl Environ Microbiol* **71**: 3235-3247.
- Morasch B, Schink B, Tebbe CC, and Meckenstock RU. (2004). Degradation of o-xylene and m-xylene by a novel sulfate-reducer belonging to the genus *Desulfotomaculum*. *Arch Microbiol* **181**: 407-417.
- Musat F, Galushko A, Jacob J, Widdel F, Kube M, Reinhardt R, Wilkes H, Schink B, and Rabus R. (2009). Anaerobic degradation of naphthalene and 2-methylnaphthalene by strains of marine sulfate-reducing bacteria. *Environ Microbiol* **11**: 209-219.
- Musat F and Widdel F. (2008). Anaerobic degradation of benzene by a marine sulfate-reducing enrichment culture, and cell hybridization of the dominant phylotype. *Environ Microbiol* **10**: 10-19.
- Niemann H, Lösekann T, de Beer D, Elvert M, Nadalig T, Knittel K, Amann R, Sauter EJ, Schlüter M, Klages M, Foucher JP, and Boetius A. (2006). Novel microbial communities of the Haakon Mosby mud volcano and their role as a methane sink. *Nature* **443**: 854-858.
- Ommedal H and Torsvik T. (2007). *Desulfotignum toluenicum* sp. nov., a novel toluene-degrading, sulphate-reducing bacterium isolated from an oil-reservoir model column. *Int J Syst Evol Microbiol* **57**: 2865-2869.
- Omeregic EO, Niemann H, Mastalerz V, de Lange GJ, Stadnitskaia A, Mascle J, Foucher JP, and Boetius A. (2009). Microbial methane oxidation and sulfate reduction at cold seeps of the deep Eastern Mediterranean Sea. *Mar Geology* **261**: 114-127.
- Orcutt BN, Joye SB, Kleindienst S, Knittel K, Ramette A, Reitz A, Samarkin V, Treude T, and Boetius A. (2010). Impact of natural oil and higher hydrocarbons on microbial diversity, distribution, and activity in Gulf of Mexico cold-seep sediments. *Deep-Sea Res Pt II* **57**: 2008-2021.
- Orphan VJ, Hinrichs K-U, Ussler W, Paull CK, Taylor LT, Sylva SP, Hayes JM, and DeLong EF. (2001). Comparative analysis of methane-oxidizing archaea and sulfate-reducing bacteria in anoxic marine sediments. *Appl Environ Microbiol* **67**: 1922-1934.
- Pachiadaki M, Kallionaki A, Dählmann A, De Lange G, and Kormas K. (2011). Diversity and spatial distribution of prokaryotic communities along a sediment vertical profile of a deep-sea mud volcano. *Microb Ecol* **62**: 655-668.
- Pachiadaki MG, Lykousis V, Stefanou EG, and Kormas KA. (2010). Prokaryotic community structure and diversity in the sediments of an active submarine mud volcano (Kazan mud volcano, East Mediterranean Sea). *FEMS Microbiol Ecol* **72**: 429-444.
- Perkins DN, Pappin DJC, Creasy DM, and Cottrell JS. (1999). Probability-based protein identification by searching sequence databases using mass spectrometry data. *Electrophoresis* **20**: 3551-3567.

- Pernthaler A, Dekas AE, Brown CT, Goffredi SK, Embaye T, and Orphan VJ. (2008). Diverse syntrophic partnerships from deep-sea methane vents revealed by direct cell capture and metagenomics. *Proc Natl Acad Sci USA* **105**: 7052-7057.
- Pernthaler A, Pernthaler J, and Amann R. (2002). Fluorescence in situ hybridization and catalyzed reporter deposition for the identification of marine bacteria. *Appl Environ Microbiol* **68**: 3094-3101.
- Pilloni G, von Netzer F, Engel M, and Lueders T. (2011). Electron acceptor-dependent identification of key anaerobic toluene degraders at a tar-oil-contaminated aquifer by Pyro-SIP. *FEMS Microbiol Ecol* **78**: 165-175.
- Rabus R, Nordhaus R, Ludwig W, and Widdel F. (1993). Complete oxidation of toluene under strictly anoxic conditions by a new sulfate-reducing bacterium. *Appl Environ Microbiol* **59**: 1444-1451.
- Rotarua A-E, Schauera R, Probiana C, Mußmann M, and Harder J. (*in press*). Visualization of candidate division OP3 cocci in limonene degrading methanogenic cultures. *J Microbiol Biotech*
- Sassen R, Roberts HH, Carney R, Milkov AV, DeFreitas DA, Lanoil B, and Zhang C. (2004). Free hydrocarbon gas, gas hydrate, and authigenic minerals in chemosynthetic communities of the northern Gulf of Mexico continental slope: relation to microbial processes. *Chem Geol* **205**: 195-217.
- Seifert J, Taubert M, Jehmlich N, Schmidt F, Völker U, Vogt C, Richnow H-H, and von Bergen M. (2012). Protein-based stable isotope probing (protein-SIP) in functional metaproteomics. *Mass Spectrometry Reviews* DOI: 10.1002/mas.21346.
- Shigematsu T, Era S, Mizuno Y, Ninomiya K, Kamegawa Y, Morimura S, and Kida K. (2006). Microbial community of a mesophilic propionate-degrading methanogenic consortium in chemostat cultivation analyzed based on 16S rRNA and acetate kinase genes. *Appl Microbiol Biotechnol* **72**: 401-415.
- Simoneit BRT and Lonsdale PF. (1982). Hydrothermal petroleum in mineralized mounds at the seabed of Guaymas Basin. *Nature* **295**: 198-202.
- Smith CJ, Danilowicz BS, Clear AK, Costello FJ, Wilson B, and Meijer WG. (2005). T-Align, a web-based tool for comparison of multiple terminal restriction fragment length polymorphism profiles. *FEMS Microbiol Ecol* **54**: 375 - 380.
- Snijders APL, de Koning B, and Wright PC. (2005). Perturbation and interpretation of nitrogen isotope distribution patterns in proteomics. *J Proteome Res* **4**: 2185-2191.
- So CM and Young LY. (1999). Isolation and characterization of a sulfate-reducing bacterium that anaerobically degrades alkanes. *Appl Environ Microbiol* **65**: 2969-2976.
- Swan BK, Martinez-Garcia M, Preston CM, Sczyrba A, Woyke T, Lamy D, Reinthaler T, Poulton NJ, Masland EDP, Gomez ML, Sieracki ME, DeLong EF, Herndl GJ, and Stepanauskas R. (2011). Potential for chemolithoautotrophy among ubiquitous bacteria lineages in the dark ocean. *Science* **333**: 1296-1300.
- Tang Y-Q, Shigematsu T, Morimura S, and Kida K. (2007). Effect of dilution rate on the microbial structure of a mesophilic butyrate-degrading methanogenic community during continuous cultivation. *Appl Microbiol Biotechnol* **75**: 451-465.
- Teske A, Hinrichs K-U, Edgcomb V, de Vera Gomez A, Kysela D, Sylva SP, Sogin ML, and Jannasch HW. (2002). Microbial diversity of hydrothermal sediments in the Guaymas Basin: evidence for anaerobic methanotrophic communities. *Appl Environ Microbiol* **68**: 1994-2007.
- Uyttebroek M, Breugelmans P, Janssen M, Wattiau P, Joffe B, Karlson U, Ortega-Calvo JJ, Bastiaens L, Ryngaert A, Hausner M, and Springael D. (2006). Distribution of the *Mycobacterium* community and polycyclic aromatic hydrocarbons (PAHs) among different size fractions of a long-term PAH-contaminated soil. *Environ Microbiol* **8**: 836-847.

- Widdel F and Bak. F. (1992) in *The prokaryotes*, edited by A. Balows, H. G. Truper, M. Dworkin et al. (Springer-Verlag, New York), pp. 3352-3378.
- Widdel F, Knittel K, and Galushko A. (2010) in *Handbook of hydrocarbon and lipid microbiology*, edited by K.N. Timmis, T. McGenity, J. R. van der Meer et al. (Springer Berlin Heidelberg), Vol. 3, pp. 1997-2021.
- Widdel F and Pfennig N. (1982). Studies on dissimilatory sulfate-reducing bacteria that decompose fatty acids II. Incomplete oxidation of propionate by *Desulfobulbus propionicus* gen. nov., sp. nov. *Arch Microbiol* **131**: 360-365.
- Winderl C, Penning H, von Netzer F, Meckenstock RU, and Lueders T. (2010). DNA-SIP identifies sulfate-reducing *Clostridia* as important toluene degraders in tar-oil-contaminated aquifer sediment. *ISME J* **4**: 1314-1325.
- Zhang F, She Y, Zheng Y, Zhou Z, Kong S, and Hou D. (2010). Molecular biologic techniques applied to the microbial prospecting of oil and gas in the Ban 876 gas and oil field in China. *Appl Microbiol Biotechnol* **86**: 1183-1194.
- Zhao C, Gao Z, Qin Q, and Ruan L. (*in press*). *Mangroviflexus xiamenensis* gen. nov., sp. nov., a member of the family *Marinilabiaceae* isolated from mangrove sediment. *Int J Syst Evol Microbiol* doi: 10.1099/ijms.1090.036137-036130
- Zhou J, Bruns MA, and Tiedje JM. (1996). DNA recovery from soils of diverse composition. *Appl Environ Microbiol* **62**: 316-322.

Supplementary Information

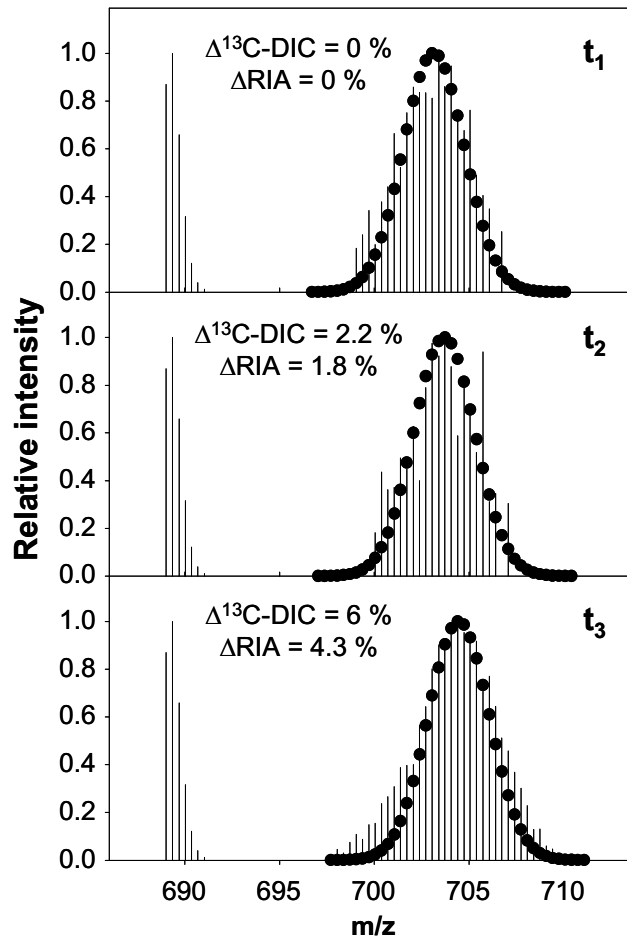


Fig. III.S1. Development of ^{13}C -incorporation into the proteome during butane incubation of Amon MV sediment visualized by mass spectrometry. The mass spectrum of peptide FTTLAGVMGGASSPGFVGHSK of carbon monoxide dehydrogenase/acetyl-CoA synthase subunit alpha (E1YL47) is shown. The natural isotopic distribution is found with an m/z of 689.01 and was artificially added to the spectrum for better illustration. Black dots represent the best fit of the Gaussian distribution model. The $\Delta^{13}\text{C-DIC}$ value shown is equivalent to 50% of the $^{13}\text{C-DIC}$ increase between time points. The slight increase of the RIA (shift to the right) correlates to approximately 50% of CO_2 -fixation as carbon source for biomass production. Furthermore a light skewness to the left is visible at t_3 , which is an evidence for increasing ^{13}C -content of used substrates.

Table SIII.1: Oligonucleotide probes used in this study

Probe name	Specificity	Forma- mide [%]	Sequence (5' to 3')	Reference
Delta495a	Most <i>Deltaproteobacteria</i> and <i>Gemmatimonadetes</i>	30	AGT TAG CCG GTG CTT CCT	Loy et al., 2002
cDelta495a	Competitor for Delta495a	-	AGT TAG CCG GTG CTT CTT	Macalady et al., 2006
Del495b	Some <i>Deltaproteobacteria</i>	30	AGT TAG CCG GCG CTT CCT	Loy et al., 2002
cDelta495b	Competitor for Delta495a	-	AGT TAG CCG GCG CTT CKT	Macalady et al., 2006
Delta495c	Some <i>Deltaproteobacteria</i>	30	AAT TAG CCG GTG CTT CCT	Loy et al., 2002
cDelta495c	Competitor for Delta495a	-	AAT TAG CCG GTG CTT CTT	Macalady et al., 2006
DSS658	<i>Desulfosarcina</i> / <i>Desulfococcus</i> clade	50	TCC ACT TCC CTC TCC CAT	Manz et al., 1998
cDSS658	Competitor for DSS658	-	TCC ACT TCC CTC TCC GGT	Kleindienst et al, submitted
SCA1-212a	SCA-SRB1	20	CAT CCC AAA ACA GTA GCT	This study
SCA1-212b	SCA-SRB1	20	CAT CCC CAA ACA GTA GCT	This study
h1_SCA1-197	Helper for SCA1-212ab	-	TAT WTA TAG AGG CCA	This study
h2_SCA1-197			TAT AWA TAG AGG CCA	This study
h3_SCA1-182			CCT TTG ATC TRA AAA	This study
h4_SCA1-182			CCT TTG ATC TGA AWA	This study
h5_SCA1-229			GCT AAT GGT ACG CGR GCT	This study
h6_SCA1-182			CCT TTG ATC TGG ATA	This study
SCA2-138	SCA-SRB2	20	CGA GTT ATC CCC GAT TCG	This study
LCA1-443	LCA-SRB1	20	CCUCAUAGGUUCUCCCA	This study
h1_LCA1-460	Helpers for LCA1-443	-	UACAAGGUGGUAAUUGGCA	This study
h2_LCA1-478			CUUCAGUGGUACCGUCAG	This study
LCA2-63	LCA-SRB2	10	GCUAAAGCUUUCUCGUUC	This study
h1_LCA2-83	Helper for LCA2-83	-	CUUACUCACUCUAGCAA	This study

Table SIII.2: Sequences of the two identified Mas proteins. Identified peptides are highlighted and average RIA and LR values given according to time points.

	T ₁	T ₂	T ₃
MasD protein #1^a			
Average RIA [%]	41.65	46.20	49.68
Average LR	0.20	0.37	0.60
MasD protein #2^b			
Average RIA [%]	43.67	47.47	50.54
Average LR	0.18	0.36	0.59

MasD partial Protein sequences provided by M. Stagars (2012)

^a MasD partial sequence #1

FE CIRHGLGYPNIRNDEVLIKSQKYWSNYTEEEARTWVAQACVVPETKECVIPARYASCTPLGSKCLELALWNGFNPFVNMQIG
PKTGDATAKMKTFEELFEATLEQYKVIHWEVGVKIRNIARYTEETIMGRPHLSAVWERCVESGLSCFEAREKGNAWHSIFWMDAL
DGLVAVKKLVFDDKKYTMEQLLEMLKANWEGYEKERMDVFKAPKWGNDE

^b masD partial sequence #2

FE CIRHGLGYPNIRNDQVLKANMFWSNTPEEEARTWVAQACIVPAPETKHGCMMPRYSSCTTLGSKCMELALWNGFNPFVQ
MQIGPKTGDP TKMNFQQLMDFIEQFKVIHWDVAVKIRNIVHHVEEIHGRPHLSATYEMCVEDGIN

Tables SIII.3 and Tables SIII.4 are provided in the Appendix of this thesis.

References for Supplementary Information

- Kleindienst S, Ramette A, Amann R, and Knittel K. (*submitted*). Distribution and in situ abundance of sulfate-reducing bacteria in diverse marine hydrocarbon seep sediments. *Environ Microbiol*
- Loy A, Lehner A, Lee N, Adamczyk J, Meier H, Ernst J, Schleifer KH, and Wagner M. (2002). Oligonucleotide microarray for 16S rRNA gene-based detection of all recognized lineages of sulfate-reducing prokaryotes in the environment. *Appl Environ Microbiol* **68**: 5064-5081.
- Macalady JL, Lyon EH, Koffman B, Albertson LK, Meyer K, Galdenzi S, and Mariani S. (2006). Dominant microbial populations in limestone-corroding stream biofilms, Frasassi cave system, Italy. *Appl Environ Microbiol* **72**: 5596-5609.
- Manz W, Eisenbrecher M, Neu TR, and Szewzyk U. (1998). Abundance and spatial organization of gram-negative sulfate-reducing bacteria in activated sludge investigated by in situ probing with specific 16S rRNA targeted oligonucleotides. *FEMS Microbiol Ecol* **25**: 43-61.
- Stagars M. (2012). Ecophysiology of key sulfate-reducing bacteria involved in anaerobic degradation of hydrocarbons at marine gas and oil seeps. Master Thesis, University of Bremen.

Chapter IV

Activity and in situ abundance of alkane-degrading sulfate-reducing bacteria at marine hydrocarbon seeps

Sara Kleindienst, Lubos Polerecky,
Florin Musat, Katrin Knittel*

In preparation

*Corresponding author: Katrin Knittel (Department of Molecular Ecology),
Phone: +49 421 2028 935, Fax: +49 421 2028 580, E-mail: kknittel@mpi-bremen.de
Max-Planck-Institute for Marine Microbiology, Celsiusstrasse 1, D-28359 Bremen, Germany

Summary

At marine seeps, the emission of reduced substrates, including gaseous and liquid hydrocarbons, fuels extraordinarily high sulfate reduction (SR) rates.

Here, we assess the environmental impact of alkane-degrading sulfate-reducing bacteria (SRB) based on in situ quantifications by catalyzed-reporter deposition fluorescence in situ hybridization (CARD-FISH) in combination with activity measurements on the cellular level by Nanometer scale secondary ion mass spectrometry (NanoSIMS). Distinct groups of *deltaproteobacterial* alkane (SCA-SRB1, SCA-SRB2) and dodecane (LCA-SRB1, LCA-SRB2) degraders were explored in situ using CARD-FISH: at diverse marine hydrocarbon seeps, groups SCA-SRB1 and SCA-SRB2 constituted up to 31 and 9% of all *Deltaproteobacteria*, respectively. In addition, LCA-SRB2 comprised up to 6% of all *Deltaproteobacteria*.

Cellular activities of specific alkane degraders were investigated in complex benthic communities from Amon Mud Volcano and Guaymas Basin hydrocarbon seeps using NanoSIMS. Two scenarios were modeled in order to obtain alkane turnover rates: values for butane oxidation were between 45 and 58 amol butane cell⁻¹ d⁻¹ assuming either ¹³C-alkane as the only carbon source, or considering additional unlabeled substrates as carbon sources, respectively. Results for dodecane oxidation rates were similar in both models yielding 1 amol dodecane cell⁻¹ d⁻¹. In addition, extrapolated data indicate that specific alkane-degrading SRB groups have the potential to contribute up to 100% of the total SR rates at seeps from the Gulf of Mexico. Thus, our obtained data suggest that alkane-degrading communities considerably influence marine carbon and sulfur cycles, particularly at seeps with complex emissions of hydrocarbons.

Introduction

Hydrocarbon seepage in form of gas and oil is widespread in the marine environment (e.g. Byrne & Emery, 1960; Simoneit & Lonsdale, 1982; Anderson et al., 1983; Kennicutt II et al., 1988; Mastalerz et al., 2009). Marine hydrocarbon seep sediments harbor a diverse microbial community that mineralizes a complex mixture of organic compounds including alkanes, cycloalkanes and aromatic hydrocarbons using sulfate, the most abundant electron acceptor in seawater (up to 28 mM). Over the last decades, microbial degradation of a wide range of hydrocarbons under oxic and anoxic conditions has been demonstrated using cultivation techniques (Aeckersberg et al., 1991; Lovley et al., 1993; Gilewicz et al., 1997; Zengler et al., 1999; Kniemeyer et al., 2007; Jaekel, 2011). Several of these enrichment cultures and isolates, obtained under sulfate-reducing conditions, originated from marine seep sediments.

At marine seeps, rates of sulfate reduction (SR) are several orders of magnitude higher compared to non-seepage sediments (up to $>1 \mu\text{mol cm}^{-3} \text{d}^{-1}$ versus a few $\text{nmol cm}^{-3} \text{d}^{-1}$; Aharon & Fu, 2000; Boetius et al., 2000; Michaelis et al., 2002; Treude et al., 2003; Joye et al., 2004). At methane-dominated seeps, SR is mainly fueled by the anaerobic oxidation of methane (AOM) which is mediated by a consortium of anaerobic methanotrophic (ANME) archaea and sulfate-reducing bacteria (SRB), leading to a ~1:1 coupling of these two processes (Nauhaus et al., 2002). In contrast, at seeps with complex hydrocarbon emission, several biogeochemical studies suggested the importance of microbial oxidation of non-methane hydrocarbons by SRB, e.g. at the Amon Mud Volcano (Amon MV) in the Mediterranean Sea (Mastalerz et al., 2009; Omeregic et al., 2009), in the Gulf of Mexico (Joye et al., 2004; Orcutt et al., 2010; Bowles et al., 2011), or the Guaymas Basin (Kallmeyer & Boetius, 2004). Ex situ rate measurements revealed that methane-dependent SR rates were less than 10% of total SR rates indicating a clear decoupling from AOM (Joye et al., 2004).

Furthermore, in situ studies demonstrated that *Deltaproteobacteria* and in particular members of the *Desulfosarcina/Desulfococcus* (DSS) clade are highly diverse and globally abundant in hydrocarbon seep sediments (e.g. Knittel et al., 2003; Wegener et al., 2008; Orcutt et al., 2010; Kleindienst et al., *in prep.*; Kleindienst et al., *submitted*). These studies suggested a metabolically diverse DSS community potentially involved in hydrocarbon degradation. Very recently, stable-isotope probing (SIP) experiments showed different groups of DSS capable of degrading alkanes in complex, benthic communities (Kleindienst et al., *in prep.*). The identified butane degraders belonged to two distinct groups (denoted as “SCA-SRB1” and “SCA-SRB2”, where SCA stands for short-chain alkane). SCA-SRB1 comprises 16S rRNA gene sequences from several propane- and butane-degrading enrichment cultures

and the butane degrading sulfate-reducing bacterium BuS5 (Kniemeyer et al., 2007; Jaekel, 2011). SCA-SRB2 comprises only sequences from uncultivated organisms. The identified dodecane degraders formed two distinct deltaproteobacterial groups (denoted as “LCA-SRB1” and “LCA-SRB2”, where LCA stands for long-chain alkane), which both contain only sequences from uncultivated organisms.

A recent study by Bowles and colleagues (2011) estimated the global median ratio between SR and AOM rates to be about 11:1. This is much higher than the 1:1 ratio, which is expected at marine seeps, assuming that SR coupled to AOM is the dominating process of anaerobic organic matter degradation there. To quantify the contribution of hydrocarbon degradation to total sulfate reduction, direct in situ measurements of hydrocarbon oxidation rates are required. However, such data are presently not available. The only available data on the cellular activity of short-chain alkane degraders were obtained from sediment-free enrichment cultures of members of SCA-SRB1 (Jaekel, 2011) but no measurements are available of cells from sediments (Kniemeyer et al., 2007; Jaekel, 2011).

Here, we present results of direct measurements of hydrocarbon assimilation and dissimilation rates in sediments collected from two well characterized marine hydrocarbon seep sites, the Amon MV and the Guaymas Basin. We focused on butane and dodecane, which are, respectively, representatives of short-chain or long-chain alkanes typically found at high concentration in marine hydrocarbon seeps. Furthermore, we focused on bacterial groups SCA-SRB1, SCA-SRB2 and LCA-SRB2 as representatives of alkane-degrading sulfate reducing bacteria commonly found in hydrocarbon seeps sediments. The hydrocarbon utilization rates were derived from incubation experiments of sediment samples with ^{13}C -labeled butane and dodecane under close to in situ conditions. Here, the assimilation and dissimilation rates of the labeled substrate by the target cells were quantified on a single-cell level using nanometer scale secondary ion mass spectrometry (NanoSIMS) coupled to catalyzed-reporter deposition fluorescence in situ hybridization (CARD-FISH), whereas the rates on the bulk level were assessed by measuring the ^{13}C -enrichments in the total organic and inorganic carbon pools. Assuming complete remineralization of the target substrate, the measured rates were converted to cellular SR rates by considering the stoichiometry of the target substrate. Subsequently, these rates were combined with in situ abundance CARD-FISH data of the target cells to estimate their potential impact on hydrocarbon turnover rates in various marine seep sites.

Results

In situ abundance of alkane-degraders at marine gas and hydrocarbon seeps

The in situ abundance of specific alkane-degrading deltaproteobacterial SRB groups (see Fig. IV.1) was determined using CARD-FISH. Analysis of selected seep sediments revealed that the DSS subgroups SCA-SRB1 and SCA-SRB2 constituted between 2 to 31% and 1 to 9% of all *Deltaproteobacteria*, respectively (Table IV.1). Only at the Haakon Mosby Mud Volcano, members of SCA-SRB1 or SCA-SRB2 were not detected. In addition, LCA-SRB2 comprised between 1 to 6% of all *Deltaproteobacteria* at several seep habitats, but were not detected in samples from Hydrate Ridge and in Black Sea microbial mats (Table IV.1).

SCA-SRB1. In situ analysis showed that SCA-SRB1 cells appeared aggregated or non-aggregated in marine hydrocarbon seep sediments (Fig. IV.1). The aggregates were found to be most abundant in sediments from the Gulf of Mexico (site 161), which was characterized by elevated concentrations of higher hydrocarbons in addition to methane. Particularly high abundances of non-aggregated SCA-SRB1 cells were found within a methanotrophic mat from the top of a Black Sea reef (site 822; 1.5×10^9 cells g^{-1} wet weight; Table IV.1) and in sediments from the Chapopote asphalt volcano in the Gulf of Mexico (site GeoB10619-6; 1.6×10^8 cells cm^{-3} ; 3% of total cells). In addition, this group was also detected in high abundances at other seep sites, for example at shallow water seeps in the Tommeliten area (site 1274-K3) or at the Amon MV (site 825) in the Mediterranean Sea indicating that they are geographically widely distributed.

SCA-SRB2. Members of the group SCA-SRB2 were generally detected in situ as non-aggregated cells (Fig. IV.1). Highest abundances were found at seeps with gas and oil emission. In general, their relative abundance was <1% of total cells. Highest absolute abundances were found in sediments from the Tommeliten (site 1274-K3; 8.5×10^7 cells cm^{-3}), the Chapopote asphalt volcano in the Gulf of Mexico (site GeoB10619-13) and Guaymas Basin (site 4489-1; Table IV.1).

Table IV.1: Overview of total cell counts and in situ abundance of all *Deltaproteobacteria*, the DSS group and alkane-degrading groups (SCA-SRB1, SCA-SRB2 and LCA-SRB2) as detected by CARD-FISH at diverse marine seeps.

Habitat	Station	Depth [cm]	Cell counts [▲]		<i>Deltaproteobacteria</i>		DSS [§]		SCA-SRB1	SCA-SRB2	LCA-SRB2
			single cells cm ⁻³ [10 ⁸]	total cells cm ⁻³ [10 ⁸]	single cells cm ⁻³ [10 ⁶] (Delta595)	total cells cm ⁻³ [10 ⁶]	single cells cm ⁻³ [10 ⁶] (DSS658)	total cells cm ⁻³ [10 ⁶]	total cells cm ⁻³ [10 ⁶] (SCA1-212)	total cells cm ⁻³ [10 ⁶] (SCA2-138)	total cells cm ⁻³ [10 ⁶] (LCA2-63)
Northern Gulf of Mexico (GoM)	156	3	20.9	35.0	225.7	1156.9	163.1	980.8	5.2	5.2	5.2
	161	5	25.5	25.5	324.8	324.8	253.7	253.7	6.4	6.4	6.4
Southern GoM:	140	1	8.6	8.6	32.3	n.d.	30.6	30.6	2.1	2.1	n.d.
Chapopote Asphalt Volcano (GoM-AV)	GeoB10619-13	0	249.2	NA	n.d.	n.d.	1113.6	NA	62.3	62.3	186.9
	GeoB10619-6	1.25	56.3	NA	616.8	n.d.	370.5	NA	160.4	14.1	14.1
	GeoB10625-16	0	19.0	NA	n.d.	n.d.	71.3	NA	4.7	n.d.	n.d.
	GeoB10625-9	3.75	38.8	NA	486.1	n.d.	246.4	NA	9.7	9.7	9.7
		13.75	24.5	NA	422.1	n.d.	198.8	NA	18.3	18.3	6.1
Guaymas Basin (GB)	4489-1	0.5	175.9	175.9	1915.4	1915.4	294.0	294.0	n.d.	44.0	44.0
		2.5	20.1	20.1	322.0	322.0	101.1	101.1	5.0	5.0	n.d.
Haakon Mosby MV (HMMV)	ATL19	1.5	48.0	194.0	791.2	791.2	230.8	230.8	n.d.	n.d.	12.0
		8.5	1.0	2.0	17.4	17.4	12.4	12.4	n.d.	n.d.	n.d.
	ATL22	3.5	32.0	33.0	506.0	506.0	358.0	358.0	n.d.	n.d.	n.d.
Amon MV (AMV)	760	2.5	6.4	11.4	79.4	598.1	32.7	496.5	4.8	1.6	4.8
	825	0.5	20.2	30.1	171.5	1162.7	142.7	1133.8	5.1	5.1	n.d.
		4.5	6.2	10.3	64.3	477.3	57.8	264.3	20.2	n.d.	1.6
Hydrate Ridge (HR)	19	4.5	76.0	250.0	388.6	16250.0	290.6	15338.6	19.0	n.d.	n.d.
	38	12.5	13.0	110.0	36.1	6820.0	57.5	6721.5	3.3	3.3	n.d.
Tommeliten (T)	1274-K1	1.5	40.0	43.0	298.9	321.3	282.1	282.1	n.d.	n.d.	n.d.
	1274-K2	1.5	50.0	53.3	730.2	778.4	299.2	299.2	37.5	12.5	12.5
	1274-K3	1.5	57.0	61.8	1005.9	1090.6	204.4	204.4	142.5	85.3	n.d.
		5.5	35.0	43.1	456.4	562.0	145.8	145.8	26.3	37.9	n.d.
		8	29.0	31.7	639.1	698.6	157.3	157.3	n.d.	8.7	n.d.
Black Sea (BS)	822 [†]	Reef's top	2000.0	2000.0	NA	NA	46000.0	46000.0	1500.0	3.3	n.d.

[▲]Total cell numbers taken from Lösekann et al. 2007 (HMMV ATL19, ATL22), Grünke et al 2011 (Amon MV 760), Felden pers. communication (Amon MV 825), Knittel et al. 2003 (HR 19, 38), Wegner et al. 2008 (T 1274-K1, 1274-K2, 1274-K3)

[§] Numbers for Deltaproteobacteria and DSS taken from Kleindienst et al. submitted

n.d: not detected; NA: not analyzed

[†] Cell numbers given in g⁻¹ wet weight

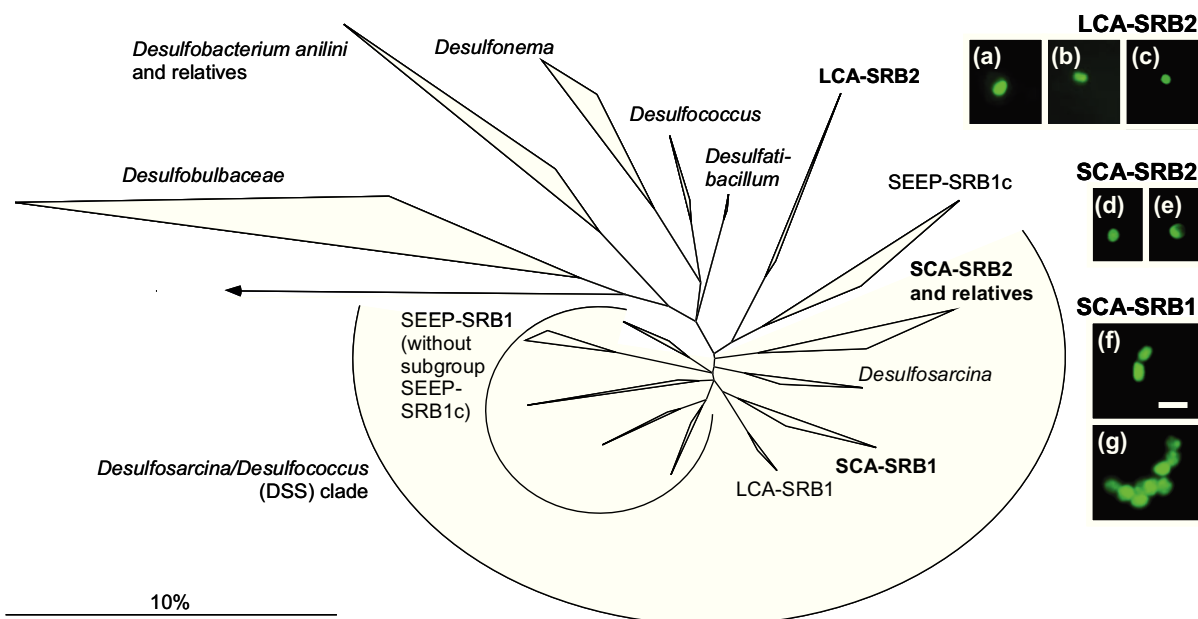


Fig. IV.1: Phylogenetic tree based on 16S rRNA genes showing the groups SCA-SRB1 and SCA-SRB2 as well as LCA-SRB2 (bold) within the *Deltaproteobacteria*. Images show LCA-SRB2 cells in sediments from Amon Mud Volcano (a, b) and Chapopote asphalt volcano (c), SCA-SRB2 cells in sediments from the Guaymas Basin (d), and the Tommeliten seeps (e) as well as SCA-SRB1 cells in sediments from the Tommeliten seeps (f) and the Chapopote asphalt volcano (g) as visualized by CARD-FISH. Scale bar represents 2 μm for all images.

LCA-SRB2. Members of the LCA-SRB2 group were detected in hydrocarbon-rich sediments from various seeps and appeared as non-aggregated cells (Fig. IV.1). LCA-SRB2 members were most abundant at hydrocarbon seeps compared to gas seeps, while their relative abundance was $<1\%$, similarly to SCA-SRB2. Highest abundances of this group were detected within a surface mat and sediments from the Chapopote asphalt volcano at the Gulf of Mexico (site GeoB10619; 1.9×10^8 cells cm^{-3}) and in sediments from the Tommeliten (site 1274-K3; 1.2×10^7 cells cm^{-3} Table IV.1).

Activity of alkane-degrading SRB in complex communities as determined by ^{13}C -labeling experiments

Assimilation of butane and dodecane. Sediments from Amon MV and Guaymas Basin were amended with ^{13}C -butane or ^{13}C -dodecane and incubated for several days. SCA-SRB1, SCA-SRB2 and LCA-SRB2 cells were selected as target cells to calculate cellular rates. All specific cells identified by CARD-FISH, showed a clear ^{13}C -enrichment resulting from the assimilation of the ^{13}C -labeled butane or dodecane. Cells that lacked the specific CARD-FISH signal (e.g. the spirillum-shaped cell in Fig. IV.2a) were not ^{13}C -enriched, indicating that they did not incorporate the substrate.

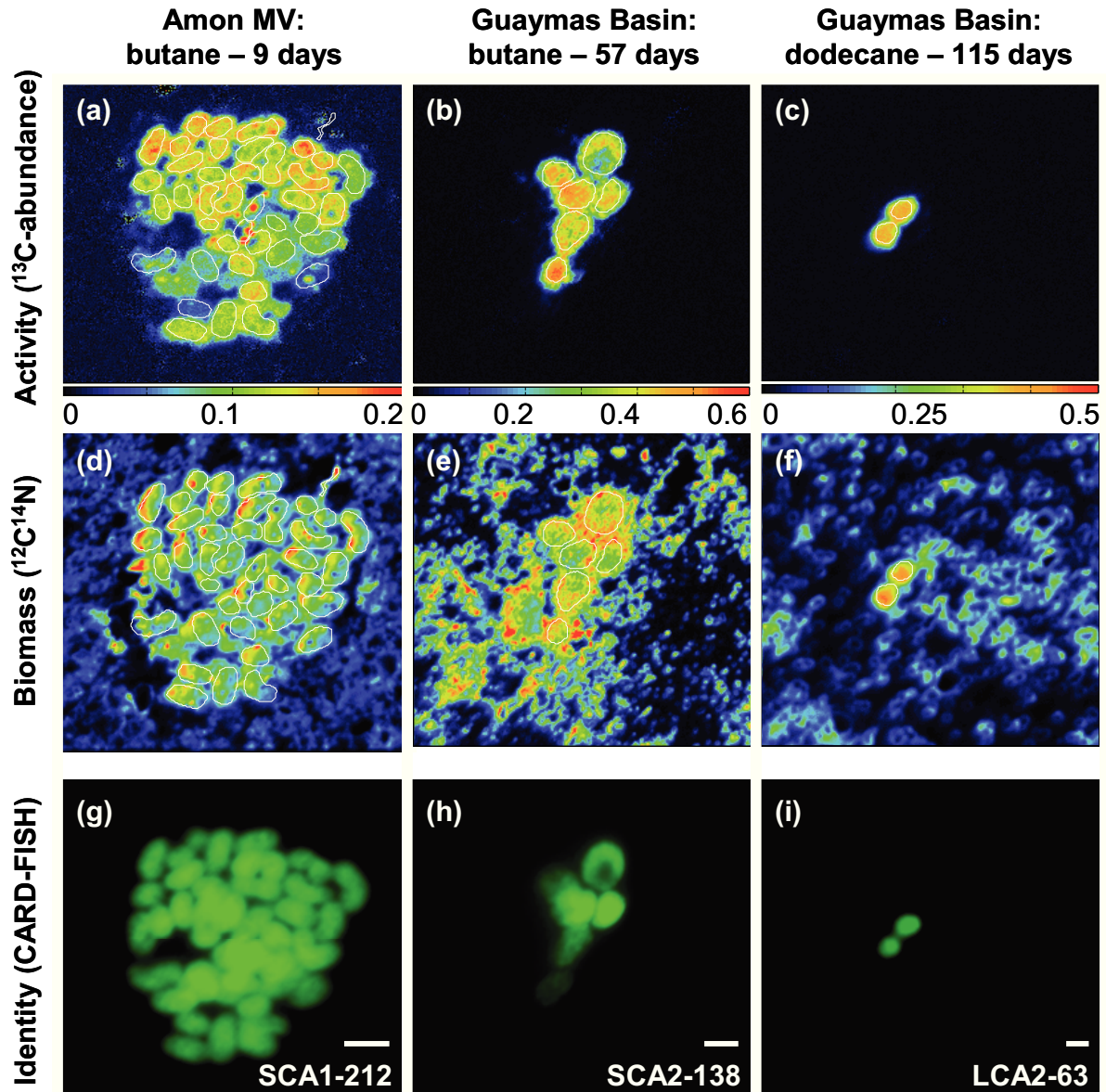


Fig. IV.2: NanoSIMS images (panels a - f) of specific butane- or dodecane-degrading cells from Amon MV and Guaymas Basin seep sediments. Cells were identified by CARD-FISH based on specific probes (panels g - i; probe names are given in the images). Scale bar represents 2 μm for all images. Regions of interest (white outlines in images a - c) were used to determine the ^{13}C -abundance in the target cells.

Cell morphologies of alkane degraders. Butane-degrading cells from the group SCA-SRB1 were oval or slightly curved (Fig IV.2g). They strongly resembled cell morphologies described previously for other SCA-SRB1 group members (strain BuS5 and the enrichments culture Butan-GMe12; Knemeyer et al., 2007; Jaekel, 2011). SCA-SRB1 cells in the ^{13}C -labeling experiments from Amon MV were, similarly as in situ, free-living or loosely aggregated and had an average size of $2.1 \times 1.5 \mu\text{m}$. The butane-degrading cells from Guaymas Basin of the group SCA-SRB2 were coccoid to oval-shaped (Fig. IV.2h) and contained vesicles. Cell sizes increased during the incubation and ranged between 1.3 μm to

4 μm in length. The average cell size was $2.5 \times 1.8 \mu\text{m}$. Dodecane-degrading cells from the groups LCA-SRB1 and LCA-SRB2 were coccoid or slightly oval-shaped and appeared non-aggregated in the incubations (Fig. IV.2i). Their size was smaller relative to the butane-degrading cells, with average cell diameters of 1 μm .

Activity of the benthic communities and specific SRB groups.

The ^{13}C -abundance in the total organic carbon (TOC) pool from the incubated sediment samples increased during the experiment (Fig. IV.3a-d), indicating active turnover and assimilation of the added ^{13}C -labeled alkanes into the biomass. Based on these measurements, time-points for single-cell NanoSIMS measurements were selected to affirm ^{13}C -incorporation into the cell biomass. Fastest increase of ^{13}C -labeled dissolved inorganic carbon (DIC) abundance was detected in the butane-amended Amon MV sediments, whereas a longer period was found in ^{13}C -butane-amended Guaymas Basin sediments as well as in both ^{13}C -dodecane-amended sediment types (Fig. IV.3e-h).

Growth of alkane degraders during the experiments. The absolute and relative abundance of most investigated alkane-degrading SRB groups (Fig. IV.3i-l, supplementary Fig. SIV.1a-d) increased in the course of the experiments. High absolute abundance already at the beginning of the experiments was detected for group SCA-SRB1 (6×10^6 cells ml^{-1} ; Fig. IV.3k). Growth of alkane degraders occurred, from the beginning of the experiment until the last sampling point for NanoSIMS analysis for the groups SCA-SRB1, SCA-SRB2 and LCA-SRB2. Highest increase in abundance, by a factor of 59, was detected for group LCA-SRB2 within 115 days (Fig. IV.3j). Also, SCA-SRB1 and SCA-SRB2 increased their abundances within 15 and 57 days by factors 3 and 2, respectively (Fig. IV.3k, i). The abundance of the LCA-SRB1 group did not increase until the last sampling point for NanoSIMS analysis (25 days). However, LCA-SRB1 started their growth afterwards and increased by a factor of 23 until 309 days of incubation (Fig. IV.3l).

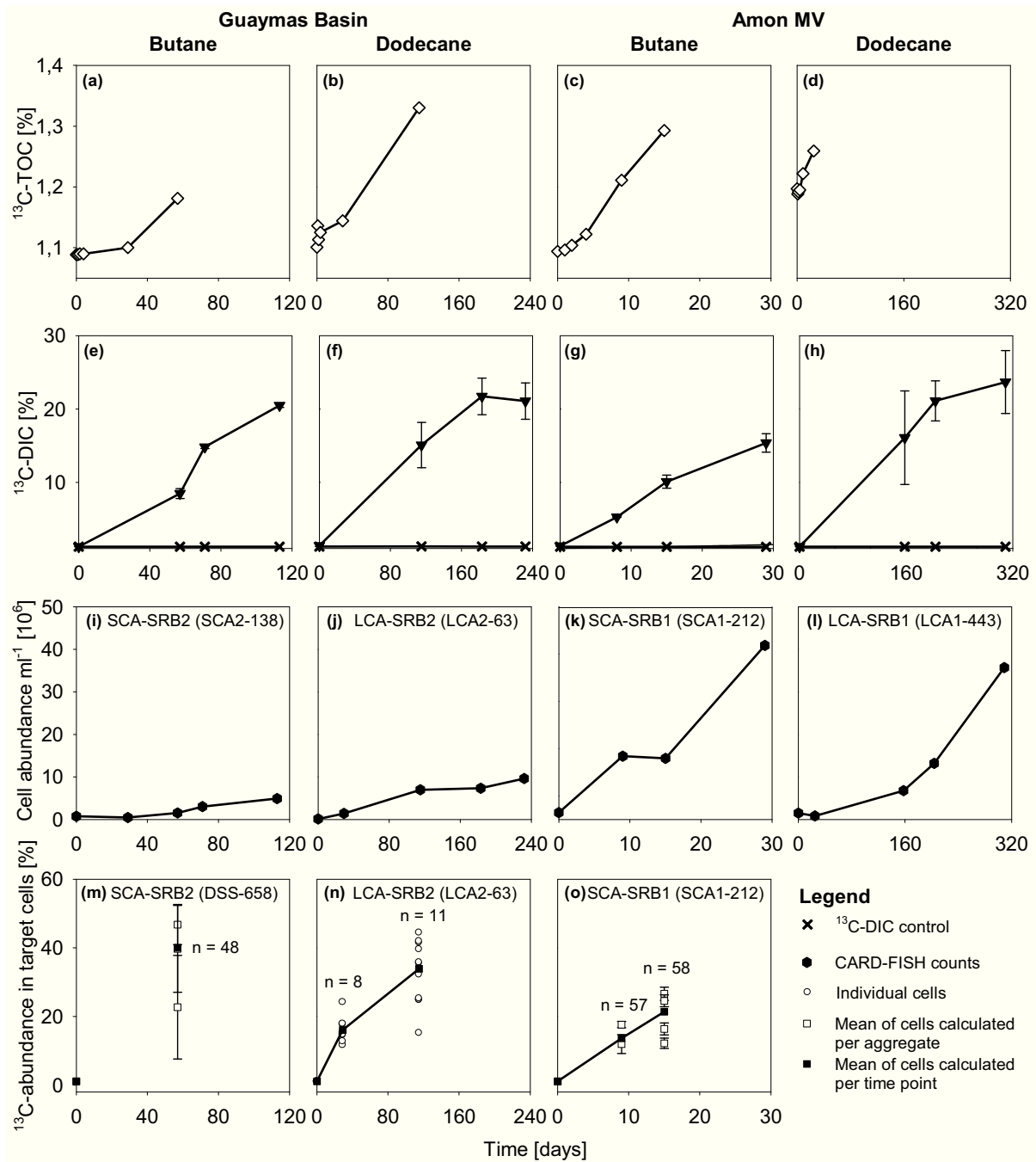


Fig. IV.3: ^{13}C -TOC (a-d), ^{13}C -DIC (e-h) and absolute cell abundance (i-l) as well as abundance of ^{13}C in alkane degraders (m-o) in sediment samples from Guaymas Basin and Amon MV amended with ^{13}C -labeled butane or dodecane. The absolute abundance and the cell identification for NanoSIMS analysis were determined using specific CARD-FISH probes for SRB groups as indicated in the panels. The ^{13}C -abundance in aggregate-building microbes (butane-degraders, Guaymas Basin and Amon MV; panels m and o) is presented as average of cells belonging to the same aggregate (□) and as an average of cells analyzed for the respective time point (■). In the dodecane-degrading incubations (panel n) ^{13}C -enriched cells were not found in aggregates and hence ^{13}C -abundance is shown for individual cells (○) and as an average of cells per time point (■). Numbers of averaged cells (indicated by n) and the standard deviations (indicated by error-bars) are illustrated. Data for the Amon MV dodecane experiment are not shown because specific target cells were not found by CARD-FISH for the NanoSIMS analysis. ^{13}C -DIC and cell abundance data (e-l) were taken from Kleindienst et al. (*in prep.*).

¹³C-abundance in target cells of alkane-degrading SRB

The ¹³C-abundance increased in all cells from alkane-degrading groups investigated during the incubation and showed highest values after 57 days (mean 40% ± 22%) and 115 days (mean 34% ± 17%; Fig. IV.3m-o). Particularly the increase of the mean ¹³C-abundance of the group SCA-SRB1 was linear (Fig. IV.3o). After a linear increase the mean ¹³C-abundance for members of the LCA-SRB2 slightly decreased after 29 days of incubation (Fig. 3n). The ¹³C-abundance of aggregated SCA-SRB1 cells indicated similar activities for individual cells, whereas the cell activities differed between aggregates (Fig. 3o and supplementary Fig. SIV.2). Although this heterogeneity with respect to ¹³C-assimilation was observed on a single cell level, we used the mean ¹³C-abundance values for the calculations of assimilation and dissimilation rates.

Activity of alkane degraders determined on the cellular level

Two model scenarios were calculated in order to obtain alkane-oxidation rates on the cellular level. The ¹³C-labeled substrate alone (first model) could not explain the observed growth of the target cells. Thus an additional unlabeled substrate was assumed to be assimilated by the target cells (second model).

Alkane-derived activity model. The “alkane-derived activity model” assumes that butane is the only carbon source for biosynthesis. Here, the cellular substrate assimilation rates of the butane-degrading SRB from Amon MV (SCA-SRB1) and Guaymas Basin (SCA-SRB2) were similar (about 45 amol C₄ cell⁻¹ d⁻¹; Table IV.2). Considering the stoichiometry of a butane oxidation with sulfate to CO₂ and a typical assimilation of 10% of the degraded substrate (Rabus et al., 2006), hereafter termed as assimilation efficiency, the cellular DIC production rates were about 1.6 fmol C cell⁻¹ d⁻¹. The corresponding cellular SR rates for groups SCA-SRB1 and SCA-SRB2 were determined to be about 1.3 fmol SO₄²⁻ cell⁻¹ d⁻¹ (Table IV.2). The doubling times estimated based on the substrate assimilation rate (46 d for cells from Amon MV and 79 d for cells from Guaymas Basin; Table IV.2) were about 2-3 fold longer than those calculated by fitting the measured cell counts with an exponential function. Furthermore, the cell counts required to match the observed ¹³C-enrichment in the DIC pool were considerably higher than those detected by CARD-FISH (about 7-fold for SCA-SRB1 and 16-fold for SCA-SRB2; Table IV.2).

The cellular assimilation rates of dodecane were about 2 orders of magnitude lower than those of butane (0.5-0.7 amol dodecane cell⁻¹ d⁻¹; Table IV.2). For the assimilation

efficiency of 10% and the stoichiometry of a dodecane oxidation with sulfate to CO₂, the cellular DIC production rates were about 60 amol C cell⁻¹ d⁻¹ and the corresponding SR rates about 50 amol SO₄²⁻ cell⁻¹ d⁻¹ (Table IV.2). Similar as for the butane incubation experiment, the estimated doubling times (276 d for LCA-SRB1 and 190 d for LCA-SRB2) were much longer than expected based on the increase in cell counts determined by CARD-FISH. Also, the cell counts required to match the observed ¹³C-enrichment in the DIC pool were about 150-fold larger than those detected by CARD-FISH (Table IV.2).

Overall activity model. Under the “overall activity model” scenario, it was assumed that carbon assimilation of the SRB groups was derived from both, i.e. from added ¹³C-labeled alkanes and from naturally occurring non-labeled organic compounds. The target substrate alone could not explain the observed growth of the target cells, as indicated by the consistently longer doubling times estimated from the assimilation rate of the target substrate in comparison to those derived directly from cell counts. Based on the ability of cultured representatives from previous studies, this additional substrate was assumed to be propane for the butane degraders and C₇-C₁₆ alkanes for the dodecane degraders. Propane was naturally occurring in the Amon MV sediments used for incubations (0.1 μM cm⁻³ from 0-8 cm sediment depth; unpublished data), while propane as well as C₇-C₁₆ alkanes are typically present in Guaymas Basin sediments. Under this assumption, the butane assimilation rates for the SCA-SRB1 and SCA-SRB2 cells from Amon MV and Guaymas Basin were about 58 amol C₄ cell⁻¹ d⁻¹ (Table IV.2), whereas the propane assimilation required to match the observed growth were about 170 amol C₃ cell⁻¹ d⁻¹ for SCA-SRB1 cells in Amon MV sediments and 45 amol C₃ cell⁻¹ d⁻¹ for SCA-SRB2 in Guaymas Basin sediments. Based on the assimilation efficiency of 10% and the stoichiometry of a complete butane and propane oxidation with sulfate to CO₂, the predicted cellular DIC production rates were about 3.3-6.7 fmol C cell⁻¹ d⁻¹ and the corresponding SR rates about 2.7-5.6 fmol SO₄²⁻ cell⁻¹ d⁻¹ (Table IV.2). Although the assumption of unlabeled substrate assimilation improved the agreement between the predicted and measured data on cellular enrichment and growth, the number of cells required to match the ¹³C-DIC enrichment data is still much higher than observed (Table IV.2). This suggests that cells numbers determined by CARD-FISH might have missed an important group of bacteria that dissimilated ¹³C-labeled substrates or metabolites.

Table IV.2: Activity of alkane-degrading SRB on the cellular level as derived by two model scenarios.

	Doubling time	Cellular C content	Target substrate		Additional substrate		Substrate assimilation rate		Target cell counts		Total DIC production rate	Cellular sulfate reduction rate due to dissimilation of substrate		
			C _{n1}	f ₁	C _{n2}	f ₂	of C _{n1}	of C _{n2}	required	detected		C _{n1}	C _{n2}	total
	days	fmol C cell ⁻¹					amol C _n cell ⁻¹ d ⁻¹		10 ⁶ cells ml ⁻¹		amol C cell ⁻¹ d ⁻¹	amol SO ₄ ²⁻ cell ⁻¹ d ⁻¹		
SCENARIO 1: alkane-derived activity model^{a,b}														
Amon MV-butane	46	12.0	4	1			44		46	6.5	1590	1290		1290
Amon MV-dodecane	276	2.4	12	1			0.49		220	1.5	52.5	40		40
Guaymas Basin-butane	79	22.2	4	1			47		12	0.75	1680	1370		1370
Guaymas Basin-dodecane	190	2.4	12	1			0.70		171	1.2	76.0	59		59
SCENARIO 2: overall activity model^{a,c}														
Amon MV-butane	11	12.0	4	0.25	3	0.75	58	171	27	6.5	6710	1710	3840	5550
Amon MV-dodecane	67	2.4	12	0.26	7	0.74	0.75	2.1	92	1.5	215	63	86	148
				0.45	16	0.55		0.93					102	165
Guaymas Basin-butane	41	22.2	4	0.56	3	0.44	58	45.2	6.8	0.75	3290	1680	1020	2700
Guaymas Basin-dodecane	72	2.4	12	0.36	7	0.64	0.91	1.6	91	1.2	200	76	65	141
				0.56	16	0.44		0.71					78	154

^a Rates obtained using the model with the assimilation efficiency set to $e = 10\%$

^b SCENARIO 1: only target substrate is assimilated + dissimilated, expected doubling time is calculated

^c SCENARIO 2: doubling time is derived from measured cell counts, fractions of target and additional substrate assimilated + dissimilated are fitted

C_n = number of carbon atoms per substrate, f = fraction of substrate turnover

Dodecane assimilation rates were under the overall activity model again about 2 orders of magnitude lower than for butane. Depending on the number of atoms in the assumed additional non-labeled oxidized substrate, the fractions of cellular activity used for dodecane turnover ranged from 26% to 56%. Based on the assimilation efficiency of 10% and the stoichiometry of a complete oxidation of dodecane and the assumed naturally occurring (C_n) alkanes with sulfate to CO_2 , the cellular DIC production rates were about $0.2 \text{ fmol C cell}^{-1} \text{ d}^{-1}$ and the corresponding SR rates about $0.15 \text{ fmol SO}_4^{2-} \text{ cell}^{-1} \text{ d}^{-1}$ (Table IV.2). The cell counts required to match the observed ^{13}C -enrichment in the DIC pool were between 60-75 fold higher than those detected by CARD-FISH (Table IV.2).

Discussion

Heterogeneous activities of the alkane degraders

Two different levels of activity were found for Amon MV butane degraders from the group SCA-SRB1 as determined by NanoSIMS analysis. Therefore, cells within the same aggregate had similar ^{13}C -abundance values, whereas a comparison of ^{13}C -abundance between aggregates indicated two activity levels. In contrast, SCA-SRB2 butane degraders from the Guaymas Basin showed a wide range of ^{13}C -abundances among aggregates. In addition, individual cells of alkane-degrading SRB groups showed varying metabolic rates. On the one hand, these heterogeneous activities may be caused by one species with different fitness levels. On the other hand, the heterogeneity likely occurs because of intragroup diversity, where distinct species feature slightly different physiologies. Heterogeneous activities were recently described for SCA-SRB1 members in sediment-free propane and butane enrichment cultures (Jaekel, 2011). In addition, naturally occurring population heterogeneity caused by physiologically distinct individual cells was prior reported for phototrophic bacteria (Musat et al., 2008). Therefore, individual butane-degrading cells within one aggregate may represent one species that divided and formed the aggregate structure, while another aggregate may represent a related species from the same phylogenetic group with a different cellular activity. This explanation is most likely true for the group SCA-SRB1, because parallel incubations analyzed by SIP-techniques revealed two distinct members of this group to be involved in butane oxidation from Amon MV sediments (Kleindienst et al., *in prep.*).

Substrate turnover of short-chain and long-chain alkane degrading SRB

Generally, the alkane turnover of specific SRB groups was significantly higher for short-chain alkane degraders compared to long-chain alkane degraders. These differences were likely caused by the different solubility of butane and dodecane in seawater and thus the different availabilities of these alkanes for microorganisms. Butane is much more soluble in water than dodecane, because the solubility of hydrocarbons is generally decreasing with increasing chain lengths. Accordingly, it was reported that the chain-length of linear alkanes influences their degradation rate in marine contaminated sediments (Grossi et al., 2002).

Calculated alkane turnover rates for SCA-SRB1 were higher than those reported for a sediment-free enrichment culture dominated by members of this group (Jaekel, 2011). This was the case for both the ^{13}C -abundance data obtained by NanoSIMS analysis (about two times higher) while considering different labeling levels of the substrates ($^{13}\text{C}_4$ -butane versus $^{13}\text{C}_1$ -butane in Jaekel et al. (2011) and for the extrapolated SR rates (about 5 times higher). Higher activities in the present study might be explained by close-to-in situ conditions. For instance, naturally occurring substances that stimulated the microbial activity, such as growth factors, may have been present in the sediments used for ^{13}C -labeling experiments that stimulated the activity of the investigated alkane degraders.

Evaluation of predicted and determined cell activities and abundances

The data obtained with the two model scenarios suggest that additional microbial processes occurred in the experiments. Thus, the two models resulted in a discrepancy between the predicted and determined cell activities and abundances. The differences with respect to cell activities were most likely due to heterotrophic carboxylation reactions such as reductive carboxylation. These carbon fixation mechanisms typically take place in parallel to those from the assimilation of hydrocarbons. Accordingly, low labeling efficiencies of about 50% atomic percent of DNA were reported previously for toluene-degrading SRB (Winderl et al., 2010). Similar low labeling efficiencies for hydrocarbon degraders were described in additional studies (Kunapuli et al., 2007; Bombach et al., 2009). Based on the overall activity model the cellular activity was estimated for parallel usage of additional non-labeled alkanes, though the model did not include carboxylation reactions. However, these reactions were probably the cause for the differences in the modeled and experimentally determined activities.

Table IV.3: Extrapolation of SR rates for all *Deltaproteobacteria*, the DSS clade and the specific alkane-degrading groups (SCA-SRB1, SCA-SRB2 and LCA-SRB2) in comparison to ex situ measured SR and AOM rates from diverse marine seep sediments.

Habitat	Station	Depth [cm]	SR rate [▼] [nmol cm ⁻³ d ⁻¹]	AOM rate [▼] [nmol cm ⁻³ d ⁻¹]	<i>Deltaproteo-</i> <i>bacteria</i> ^{§,▲}		DSS ^{§,▲}		SCA-SRB1		SCA-SRB2		LCA-SRB2		Sum of specific alkane degraders			
					scenario 1	scenario 2	scenario 1	scenario 2	scenario 1	scenario 2	scenario 1	scenario 2	scenario 1	scenario 2	scenario 1	scenario 2	scenario 1	scenario 2
					[nmol cm ⁻³ d ⁻¹]	[nmol cm ⁻³ d ⁻¹]	[nmol cm ⁻³ d ⁻¹]	[nmol cm ⁻³ d ⁻¹]	[nmol cm ⁻³ d ⁻¹]	[nmol cm ⁻³ d ⁻¹]	[nmol cm ⁻³ d ⁻¹]	[nmol cm ⁻³ d ⁻¹]	[nmol cm ⁻³ d ⁻¹]	[nmol cm ⁻³ d ⁻¹]	[nmol cm ⁻³ d ⁻¹]	[nmol cm ⁻³ d ⁻¹]	[nmol cm ⁻³ d ⁻¹]	[nmol cm ⁻³ d ⁻¹]
Northern Gulf of Mexico (GoM)	156	3	95	38	156	483	113	349	7	29	7	14	0	1	14	44		
	161	5	NA	NA	224	695	175	542	8	35	9	17	0	1	17	54		
Southern GoM:	140	1	1	1	22	69	21	65	3	12	3	6	-	-	6	18		
Chapopote Asphalt	GeoB10619-13	0	NA	NA	-	-	768	2381	80	346	85	168	11	28	177	542		
Volcano (GoM-AV)	GeoB10619-6	1.25	38	3	425	1319	256	792	207	890	19	38	1	2	227	930		
	GeoB10625-16	0	NA	NA	-	-	49	152	6	26	-	-	-	-	6	26		
	GeoB10625-9	3.75	404	NA	335	1040	170	527	13	54	13	26	1	1	26	81		
		13.75	7	NA	291	903	137	425	24	102	25	50	0	1	49	152		
Guaymas Basin (GB)	4489-1	0.5	NA	NA	1321	4096	203	629	-	-	60	119	3	6	63	125		
		2.5	NA	NA	222	689	70	216	6	28	7	14	-	-	13	41		
Haakon Mosby MV (HMMV)	ATL19	1.5	275	234	546	1692	159	494	-	-	-	-	1	2	1	2		
		8.5	46	38	12	37	9	27	-	-	-	-	-	-	-	-		
	ATL22	3.5	0	3	349	1082	247	766	-	-	-	-	-	-	-	-		
Amon MV (AMV)	760	2.5	37	4	55	170	23	70	6	27	2	4	0	1	9	32		
	825	0.5	519	61	118	367	98	305	7	28	7	14	-	-	13	42		
		4.5	1321	205	44	138	40	124	26	112	-	-	0	0	26	112		
Hydrate Ridge (HR)	19	4.5	757	107	268	831	200	622	25	105	-	-	-	-	25	105		
	38	12.5	153	389*	25	77	40	123	4	18	4	9	-	-	9	27		
Tommeliten (T)	1274-K1	1.5	NA	NA	206	639	195	603	-	-	-	-	-	-	-	-		
	1274-K2	1.5	NA	NA	504	1562	206	640	48	208	17	34	1	2	66	244		
	1274-K3	1.5	NA	NA	694	2151	141	437	184	791	117	230	-	-	301	1021		
		5.5	NA	NA	315	976	101	312	34	146	52	102	-	-	86	248		
		8	3*	1*	441	1367	108	336	-	-	12	23	-	-	12	23		

[▼]Sulfate reduction rates taken from: Orcutt et al. 2010, Wegener pers. communication, Niemann et al. 2005, Felden 2009, Treude et al. 2003

[▲]Averaged cellular activity according to groups SCA-SRB1, SCA-SRB2, LCA-SRB1 and LCA-SRB2

[§] Numbers for *Deltaproteobacteria* and DSS taken from Kleindienst et al. *submitted*. Extrapolation was done assuming that all non-aggregated cells of *Deltaproteobacteria* or all non-aggregated cells of the DSS group represent the alkane-degrading SRB community (AOM aggregates were excluded). Furthermore, the average activity of all specific alkane-degrading SRB based on the two model scenarios (scenario 1: 690 amol SO₄²⁻ cell⁻¹ d⁻¹, scenario 2: 2139 amol SO₄²⁻ cell⁻¹ d⁻¹) was assumed to be the average activity of the whole alkane-degrading SRB community.

Scenario 1: alkane-derived activity, scenario 2: overall activity, NA: not analyzed; -: extrapolation not conducted because target cells were not detected

* Rates obtained from sites close by

In addition, both model scenarios revealed a discrepancy between the predicted and the determined cell abundances, for instance when fitting these numbers with the ^{13}C -DIC pool. As described previously, the selected seep sediments harbor a complex and diverse sulfate-reducing microbial community (Kleindienst et al., *in prep.*; Kleindienst et al., *submitted*). Thus, it cannot be excluded that other unexplored alkane-degrading microbes contributed to the ^{13}C -DIC and ^{13}C -TOC production. As the present study was a follow-up of a SIP study (Kleindienst et al., *in prep.*), major primary consumers, which were identified by various SIP-techniques, were most likely detected by CARD-FISH. However, this SIP-study showed that phylogenetically distinct bacteria were secondarily labeled, which most likely contributed significantly to the production of ^{13}C -TOC and ^{13}C -DIC. These secondary consumers, which were actively involved in the ^{13}C -carbon flow of alkane degradation processes, were uncultured *Bacteroidetes*, uncultured *Desulfobacteraceae* as well as OP3 (Kleindienst et al., *in prep.*). Thus, focusing on one rather than all active groups may explain the difference between the detected and determined cell numbers for active alkane degraders, which were needed to fit the ^{13}C -pools in the models.

Extrapolation of sulfate-reduction rates for alkane degrading SRB at marine seeps

The extrapolation of SR rates for the alkane-degrading groups SCA-SRB1-SCA-SRB2 and LCA-SRB2 indicated that these specific organisms have the potential to significantly contribute to hydrocarbon degradation processes at marine seeps. This assumption was obtained for both model scenarios, which were used to calculate assimilation and dissimilation activities. Furthermore, it is likely that these groups are mostly responsible for these ex situ SR rates, which were determined in particular for seep sediments characterized by an emission of non-methane hydrocarbons. For instance, the highest potential for SR rates that are coupled to alkane degradation was extrapolated for sediments at the Gulf of Mexico with $1 \mu\text{mol cm}^{-3} \text{ d}^{-1}$ (Chapopote Asphalt Volcano, site GeoB10619-6; Table IV.3). Comparing the extrapolated values with ex situ rate measurements suggests that between 7 to >100% may be derived by the sum of specific alkane-degrading SRB at different Gulf of Mexico sites. Also, previous studies suggested that complex hydrocarbon mixtures, found at these seeps, fuel a diverse SRB community, leading to high SR rates that are coupled to hydrocarbon turnover (Orcutt et al., 2010; Bowles et al., 2011). In contrast, the potential for non-methane hydrocarbon degradation coupled to SR is rather low in sediments that are mainly influenced by methane seepage, e.g. at the Haakon Mosby MV or Hydrate Ridge. Here, dominant methane seepage most likely facilitates AOM-mediating communities, which

in turn may contribute more to SR than alkane degraders (e.g. Boetius et al., 2000; Niemann et al., 2006).

Comparing the rates of the present study with ex situ SR rates from previous studies (Orcutt et al., 2010) it becomes obvious, that the extrapolated data even exceed ex situ rates for particular samples. While both types of data were derived under laboratory conditions, alkane degraders in the present study were not limited by the substrate concentrations, which were about 100 to 1000 times higher as compared to natural marine seep sediments (e.g. Kleindienst et al., *in prep.*, M. Kellermann, MARUM, *pers. communication*). Also, sulfate may become limited in marine seep sediments. This was for example discussed for sites at the Gulf of Mexico, where diffusion alone is too slow to provide enough sulfate needed to sustain the high SR rates at particular sites already within a few cm below seafloor (Bowles et al., 2011). In contrast, electron donors and acceptors were not limiting for alkane degraders in our experiments and this is most likely the main reason for an overall higher activity. Higher activity may also be the result of slightly elevated temperatures in our experiments, which may have stimulated enzymatic processes, if temperature changed towards their optimum (reviewed in Farrell & Rose, 1967). Furthermore, small changes in temperature may generally affect the efficiency of organic matter turnover in anoxic marine sediments (Weston & Joye, 2005).

While our data suggest that specific alkane degraders at marine seeps have the potential to mediate SR at high rates, the in situ active community is assumed to be highly diverse. It can be expected that several SRB groups, which are able to oxidize hydrocarbons at marine seeps have not yet been identified. Therefore, an extrapolation was also conducted for the maximal SRB community, which may be involved in alkane degradation. For this purpose, all non-aggregated *Deltaproteobacteria* or all non-aggregated DSS members that typically dominate hydrocarbon seeps (Kleindienst et al., *submitted*) were used as a proxy for the SRB community. Furthermore it was assumed that these *Deltaproteobacteria* or DSS members are alkane degraders. In addition, calculations were performed based on the average activities, determined for specific alkane-degrading SRB groups. The extrapolated rates of this approach suggest that, the reported SR rates may be mainly derived from alkane-degradation coupled to SR as the dominant organic matter degradation process. However, this approach likely overestimates in situ SR rates, because the in situ community can be assumed to be involved in additional organic matter degradation processes too. Nevertheless, it demonstrates that the potential of the whole alkane-degrading SRB community may be highly significant for marine hydrocarbon seep ecosystems.

Conclusion

In the present study, we demonstrated that alkane-degrading groups SCA-SRB1, SCA-SRB2 and LCA-SRB2 are abundant in several seep sediments, constituting a considerable fraction of the deltaproteobacterial community. Furthermore, the extrapolated SR rates clearly indicated that these specific groups have the potential to significantly contribute to highly elevated SR rates as reported for various marine hydrocarbon seeps. These conclusions were derived from cellular activities of specific short-chain and long-chain alkane degraders from the complex benthic community, which were prior to this study only explored for sediment-free enrichment cultures using short-chain alkanes (Jaekel, 2011). In addition, when focusing on the whole SRB community, extrapolated data indicated that the overall methane-independent SR is potentially mainly coupled to hydrocarbon degradation at these marine seep sites. Thus, hydrocarbon degradation processes do likely considerably impact marine carbon and sulfur cycles in particular in those ecosystems with high sulfate accessibility and hydrocarbon emission. For example, Bowles et al. (2011) discussed that the extreme sulfate turnover, likely caused by hydrocarbon degraders, is so immense that sulfate diffusion alone cannot provide enough of this highly abundant electron acceptor (up to 28 mM in seawater). Therefore, the amount of hydrocarbons coupled to SR is most probably highly influencing the carbon cycle. Accordingly, Quistad et al. (2011) suggested, that microbial propane oxidation has the capacity to function as a propane sink in the marine subsurface.

Following studies could reveal, if similar activities can be demonstrated in situ by using state-of-the-art deep-sea sampling and incubation technology.

Experimental procedures

Sample collection

Sites at the Amon MV are characterized by gaseous hydrocarbons and are referred to as gas seeps, while sites at Guaymas Basin are characterized by a seepage of complex hydrocarbon composition and are referred to as hydrocarbon seeps. Anoxic sediments were collected from a cold seep at Amon MV and a hydrothermal vent site at Guaymas Basin during the cruises MSM13-3 (RV Maria S. Merian; ROVQUEST4000, MARUM) and AT 15-56 (RV Atlantis, submersible Alvin) in 2009. Sediment samples from Amon Mud Volcano of the Nile Deep Sea Fan were collected from 2-20 cm below a microbial mat (PANGAEA EventLabel MSM13/3_929-1_PUC1; MSM13/3_929-1_PUC9, MSM13/3_929-1_PUC20; water depth 1122 m, 32°20.1321N, 31°42.6543E). A detailed description of the sampling site can be

found in (Grünke et al., 2011). Guaymas Basin in the central Gulf of California harbors petroleum-rich hydrothermal sediments, covered with organic-rich layers of buried sedimentary organic matter. Hydrothermal fluids contain remarkable concentrations of hydrocarbons including alkanes and aromatic hydrocarbons (Didyk & Simoneit, 1989). Fine-grained sediment samples below a white *Beggiatoa* mat from 0-10 cm sediment depth (push cores 9 and 10, water depth 2010 m, 27°0.696N, 111°24.265W) with conspicuous hydrocarbon smell were collected during dive 4573 with the submersible Alvin.

Incubations with labeled substrates, sampling and analysis of ¹³C-TOC abundance

After sampling and the cruises, sediments were stored for 4 months at 4°C while pre-incubations were carried out with a subset of sediments, in order to select sediments with highest alkane-degrading microbial activities as determined by sulfide- and ¹³CO₂-production (data of pre-incubations not shown). For incubations 4 mL sediment slurries (1:1 with artificial anoxic seawater; Widdel & Bak., 1992) under anoxic atmosphere (N₂/CO₂ 90/10 v/v) were used and sacrificed at each time point. Fully ¹³C-labeled butane or dodecane (Campro Scientific, Germany) were added to incubations. Hydrocarbon concentrations in our experiments (2.1 mM butane; 1.8 mM dodecane) exceeded the natural concentrations by >100× to prevent substrate-diffusion limitations for the bacteria. However, butane is a natural substrate at both seeps types (Amon MV at same site: 0.5-1.1 μM butane cm⁻³ sediment in 0-8 cm depth, (data not shown); Guaymas Basin at site close by: 6-16 μM butane in 0-8 cm depth; M. Kellermann, MARUM, pers. communication), while dodecane is typically found at hydrocarbon seeps from Guaymas Basin (cf. Bazylynski et al., 1988). Sediments were incubated at 20°C and 28°C for Amon Mud Volcano and Guaymas Basin sites, respectively. Samples were taken at 0, 1, 2 and 4 days as well as at 9 and 15 days for Amon Mud Volcano butane-incubations, 9 and 25 days for Amon Mud Volcano dodecane-experiments, 29 and 57 days for Guaymas Basin butane-stimulations and 29 and 115 days for Guaymas Basin dodecane-incubations. 2 ml slurries were fixed for 1 h at 4°C with paraformaldehyde (PFA), at a final concentration of 1% PFA, washed with PBS and stored in 6 ml 1:1 ethanol/PBS at -20°C.

For ¹³C-total organic carbon analysis of NanoSIMS samples, bulk ¹³C- and ¹²C-abundance was determined. Therefore, 500 μl of fixed sediments sample was decarbonized using 1M HCl, dried and packed into tin-cups. Subsequently, bulk samples were analyzed with an automated elemental analyzer (Thermo Flash EA, 1112 Series, Thermo Fischer,

Dreieich-Germany) and a Finnigan Delta Plus Advantage mass spectrometer (Thermo Fischer), using CO₂ released by flash combustion in excess oxygen at 1050°C.

Cell separation and CARD-FISH

Density gradient centrifugation was used to separate cells from sediments for subsequent secondary ion mass spectroscopy analysis. Sonication treatment was used, for 20 s with a MS73 probe (Sonopuls HD70, Bandelin) at an amplitude of 42 mm and a power of <10W, to detach cells from particles. 200 µl of PFA-fixed sample were mixed with 800 µl 1× PBS in sterile tubes. 1 ml density gradients 60% (histodenz w/v in 1x PBS) were carefully placed with syringe and needle underneath the sample. Centrifugation was performed (14.000× g, 20 min, 20°C). After the centrifugation 1500 µl of the supernatant was sampled, while the sediment pellet was re-used for an additional cell extraction using the same protocol as above without further sonication. Purified supernatants were directly filtered on three iosopore membrane filters (GTTP filters, 5 mm diameter, 0.2 µm pore size; Millipore), which were sputtered with Au/Pd (sputter coater; GaLa - Gabler Labor Instrumente; Germany).

In situ hybridizations with horseradish peroxidase (HRP)-labeled probes followed by fluorescently-labeled-tyramide signal amplification (catalyzed reporter deposition; CARD) were carried out as described previously (Pernthaler et al., 2002; Kleindienst et al., *submitted*). Probe sequences (probes purchased from biomers.net; Ulm, Germany) and formamide concentrations required for specific hybridization are given in supplementary Table SIV.1. CARD-FISH signals were used to identify alkane degraders, which only accounted for a small proportion of the total community at Amon MV and Guaymas Basin, respectively. Specific signals were used to mark fields with cells for Nano-SIMS analysis using laser microdissection (LMD model DM6000B; Leica Microsystems).

Nanometer scale secondary ion mass spectrometry (NanoSIMS)

Fields on the Au/Pd coated polycarbonate filters containing hybridized target cells were selected, marked with a laser dissection microscope and analyzed with a NanoSIMS 50L (Cameca, Gennevilliers Cedex-France) at the Max Planck Institute for Marine Microbiology in Bremen, Germany. First, the areas of interest were pre-sputtered with a primary Cs⁺ ion beam of 100 pA to remove surface contamination, to implant Cs⁺ ions in the sample and to achieve an approximately stable ion emission rate. Subsequently, the primary Cs⁺ beam (current between 0.8 and 1 pA, beam diameter between 50 and 100 nm) was rastered across the sample area (10 x 10 µm to 20 x 20 µm in size, 256 x 256 pixels) with a dwell time of 1

ms per pixel while the counts of the emitted secondary ion counts $^{12}\text{C}^-$, $^{13}\text{C}^-$, $^{19}\text{F}^-$, $^{12}\text{C}^{14}\text{N}^-$ and $^{32}\text{S}^-$ were simultaneously recorded by separate electron multiplier detectors. To minimize interferences for $^{13}\text{C}^-$ the instrument was tuned for high mass resolution (around 7000 MRP).

NanoSIMS data were processed with the Look@NanoSIMS program (Polerecky et al., 2012). First, individual planes of detected secondary ions were drift corrected based on the biomass signal ($^{12}\text{C}^{14}\text{N}^-$) and accumulated. Subsequently, CARD-FISH images of the same field of view were aligned and overlaid with the accumulated $^{12}\text{C}^{14}\text{N}^-$ images, and used to draw regions of interest (ROIs) corresponding to individual target cells. Finally, ^{13}C -abundances in the target cells were calculated as $^{13}\text{C}/(^{12}\text{C}+^{13}\text{C})$, where ^{13}C and ^{12}C correspond to total counts of the respective ions accumulated over all pixels in the ROIs. The depth profiles of the ^{13}C abundance did not exhibit significant trends with depth, which justified this calculation (Polerecky et al. 2012). More than 50 cells (corresponding to 2-4 fields) and about 8-11 cells (corresponding to 8-9 fields) were analyzed for every sampling point of the butane and dodecane incubations, respectively, and the mean values and standard deviations were calculated. The mean values were used for the calculation of substrate assimilation and dissimilation rates (see below).

Calculation of substrate assimilation and dissimilation rates

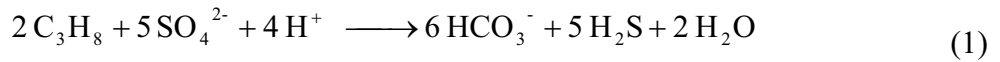
The rates of substrate assimilation and dissimilation by the target alkane degrading cells were estimated by fitting the experimental data with a mathematical model described in the Supporting Information (SI). The model considered two scenarios. In the first model scenario, referred to as the target alkane-derived activity model, only the target (i.e. labeled) substrate was assumed to be assimilated by the target cells (i.e., $f_1 = 1, f_2 = 0$). The estimation of the model parameters proceeded as follows: first, the ^{13}C -abundances measured in the single cells (A_{cell}) and in the DIC pool (A_{DIC}) were fitted with functions 8 and 11 with $F = A_s = 1$ to estimate the cellular substrate turnover rate (r_s) and the initial cell counts ($N(0)$). Based on these estimates, the cellular substrate assimilation rate was calculated as ϵr_s , substrate dissimilation as $(1-\epsilon)r_s$, and the cellular DIC production rate as $(1-\epsilon)r_s n_s$, where n_s is the number of C atoms in the labeled substrate (4 for butane and 12 for dodecane). Subsequently, these values were used to calculate the expected doubling times (equation 3 in SI), the cell counts as a function of time (equation 1 in SI), and the ^{13}C -abundance in the total organic carbon pool (A_{TOC}) as a function of time (equation 10 in SI).

In the second model scenario, referred to as the overall activity model, the target cells were assumed to assimilate a non-labeled substrate in addition to the labeled target substrate.

The number of C atoms in this non-labeled substrate was assumed to be equal to $n_{s2} = 3$ for the butane degrading target cell, and $n_{s2} = 7$ or 16 for the dodecane degrading target cells. These values were chosen because it was reported for alkane-degrading SRB that they use a narrow range of different chain lengths, e.g. C₃-C₄ for short-chain alkane degraders and C₆-C₂₀ for long-chain alkane degraders (cf. Widdel et al., 2010). The estimation of the model parameters proceeded as follows. First, the doubling time of the target cells was estimated by fitting the determined cell counts with equation 1 in SI, leading to the estimate of the total substrate assimilation rate required to support observed growth (equation 2, SI). Second, the measured ¹³C-abundances in the target cells (A_{cell}) and in the DIC pool (A_{DIC}) were fitted with functions 8 and 11, with the factor F given by equation 7. This yielded estimates of the fractions f_1 and $f_2 = 1 - f_1$ and of the initial count of the target cells $N(0)$. Based on these values, the cellular rates of assimilation of the labeled and non-labeled substrates were calculated as $\epsilon r_s f_1$ and $\epsilon r_s f_2$, respectively. Similarly, the dissimilation rates of the two substrates were calculated as $(1 - \epsilon) r_s f_1$ and $(1 - \epsilon) r_s f_2$, and the cellular DIC production rate as $(1 - \epsilon) r_s (n_{s1} f_1 + n_{s2} f_2)$.

In both scenarios, the efficiency of the substrate assimilation was assumed to be 10%, which was reported for SRB (Rabus et al., 2006). Furthermore, the average cellular carbon content was calculated as $C_{\text{avg}} = \rho V_{\text{avg}}$, where ρ is the cellular carbon density (the value of 4.6 fmol C μm^{-3} was used as determined for the closest model organisms strain Bus5; Jaekel, 2011) and V_{avg} is the cell volume calculated as $V_{\text{avg}} = \pi W^2 (L/4 - W/12)$, assuming a rod-like cell shape with dimensions W (width) and L (length), as described by Musat et al. (Musat & Widdel, 2008).

The stoichiometry of complete oxidation of propane, butane, heptane, dodecane and hexadecane by sulfate-reducing bacteria used for calculation of rates was



Acknowledgements

We would like to thank Antje Boetius, Janine Felden, Andreas Teske, Gunter Wegener and Thomas Holler for sampling sediments. Samples were obtained via funding of the EU FP6 program HERMIONE (contract number 226354) and the DFG (METEOR/MERIAN SPP, MSM13-3 awarded to Antje Boetius) and the Max Planck Society. We acknowledge the officers, crews, and shipboard scientific parties of the cruises MSM13-3 and AT 15-56 in 2009. We especially acknowledge Daniela Franzke, Sten Littmann and Thomas Max (MPI Bremen; Germany) for analytical support. We also would like to thank Victoria Orphan (Caltech, Pasadena, CA; USA) for sharing methods for NanoSIMS sample preparation. This study is part of the DFG Priority Program SPP1319 “Transformation of hydrocarbons under anoxic conditions: from molecular to global scale” within the Deutsche Forschungsgemeinschaft. Further support was provided by the Max Planck Society, Germany.

References

- Aeckersberg F, Bak F, and Widdel F. (1991). Anaerobic oxidation of saturated-hydrocarbons to CO₂ by a new type of sulfate-reducing bacterium. *Arch Microbiol* **156**: 5-14.
- Aharon P and Fu B. (2000). Microbial sulfate reduction rates and sulfur and oxygen isotope fractionations at oil and gas seeps in deepwater Gulf of Mexico. *Geochim Cosmochim Acta* **64**: 233-246.
- Anderson RK, Scalan RS, Parker PL, and Behrens EW. (1983). Seep oil and gas in Gulf of Mexico slope sediment. *Science* **222**: 619-621.
- Bazylinski DA, Farrington JW, and Jannasch HW. (1988). Hydrocarbons in surface sediments from a Guaymas Basin hydrothermal vent site. *Org Geochem* **12**: 547-558.
- Boetius A, Ravensschlag K, Schubert CJ, Rickert D, Widdel F, Gieseke A, Amann R, Jørgensen BB, Witte U, and Pfannkuche O. (2000). A marine microbial consortium apparently mediating anaerobic oxidation of methane. *Nature* **407**: 623-626.
- Bombach P, Chatzinotas A, Neu TR, Kästner M, Lueders T, and Vogt C. (2009). Enrichment and characterization of a sulfate-reducing toluene-degrading microbial consortium by combining in situ microcosms and stable isotope probing techniques. *FEMS Microbiol Ecol* **71**: 237-246.
- Bowles MW, Samarkin VA, Bowles KM, and Joye SB. (2011). Weak coupling between sulfate reduction and the anaerobic oxidation of methane in methane-rich seafloor sediments during ex situ incubation. *Geochim Cosmochim Acta* **75**: 500-519.
- Byrne JV and Emery KO. (1960). Sediments of the Gulf of California. *Geol Soc Am Bull* **71**: 983-1010.
- Didyk BM and Simoneit BRT. (1989). Hydrothermal oil of Guaymas Basin and implications for petroleum formation mechanisms. *Nature* **342**: 65-69.
- Farrell J and Rose A. (1967). Temperature Effects on Microorganisms. *Annu Rev Microbiol* **21**: 101-120.
- Felden J. (2009). Methane fluxes and associated biogeochemical processes in cold seep ecosystems. Doctoral dissertation, Jacobs University Bremen.
- Gilewicz M, Ni'matuzahroh, Nadalig T, Budzinski H, Doumenq P, Michotey V, and Bertrand JC. (1997). Isolation and characterization of a marine bacterium capable of utilizing 2-methylphenanthrene. *Appl Microbiol Biotechnol* **48**: 528-533.
- Grossi V, Massias D, Stora G, and Bertrand JC. (2002). Burial, exportation and degradation of acyclic petroleum hydrocarbons following a simulated oil spill in bioturbated Mediterranean coastal sediments. *Chemosphere* **48**: 947-954.
- Grünke S, Felden J, Lichtschlag A, Girnth AC, de Beer D, Wenzhöfer F, and Boetius A. (2011). Niche differentiation among mat-forming, sulfide-oxidizing bacteria at cold seeps of the Nile Deep Sea Fan (Eastern Mediterranean Sea). *Geobiology* **9**: 330-348.
- Jaekel U. (2011). Anaerobic oxidation of short-chain and cyclic alkanes by sulfate-reducing bacteria. Doctoral dissertation, University Bremen.
- Joye SB, Boetius A, Orcutt BN, Montoya JP, Schulz HN, Erickson MJ, and Lugo SK. (2004). The anaerobic oxidation of methane and sulfate reduction in sediments from Gulf of Mexico cold seeps. *Chem Geol* **205**: 219-238.
- Kallmeyer J and Boetius A. (2004). Effects of temperature and pressure on sulfate reduction and anaerobic oxidation of methane in hydrothermal sediments of Guaymas Basin. *Appl Environ Microbiol* **70**: 1231-1233.
- Kennicutt II MC, Brooks JM, and Denoux GJ. (1988). Leakage of deep, reservoired petroleum to the near-surface on the Gulf of Mexico continental-slope. *Mar Chem* **24**: 39-59.

- Kleindienst S, Herbst FA, von Netzer F, Amann R, Peplies J, von Bergen M, Seifert J, Musat F, Lueders T, and Knittel K. (*in prep.*). Specialists instead of generalists oxidize alkanes in anoxic marine hydrocarbon seep sediments.
- Kleindienst S, Ramette A, Amann R, and Knittel K. (*submitted*). Distribution and in situ abundance of sulfate-reducing bacteria in diverse marine hydrocarbon seep sediments. *Environ Microbiol*
- Kniemeyer O, Musat F, Sievert SM, Knittel K, Wilkes H, Blumenberg M, Michaelis W, Classen A, Bolm C, Joye SB, and Widdel F. (2007). Anaerobic oxidation of short-chain hydrocarbons by marine sulphate-reducing bacteria. *Nature* **449**: 898-910.
- Knittel K, Boetius A, Lemke A, Eilers H, Lochte K, Pfannkuche O, Linke P, and Amann R. (2003). Activity, distribution, and diversity of sulfate reducers and other bacteria in sediments above gas hydrate (Cascadia margin, Oregon). *Geomicrobiol J* **20**: 269-294.
- Kunapuli U, Lueders T, and Meckenstock RU. (2007). The use of stable isotope probing to identify key iron-reducing microorganisms involved in anaerobic benzene degradation. *ISME J* **1**: 643-653.
- Lösekan T, Knittel K, Nadalig T, Fuchs B, Niemann H, Boetius A, and Amann R. (2007). Diversity and abundance of aerobic and anaerobic methane oxidizers at the Haakon Mosby Mud Volcano, Barents Sea. *Appl Environ Microbiol* **73**: 3348-3362.
- Lovley DR, Giovannoni SJ, White DC, Champine JE, Phillips EJP, Gorby YA, and Goodwin S. (1993). *Geobacter metallireducens* gen. nov. sp. nov., a microorganism capable of coupling the complete oxidation of organic-compounds to the reduction of iron and other metals. *Arch Microbiol* **159**: 336-344.
- Mastalerz V, de Lange GJ, and Dählmann A. (2009). Differential aerobic and anaerobic oxidation of hydrocarbon gases discharged at mud volcanoes in the Nile deep-sea fan. *Geochim Cosmochim Acta* **73**: 3849-3863.
- Michaelis W, Seifert R, Nauhaus K, Treude T, Thiel V, Blumenberg M, Knittel K, Gieseke A, Peterknecht K, Pape T, Boetius A, Amann R, Jørgensen B, B., Widdel F, Peckmann J, Pimenov NV, and Gulin MB. (2002). Microbial reefs in the Black Sea fueled by anaerobic oxidation of methane. *Science* **297**: 1013-1015.
- Musat F and Widdel F. (2008). Anaerobic degradation of benzene by a marine sulfate-reducing enrichment culture, and cell hybridization of the dominant phylotype. *Environ Microbiol* **10**: 10-19.
- Musat N, Halm H, Winterholler B, Hoppe P, Peduzzi S, Hillion F, Horreard F, Amann R, Jørgensen BB, and Kuypers MMM. (2008). A single-cell view on the ecophysiology of anaerobic phototrophic bacteria. *Proc Natl Acad Sci USA* **105**: 17861-17866.
- Nauhaus K, Boetius A, Krüger M, and Widdel F. (2002). *In vitro* demonstration of anaerobic oxidation of methane coupled to sulphate reduction in sediment from a marine gas hydrate area. *Environ Microbiol* **4**: 296-305.
- Niemann H, Elvert M, Hovland M, Orcutt B, Judd A, Suck I, Gutt J, Joye SB, Damm E, Finster K, and Boetius A. (2005). Methane emission and consumption at a North Sea gas seep (Tommeliten area). *Biogeosciences* **2**: 335-351.
- Niemann H, Lösekan T, de Beer D, Elvert M, Nadalig T, Knittel K, Amann R, Sauter EJ, Schlüter M, Klages M, Foucher JP, and Boetius A. (2006). Novel microbial communities of the Haakon Mosby mud volcano and their role as a methane sink. *Nature* **443**: 854-858.
- Omeregge EO, Niemann H, Mastalerz V, de Lange GJ, Stadnitskaia A, Mascle J, Foucher JP, and Boetius A. (2009). Microbial methane oxidation and sulfate reduction at cold seeps of the deep Eastern Mediterranean Sea. *Mar Geology* **261**: 114-127.
- Orcutt BN, Joye SB, Kleindienst S, Knittel K, Ramette A, Reitz A, Samarkin V, Treude T, and Boetius A. (2010). Impact of natural oil and higher hydrocarbons on microbial

- diversity, distribution, and activity in Gulf of Mexico cold-seep sediments. *Deep-Sea Res Pt II* **57**: 2008-2021.
- Pernthaler A, Pernthaler J, and Amann R. (2002). Fluorescence in situ hybridization and catalyzed reporter deposition for the identification of marine bacteria. *Appl Environ Microbiol* **68**: 3094-3101.
- Polerecky L, Adam B, Milucka J, Musat N, Vagner T, and Kuypers MMM. (2012). Look@NanoSIMS – a tool for the analysis of nanoSIMS data in environmental microbiology. *Environ Microbiol* DOI: 10.1111/j.1462-2920.2011.02681.x.
- Quistad SD and Valentine DL. (2011). Anaerobic propane oxidation in marine hydrocarbon seep sediments. *Geochim Cosmochim Acta* **75**: 2159-2169.
- Rabus R, Hansen TA, and Widdel F. (2006) in *The prokaryotes: Proteobacteria: alpha and beta subclasses: a handbook on the biology of bacteria*, edited by M. Dworkin, S. Falkow, and E. Rosenberg (Springer, Berlin), Vol. 5, pp. 659-768.
- Simoneit BRT and Lonsdale PF. (1982). Hydrothermal petroleum in mineralized mounds at the seabed of Guaymas Basin. *Nature* **295**: 198-202.
- Treude T, Boetius A, Knittel K, Wallmann K, and Jørgensen BB. (2003). Anaerobic oxidation of methane above gas hydrates at Hydrate Ridge, NE Pacific Ocean. *Mar Ecol Prog Ser* **264**: 1-14.
- Wegener G, Shovitri M, Knittel K, Niemann H, Hovland M, and Boetius A. (2008). Biogeochemical processes and microbial diversity of the Gullfaks and Tommeliten methane seeps (Northern North Sea). *Biogeosciences* **5**: 1127-1144.
- Weston NB and Joye SB. (2005). Temperature-driven decoupling of key phases of organic matter degradation in marine sediments. *Proc Natl Acad Sci USA* **102**: 17036-17040.
- Widdel F and Bak. F. (1992) in *The prokaryotes*, edited by A. Balows, H. G. Truper, M. Dworkin et al. (Springer-Verlag, New York), pp. 3352-3378.
- Widdel F, Knittel K, and Galushko A. (2010) in *Handbook of hydrocarbon and lipid microbiology*, edited by K.N. Timmis, T. McGenity, J. R. van der Meer et al. (Springer Berlin Heidelberg), Vol. 3, pp. 1997-2021.
- Winderl C, Penning H, von Netzer F, Meckenstock RU, and Lueders T. (2010). DNA-SIP identifies sulfate-reducing *Clostridia* as important toluene degraders in tar-oil-contaminated aquifer sediment. *ISME J* **4**: 1314-1325.
- Zengler K, Richnow HH, Rosselló-Móra R, Michaelis W, and Widdel F. (1999). Methane formation from long-chain alkanes by anaerobic microorganisms. *Nature* **401**: 266-269.

Table SIV.1: CARD-FISH probes used in this study

Probe name	Specificity	Formamide	Sequence (5' to 3')	Reference
Del495a	Most <i>Deltaproteobacteria</i> and <i>Gemmatimonadetes</i>	30	AGT TAG CCG GTG CTT CCT	Loy et al., 2002
	Competitor for Delta495a	30	AGT TAG CCG GTG CTT CTT	Macalady et al., 2006
Del495b	Some <i>Deltaproteobacteria</i>		AGT TAG CCG GCG CTT CCT	Loy et al., 2002
	Competitor for Delta495a	30	AGT TAG CCG GCG CTT CKT	Lücker et al., 2007
Del495c	Some <i>Deltaproteobacteria</i>		AAT TAG CCG GTG CTT CCT	Loy et al., 2002
	Competitor for Delta495a	-	AAT TAG CCG GTG CTT CTT	Lücker et al., 2007
DSS658	<i>Desulfosarcina/Desulfococcus</i> branch	50	TCC ACT TCC CTC TCC CAT	Manz et al., 1998
cDSS658	Competitor for DSS658	-	TCC ACT TCC CTC TCC GGT	Kleindienst et al, in prep.
SCA1-212a [▼]	SCA-SRB1 group within the DSS branch	20	CAT CCC AAA ACA GTA GCT	Kleindienst et al, in prep.
SCA1-212b [▼]	SCA-SRB1 group within the DSS branch	20	CAT CCC CAA ACA GTA GCT	Kleindienst et al, in prep.
SCA2-138	SCA-SRB2 group within the DSS branch	25	CGA GTT ATC CCC GAT TCG	Kleindienst et al, in prep.
LCA1-443 [▼]	LCA-SRB1 group within the DSS branch	20	CCU CAU AGG UUC UUC CCA	Kleindienst et al, in prep.
LCA2-63 [▼]	LCA-SRB2 group within the <i>Desulfobacteraceae</i>	10	GCU AAA GCU UUC UCG UUC	Kleindienst et al, in prep.
SEEP-SRB1a-473 [▼]	SEEP-SRB1a	30	TTC AGT GAT ACC GTC AGT ATC CC	Schreiber et al., 2010
SEEP-SRB1a 1441	SEEP-SRB1a	45	CCC CTT GCG GGT TGG TCC	Schreiber et al., 2010
SEEP1-SRBc-1309	SEEP-SRB1c	30	ATG GAG TCG AAT TGC AGA CTC	Schreiber et al., 2010
SEEP1-SRBd-1420	SEEP-SRB1d	30	CAA CTT CTG GTA CAG CCA	Schreiber et al., 2010
cSEEP1-SRBd-1420	Competitor for SEEP1-SRBd-1420	-	CAA CTT CTG GTA CAA CCA	Schreiber et al., 2010
SEEP-SRB1e-632	SEEP-SRB1e	45	CTC CCA TAC TCA AGC CCT TTA GTT	Schreiber et al., 2010
cSEEP1e-632	Competitor for SEEP-SRB1e-632	-	CTC CCA TAC TCA AGT CCC TTA GTT	Schreiber et al., 2010
SEEP-SRB1f-153	SEEP-SRB1f	35	AGC ATC GCT TTC GCG GTG	Schreiber et al., 2010

[▼]Used with helper according to Kleindienst et al. submitted, Schreiber et al. 2010

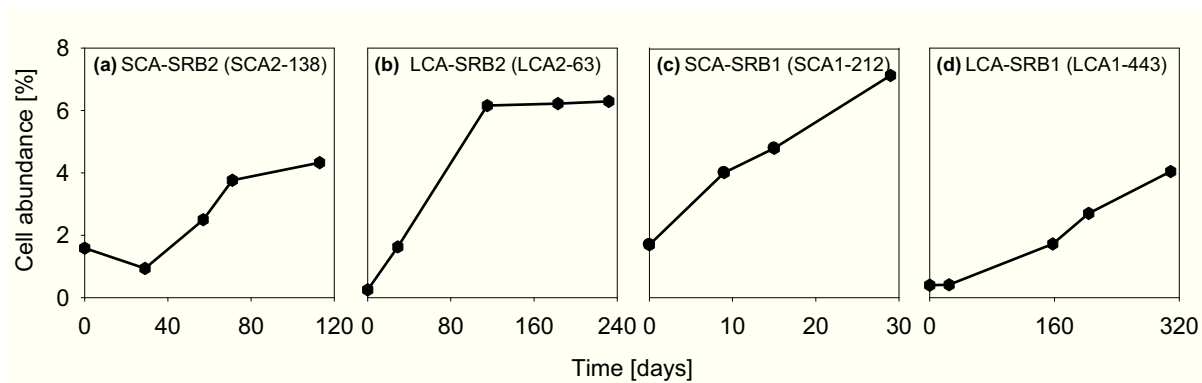


Fig. SIV.1: Relative abundance of alkane degraders within NanoSIMS samples over the course of hydrocarbon degradation for Amon MV butane (a), Amon MV dodecane (b), Guaymas Basin butane (c) and Guaymas Basin dodecane (d) experiments. Abundances were determined using specific CARD-FISH probes as indicated in the panels.

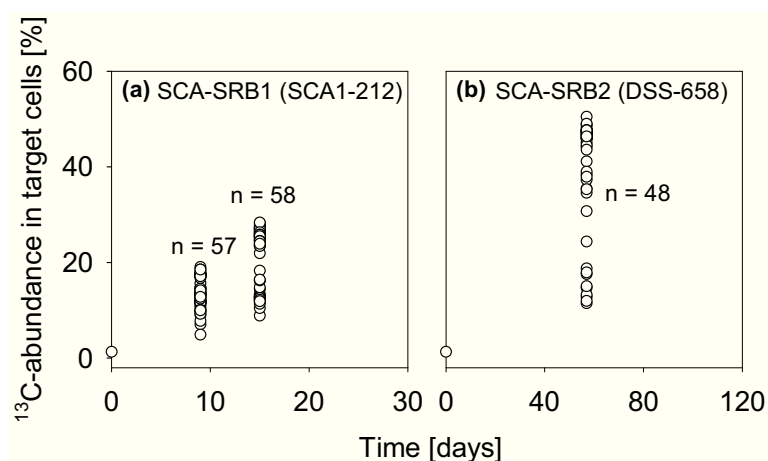


Fig. SIV.2: ^{13}C -abundance in individual cells (\circ ; n = number of cells) as determined by NanoSIMS analysis. Seep sediments from Amon Mud Volcano- (Amon MV; a) and Guaymas Basin (GB; b) were incubated with ^{13}C -labeled butane. Amon Mud Volcano samples were analyzed after 9 and 15 days of incubation, while Guaymas Basin samples were analyzed after 57 days.

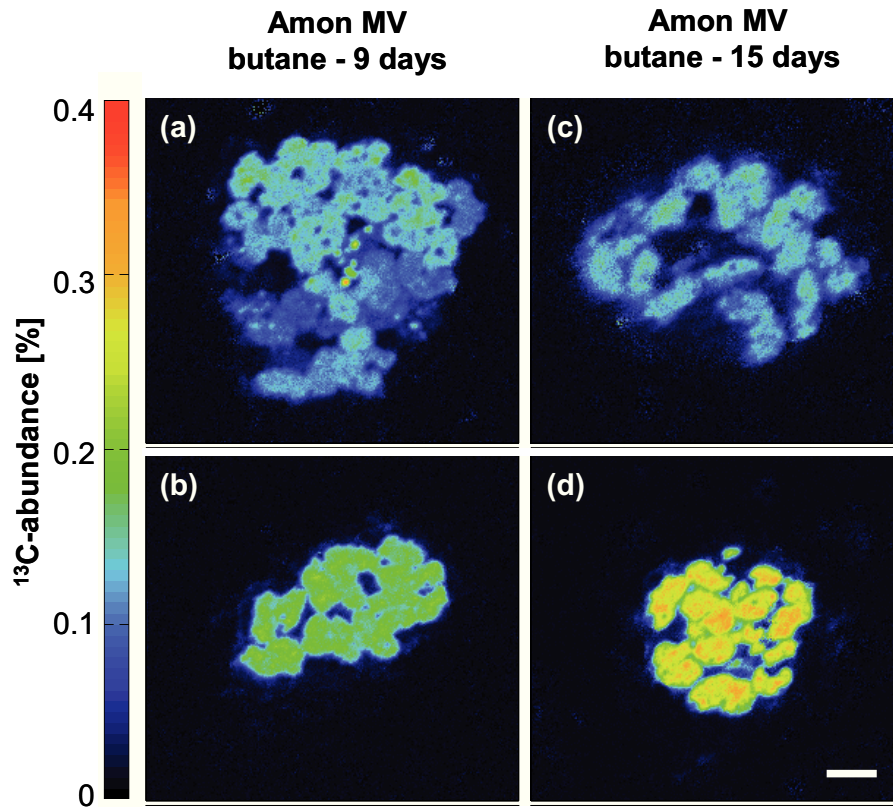


Fig. SIV.3: NanoSIMS images of selected aggregate forming ^{13}C -butane consumers of group SCA-SRB1 from Amon Mud Volcano (Amon MV) marine seep sediments after incubation for 9 (a-b) and 15 days (c-d). The activity (^{13}C -abundance) was used to determine label incorporation on the single cell level and revealed similar activities for cells within one aggregate. However, comparing the mean ^{13}C -abundances for each aggregate separately (as shown in Fig. IV.3j), activities of aggregates differed among each other and likely at least two different levels of activity were most apparent after 15 days of incubation. Scale bar indicates 2 μm .

Model of hydrocarbon assimilation by a population of growing cells

Let's assume that sediment slurry contains a population of cells that degrade two types of substrates, one ^{13}C -labeled (with the ^{13}C -abundance equal to A_{s1}) and one non-labeled (^{13}C -abundance equal to the natural abundance, $A_{s2} = A_0 = 0.011$). The first substrate contains n_{s1} carbon atoms (e.g., $n_{s1} = 4$ for butane, $n_{s1} = 12$ for dodecane), whereas the second one contains n_{s2} carbon atoms. Furthermore, let's assume that due to assimilation of these substrates the cells multiply and therefore the population grows exponentially as

$$N(t) = N(0)2^{t/\tau}, \quad (1)$$

where τ is the doubling time and $N(t)$ is the number of cells per ml of the sediment slurry at time point t . In the following we derive expressions for the ^{13}C -abundance in the substrate degrading cells (A_{cell}), in the total organic carbon pool (A_{TOC}) and in the total dissolved inorganic carbon pool (A_{DIC}) as a function of time.

We first consider that during a life-cycle the cell increases its cellular carbon content from C_{cell} (i.e., when it has just divided) to $2C_{\text{cell}}$ (i.e., just before the next division). For a randomly chosen cell, its cellular carbon content $C(t)$ at an arbitrary time point t between two subsequent cell divisions has a value that is uniformly distributed between C_{cell} and $2C_{\text{cell}}$. Therefore, the carbon content of an average cell is $C_{\text{avg}} = 1.5C_{\text{cell}}$. Let's further assume that the carbon content of the cell increases linearly as $C(t) = C(0) + r_a t$ as a result of assimilation of carbon atoms from the substrates at a rate r_a (in $\text{mol C cell}^{-1} \text{d}^{-1}$), and that the cell divides when its carbon content increases by C_{cell} . Using these assumptions, we can find the relationship between the doubling time τ and the carbon assimilation rate r_a as $C_{\text{cell}} = r_a \tau$. Using the carbon content of an average cell, this relationship can be written as

$$\tau = \frac{C_{\text{avg}}}{1.5r_a}. \quad (2)$$

In general, the carbon assimilation rate can be written as $r_a = \epsilon(r_{s1}n_{s1} + r_{s2}n_{s2})$, where r_{si} is the cellular turnover rate of substrate i ($i = 1, 2$; in $\text{mol substrate cell}^{-1} \text{d}^{-1}$) and ϵ is the substrate assimilation efficiency (assumed equal for both substrates). Without loss of generality, we can write $r_{si} = r_s f_i$, where f_i is the fraction of the total substrate turnover rate r_s that is used for turnover of substrate i ($f_1 + f_2 = 1$). Assuming that all assimilated carbon from the substrates is used to increase the cellular biomass, which will result in cell division when the increase reaches C_{cell} , the relationship between the cellular doubling time and the cellular substrate turnover rates can be written as

$$\tau = \frac{C_{\text{avg}}}{1.5\epsilon r_s (f_1 n_{s1} + f_2 n_{s2})}. \quad (3)$$

If the sediment contains N cells per ml with an average carbon content of C_{avg} , the total carbon concentration in this organic carbon pool is $C = NC_{\text{avg}}$. Taking into account equations 1–3, the rate of increase in C is therefore given by

$$\frac{dC}{dt} = \frac{1.5 \ln(2)}{C_{\text{avg}}} \epsilon_s (f_1 n_{s1} + f_2 n_{s2}) C. \quad (4)$$

The probability of utilizing a ^{13}C -labeled substrate molecule is equal to the ^{13}C -abundance of the substrate. Therefore, the ^{13}C -carbon content of the cell population increases at a rate

$$\frac{d^{13}\text{C}}{dt} = \frac{1.5 \ln(2)}{C_{\text{avg}}} \epsilon_s (f_1 n_{s1} A_{s1} + f_2 n_{s2} A_0) C. \quad (5)$$

Using equation 1, the ^{13}C -carbon content at time t can easily be calculated by integration of equation 5, which gives

$$^{13}\text{C}(t) = ^{13}\text{C}(0) + \int_0^t \frac{d^{13}\text{C}}{dt} dt = ^{13}\text{C}(0) + C(0)F(2^{t/\tau} - 1), \quad (6)$$

where

$$F = \frac{f_1 n_{s1} A_{s1} + f_2 n_{s2} A_0}{f_1 n_{s1} + f_2 n_{s2}}. \quad (7)$$

Consequently, the ^{13}C -abundance in the average cell from the population of substrate degrading cells is equal to

$$A_{\text{cell}}(t) = \frac{^{13}\text{C}(t)}{C(t)} = \frac{A_0 + Ff(t)}{1 + f(t)}, \quad (8)$$

where

$$f(t) = 2^{t/\tau} - 1 \quad (9)$$

and A_0 is the initial ^{13}C -abundance in the cells. Equation 8 depends only on the parameters characterizing the cell (C_{avg}) and its carbon assimilation (ϵ , r_s , f_1 and $f_2 = 1 - f_1$). Provided that the doubling time of the cell (and thus the total substrate assimilation rate r_a ; Eq. 3) and the substrate's ^{13}C -abundances are known, the fractions f_1 and $f_2 = 1 - f_1$ can be estimated by measuring ^{13}C -abundances in single cells at different time points and fitting these measurements with the function 8.

Assuming that the total organic carbon (TOC) in the sediment slurry increases solely due to the increase in the carbon content of the substrates degrading cell population, and that the initial ^{13}C -abundance of TOC is A_0 , the TOC and ^{13}C -TOC as a function of time can be calculated by a similar integration as $^{13}\text{C}(t)$ in Eq. 6. After performing this integration, we arrive at the following expression for the ^{13}C -abundance in the TOC pool:

$$A_{\text{TOC}}(t) = \frac{A_0 + \text{GFf}(t)}{1 + \text{Gf}(t)}, \quad (10)$$

where

$$G = \frac{N(0)C_{\text{avg}}}{\text{TOC}_0} \frac{1}{1.5 \ln 2}$$

and TOC_0 is the initial TOC content in the sediment (in $\text{mol C L}^{-1}_{\text{sed}}$).

Due to the substrate degrading activity of the cell population, the carbon content in the porewater DIC pool increases at a rate $(1-\varepsilon)N(t)r_s(f_1n_{s1} + f_2n_{s2})/\phi$, where ϕ is the sediment porosity and $N(t)$ is the momentary cell density. Similarly, the ^{13}C -DIC increases at a rate $(1 - \varepsilon)N(t)r_s(f_1n_{s1}A_{s1} + f_2n_{s2}A_0)/\phi$. Integration of these rates gives the following expression for the ^{13}C -abundance in the DIC pool:

$$A_{\text{DIC}}(t) = \frac{A_0 + \text{HFf}(t)}{1 + \text{Hf}(t)}, \quad (11)$$

where

$$H = \frac{N(0)C_{\text{avg}}}{\phi \text{DIC}_0} \frac{1 - \varepsilon}{\varepsilon} \frac{1}{1.5 \ln 2}$$

and DIC_0 is the initial DIC content in the porewater (in $\text{mol C L}^{-1}_{\text{pw}}$). Therefore, by measuring the initial carbon contents TOC_0 and DIC_0 , the parameters ε and $N(0)$ can be estimated by fitting the measured ^{13}C -abundances in the TOC and DIC pools with functions 10–11.

If the initial TOC and DIC contents are large compared to the carbon content in the substrate degrading cell population, i.e., $\text{TOC}_0 \gg N(0)C_{\text{avg}}$ and $\text{DIC}_0 \gg N(0)C_{\text{avg}}$, equations 10-11 can be combined to yield the following equation:

$$\varepsilon \approx \left(1 + \frac{A_{\text{DIC}}(t) - A_0}{A_{\text{TOC}}(t) - A_0} \frac{\phi \text{DIC}_0}{\text{TOC}_0} \right)^{-1}. \quad (12)$$

This expression can be used to estimate the substrate assimilation efficiency, ε , provided that assimilation (at a cellular rate $\varepsilon r_s(f_1n_{s1} + f_2n_{s2})$) and dissimilation (at a cellular rate $(1 - \varepsilon)r_s(f_1n_{s1} + f_2n_{s2})$) of the substrates by the substrate degrading cells are the only processes that convert the substrates into biomass and inorganic carbon. It should be noted that as long as the same substrates are assimilated and dissimilated, expression 12 is independent of the cellular carbon content, the total substrate turnover rate and the number of C-atoms in the degraded substrates.

Finally, it is useful to show that the above equations lead to the expression that is commonly used to calculate substrate assimilation rates from the measured ^{13}C -abundance in

cells incubated with a labeled substrate. Assuming that the cells assimilate only the labeled substrate (i.e., $f_1 = 1, f_2 = 0$), and that the incubation interval is sufficiently short to prevent cell division or substantial increase in their C-content (i.e., $t \ll \tau$), equation 8 can be simplified to

$$A_{\text{cell}}(t) \approx A_{\text{cell}}(0) + A_s \frac{1.5 \ln 2}{C_{\text{avg}}} \epsilon r_s n_s t.$$

Thus, under these conditions, the cellular substrate assimilation rate can be calculated simply from the cell's ^{13}C -abundances measured at different time points, i.e.,

$$r_a = \epsilon r_s n_s = \frac{A_{\text{cell}}(t) - A_{\text{cell}}(0)}{t} \frac{C_{\text{avg}}}{1.5 \ln(2) A_s}. \quad (13)$$

Fitting of the experimental data

The measured cell abundances and ^{13}C -abundances in the substrate degrading cells and in the TOC and DIC pools were fitted with functions 1, 8, 10 and 11 to yield estimates of the doubling time (τ), total cellular carbon turnover rate (r_s), the substrates assimilation rates ($\epsilon r_s f_1$ and $\epsilon r_s f_2$), the carbon assimilation rate ($\epsilon r_s (f_1 n_{s1} + f_2 n_{s2})$) and the initial cell abundance ($N(0)$). The results are shown in Fig. IV.1 and Fig. IV2.

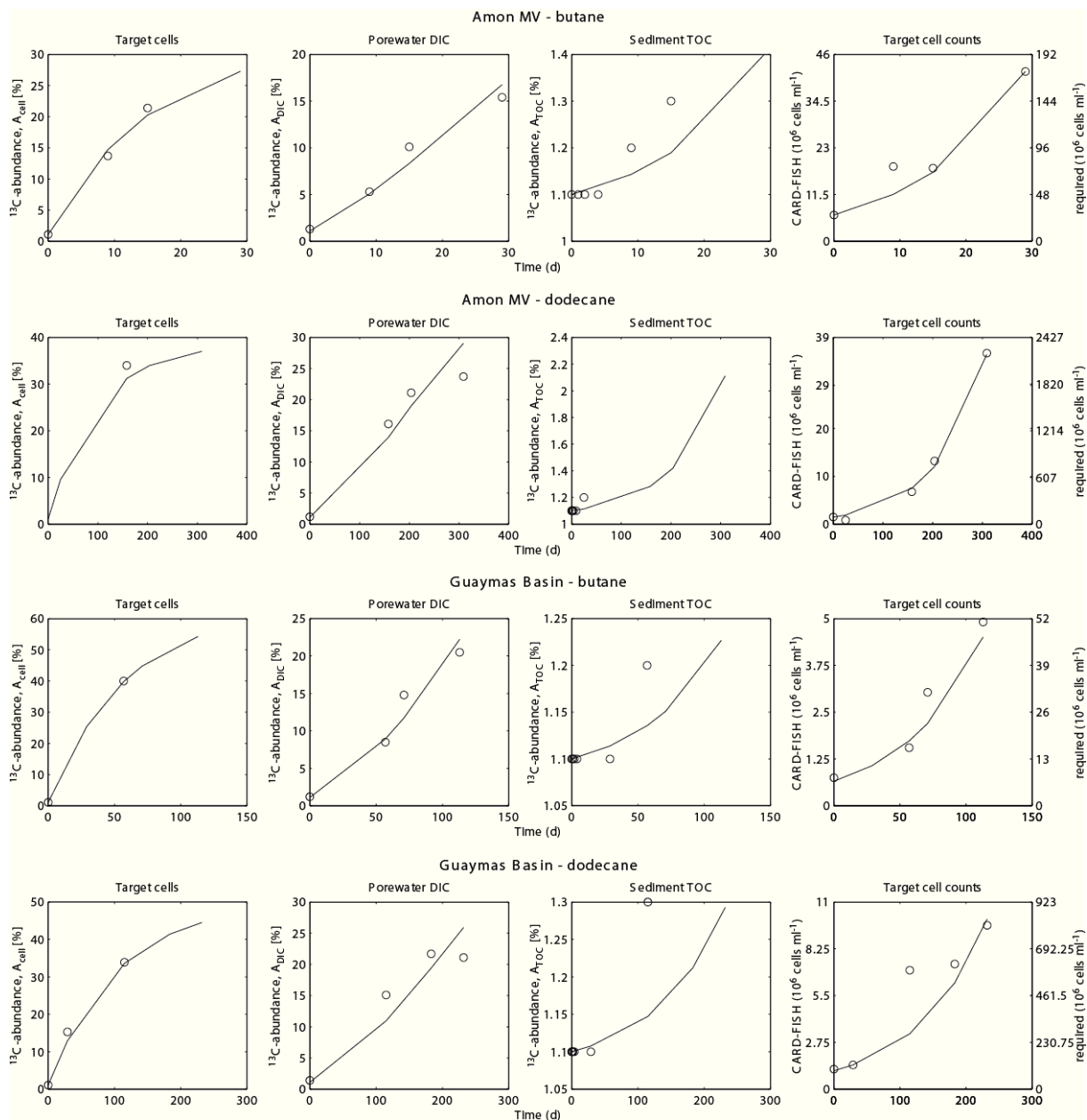


Fig. SIV.4: ^{13}C -abundances in the single cells of the substrate degrading sulfate-reducing bacteria (A_{cell}) and in the DIC (A_{DIC}) and TOC (A_{TOC}) pools, plotted as a function of time. Shown are experimental data (symbols) and the best fits by the model (lines). In this scenario, the assimilation efficiency ϵ was set to 10%. Fitting was done assuming $\text{DIC}_0 = 20\text{mM}$ and the measured TOC_0 values. The far-right graphs for each incubation show the comparison between the cell counts required to fit the experimental data (right axis) and those measured by the CARD-FISH method (left axis). The measured and required cell counts increase exponentially with the same doubling time. The ^{13}C -abundance in the cells from the AMV-dodecane incubation was estimated based on those determined for the GB-dodecane incubation.

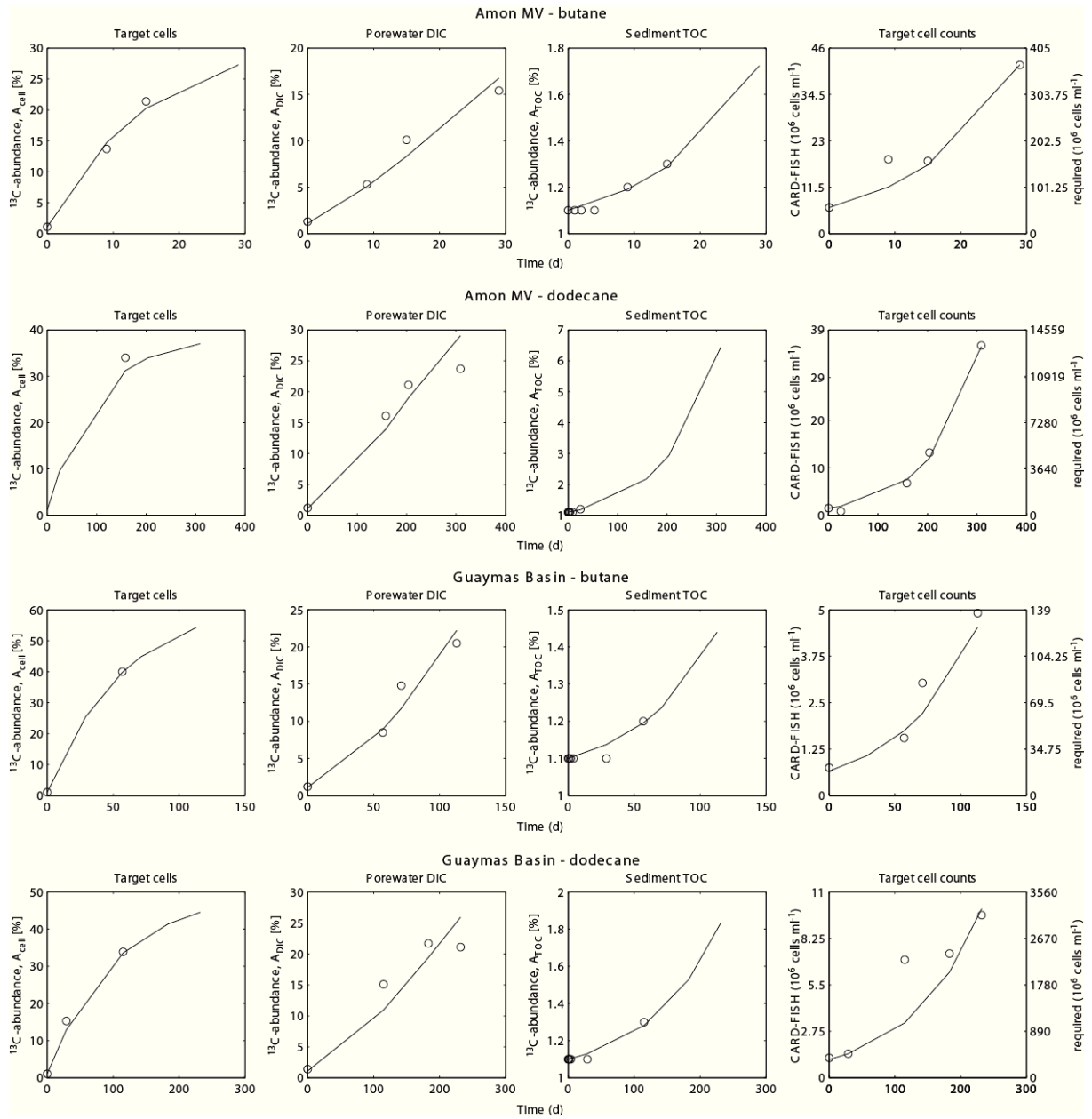


Fig. SIV.5: The same as in Fig. S4, except the substrate assimilation efficiency was estimated based on the bulk TOC and DIC data (concentrations and ¹³C-abundances) using equation 12.

References for Supplementary Information

- Kleindienst S, Herbst FA, von Netzer F, Amann R, Peplies J, von Bergen M, Seifert J, Musat F, Lueders T, and Knittel K. (*in prep.*). Specialists instead of generalists oxidize alkanes in anoxic marine hydrocarbon seep sediments.
- Kleindienst S, Ramette A, Amann R, and Knittel K. (*submitted*). Distribution and in situ abundance of sulfate-reducing bacteria in diverse marine hydrocarbon seep sediments. *Environ Microbiol*
- Loy A, Lehner A, Lee N, Adamczyk J, Meier H, Ernst J, Schleifer KH, and Wagner M. (2002). Oligonucleotide microarray for 16S rRNA gene-based detection of all recognized lineages of sulfate-reducing prokaryotes in the environment. *Appl Environ Microbiol* **68**: 5064-5081.
- Lücker S, Steger D, Kjeldsen KU, MacGregor BJ, Wagner M, and Loy A. (2007). Improved 16S rRNA-targeted probe set for analysis of sulfate-reducing bacteria by fluorescence in situ hybridization. *J Microbiol Methods* **69**: 523-528.
- Macalady JL, Lyon EH, Koffman B, Albertson LK, Meyer K, Galdenzi S, and Mariani S. (2006). Dominant microbial populations in limestone-corroding stream biofilms, Frasassi cave system, Italy. *Appl Environ Microbiol* **72**: 5596-5609.
- Manz W, Eisenbrecher M, Neu TR, and Szewzyk U. (1998). Abundance and spatial organization of gram-negative sulfate-reducing bacteria in activated sludge investigated by in situ probing with specific 16S rRNA targeted oligonucleotides. *FEMS Microbiol Ecol* **25**: 43-61.
- Schreiber L, Holler T, Knittel K, Meyerdierks A, and Amann R. (2010). Identification of the dominant sulfate-reducing bacterial partner of anaerobic methanotrophs of the ANME-2 clade. *Environ Microbiol* **12**: 2327-2340.

Chapter V

Impact of natural oil and higher hydrocarbons on microbial diversity, distribution and activity in Gulf of Mexico cold seep sediments

Beth N. Orcutt^{a,*}, Samantha B. Joye^a, Sara Kleindienst^b, Katrin Knittel^b,
Alban Ramette^b, Anja Reitz^d, Vladimir Samarkin^a, Tina Treude^{b,1}, Antje Boetius^{b,c}

Published in *Deep Sea Research Part II: Topical Studies in Oceanography*

Volume 57, Pages 2008–2021, 2010

© Copyright 2010 Elsevier Ltd.

* Corresponding author. Present address: The Center for Geomicrobiology, Aarhus University, DK-8000 Aarhus, Denmark. E-mail: beth.orcutt@biology.au.dk

^a Department of Marine Sciences, University of Georgia, Athens, GA 30602, USA

^b Max Planck Institute for Marine Microbiology, 28359 Bremen, Germany

^c HGF MPG Joint Research Group on Deep Sea Ecology and Technology, AWI, 27515 Bremerhaven, Germany

^d Leibniz-Institute of Marine Sciences, IFM-GEOMAR, 24148 Kiel, Germany

¹ Present address: Leibniz-Institute of Marine Sciences, IFM-GEOMAR, 24148 Kiel, Germany

Abstract

Gulf of Mexico cold seeps characterized by variable compositions and magnitudes of hydrocarbon seepage were sampled in order to investigate the effects of natural oils, methane, and non-methane hydrocarbons on microbial activity, diversity, and distribution in seafloor sediments. Though some sediments were characterized by relatively high quantities of oil, which may be toxic to some microorganisms, high rates of sulfate reduction (SR, $27.9 \pm 14.7 \text{ mmol m}^{-2} \text{ d}^{-1}$), anaerobic oxidation of methane (AOM, $16.2 \pm 6.7 \text{ mmol m}^{-2} \text{ d}^{-1}$), and acetate oxidation ($2.74 \pm 0.76 \text{ mmol m}^{-2} \text{ d}^{-1}$) were observed in radiotracer measurements. In many instances, the SR rate was higher than the AOM rate, indicating that non-methane hydrocarbons fueled SR. Analysis of 16S rRNA gene clone libraries revealed phylogenetically diverse communities that were dominated by phylotypes of sulfate-reducing bacteria (SRB) and anaerobic methanotrophs of the ANME-1 and ANME-2 varieties. Another group of archaea forms a Gulf of Mexico-specific clade (GOM ARC2) that may be important in brine-influenced, oil-impacted sediments from deeper water. Additionally, species grouping within the uncultivated *Deltaproteobacteria* clades SEEP-SRB3 and -SRB4, as well as relatives of *Desulfobacterium anilini*, were observed in relatively higher abundance in the oil-impacted sediments, suggesting that these groups of SRB may be involved in or influenced by degradation of higher hydrocarbons or petroleum byproducts.

Chapter VI

Synopsis of Results, General Discussion and Conclusions

In the present thesis, the ecology, function and physiology of SRB involved in hydrocarbon degradation processes at marine seeps were examined. The obtained results deepened our knowledge about the abundance and distribution of hydrocarbon-degrading SRB in marine seep sediments. In addition, the spectrum of SRB groups involved in hydrocarbon-degradation at marine seeps was substantially broadened: three groups of yet uncultured alkane-degrading SRB as well as one novel ANME partner were discovered. Furthermore, the achieved data considerably advance our understanding of the high diversity of SRB key players and their important impact on marine seep ecosystems.

In the following, the results obtained in this thesis are shortly summarized and discussed in a broader context with respect to the original objectives. Finally, conclusions and main achievements obtained in this study are presented. For detailed results and discussions the reader is referred to Chapters II to IV.

1. DSS hydrocarbon degraders at marine seeps

Prior to this study several SRB able to degrade non-methane hydrocarbons were isolated (reviewed in Widdel et al., 2010), while knowledge about the in situ abundance was largely lacking. Some of the DSS microorganisms described to oxidize alkanes and aromatic hydrocarbons had been isolated from marine seep sediments (Kniemeyer et al., 2003; Kniemeyer et al., 2007). In the present study, the class *Deltaproteobacteria* and the genus *Desulfotomaculum* (*Firmicutes*) were analyzed by CARD-FISH as a proxy for SRB. Analysis revealed that the DSS group dominated most hydrocarbon seep sediments. They accounted for instance up to 53% of total cells (89% of all *Deltaproteobacteria*) at the Amon Mud Volcano (Chapter II). Furthermore, total DSS members accounted for up to 36% of total cells (92% of all *Deltaproteobacteria*) at the Gulf of Mexico and even up to 61% of total cells (99% of all *Deltaproteobacteria*) at Hydrate Ridge. Therefore, the DSS group was assumed to play an important role in hydrocarbon degradation processes. Their abundance was high in both cells associated with ANME archaea (also referred to as aggregated cells) and non-aggregated cells (also referred to as single cells). DSS organisms that live associated with ANME archaea were found to be particularly abundant at Hydrate Ridge and are most probably involved in AOM (Boetius et al., 2000; Orphan et al., 2001; Michaelis et al., 2002; Orphan et al., 2002; Knittel et al., 2003; Knittel et al., 2005). Therefore, single DSS cells at marine seeps were, similar to their isolated counterparts, assumed to oxidize non-methane hydrocarbons, and the apparent

dominance of the DSS group was hence a first indication for their involvement in non-methane hydrocarbon degradation. As part of this thesis, this hypothesis was tested by SIP-techniques. The majority of key players involved in butane and dodecane degradation in marine gas and hydrocarbon seep sediments was identified as DSS members (Chapter III). This confirmed that the dominant DSS community is actually capable to mediate these processes under similar conditions as found in marine seep sediments.

At gas seeps potential non-methane hydrocarbon substrates for DSS members are mainly short-chain alkanes, while at gas and oil emitting seeps DSS microorganisms probably oxidize alkanes and aromatic hydrocarbons. Alkenes are absent or only present in traces at marine habitats (cf. Bazylinski et al., 1988; Didyk & Simoneit, 1989), and are therefore not assumed to be an important energy source for marine microbes.

DSS members have been reported to be abundant in marine non-seep coastal sediments as well (e.g. Ravensschlag et al., 2000; Mußmann et al., 2005; Musat et al., 2006). Furthermore, DSS organisms are metabolically versatile and possess numerous oxidative capabilities with respect to electron donors such as hydrogen, fatty acids and alcohols (e.g. Brysch et al., 1987; Liesack & Finster, 1994; Knoblauch et al., 1999). This metabolic diversity is not surprisingly considering the large DSS intragroup diversity with 16S rRNA gene similarity values as low as 80%. Although isolates were taxonomically classified as *Desulfobacteraceae* this is far below the proposed cut-off of $87.7\% \pm 2.5$ minimum level for family boundaries and the DSS clade may rather be regarded as a novel order according to the classification boundaries proposed by Yarza and colleagues (2010). Because of this vast diversity, DSS members at marine seeps may comprise microbes with so far unknown metabolic pathways. Nevertheless, based on SR rates in combination with molecular and isotopic analysis of hydrocarbons (Sassen et al., 2004; Niemann et al., 2006a; Mastalerz et al., 2009; Bowles et al., 2011; Schubotz et al., 2011) it is expected that hydrocarbons and their metabolic byproducts are among the dominant electron donors, which are used by DSS members at marine seeps. In depth analysis of the abundance of cultured strain BuS5 and the enrichment culture Butane12-GMe revealed a very low abundance at seeps (below 0.5% of total cells; Chapter II). Thus, the results obtained in this thesis strongly suggest that the highly diverse DSS group is globally abundant and that at least some of its members play an important ecological role in marine seep sediments by oxidizing non-methane hydrocarbons.

SCA-SRB1, SCA-SRB2, LCA-SRB1 and SEEP-SRB1. In the present thesis, it was proven (for groups SCA-SRB1, SCA-SRB2 and LCA-SRB1) or hypothesized (for subgroups SEEP-SRB1b-f) that specific DSS subgroups are involved in hydrocarbon degradation

(Fig. VI.1). These DSS subgroups will in the following be discussed with respect to their abundance and distribution at marine seeps and their potential to use distinct hydrocarbons as carbon and energy sources in situ.

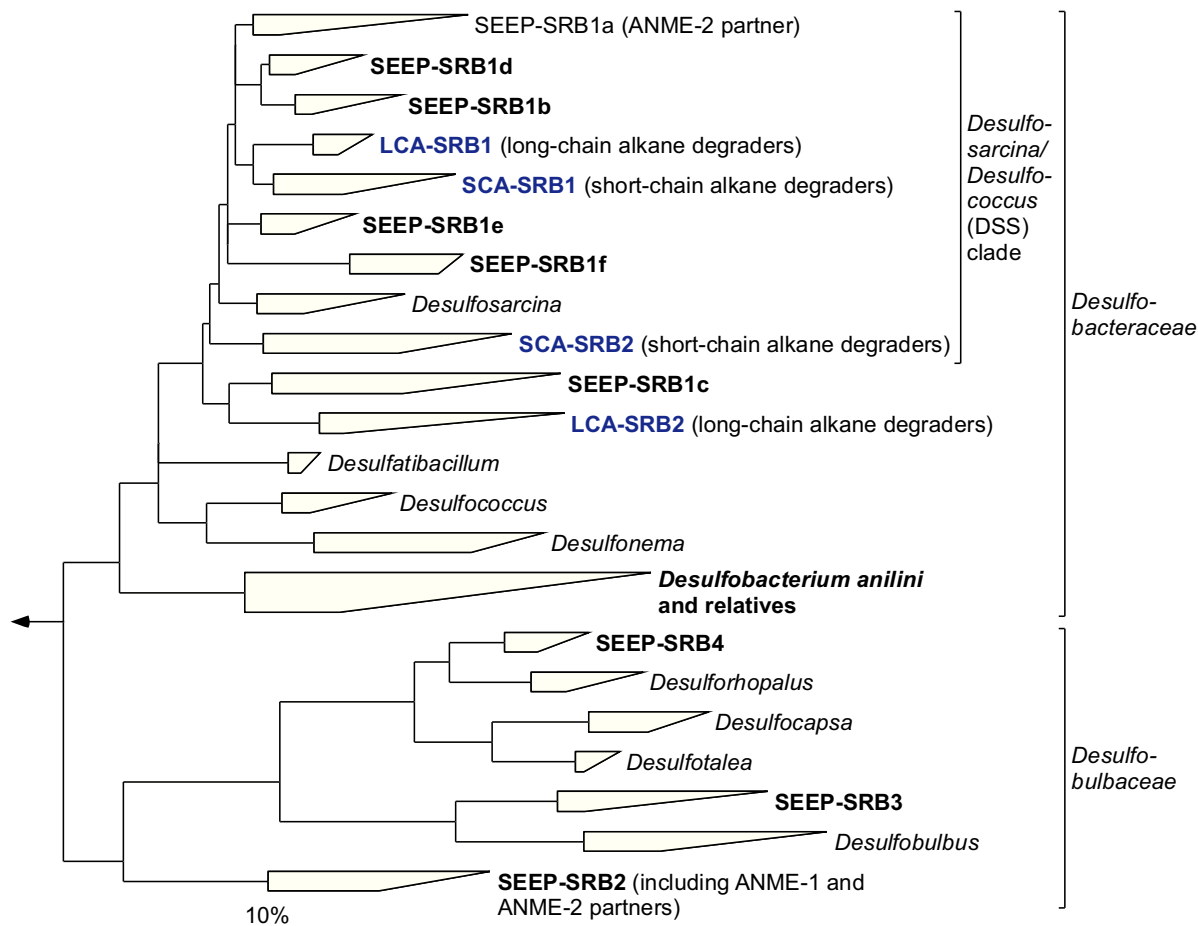


Fig. VI.1: Phylogenetic tree showing the affiliation of proposed hydrocarbon-degrading SRB groups within the *Deltaproteobacteria*. Groups, which were proven to be capable of alkane degradation are shown in blue, those which were hypothesized but not yet proven are in bold type. The tree was calculated by maximum-likelihood analysis in combination with filters, which consider only 50% conserved regions of the 16S rRNA of *Deltaproteobacteria*. The bar represents 10% estimated sequence divergence.

1.1. SCA-SRB1 are global key players involved in short-chain alkane degradation

This study supports recent findings obtained by traditional cultivation techniques that SCA-SRB1 members are catalyzing propane and butane degradation. Strain BuS5 and enrichment cultures But12-GMe, Prop12-GMe and But12-HyR were isolated or enriched from seeps at Guaymas Basin, Gulf of Mexico and Hydrate Ridge (Kniemeyer et al., 2007; Jaekel, 2011).

These propane- and butane-oxidizing isolates and enrichment cultures clustered in a phylogenetically distinct group. In the present thesis, the 16S rRNA intragroup similarity of SCA-SRB1 was analyzed and shown to be >94%, suggesting that SCA-SRB1 is likely a single genus (Chapter III). Thus, all SCA-SRB1 members may have highly similar metabolic capabilities with respect to propane and butane degradation.

Based on the origin of isolates and enrichment cultures, SCA-SRB1 members seem to be globally distributed at various hydrocarbon seeps including Guaymas Basin, Gulf of Mexico and Amon Mud Volcano. In addition, based on the enrichment culture But12-HyR (Jaekel, 2011) they occur even in methane-dominated seeps such as Hydrate Ridge, where they probably use short-chain alkanes that are present in variable, yet often low concentrations (mostly <1%; Milkov et al., 2004). Furthermore, in this study the in situ quantification of SCA-SRB1 (Chapter IV) supported the assumption that this group is globally distributed. SCA-SRB1 were determined to be particularly abundant in sediment samples from Amon Mud Volcano, Tommeliten and Gulf of Mexico as well as in Black Sea microbial mats. In addition, clone libraries from previous studies and the present thesis comprised SCA-SRB1 sequences in a high frequency at seeps from Gulf of Mexico, Guaymas Basin, several Mediterranean mud volcanoes and Gulf of Cadiz (Table VI.1 and Chapter II). In conclusion, members of the group SCA-SRB1 are proposed to be global key players for degradation of short-chain alkanes at marine seeps.

Table VI.1: Distribution of specific hydrocarbon-degrading SRB groups as revealed by 16S rRNA gene sequence retrieval.

Habitat/Enrichment	Sequence # and representative sequence (accession #)										
	Bac- teria [▲]	Delta- proteo- bacteria	DBA and relatives	SCA- SRB1	SCA- SRB2	LCA- SRB1	LCA- SRB2	SEEP- SRB1	SEEP- SRB2	SEEP- SRB3	SEEP- SRB4
Enrichments											
Butane (GB & GoM)	4	2	-	2 (EF077225)	-	-	-	-	-	-	-
Propane & butane (GB, GoM & HR)	16	16	-	2 (FR823373)	1 (FR823364)	-	-	-	-	-	-
Butane (GB)	109 [*]	65	10 (NA)	4 (NA)	14[§] (NA)	-	-	9 (NA)	1 (NA)	-	-
Propane & pentane (Zodlone) [§]	61	40	1 (GU211136)	-	-	-	3 (GU211129)	2 (GU211116)	-	-	-
Phenanthrene (San Diego Bay)	2	2	-	-	1 (EF467180)	-	-	-	-	-	-
Benzene (GB)	12	4	2 (AF029045)	-	-	-	-	-	-	-	-
Oil (estuarine sediments)	79	79	-	-	5 (HQ622295)	-	1 (HQ622287)	-	-	-	-
Methane (GB)	46	17	4 (FR682625)	-	-	-	1 (FR682640)	1 (FR682642)	2 (FR682636)	-	-
Methane (Gulf of Cadiz)	90	15	-	-	-	-	1 (HQ405625)	7 (HQ405690)	-	-	-
Gulf of Mexico sediments											
	67	31	5 (AY542205)	3 (AY542263)	2	-	-	1 (AY542242)	5 (AY542201)	2 (AY542555)	0
	35	21	-	5 (AY324503)	2 (AY324491)	-	-	4 (AY324502)	5 (AY324500)	1 (AY324519)	1 (AY324495)
	117	95	18 (FR872003)	3 (FR872044)	-	-	-	8 (FR872040)	29 (FR871996)	-	-
	134 [§]	128	12 (FR872081)	16 (FR872057)	-	-	-	46 (FR872100)	16 (FR872088)	-	-
	55	14	4 (AY542613)	1 (AY542599)	4 (AY542569)	-	-	-	-	-	-
	268	71	9 (AM745206)	-	-	1 (FN421142)	-	10 (AM745144)	6 (AM746088)	7 (AM746069)	3 (AM745168)
	34	16	2 (AM404376)	-	-	-	-	4 (AM404373)	2 (AM404377)	-	1 (AM404379)
	63	27	13 (AY211731)	-	-	-	-	-	7 (AY211752)	-	-
Tommeliten sediments											
	77	31	3 (FM179888)	-	-	-	-	-	5 (FM179871)	1 (FM179901)	1 (FM179898)
	7	4	1 (DQ007536)	-	-	-	-	1 (DQ007534)	1 (DQ007535)	-	-
Eastern Mediterranean mud volcano sediments											
Amon	920	295	8 (FR798170)	4 (FR798655)	-	-	-	8 (FR798175)	-	111 (FR798178)	23 (FR798158)
Amon & Isis	142	69	2 (EU179164)	3 (EU178996)	1 (EU179041)	1 (EU179001)	-	32 (EU178998)	-	1 (EU179157)	3 (EU179027)
Amsterdam	276	60	8 (HQ588565)	2 (HQ588475)	3 (HQ588569)	-	-	13 (HQ588556)	4 (HQ588449)	1 (HQ588389)	3 (HQ588501)
Kazan	199	43	2 (FJ712483)	-	1 (FJ712462)	-	-	7 (FJ712461)	-	-	2 (FJ712508)
Chefren	376	91	1 (EF687258)	-	-	-	2 (EF687267)	17 (EF687289)	1 (EF687326)	1 (EF687511)	2 (EF687149)
Milano	90	15	-	-	-	-	-	-	-	3 (AY592930)	1 (AY592880)
Haakon Mosby Mud Volcano sediments											
	71	28	1 (AJ704686)	-	-	-	2 (AJ704684)	5 (AJ704677)	-	-	3 (AJ704692)
Hydrate Ridge											
	44	25	-	-	-	-	-	4 (AJ535249)	3 (AJ535250)	2 (AJ535236)	4 (AJ535218)
	23	8	-	-	-	-	-	-	4 (AM713448)	-	-
	41	18	2 (AM229200)	-	-	-	-	12 (AM229208)	2 (AM229205)	-	-
Gulf of Cadiz											
	139	59	4 (FJ813591)	8 (FN820354)	-	-	-	21 (FJ813564)	-	-	-
	174	76	-	-	-	-	4 (GQ249590)	1 (GQ249585)	-	-	-

(continued on next page)

Table VI.1: continued

Habitat/Enrichment	Sequence # and representative sequence (accession #)										
	Bac- teria [▲]	<i>Delta- proteo- bacteria</i>	DBA and relatives	SCA- SRB1	SCA- SRB2 and rel. [▼]	LCA- SRB1	LCA- SRB2	SEEP- SRB1	SEEP- SRB2	SEEP- SRB3	SEEP- SRB4
<i>Eel River Basin and Santa Barbara Basin sediments</i>											
	119	37	4 (GQ357040)	-	-	-	-	6 (GQ356958)	-	2 (GQ356972)	1 (GQ356948)
	121 (122)	34	1 (FJ264650)	-	-	-	-	2 (FJ264753)	1 (FJ264786)	2 (FJ264778)	1 (FJ264573)
	21	7	1 (EU622296)	-	1 (EU622291)	-	-	1 (EU622295)	-	-	-
	22	19	1	-	2 (AF354159)	-	-	6 (AF354158)	4 (AF354156)	1 (AF354166)	1 (AF354148)
<i>Japan Sea sediments</i>											
Deep-Sea	37	8	-	-	-	-	-	1 (AB525448)	5 (AB525460)	1 (AB525452)	-
	15	4	-	-	-	-	-	-	-	-	2 (AB121099)
	75	3	-	-	-	-	-	-	-	-	1 (AB015588)
Okhotsk Sea	116	13	-	-	-	-	-	1 (FJ873366)	-	-	1 (FJ873360)
<i>Arctica and Antarctica sediments</i>											
Arctica	79	34	1 (AJ241002)	-	-	-	-	-	-	-	2 (AJ240992)
	114	12	-	-	-	-	1 (GQ259270)	1 (GQ259269)	-	-	1 (GQ259295)
	463	26	-	-	-	-	-	6 (EU287209)	-	-	1 (EU287257)
	172	47	3 (FN396676)	-	-	-	-	4 (FN396621)	-	5 (FN396701)	3 (FN396689)
Antarctica	17	17	-	-	-	-	-	-	-	-	1 (AY177789)
	28	16	-	-	-	1 (FN429813)	-	1 (FN429809)	-	-	-
<i>New Zealand sediments</i>											
	77	58	1	-	-	1 (JF268407)	2 (JF268340)	-	-	-	4 (JF268369)
<i>Submarine volcano (Vailulu'u; South Pacific)</i>											
	502	24	-	-	-	1 (FJ497421)	-	-	-	-	-
<i>Guaymas Basin sediments</i>											
	78	32	4 (GU302445)	-	1 (GU302470)	-	-	9 (GU302442)	4 (GU302423)	1 (GU302491)	1 (GU302432)
	78	20	-	-	-	-	-	-	2 (AF420337)	2 (AF420335)	3 (AF420368)
<i>Additional hydrothermal vent sediments</i>											
Rainbow (Mid-Atlantic Ridge)	52	13	-	-	-	-	-	-	1 (AJ969442)	-	1 (AJ969502)
Yonaguni Knoll IV (Okinawa Trough)	16	5	-	-	-	-	-	-	1 (AB252432)	-	-
Brothers seamount (New Zealand)	31	6	-	-	-	-	-	-	1 (AM712339)	-	-
Indien Ridge (Indian Ocean)	76	10	-	-	-	-	-	-	-	6 (AY355301)	-
<i>Non-seep sediments</i>											
Saline lake (California) [§]	164	28	13 (EU592450)	-	-	-	-	1 (EU592487)	1 (EU592452)	-	-
Salt marsh (San Francisco) [§]	27	10	4 (GU291340)	-	-	-	1 (GU291339)	-	-	-	-
Mahomet aquifer (Illinois) [§]	86	38	-	-	1 (HM141837)	-	3 (HM141854)	-	-	-	-
Oil polluted beach (Greece)	730	241	4 (JF344708)	-	1 (JF344129)	3 (JF344559)	-	15 (JF344433)	-	-	-
Oil polluted coast (France) [*]	28	14	1 (DQ176610)	-	-	5 (DQ176606)	-	-	-	-	-
Lake Cadagno (Switzerland) [§]	31	7	-	-	-	1 (FJ502253)	-	-	-	-	-
Water filled sinkhole (Mexico) [§]	1342	295	20 (FJ484434)	-	-	2 (FJ484544)	-	1 (FJ485022)	-	-	-
Polluted harbor sediments (China)	176	45	3 (DQ395003)	-	-	-	-	1 (DQ394951)	-	-	-
Mangrove sediments (China) [§]	65	10	-	-	-	-	1 (AM176871)	-	-	-	-

[▲] Sequence # as analyzed in SILVA database Parc108 (release date Sept. 1st 2011); sequence # in bold face type are ≥10% of deltaproteobacterial sequences.

[•] Sequences taken from Stagers (2012).

[▼] SCA-SRB2 were analyzed including next relatives, because SCA-SRB2 specific sequences (indicated by [§]) were only retrieved from GB.

[§] Clone library specific for the DSS group.

^{*} In situ experiment.

[§] Non-marine habitat

Not available (NA), Guaymas Basin (GB), Gulf of Mexico (GoM), Hydrate Ridge (HR)

1.2. SCA-SRB2 are Guaymas Basin-endemic short-chain alkane degraders

Based on SIP-techniques, the dominant butane degraders in Guaymas Basin sediments were affiliated with the DSS clade and were defined as SCA-SRB2 group in this thesis (Chapter III). Group SCA-SRB2, comprised exclusively the identified butane degraders as well as sequences from butane enrichment cultures that originated from Guaymas Basin sediments. These enrichment cultures were obtained during the present thesis as a follow-up of the SIP-incubations and further investigated by M. Stagers (2012). SCA-SRB2 identified in the present study had a 16S rRNA sequence similarity of 100%. When including sequences from Guaymas Basin butane enrichment cultures, the sequences similarity of SCA-SRB2 was 93% (Stagers, 2012). And lastly, when including next relatives from other habitats, referred to as “SCA-SRB2 and relatives” (Table VI.1), the sequence similarity of the 16S rRNA gene was only >86% (Chapter III), which would be rather on the family than on the genus level (Yarza et al., 2010).

SCA-SRB2 members were found to be usually low abundant (below 1% of total cells) at various hydrocarbon seeps as determined by CARD-FISH (Chapter IV). Only at Tommeliten SCA-SRB2 were detected to account for 1% of total cells. Also, 16S rRNA sequences affiliating with the group SCA-SRB2 were so far only reported from Guaymas Basin sediments (Chapter III, Stagers, 2012). Sequences affiliating with SCA-SRB2 and relatives were reported from previous studies and found at diverse habitats including the Gulf of Mexico, Guaymas Basin, several Mediterranean mud volcanoes, Eel River Basin and non-seep habitats (Table VI.1). It is assumed that SCA-SRB2 and relatives may not be exclusively involved in short-chain alkane degradation, while SCA-SRB2 members likely are restricted to butane and propane oxidation. Concluding, SCA-SRB2 group members might be endemic at Guaymas Basin rather than globally distributed. Nevertheless, it remains hypothetical if SCA-SRB2 members are specifically adapted to the special conditions (e.g. steep temperature gradients caused by hydrothermal vent activity in combination with hydrocarbon seepage) found at Guaymas Basin. Special adaptations seem to be present for other cluster as well. Also, 16S rRNA analysis from previous studies revealed clusters comprising sequences retrieved only from Guaymas Basin sediments (e.g. Teske et al., 2002; Dhillon et al., 2003; Holler et al., 2011).

1.3. LCA-SRB1 are long-chain alkane degraders

LCA-SRB1 were defined as a distinct DSS subgroup, with the potential ability to degrade hydrocarbons. LCA-SRB1 members have an intragroup similarity of >94% based on the 16S rRNA and comprise identified dodecane-degrading SRB from Amon Mud Volcano (Chapter III) as well as sequences retrieved from various habitats. These habitats included seeps from the Gulf of Mexico, submarine mud volcanoes, Eel River Basin, New Zealand as well as sediments from Antarctica and additional non-seep habitats (Table VI.1). Also, LCA-SRB1 accounted for 35% of deltaproteobacterial sequences in a previous study (Miralles et al., 2007), where in situ experiments were carried out in coastal sediments (Mediterranean Sea, France). Here, sediments were in the field amended with oil and LCA-SRB1 members were discussed to be responsible for hydrocarbon degradation of C₁₇ to C₃₀ alkanes. Therefore, members of this group are potential alkane degraders and probably globally distributed and not only restricted to seep habitats. Data obtained in this thesis showed LCA-SRB1 members as long-chain alkane degraders at Amon Mud Volcano. In situ quantifications of this specific group, besides the Amon Mud Volcano, are still needed to evaluate their global distribution and abundance at marine seeps. Based on the low sequence frequency it is expected that this group may be rather low abundant.

Dodecane is not a naturally occurring compound in Amon Mud Volcano sediments and experiments from this study showed a lag phase until sulfate-dependent hydrocarbon degradation started. This lag phase may be either due to a very low abundance of LCA SRB1 members at this habitat (Chapter IV) and/or due to a need to induce the synthesis of enzymes needed for the degradation of dodecane. LCA-SRB1 members potentially have the capability to degrade non-hydrocarbon substrates, if hydrocarbons are not available. In numerous studies, organisms were shown to have the ability to degrade hydrocarbons and non-hydrocarbon compounds such as fatty acids (e.g. Beller et al., 1996; Galushko et al., 1999; Kniermeyer et al., 2003).

1.4. SEEP-SRB1 are globally abundant candidates for hydrocarbon degradation

Members of SEEP-SRB1a have been described as dominant ANME2-partners in various marine seeps (Schreiber et al., 2010), and were assumed to be involved in AOM. Prior to this thesis, the ecological role of the remaining SEEP-SRB1 subgroups, i.e. SEEP-SRB1b to SEEP-SRB1f was unknown. These subgroups comprise only sequences from marine seep

sites, thus suggesting that corresponding organisms may have hydrocarbon degrading capabilities. In this study, the hypothesis was supported by showing high abundances of SEEP-SRB1c, SEEP-SRB1e and SEEP-SRB1f at Amon Mud Volcano, Haakon Mosby Mud Volcano and Tommeliten (Chapter II). In addition, cDNA-based clone libraries constructed from hydrate-bearing oily sediments revealed a high frequency of sequences belonging to these groups (Chapter II). These organisms potentially have a preference for short-chain alkanes such as propane and butane, present at most seep sites where they were retrieved from, but also other hydrocarbons, e.g. longer alkanes and aromatic hydrocarbons, may serve as energy sources. However, SIP-experiments performed in this thesis did not give evidence for butane or dodecane degradation by SEEP-SRB1 in Amon Mud Volcano sediments (Chapter III). Thus, a next step towards the clarification of the ecological roles of SEEP-SRB1b-f members may be NanoSIMS analysis of single cells from the SIP-incubation or single-cell genomics. Through these analyses, an involvement in alkane degradation may still be proven.

2. Non-DSS hydrocarbon degraders at marine seeps

Besides the dominant DSS clade additional groups of *Deltaproteobacteria* were (i) shown to be abundant at hydrocarbon seeps and some were (ii) shown to be involved in hydrocarbon degradation. These groups belong to the families *Desulfobacteraceae* (*Desulfobacterium anilini* and relatives, LCA-SRB2 members) and *Desulfobulbaceae* (SEEP-SRB2, SEEP-SRB3 and SEEP-SRB4; Fig. VI.1).

2.1. SEEP-SRB2 are novel ANME-partners involved in AOM

Known SRB that live associated with ANME-1, ANME-2 and ANME-3 archaea were identified as members of the DSS clade (e.g. Boetius et al., 2000; Knittel et al., 2005; Schreiber et al., 2010). One group of these DSS members was further designated SEEP-SRB1a (Schreiber et al., 2010). Additional SRB associated with ANME-2c or ANME3 archaea were identified as *Desulfobulbaceae* (Lösekann et al., 2007; Pernthaler et al., 2008). In the present study, associated SEEP-SRB2 members were identified as novel ANME-partners either in ANME-2/SEEP2 consortia or in ANME-1/SEEP2 associations. One reason is that probe DSS658 targeting the DSS group, which was intensively used within numerous FISH studies, cross-hybridizes with group SEEP-SRB2 (Chapter II). Only after development and application of competitors, a clear distinction between the two groups was possible. Therefore, previous studies most likely overestimated the DSS community by counting false-

positive single cells or associated ANME partners. However, the identification of SEEP-SRB1a members as the dominant ANME-2 partner (Schreiber et al., 2010) still proves true because probes used (SEEP1a-473, SEEP1a-1441) were highly specific in this case.

In this study, novel associations of SEEP-SRB2 and ANME archaea were found in particular in sediments from the northern and southern Gulf of Mexico. Here, SEEP-SRB2/ANME-2 and DSS/ANME-2 aggregates co-existed. DSS/ANME-2 aggregates were generally more abundant, while in distinct sediment layers SEEP-SRB2/ANME-2 dominated all aggregates. In bacterial mats from Black Sea reef-like structures, the SEEP-SRB2 abundance was determined to correlate with ANME-1, while DSS was mainly found to co-exist with ANME-2. Here, SEEP-SRB2 and DSS organisms potentially have their own niches. SEEP-SRB2 clearly dominated also methane seep sediments at Tommeliten. In addition to all indications obtained in this study, SEEP-SRB2 were found in high abundance associated with ANME-2 and ANME-1 archaea in AOM-enrichments cultures from Gulf of Mexico and Guaymas Basin sediments (Holler and Krukenberg, MPI Bremen; pers. communication) supporting their hypothesized involvement in AOM.

The selecting factors influencing the distribution of SEEP-SRB2 remain largely unknown. Based on the distribution of SEEP-SRB2, members are likely not influenced by temperature, water depth, pressure, and methane accessibility (cf. Table VI.2). Sulfate concentrations may affect the distribution of SEEP-SRB2. ANME-2/SEEP-SRB2 consortia were detected to be more abundant in sediments below 7 cm sediment depth at the Gulf of Mexico site 156 (Chapter II). In contrast, ANME-2/SEEP-SRB1a consortia were at the same site shown to be more abundant in sediments above 7 cm. Accordingly, these upper sediment layers contained highest sulfate concentration of 4-22 mM (Orcutt et al., 2010), indicating that sulfate may influence the distribution of consortia.

Single SEEP-SRB2. The majority of SEEP-SRB2 was found as single, non-associated cells (Chapter II) and may be involved in other metabolic processes than AOM. In some seeps such as sediments from the Gulf of Mexico and Tommeliten, they even exceeded the abundance of the DSS group. Interestingly, the abundance of free-living cells was found to be correlated with the appearance of SEEP-SRB2 associated with ANME archaea. For example, highest numbers of free-living cells were found in habitats where they also occurred associated. Nevertheless, it needs further investigation to determine whether these high numbers of detected single cells originated from aggregates. For comparison, SEEP-SRB1a cells were in this and previous studies almost exclusively detected in an aggregated life style (Schreiber et al., 2010).

Table VI.2: SEEP-SRB2: Overview of habitats, cell abundance and occurrence in aggregated and non-aggregated cells at marine seeps investigated.

Feature	Gas seeps				Hydrocarbon seeps			
	Hydrate Ridge	Amon Mud Volcano	Haakon Mosby Mud Volcano	Tommeliten	Black Sea	Gulf of Mexico	Chapopote Asphalt Volcano	Guaymas Basin
<i>Habitat characterization</i>								
Location	NE Pacific Ocean	Mediterranean Sea	Barents Sea	North Sea	NW shelf of the Black Sea	Northern Gulf of Mexico	Southern Gulf of Mexico	Gulf of California
Sample type	Hydrate bearing sediment	Sediment	Sediment	Sediment	Microbial mat from reef-like structure	Sediment	Sediment with tar deposits	Sediment
Dominant hydrocarbon compounds	Methane (>95%)	Mainly C ₁ ; C ₂ -C ₄	Methane (>99%)	Methane (>99%)	Methane (>95%)	Methane and/or crude oil dominated	Crude oil dominated	Crude oil-like hydrocarbons
Water depth [m]	780	1100	1300	75	190	400-1400	2900	2000
Temperature [°C]	2-4	14	-1	4	8	4	4	3 to 50 ^a
<i>SEEP-SRB2 features</i>								
ANME partner of SEEP-SRB2	–	ANME-2	–	ANME-2	ANME-1	ANME-2	ANME-2	NA
Consortia type	–	Shell-type	–	Shell- and mixed-type	Association in bacterial mats	Shell-type	Shell-type	NA
Free-living SEEP-SRB2	+	+	+	+	+	+	+	+
SEEP-SRB2 sequences	+	–	–	+	NA	+	+	+
	(AM713448)			(DQ007535)		(FR871996)	(AM746088)	(GU302423)
References	This study, Suess et al. 1999, Treude et al. 2003, Knittel et al. 2005	This study, Grünke et al. 2011	This study, Ginsburg et al. 1999, Niemann et al. 2006b, Lösekann et al. 2007	This study, Hovland et al. 2002, Niemann et al. 2005, Wegener et al. 2008	This study, Michaelis et al. 2002, Treude et al. 2005	This study, Joye et al. 2004	This study, MacDonald et al. 2004, Schubotz et al. 2011	This study, Bazylinski et al. 1988, Teske et al. 2002, McKay pers. communication

^a Typical temperature gradient from 0 to 20 cm sediment depth (McKay; pers. communication).

Not detected (–), present (+), not analyzed (NA)

Results obtained in this thesis are indicated in blue.

Also, similarly to SEEP-SRB1, SEEP-SRB2 was not observed to degrade butane or dodecane in incubations with Amon Mud Volcano sediments (Chapter III). However, based on their abundance and distribution as well as the frequency of sequences retrieved from various habitats, particularly at Gulf of Mexico, Tommeliten and Hydrate Ridge (Table VI.1), SEEP-SRB2 are most likely involved in AOM or non-methane hydrocarbon degradation.

2.2. SEEP-SRB3 and SEEP-SRB4 are candidates for hydrocarbon degradation

SEEP-SRB3 and SEEP-SRB4 belong to the family *Desulfobulbaceae* and are closely related to the genera *Desulfobulbus* and *Desulforhopalus*. SEEP-SRB3 and SEEP-SRB4 sequences were exclusively derived from marine seep habitats (Table VI.1). Therefore, their lifestyle is likely connected with dominant metabolic pathways carried out at marine seeps. In the present study cell numbers and distribution patterns were for the first time determined at diverse seep sites.

SEEP-SRB3 cells were found being most abundant in oily sediments from the Gulf of Mexico. A significant correlation between the presence of *Desulfobacterium anilini* relatives and SEEP-SRB3 cells was determined based on the CARD-FISH results (Chapter II). Interestingly, *Desulfobacterium anilini* relatives are known to degrade aromatic hydrocarbons (Widdel et al., 2010 and references therein). Furthermore, sequences affiliating with SEEP-SRB3 were retrieved from several habitats in previous studies and were found in a high frequency especially at Gulf of Mexico, Mediterranean mud volcanoes and additional habitats with potential hydrocarbon impact (see Table VI.1). Therefore, SEEP-SRB3 might be involved in alkane or aromatic hydrocarbon degradation.

SEEP-SRB4 dominated all *Desulfobulbaceae* within surface sediments under *Beggiatoa* mats especially at the Haakon Mosby Mud Volcano and at the Amon Mud Volcano (Chapter II). This finding was supported by the frequent retrieval of SEEP-SRB4 sequences especially from submarine volcanoes, but also from Hydrate Ridge, Guaymas Basin and Deep-Sea sediments from Japan (Table VI.1). Since mud volcanoes are characterized by a high alkane gas-flow (Niemann et al., 2005; Mastalerz et al., 2009), SEEP-SRB4 is likely involved in short-chain alkane degradation. Its involvement is supposed to be either direct by oxidation of non-methane alkanes or indirect by thriving on intermediates or biomass produced in the degradation of non-methane hydrocarbons.

2.3. LCA-SRB2 are global key players involved in long-chain alkane degradation

LCA-SRB2 members are likely global key players involved in long-chain alkane degradation including dodecane-degrading organisms from Guaymas Basin (Chapter III) as well as other bacteria from various seeps and non-seep habitats. On the currently available sequence dataset, LCA-SRB2 includes sequences from seeps at Guaymas Basin, several submarine volcanoes,

Gulf of Cadiz, Svalbard and New Zealand (Table VI.1). Phylogenetic analysis determined a high group similarity of the 16S rRNA genes which was with >94% on the genus level. Therefore, members of the group LCA-SRB2 might all have the same metabolic potential to oxidize long-chain alkanes. However, similar to the group LCA-SRB1, it remains to be investigated whether LCA-SRB2 organisms are exclusively involved in hydrocarbon degradation or if they can also gain their energy from other substrates such as fatty acids. Nevertheless, CARD-FISH results of the present study indicated the highest abundance of this group at hydrocarbon seeps from the Gulf of Mexico (Chapter IV), which further supports the involvement of LCA-SRB2 in long-chain alkane degradation.

2.4. *Desulfobacterium anilini* and relatives are involved in oil degradation

Besides organism using short-chain and long-chain alkanes as energy source, aromatic hydrocarbon degraders such as *Desulfobacterium anilini* and relatives might be important in marine hydrocarbon seep sediments which naturally contain high concentrations of aromatic hydrocarbons. Biogeochemical and tracer studies indicated microbial long-chain alkane and aromatic hydrocarbon degradation at seeps from the Gulf of Mexico and Guaymas Basin (Bazylnski et al., 1989; Schubotz et al., 2011). Furthermore, using cultivation techniques organisms degrading aromatic hydrocarbons (e.g. naphthalene, benzene, and toluene for review see Widdel et al., 2010) were isolated from marine sediments including seep from Guaymas Basin (strain EBS7 Kniermeyer et al., 2003). These organisms form one phylogenetic cluster together with *Desulfobacterium anilini* and belong to the family *Desulfobacteraceae* outside of the DSS clade (Fig. VI.1). In this study, members of *Desulfobacterium anilini* and relatives showed a significant preference for two samples from the oily Gulf of Mexico station 161 (Chapter II). In other seep sediments they were not detected or only found in low abundance. In addition, the cDNA-based clone library constructed from oily Gulf of Mexico sediments showed a high frequency of sequences affiliating with *Desulfobacterium anilini* and relatives (Chapter II). Previous studies confirmed the high frequency of sequences from *Desulfobacterium anilini* and relatives at various habitats, including Gulf of Mexico, Tommeliten, several submarine volcanoes, Eel River Basin, Guaymas Basin and several non-seep habitats (Table VI.1). It is assumed that these organisms have an important ecological role by being involved in the degradation of aromatic hydrocarbons and additional substrates in marine sediments with oil seepage.

3. Unexplored groups involved in hydrocarbon degradation at marine seeps

In the present thesis, several groups have been investigated, which were on the one hand proven to degrade hydrocarbons or were on the other hand putative candidates to be involved in these processes (see Fig. VI.1). The majority of *Deltaproteobacteria* was assigned to specific SRB groups, i.e. $83\% \pm 14\%$ at gas seeps and $61\% \pm 35\%$ at hydrocarbon seeps as determined by CARD-FISH, indicating that the approach used was sufficient for classification of most SRB at the sites investigated (Chapter II). However, it cannot be excluded that some groups involved in hydrocarbon degradation at marine seeps remained undetected. This would be mostly due to methodological limitations. In this study, sediment samples from a wide range of oceanic habitats were selected based on differences in the hydrocarbon composition, and in order to accomplish a broad geographic distribution. Nevertheless global extrapolations have to be done carefully, since still only a limited set of samples was used for analysis. Also the choice of already established and newly designed probes was done on the current state of the art. Probe coverage of the target groups was mostly not 100%. In addition, it has to be considered that several groups involved in hydrocarbon degradation are most likely still unexplored. A strong argument for this assumption is the discovery of three groups comprising novel key players that were identified in this study (Chapter III). Furthermore, SIP-incubations were done under in situ-like conditions, meaning that the organisms had to cope with quite different conditions e.g. a much lower pressure. Also the so called ‘bottle effect’ (Eilers et al., 2000) has to be considered which refers to changes in community composition upon sampling. Thus, some SRB groups may not be capable to perform anaerobic hydrocarbon degradation under the experimental conditions as compared to those present in situ. This may also explain the remaining uncertainty about the ecological role of the single-celled members of groups SEEP-SRB1 to SEEP-SRB4.

Unexplored DSS subgroups. In depth analysis of the dominant DSS clade by CARD-FISH revealed that up to 81% of single cells were in this study further assigned to DSS subgroups (Tommeliten), while in other habitats only 15% was attributed to DSS subgroups (Hydrate Ridge; Fig. VI.2). Therefore, some DSS subgroups at marine seeps remained unassigned. The identification of the hydrocarbon-degrading groups SCA-SRB1 and SCA-SRB2 in addition to SEEP-SRB1, which was already defined prior to this study, broadened substantially the spectrum of DSS subgroups at marine seeps. Including these newly defined groups into the detailed investigation of the dominant DSS clade, additional 8 to 35% of DSS members could be assigned to specific subgroups (cf. Chapter IV).

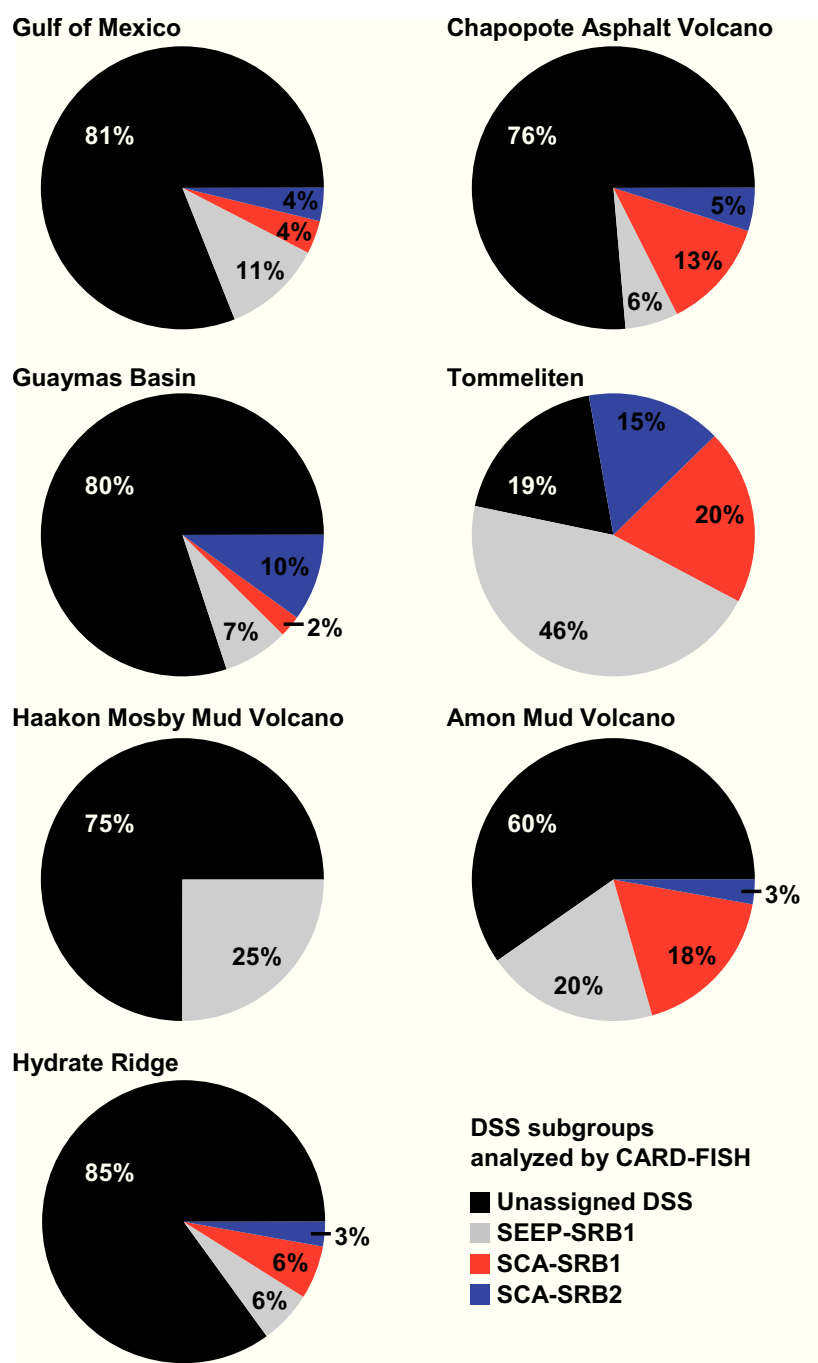


Fig. VI.2: Relative fractions of DSS subgroups in marine seep sediments investigated. Fractions were calculated based on single, non-associated SRB as determined by CARD-FISH. Results consider all depths and sites investigated per habitat. The following sites are summarized: Gulf of Mexico (156, 161) Chapopote Asphalt Volcano (140, 106-19-6, 106-19-13, 106-25-9, 106-25-16), Guaymas Basin (4489-1), Tommeliten (K1-1274, K2-1274, K3-1274), Haakon Mosby Mud Volcano (ATL19, ATL22), Amon Mud Volcano (760, 825), and Hydrate Ridge (19, 38).

Only at the Haakon Mosby Mud Volcano, none of these newly defined DSS subgroups were detected. Thus, the approach used in this study is very useful to identify and subsequently quantify yet unexplored DSS subgroup. Based on the high diversity detected in clone libraries

and the 454-pyrosequencing approach during this thesis (Chapters II and III) as well as in clone libraries of previous studies (e.g. Teske et al., 2002; Knittel et al., 2003; Lösekann et al., 2007; Wegener et al., 2008; Orcutt et al., 2010), it can be concluded that similar SIP-studies using different seep sediments or hydrocarbon substrates, will detect additional DSS subgroups involved in hydrocarbon degradation.

4. Environmental impact of hydrocarbon-degrading SRB

Emissions of reduced substrates, including gaseous and liquid hydrocarbons, fuel extraordinarily high SR rates at marine seeps. However, direct measurements of hydrocarbon oxidation rates were required to better understand the influence of non-methane degrading SRB on the marine seep environment. In the present thesis, the environmental impact of alkane-degrading SRB groups SCA-SRB1, SCA-SRB2 and LCA-SRB2 was assessed based on in situ quantifications by CARD-FISH in combination with activity measurements on the cellular level by NanoSIMS. The obtained data indicate that alkane-degrading communities considerably influence marine carbon and sulfur cycles, in particular at seeps with complex hydrocarbon emission.

4.1. Cellular activities of alkane-degrading SRB

Prior to this thesis, the only available data on the cellular activity of short-chain alkane degraders were achieved from sediment-free enrichment cultures of SCA-SRB1 (Jaekel, 2011), while for long-chain alkane degraders no cellular activity data were available. Cellular alkane-oxidation rates were determined by two different model scenarios (Chapter IV). The first scenario described the cellular activity based on the turnover of ^{13}C -alkanes. The second scenario estimated the overall cellular activity, assuming the turnover of ^{13}C -alkanes and additional organic compounds. Cellular rates were on average between 45 to 58 amol butane and 1 amol dodecane $\text{cell}^{-1} \text{d}^{-1}$, respectively. The single cell ^{13}C -abundances of butane degraders were on average up to two times higher as those reported for other SCA-SRB1 members in sediment-free enrichment cultures (Jaekel, 2011), leading to overall higher extrapolated SR rates. Higher cellular activities may result from close-to-in situ conditions. For instance, naturally occurring substances that stimulated the microbial activity such as growth factors may have been present in the sediments used for ^{13}C -labeling experiments that stimulated the activity of the investigated alkane degraders.

Accordingly, both model scenarios indicated that unlabeled compounds were potentially used for assimilatory processes, in addition to the ^{13}C -labeled alkanes (Chapter IV). Protein-SIP analysis from parallel incubations showed that the relative ^{13}C -abundance of proteins remained below 60% even after an incubation for more than 300 days (Chapter III). These findings were in line with earlier studies, where the ^{13}C -abundance of DNA remained below 50% for hydrocarbon-degrading SRB (e.g. Winderl et al., 2010). Additional carbon sources for biomass synthesis besides ^{13}C -alkanes are hydrocarbons that were already present in the sediments. Furthermore, in parallel to carbon fixation from ^{13}C -alkanes, heterotrophic carbon fixation may proceed by reductive carboxylation of acetyl-CoA as discussed previously (e.g. Winderl et al., 2010). Both scenarios would lead to a lower ^{13}C -incorporation into the biomass. In this study, indications for reductive carboxylation of specific alkane-degrading SRB were retrieved by Protein-SIP analysis (Chapter III). Thus, heterotrophic carbon fixation is likely important for non-methane degrading SRB at marine seeps.

4.2. SR rates coupled to alkane oxidation at hydrocarbon seeps

An extrapolation of SR rates based on in situ abundances and cellular activities revealed that specific alkane-degrading SRB groups potentially contribute a substantial fraction of the ex situ measured SR rates at certain hydrocarbon seeps. For instance, the sum of analyzed alkane-degrading SRB groups may be responsible for 7-100% of overall ex situ rates from Gulf of Mexico seeps. These rates were calculated to be in the range of $>1 \mu\text{mol cm}^{-3} \text{d}^{-1}$ if sulfate and short-chain alkanes are not limiting (Chapter IV). Based on the extrapolated data it can be assumed that SR is mainly coupled to non-methane alkane degradation at habitats with complex hydrocarbon emission such as seeps from the Gulf of Mexico. In contrast, extrapolations for seeps at Hydrate Ridge and Haakon Mosby Mud Volcano, two methane-dominated habitats, suggested that non-methane alkane-oxidation plays only a minor role for the SRB community at these sites.

At hydrocarbon seeps, it is likely that in addition to SCA-SRB1, SCA-SRB2 and LCA-SRB2 other groups have the capabilities to oxidize alkanes. Therefore, it can be hypothesized that SR rates at marine seeps are even higher as the ones extrapolated for these specific groups investigated in this thesis (Chapter IV). Thus, microbial alkane degradation by SRB is likely an important process for organic matter degradation in sediments with complex hydrocarbon seepage.

5. Future Perspectives

In the present study, the identification and quantification of active hydrocarbon degraders based on SIP-techniques was achieved. This identification in combination with subsequent probe design for key players and finally their in situ quantification at marine seeps turned out to be a very successful approach. It can be assumed that similar SIP-studies would further extend the spectrum of marine hydrocarbon degraders, particularly when sediments of different habitats or additional substrates, others than in this study, are used. The experimental SIP-techniques could be further improved towards in situ conditions, e.g. by applying pressure. For example, using an instrument such as the Deep Ocean Benthic Sampler (Sheryll, 2009) during cruises, will allow to obtain contamination-free sediment cores and to preserve the in situ conditions upon retrieval to the ship. However, a SIP-experiment would be ideal when carrying out directly in the field e.g. according to Takano et al. (2010), who performed in situ tracer experiments with marine sediments at 1,500 m water depth.

The enrichment and isolation of uncultured organisms is still essential to understand the physiology of organisms in detail and to explore the biochemistry of yet unknown metabolic pathways. During this thesis, the enrichment of novel alkane-degrading SRB was achieved as a follow-up of the SIP-incubations. These enrichment cultures are promising for an intended isolation. Therefore, the investigations of hydrocarbon degraders should be continued using traditional cultivation techniques. In addition, it is crucial to pursue the cultivation of SEEP-SRB organisms, in order to resolve their metabolic pathways and to test their hydrocarbon oxidation capabilities, since they constituted a remarkable fraction of the sulfate-reducing microbial community. A promising approach would be to use cultivation techniques in combination with high pressure equipment, again to optimally mimic in situ conditions.

A parallel single cell genomics approach (e.g. Stepanauskas & Sieracki, 2007) could reveal the genomic capabilities of so far uncultured, abundant organisms. This approach was successfully initiated during this thesis and yielded partial genomes of single cells (SEEP-SRB1b, SEEP-SRB1d, SEEP-SRB1e, SEEP-SRB1f and SEEP-SRB3). A manual annotation of partial genomes was not possible because of time restrictions but should of course be done to explore the genetic capabilities of these organisms. Subsequently, particular genes could be explored with methods such as mRNA-FISH (Pernthaler & Amann, 2004), metatranscriptomics (e.g. Frias-Lopez et al., 2008) or metaproteomics (Wilmes & Bond, 2006), to determine whether these genes are actually expressed in the organisms.

The results of this thesis also contribute to a better understanding of natural recovery mechanisms after accidental oil spillage. Currently, strong research needs exist after the Deepwater Horizon catastrophe in the Gulf of Mexico. Thus, for future projects it is tempting to transfer the developed and successfully applied methods from this thesis to such an anthropogenically contaminated marine benthic environment. The obtained data provide the background to accomplish comparative studies with respect to hydrocarbon-degrading organisms and in situ turnover rate measurements of the responsible groups at these sites.

References

- Aeckersberg F, Bak F, and Widdel F. (1991). Anaerobic oxidation of saturated-hydrocarbons to CO₂ by a new type of sulfate-reducing bacterium. *Arch Microbiol* **156**: 5-14.
- Aeckersberg F, Rainey FA, and Widdel F. (1998). Growth, natural relationships, cellular fatty acids and metabolic adaptation of sulfate-reducing bacteria that utilize long-chain alkanes under anoxic conditions. *Arch Microbiol* **170**: 361-369.
- Aharon P. (1994). Geology and biology of modern and ancient submarine hydrocarbon seeps and vents: An introduction. *Geo-Mar Lett* **14**: 69-73.
- Anderson RK, Scalan RS, Parker PL, and Behrens EW. (1983). Seep oil and gas in Gulf of Mexico slope sediment. *Science* **222**: 619-621.
- Bazylynski DA, Farrington JW, and Jannasch HW. (1988). Hydrocarbons in surface sediments from a Guaymas Basin hydrothermal vent site. *Org Geochem* **12**: 547-558.
- Bazylynski DA, Wirsén CO, and Jannasch HW. (1989). Microbial utilization of naturally occurring hydrocarbons at the Guaymas Basin hydrothermal vent site. *Appl Environ Microbiol* **55**: 2832-2836.
- de Beer D, Sauter E, Niemann H, Kaul N, Foucher JP, Witte U, Schlüter M, and Boetius A. (2006). In situ fluxes and zonation of microbial activity in surface sediments of the Haakon Mosby Mud Volcano. *Limnol Oceanogr* **51**: 1315-1331.
- Behrens EW. (1988). Geology of a continental slope oil seep, northern Gulf of Mexico. *AAPG Bull* **72**: 105-114.
- Beller HR and Spormann AM. (1997). Anaerobic activation of toluene and o-xylene by addition to fumarate in denitrifying strain T. *J Bacteriol* **179**: 670-676.
- Beller HR, Spormann AM, Sharma PK, Cole JR, and Reinhard M. (1996). Isolation and characterization of a novel toluene-degrading, sulfate-reducing bacterium. *Appl Environ Microbiol* **62**: 1188-1196.
- Biegert T, Fuchs G, and Heider J. (1996). Evidence that anaerobic oxidation of toluene in the denitrifying bacterium *Thauera aromatica* is initiated by formation of benzylsuccinate from toluene and fumarate. *Europ J Biochem* **238**: 661-668.
- Birch LD and Bachofen R. (1988) in *Biotechnology: special microbial processes*, edited by H.J. Rehm and G. Reed (VCH Verlagsgesellschaft, Weinheim), Vol. Vol 6b, pp. 71-99.
- Black MB, Halanych KM, Maas PAY, Hoeh WR, Hashimoto J, Desbruyères D, Lutz RA, and Vrijenhoek RC. (1997). Molecular systematics of vestimentiferan tubeworms from hydrothermal vents and cold-water seeps. *Mar Biol* **130**: 141-149.
- Boetius A, Ravensschlag K, Schubert CJ, Rickert D, Widdel F, Gieseke A, Amann R, Jørgensen BB, Witte U, and Pfannkuche O. (2000). A marine microbial consortium apparently mediating anaerobic oxidation of methane. *Nature* **407**: 623-626.
- Bohrmann G, Greinert J, Suess E, and Torres M. (1998). Authigenic carbonates from the Cascadia subduction zone and their relation to gas hydrate stability. *Geology* **26**: 647-650.
- Boschker HTS and Middelburg JJ. (2002). Stable isotopes and biomarkers in microbial ecology. *FEMS Microbiol Ecol* **40**: 85-95.
- Boschker HTS, Nold SC, Wellsbury P, Bos D, de Graaf W, Pel R, Parkes RJ, and Cappenberg TE. (1998). Direct linking of microbial populations to specific biogeochemical processes by ¹³C-labelling of biomarkers. *Nature* **392**: 801-805.
- Bowles MW, Samarkin VA, Bowles KM, and Joye SB. (2011). Weak coupling between sulfate reduction and the anaerobic oxidation of methane in methane-rich seafloor sediments during ex situ incubation. *Geochim Cosmochim Acta* **75**: 500-519.

- Brooks JM, Cox HB, Bryant WR, Kennicutt II MC, Mann RG, and McDonald TJ. (1986). Association of gas hydrates and oil seepage in the Gulf of Mexico. *Org Geochem* **10**: 221-234.
- Brooks JM, Kennicutt II MC, Fay RR, McDonald TJ, and Sassen R. (1984). Thermogenic gas hydrates in the Gulf of Mexico. *Science* **225**: 409-411.
- Brysch K, Schneider C, Fuchs G, and Widdel F. (1987). Lithoautotrophic growth of sulfate-reducing bacteria, and description of *Desulfobacterium autotrophicum* gen. nov., sp. nov. *Arch Microbiol* **148**: 264-274.
- Callaghan AV, Wawrik B, Ní Chadhain SM, Young LY, and Zylstra GJ. (2008). Anaerobic alkane-degrading strain AK-01 contains two alkylsuccinate synthase genes. *Biochem Biophys Res Commun* **366**: 142-148.
- Camilli R, Reddy CM, Yoerger DR, Van Mooy BAS, Jakuba MV, Kinsey JC, McIntyre CP, Sylva SP, and Maloney JV. (2010). Tracking hydrocarbon plume transport and biodegradation at Deepwater Horizon. *Science* **330**: 201-204.
- Campbell KA. (2006). Hydrocarbon seep and hydrothermal vent paleoenvironments and paleontology: Past developments and future research directions. *Palaeogeogr Paleoclimatol Paleoecol* **232**: 362-407.
- Childress JJ, Fisher CR, Brooks JM, Kennicutt II MC, Bidigare R, and Anderson AE. (1986). A methanotrophic marine molluscan (*Bivalvia*, *Mytilidae*) symbiosis: mussels fueled by gas. *Science* **233**: 1306-1308.
- Corliss JB, Dymond J, Gordon LI, Edmond JM, von Herzen RP, Ballard RD, Green K, Williams D, Bainbridge A, Crane K, and van Andel TH. (1979). Submarine thermal springs on the Galápagos Rift. *Science* **203**: 1073-1083.
- Cravo-Laureau C, Matheron R, Joulian C, Cayol JL, and Hirschler-Rea A. (2004). *Desulfatibacillum alkenivorans* sp nov., a novel *n*-alkene-degrading, sulfate-reducing bacterium, and emended description of the genus *Desulfatibacillum*. *Int J Syst Evol Microbiol* **54**: 1639-1642.
- DeRito CM, Pumphrey GM, and Madsen EL. (2005). Use of field-based stable isotope probing to identify adapted populations and track carbon flow through a phenol-degrading soil microbial community. *Appl Environ Microbiol* **71**: 7858-7865.
- Dhillon A, Teske A, Dillon J, Stahl DA, and Sogin ML. (2003). Molecular characterization of sulfate-reducing bacteria in the Guaymas Basin. *Appl Environ Microbiol* **69**: 2765-2772.
- Didyk BM and Simoneit BRT. (1989). Hydrothermal oil of Guaymas Basin and implications for petroleum formation mechanisms. *Nature* **342**: 65-69.
- Dupré S, Buffet G, Mascle J, Foucher JP, Gauger S, Boetius A, Marfia C, Team AsterXAUV, Team QuestROV, and Scientific party BIONIL. (2008). High-resolution mapping of large gas emitting mud volcanoes on the Egyptian continental margin (Nile Deep Sea Fan) by AUV surveys. *Mar Geophys Res* **29**: 275-290.
- Dupré S, Woodside J, Foucher JP, de Lange G, Mascle J, Boetius A, Mastalerz V, Stadnitskaia A, Ondréas H, Huguen C, Harmégnies FO, Gontharet S, Loncke L, Deville E, Niemann H, Omeregie E, Roy KOL, Fiala-Medioni A, Dählmann A, Caprais JC, Prinzhofer A, Sibuet M, Pierre C, Damsté JSS, and Scientific Party NAUTINIL. (2007). Seafloor geological studies above active gas chimneys off Egypt (Central Nile Deep Sea Fan). *Deep-Sea Res Pt I* **54**: 1146-1172.
- Eilers H, Pernthaler J, and Amann R. (2000). Succession of pelagic marine bacteria during enrichment: a close look at cultivation-induced shifts. *Appl Environ Microbiol* **66**: 4634-4640.
- Elvert M, Suess E, and Whiticar MJ. (1999). Anaerobic methane oxidation associated with marine gas hydrates: superlight C-isotopes from saturated and unsaturated C₂₀ and C₂₅ irregular isoprenoids. *Naturwissenschaften* **86**: 295-300.

- Felden J. (2009). Methane fluxes and associated biogeochemical processes in cold seep ecosystems. Doctoral dissertation, Jacobs University Bremen.
- Fiala-Médioni A, Boulègue J, Ohta S, Felbeck H, and Mariotti A. (1993). Source of energy sustaining the *Calyptogen* populations from deep trenches in subduction zones off Japan. *Deep Sea Res Part I* **40**: 1241-1258.
- Fisher CR, Brooks JM, Vodenichar JS, Zande JM, Childress JJ, and Burke Jr RA. (1993). The co-occurrence of methanotrophic and chemoautotrophic sulfur-oxidizing bacterial symbionts in a deep-sea mussel. *Mar Ecol* **14**: 277-289.
- Formolo MJ, Lyons TW, Zhang C, Kelley C, Sassen R, Horita J, and Cole DR. (2004). Quantifying carbon sources in the formation of authigenic carbonates at gas hydrate sites in the Gulf of Mexico. *Chem Geol* **205**: 253-264.
- Frias-Lopez J, Shi Y, Tyson GW, Coleman ML, Schuster SC, Chisholm SW, and DeLong EF. (2008). Microbial community gene expression in ocean surface waters. *Proc Natl Acad Sci USA* **105**: 3805-3810.
- Froelich PN, Klinkhammer GP, Bender ML, Luedtke NA, Heath GR, Cullen D, Dauphin P, Hammond D, Hartman B, and Maynard V. (1979). Early oxidation of organic matter in pelagic sediments of the eastern equatorial Atlantic: suboxic diagenesis. *Geochim Cosmochim Acta* **43**: 1075-1090.
- Gallagher E, McGuinness L, Phelps C, Young LY, and Kerkhof LJ. (2005). ¹³C-carrier DNA shortens the incubation time needed to detect benzoate-utilizing denitrifying bacteria by stable-isotope probing. *Appl Environ Microbiol* **71**: 5192-5196.
- Galushko A, Minz D, Schink B, and Widdel F. (1999). Anaerobic degradation of naphthalene by a pure culture of a novel type of marine sulphate-reducing bacterium. *Environ Microbiol* **1**: 415-420.
- Gilewicz M, Ni'matuzahroh, Nadalig T, Budzinski H, Doumenq P, Michotey V, and Bertrand JC. (1997). Isolation and characterization of a marine bacterium capable of utilizing 2-methylphenanthrene. *Appl Microbiol Biotechnol* **48**: 528-533.
- Ginsburg GD, Milkov AV, Soloviev VA, Egorov AV, Cherkashev GA, Vogt PR, Crane K, Lorenson TD, and Khutorskoy MD. (1999). Gas hydrate accumulation at the Haakon Mosby Mud Volcano. *Geo-Mar Lett* **19**: 57-67.
- Grundmann O, Behrends A, Rabus R, Amann J, Halder T, Heider J, and Widdel F. (2008). Genes encoding the candidate enzyme for anaerobic activation of *n*-alkanes in the denitrifying bacterium, strain HxN1. *Environ Microbiol* **10**: 376-385.
- Gundersen JK, Jørgensen BB, Larsen E, and Jannasch HW. (1992). Mats of giant sulphur bacteria on deep-sea sediments due to fluctuating hydrothermal flow. *Nature* **360**: 454-456.
- Grünke S, Felden J, Lichtschlag A, Girnth AC, de Beer D, Wenzhöfer F, and Boetius A. (2011). Niche differentiation among mat-forming, sulfide-oxidizing bacteria at cold seeps of the Nile Deep Sea Fan (Eastern Mediterranean Sea). *Geobiology* **9**: 330-348.
- Harms G, Zengler K, Rabus R, Aeckersberg F, Minz D, Rosselló-Móra R, and Widdel F. (1999). Anaerobic oxidation of *o*-xylene, *m*-xylene, and homologous alkylbenzenes by new types of sulfate-reducing bacteria. *Appl Environ Microbiol* **65**: 999-1004.
- Hayes JM. (2001). Fractionation of carbon and hydrogen isotopes in biosynthetic processes. *Rev Mineral Geochem* **43**:
- Haymon RM, Fornari DJ, Edwards MH, Carbotte S, Wright D, and MacDonald KC. (1991). Hydrothermal vent distribution along the East Pacific Rise crest (9°09'–54'N) and its relationship to magmatic and tectonic processes on fast-spreading mid-ocean ridges. *Earth Planet Sci Lett* **104**: 513-534.
- Hensen C, Nuzzo M, Hornibrook E, Pinheiro LM, Bock B, Magalhães VH, and Brückmann W. (2007). Sources of mud volcano fluids in the Gulf of Cadiz - indications for hydrothermal imprint. *Geochim Cosmochim Acta* **71**: 1232-1248.

- Higashioka Y, Kojima H, Nakagawa T, Sato S, and Fukui M. (2009). A novel *n*-alkane-degrading bacterium as a minor member of p-xylene-degrading sulfate-reducing consortium. *Biodegradation* **20**: 383-390.
- Hinrichs K-U and Boetius A. (2002) *The anaerobic oxidation of methane: new insights in microbial ecology and biogeochemistry*. (Springer Verlag, Berlin, Germany).
- Hinrichs K-U, Hayes JM, Sylva SP, Brewer PG, and DeLong EF. (1999). Methane-consuming archaeobacteria in marine sediments. *Nature* **398**: 802-805.
- Holler T, Widdel F, Knittel K, Amann R, Kellermann MY, Hinrichs K-U, Teske A, Boetius A, and Wegener G. (2011). Thermophilic anaerobic oxidation of methane by marine microbial consortia. *ISME J* **5**: 1946-1956.
- Hovland M. (2002). On the self-sealing nature of marine seeps. *Continent Shelf Res* **22**: 2387-2394.
- Hovland M and Judd AG. (1988) *Seabed pockmarks and seepages: Impact on geology, biology and the marine environment*. (Graham & Trotman, London).
- Hovland M, Judd AG, and Burke RA. (1993). The global flux of methane from shallow submarine sediments. *Chemosphere* **26**: 559-578.
- Hovland M and Sommerville JH. (1985). Characteristics of two natural gas seepages in the North Sea. *Mar Petrol Geol* **2**: 319-326.
- Jaekel U. (2011). Anaerobic oxidation of short-chain and cyclic alkanes by sulfate-reducing bacteria. Doctoral dissertation, University Bremen.
- Jannasch HW. (1985). Review lecture: The chemosynthetic support of life and the microbial diversity at deep-sea hydrothermal vents. *Proc R Soc Lond B Biol Sci* **225**: 277-297.
- Jannasch HW and Mottl MJ. (1985). Geomicrobiology of deep-sea hydrothermal vents. *Science* **229**: 717-725.
- Jehmlich N, Schmidt F, von Bergen M, Richnow H-H, and Vogt C. (2008a). Protein-based stable isotope probing (Protein-SIP) reveals active species within anoxic mixed cultures. *ISME J* **2**: 1122-1133.
- Jehmlich N, Schmidt F, Hartwich M, von Bergen M, Richnow H-H, and Vogt C. (2008b). Incorporation of carbon and nitrogen atoms into proteins measured by protein-based stable isotope probing (Protein-SIP). *Rapid Commun Mass Spectrom* **22**: 2889-2897.
- Jehmlich N, Schmidt F, Taubert M, Seifert J, Bastida F, von Bergen M, Richnow H-H, and Vogt C. (2010). Protein-based stable isotope probing. *Nat. Protocols* **5**: 1957-1966.
- Jeon CO, Park W, Padmanabhan P, DeRito C, Snape JR, and Madsen EL. (2003). Discovery of a bacterium, with distinctive dioxygenase, that is responsible for in situ biodegradation in contaminated sediment. *Proc Natl Acad Sci USA* **100**: 13591-13596.
- Johann H. (2007). Adding handles to unhandy substrates: anaerobic hydrocarbon activation mechanisms. *Curr Opin Chem Biol* **11**: 188-194.
- Jørgensen B, B. and Revsbech N, P. (1985). Diffusive boundary layers and the oxygen uptake of sediments and detritus. *Limnol Oceanogr* **30**: 111-122.
- Jørgensen BB. (1982). Mineralization of organic-matter in the sea bed - the role of sulfate reduction. *Nature* **296**: 643-645.
- Joye SB, Boetius A, Orcutt BN, Montoya JP, Schulz HN, Erickson MJ, and Lugo SK. (2004). The anaerobic oxidation of methane and sulfate reduction in sediments from Gulf of Mexico cold seeps. *Chem Geol* **205**: 219-238.
- Joye SB, MacDonald IR, Leifer I, and Asper V. (2011). Magnitude and oxidation potential of hydrocarbon gases released from the BP oil well blowout. *Nature Geosci* **4**: 160-164.
- Kallmeyer J and Boetius A. (2004). Effects of temperature and pressure on sulfate reduction and anaerobic oxidation of methane in hydrothermal sediments of Guaymas Basin. *Appl Environ Microbiol* **70**: 1231-1233.

- Kasai Y, Takahata Y, Manefield M, and Watanabe K. (2006). RNA-based stable isotope probing and isolation of anaerobic benzene-degrading bacteria from gasoline-contaminated groundwater. *Appl Environ Microbiol* **72**: 3586-3592.
- Kawka OE and Simoneit BRT. (1987). Survey of hydrothermally-generated petroleum from the Guaymas Basin spreading center. *Org Geochem* **11**: 311-328.
- Kenk V and Wilson B. (1985). A new mussel (*Bivalvia*, *Mytilidae*) from hydrothermal vents in the Galapagos Rift Zone. *Malacologia* 253-271.
- Kennicutt II MC, Brooks JM, Bidigare RR, and Denoux GJ. (1988a). Gulf of Mexico hydrocarbon seep communities-I. Regional distribution of hydrocarbon seepage and associated fauna. *Deep-Sea Res* **35**: 1639-1651.
- Kennicutt II MC, Brooks JM, Bidigare RR, Fay RR, Wade TL, and McDonald TJ. (1985). Vent-type taxa in a hydrocarbon seep region on the Louisiana slope. *Nature* **317**: 351-353.
- Kennicutt II MC, Brooks JM, and Denoux GJ. (1988b). Leakage of deep, reservoired petroleum to the near-surface on the Gulf of Mexico continental-slope. *Mar Chem* **24**: 39-59.
- Killops SD and Killops VJ. (2004) *An Introduction to Organic Geochemistry*, 2 ed. (Longman Scientific and Technical, New York).
- Klapp SA, Bohrmann G, Kuhs WF, Mangir Murshed M, Pape T, Klein H, Techmer KS, Heeschen KU, and Abegg F. (2010). Microstructures of structure I and II gas hydrates from the Gulf of Mexico. *Mar Petrol Geol* **27**: 116-125.
- Kniemeyer O, Fischer T, Wilkes H, Glöckner FO, and Widdel F. (2003). Anaerobic degradation of ethylbenzene by a new type of marine sulfate-reducing bacterium. *Appl Environ Microbiol* **69**: 760-768.
- Kniemeyer O, Musat F, Sievert SM, Knittel K, Wilkes H, Blumenberg M, Michaelis W, Classen A, Bolm C, Joye SB, and Widdel F. (2007). Anaerobic oxidation of short-chain hydrocarbons by marine sulphate-reducing bacteria. *Nature* **449**: 898-910.
- Knittel K and Boetius A. (2009). Anaerobic oxidation of methane: progress with an unknown process. *Annu Rev Microbiol* **63**: 311-334.
- Knittel K, Boetius A, Lemke A, Eilers H, Lochte K, Pfannkuche O, Linke P, and Amann R. (2003). Activity, distribution, and diversity of sulfate reducers and other bacteria in sediments above gas hydrate (Cascadia margin, Oregon). *Geomicrobiol J* **20**: 269-294.
- Knittel K, Lösekann T, Boetius A, Kort R, and Amann R. (2005). Diversity and distribution of methanotrophic archaea at cold seeps. *Appl Environ Microbiol* **71**: 467-479.
- Knoblauch C, Jørgensen B, B., and Harder J. (1999). Community size and metabolic rates of psychrophilic sulfate-reducing bacteria in Arctic marine sediments. *Appl Environ Microbiol* **65**: 4230-4233.
- Krüger M, Treude T, Wolters H, Nauhaus K, and Boetius A. (2005). Microbial methane turnover in different marine habitats. *Palaogeogr Paleoclimatol Paleoecol* **227**: 6-17.
- Kulm LD, Suess E, Moore JC, Carson B, Lewis BT, Ritger SD, Kadko DC, Thornburg TM, Embley RW, Rugh WD, Massoth GJ, Langseth MG, Cochrane GR, and Scamman RL. (1986). Oregon subduction zone: venting, fauna, and carbonates. *Science* **231**: 561-566.
- Kunapuli U, Lueders T, and Meckenstock RU. (2007). The use of stable isotope probing to identify key iron-reducing microorganisms involved in anaerobic benzene degradation. *ISME J* **1**: 643-653.
- Kvenvolden KA. (1993). Gas hydrates - geological perspective and global change. *Rev Geophys* **31**: 173-187.
- Larkin JM and Strohl WR. (1983). *Beggiatoa*, *Thiothrix*, and *Thioploca*. *Annu Rev Microbiol* **37**: 341-367.

- Leigh MB, Pellizari VH, Uhlik O, Sutka R, Rodrigues J, Ostrom NE, Zhou J, and Tiedje JM. (2007). Biphenyl-utilizing bacteria and their functional genes in a pine root zone contaminated with polychlorinated biphenyls (PCBs). *ISME J* **1**: 134-148.
- Li T, Wu T-D, Mazéas L, Toffin L, Guerquin-Kern J-L, Leblon G, and Bouchez T. (2008). Simultaneous analysis of microbial identity and function using NanoSIMS. *Environ Microbiol* **10**: 580-588.
- Liesack W and Finster K. (1994). Phylogenetic analysis of five strains of gram-negative, obligately anaerobic, sulfur-reducing bacteria and description of *Desulfuromusa* gen. nov., including *Desulfuromusa kysingii* sp. nov., *Desulfuromusa bakii* sp. nov., and *Desulfuromusa succinoxidans* sp. nov. *Int J Syst Bacteriol* **44**: 753-758.
- Liu A, Garcia-Dominguez E, Rhine ED, and Young LY. (2004). A novel arsenate respiring isolate that can utilize aromatic substrates. *FEMS Microbiol Ecol* **48**: 323-332.
- Lonsdale P and Becker K. (1985). Hydrothermal plumes, hot springs, and conductive heat flow in the Southern Trough of Guaymas Basin. *Earth Planet Sci Lett* **73**: 211-225.
- Lösekan T, Knittel K, Nadalig T, Fuchs B, Niemann H, Boetius A, and Amann R. (2007). Diversity and abundance of aerobic and anaerobic methane oxidizers at the Haakon Mosby Mud Volcano, Barents Sea. *Appl Environ Microbiol* **73**: 3348-3362.
- Lovley DR, Giovannoni SJ, White DC, Champine JE, Phillips EJP, Gorby YA, and Goodwin S. (1993). *Geobacter metallireducens* gen. nov. sp. nov., a microorganism capable of coupling the complete oxidation of organic-compounds to the reduction of iron and other metals. *Arch Microbiol* **159**: 336-344.
- MacDonald IR, Bohrmann G, Escobar E, Abegg F, Blanchon P, Blinova V, Bruckmann W, Drews M, Eisenhauer A, Han X, Heeschen K, Meier F, Mortera C, Naehr T, Orcutt B, Bernard B, Brooks J, and de Farago M. (2004). Asphalt volcanism and chemosynthetic life in the Campeche Knolls, Gulf of Mexico. *Science* **304**: 999-1002.
- Mahmood S, Paton GI, and Prosser JJ. (2005). Cultivation-independent in situ molecular analysis of bacteria involved in degradation of pentachlorophenol in soil. *Environ Microbiol* **7**: 1349-1360.
- Manefield M, Griffiths RI, Leigh MB, Fisher R, and Whiteley AS. (2005). Functional and compositional comparison of two activated sludge communities remediating coking effluent. *Environ Microbiol* **7**: 715-722.
- Manefield M, Whiteley AS, Griffiths RI, and Bailey MJ. (2002). RNA stable isotope probing, a novel means of linking microbial community function to phylogeny. *Appl Environ Microbiol* **68**: 5367-5373.
- Martens CS. (1990). Generation of short chain acid anions in hydrothermally altered sediments of the Guaymas Basin, Gulf of California. *Appl Geochem* **5**: 71-76.
- Masclé J, Zitter T, Bellaiche G, Droz L, Gaullier V, Loncke L, and Party PS. (2001). The Nile deep sea fan: preliminary results from a swath bathymetry survey. *Mar Petrol Geol* **18**: 471-477.
- Mastalerz V, de Lange GJ, and Dählmann A. (2009). Differential aerobic and anaerobic oxidation of hydrocarbon gases discharged at mud volcanoes in the Nile deep-sea fan. *Geochim Cosmochim Acta* **73**: 3849-3863.
- McNeill AM, Hood RC, and Wood M. (1994). Direct measurement of nitrogen-fixation by *Trifolium repens* L and *Alnus glutinosa* L using $^{15}\text{N}_2$. *J Exp Bot* **45**: 749-755.
- Meckenstock RU, Annweiler E, Michaelis W, Richnow HH, and Schink B. (2000). Anaerobic naphthalene degradation by a sulfate-reducing enrichment culture. *Appl Environ Microbiol* **66**: 2743-2747.
- Michaelis W, Seifert R, Nauhaus K, Treude T, Thiel V, Blumenberg M, Knittel K, Gieseke A, Peterknecht K, Pape T, Boetius A, Amann R, Jørgensen B, B., Widdel F, Peckmann J, Pimenov NV, and Gulin MB. (2002). Microbial reefs in the Black Sea fueled by anaerobic oxidation of methane. *Science* **297**: 1013-1015.

- Milkov AV, Claypool GE, Lee Y-J, Torres ME, Borowski WS, Tomaru H, Sassen R, and Long PE. (2004). Ethane enrichment and propane depletion in subsurface gases indicate gas hydrate occurrence in marine sediments at southern Hydrate Ridge offshore Oregon. *Org Geochem* **35**: 1067-1080.
- Miralles G, Grossi V, Acquaviva M, Duran R, Bertrand JC, and Cuny P. (2007). Alkane biodegradation and dynamics of phylogenetic subgroups of sulfate-reducing bacteria in an anoxic coastal marine sediment artificially contaminated with oil. *Chemosphere* **68**: 1327-1334.
- Miroshnichenko M and Bonch-Osmolovskaya E. (2006). Recent developments in the thermophilic microbiology of deep-sea hydrothermal vents. *Extremophiles* **10**: 85-96.
- Molin S and Givskov M. (1999). Application of molecular tools for in situ monitoring of bacterial growth activity. *Environ Microbiol* **1**: 383-391.
- Morasch B, Schink B, Tebbe CC, and Meckenstock RU. (2004). Degradation of o-xylene and m-xylene by a novel sulfate-reducer belonging to the genus *Desulfotomaculum*. *Arch Microbiol* **181**: 407-417.
- Musat F, Galushko A, Jacob J, Widdel F, Kube M, Reinhardt R, Wilkes H, Schink B, and Rabus R. (2009). Anaerobic degradation of naphthalene and 2-methylnaphthalene by strains of marine sulfate-reducing bacteria. *Environ Microbiol* **11**: 209-219.
- Musat N, Halm H, Winterholler B, Hoppe P, Peduzzi S, Hillion F, Horreard F, Amann R, Jørgensen BB, and Kuypers MMM. (2008). A single-cell view on the ecophysiology of anaerobic phototrophic bacteria. *Proc Natl Acad Sci USA* **105**: 17861-17866.
- Musat N, Werner U, Knittel K, Kolb S, Dodenhof T, van Beusekom JEE, de Beer D, Dubilier N, and Amann R. (2006). Microbial community structure of sandy intertidal sediments in the North Sea, Sylt-Rømø Basin, Wadden Sea. *Syst. Appl. Microbiol.* **29**: 333-348.
- Mußmann M, Ishii K, Rabus R, and Amann R. (2005). Diversity and vertical distribution of cultured and uncultured *Deltaproteobacteria* in an intertidal mud flat of the Wadden Sea. *Environ Microbiol* **7**: 405-418.
- Muyzer G and Stams AJM. (2008). The ecology and biotechnology of sulphate-reducing bacteria. *Nat Rev Micro* **6**: 441-454.
- National Research Council. (2003) *Committee on Oil in the Sea III: Inputs, Fates, and Effects*. (The National Academic Press, Washington, D.C.).
- Niemann H, Duarte J, Hensen C, Omoregie E, Magalhães VH, Elvert M, Pinheiro LM, Kopf A, and Boetius A. (2006a). Microbial methane turnover at mud volcanoes of the Gulf of Cadiz. *Geochim Cosmochim Acta* **70**: 5336-5355.
- Niemann H, Elvert M, Hovland M, Orcutt B, Judd A, Suck I, Gutt J, Joye SB, Damm E, Finster K, and Boetius A. (2005). Methane emission and consumption at a North Sea gas seep (Tommeliten area). *Biogeosciences* **2**: 335-351.
- Niemann H, Lösekann T, de Beer D, Elvert M, Nadalig T, Knittel K, Amann R, Sauter EJ, Schlüter M, Klages M, Foucher JP, and Boetius A. (2006b). Novel microbial communities of the Haakon Mosby mud volcano and their role as a methane sink. *Nature* **443**: 854-858.
- Ommedal H and Torsvik T. (2007). *Desulfotignum toluenicum* sp. nov., a novel toluene-degrading, sulphate-reducing bacterium isolated from an oil-reservoir model column. *Int J Syst Evol Microbiol* **57**: 2865-2869.
- Omoregie EO, Niemann H, Mastalerz V, de Lange GJ, Stadnitskaia A, Mascle J, Foucher JP, and Boetius A. (2009). Microbial methane oxidation and sulfate reduction at cold seeps of the deep Eastern Mediterranean Sea. *Mar Geology* **261**: 114-127.
- Orcutt B, Boetius A, Elvert M, Samarkin V, and Joye SB. (2005). Molecular biogeochemistry of sulfate reduction, methanogenesis and the anaerobic oxidation of methane at Gulf of Mexico cold seeps. *Geochim Cosmochim Acta* **69**: 4267-4281.

- Orcutt BN, Boetius A, Lugo SK, MacDonald IR, Samarkin VA, and Joye SB. (2004). Life at the edge of methane ice: microbial cycling of carbon and sulfur in Gulf of Mexico gas hydrates. *Chem Geol* **205**: 239-251.
- Orcutt BN, Joye SB, Kleindienst S, Knittel K, Ramette A, Reitz A, Samarkin V, Treude T, and Boetius A. (2010). Impact of natural oil and higher hydrocarbons on microbial diversity, distribution, and activity in Gulf of Mexico cold-seep sediments. *Deep-Sea Res Pt II* **57**: 2008-2021.
- Orphan VJ, Hinrichs K-U, Ussler W, Paull CK, Taylor LT, Sylva SP, Hayes JM, and DeLong EF. (2001). Comparative analysis of methane-oxidizing archaea and sulfate-reducing bacteria in anoxic marine sediments. *Appl Environ Microbiol* **67**: 1922-1934.
- Orphan VJ, House CH, Hinrichs K-U, McKeegan KD, and DeLong EF. (2002). Multiple archaeal groups mediate methane oxidation in anoxic cold seep sediments. *Proc Natl Acad Sci USA* **99**: 7663-7668.
- Padmanabhan P, Padmanabhan S, DeRito C, Gray A, Gannon D, Snape JR, Tsai CS, Park W, Jeon C, and Madsen EL. (2003). Respiration of ¹³C-labeled substrates added to soil in the field and subsequent 16S rRNA gene analysis of ¹³C-labeled soil DNA. *Appl Environ Microbiol* **69**: 1614-1622.
- Pernthaler A and Amann R. (2004). Simultaneous fluorescence in situ hybridization of mRNA and rRNA in environmental bacteria. *Appl Environ Microbiol* **70**: 5426-5433.
- Pernthaler A, Dekas AE, Brown CT, Goffredi SK, Embaye T, and Orphan VJ. (2008). Diverse syntrophic partnerships from deep-sea methane vents revealed by direct cell capture and metagenomics. *Proc Natl Acad Sci USA* **105**: 7052-7057.
- Peter L. (1977). Clustering of suspension-feeding macrobenthos near abyssal hydrothermal vents at oceanic spreading centers. *Deep Sea Res* **24**: 857-863.
- Petersen JM, Zielinski FU, Pape T, Seifert R, Moraru C, Amann R, Hourdez S, Girguis PR, Wankel SD, Barbe V, Pelletier E, Fink D, Borowski C, Bach W, and Dubilier N. (2011). Hydrogen is an energy source for hydrothermal vent symbioses. *Nature* **476**: 176-180.
- Peterson BJ and Fry B. (1987). Stable isotopes in ecosystem studies. *Annu Rev Ecol Syst* **18**: 293-320.
- Pilloni G, von Netzer F, Engel M, and Lueders T. (2011). Electron acceptor-dependent identification of key anaerobic toluene degraders at a tar-oil-contaminated aquifer by Pyro-SIP. *FEMS Microbiol Ecol* **78**: 165-175.
- Pimenov NV, Rusanov II, Poglazova MN, Mityushina LL, Sorokin DY, Khmelenina VN, and Trotsenko YA. (1997). Bacterial mats on coral-like structures at methane seeps in the Black Sea. *Microbiol* **66**: 354-360.
- Putscher RE. (1952). Isolation of olefins from Bradford crude oil. *Anal Chem* **24**: 1551-1558.
- Quistad SD and Valentine DL. (2011). Anaerobic propane oxidation in marine hydrocarbon seep sediments. *Geochim Cosmochim Acta* **75**: 2159-2169.
- Rabus R, Nordhaus R, Ludwig W, and Widdel F. (1993). Complete oxidation of toluene under strictly anoxic conditions by a new sulfate-reducing bacterium. *Appl Environ Microbiol* **59**: 1444-1451.
- Radajewski S, Ineson P, Parekh NR, and Murrell JC. (2000). Stable-isotope probing as a tool in microbial ecology. *Nature* **403**: 646-649.
- Rappé MS and Giovannoni SJ. (2003). The uncultured microbial majority. *Annu Rev Microbiol* **57**: 369-394.
- Ravenschlag K, Sahm K, Knoblauch C, Jørgensen BB, and Amann R. (2000). Community structure, cellular rRNA content and activity of sulfate-reducing bacteria in marine Arctic sediments. *Appl Environ Microbiol* **66**: 3592-3602.
- Reeburgh WS. (2007). Oceanic methane biogeochemistry. *Chem Rev* **107**: 486-513.

- Reed A, Lutz R, and Vetriani C. (2006). Vertical distribution and diversity of bacteria and archaea in sulfide and methane-rich cold seep sediments located at the base of the Florida Escarpment. *Extremophiles* **10**: 199-211.
- Reitner J, Peckmann J, Blumenberg M, Michaelis W, Reimer A, and Thiel V. (2005a). Concretionary methane-seep carbonates and associated microbial communities in Black Sea sediments. *Palaogeogr Paleoclimatol Paleoecol* **227**: 18-30.
- Reitner J, Peckmann J, Reimer A, Schumann G, and Thiel V. (2005b). Methane-derived carbonate build-ups and associated microbial communities at cold seeps on the lower Crimean shelf (Black Sea). *Facies* **51**: 66-79.
- Rossel PE, Lipp JS, Fredricks HF, Arnds J, Boetius A, Elvert M, and Hinrichs K-U. (2008). Intact polar lipids of anaerobic methanotrophic archaea and associated bacteria. *Org Geochem* **39**: 992-999.
- Rueter P, Rabus R, Wilkes H, Aeckersberg F, Rainey FA, Jannasch HW, and Widdel F. (1994). Anaerobic oxidation of hydrocarbons in crude-oil by new types of sulfate-reducing bacteria. *Nature* **372**: 455-458.
- Sassen R, Joye SB, Sweet ST, DeFreitas DA, Milkov AV, and MacDonald IR. (1999). Thermogenic gas hydrates and hydrocarbon gases in complex chemosynthetic communities, Gulf of Mexico continental slope. *Org Geochem* **30**: 485-497.
- Sassen R, MacDonald IR, Guinasso NL, Joye SB, Requejo AG, Sweet ST, Alcalá-Herrera J, DeFreitas DA, and Schink DR. (1998). Bacterial methane oxidation in sea-floor gas hydrate: Significance to life in extreme environments. *Geology* **26**: 851-854.
- Sassen R, Roberts HH, Carney R, Milkov AV, DeFreitas DA, Lanoil B, and Zhang C. (2004). Free hydrocarbon gas, gas hydrate, and authigenic minerals in chemosynthetic communities of the northern Gulf of Mexico continental slope: relation to microbial processes. *Chem Geol* **205**: 195-217.
- Schreiber L, Holler T, Knittel K, Meyerdierks A, and Amann R. (2010). Identification of the dominant sulfate-reducing bacterial partner of anaerobic methanotrophs of the ANME-2 clade. *Environ Microbiol* **12**: 2327-2340.
- Schubotz F, Lipp JS, Elvert M, Kasten S, Mollar XP, Zabel M, Bohrmann G, and Hinrichs K-U. (2011). Petroleum degradation and associated microbial signatures at the Chapopote asphalt volcano, Southern Gulf of Mexico. *Geochim Cosmochim Acta* **75**: 4377-4398.
- Schulz HN and de Beer D. (2002). Uptake rates of oxygen and sulfide measured with individual *Thiomargarita namibiensis* cells by using microelectrodes. *Appl Environ Microbiol* **68**: 5746-5749.
- Schulz HN and Schulz HD. (2005). Large sulfur bacteria and the formation of phosphorite. *Science* **307**: 416-418.
- Sheryll RP. (2009). New technology for uncontaminated and pressure controlled deep-sea sampling: "Deep Ocean Benthic Sampler" (DOBS), Stevens Institute of Technology.
- Simoneit BRT and Lonsdale PF. (1982). Hydrothermal petroleum in mineralized mounds at the seabed of Guaymas Basin. *Nature* **295**: 198-202.
- Simoneit BRT, Lonsdale PF, Edmond JM, and Shanks III WC. (1990). Deep-water hydrocarbon seeps in Guaymas Basin, Gulf of California. *Appl Geochem* **5**: 41-49.
- Singleton DR, Hunt M, Powell SN, Frontera-Suau R, and Aitken MD. (2007). Stable-isotope probing with multiple growth substrates to determine substrate specificity of uncultivated bacteria. *J Microbiol Methods* **69**: 180-187.
- Singleton DR, Powell SN, Sangaiah R, Gold A, Ball LM, and Aitken MD. (2005). Stable-isotope probing of bacteria capable of degrading salicylate, naphthalene, or phenanthrene in a bioreactor treating contaminated soil. *Appl Environ Microbiol* **71**: 1202-1209.

- So CM and Young LY. (1999). Isolation and characterization of a sulfate-reducing bacterium that anaerobically degrades alkanes. *Appl Environ Microbiol* **65**: 2969-2976.
- Stadnitskaia A, Ivanov MK, Blinova V, Kreulen R, and van Weering TCE. (2006). Molecular and carbon isotopic variability of hydrocarbon gases from mud volcanoes in the Gulf of Cadiz, NE Atlantic. *Mar Petrol Geol* **23**: 281-296.
- Stagars M. (2012). Ecophysiology of key sulfate-reducing bacteria involved in anaerobic degradation of hydrocarbons at marine gas and oil seeps. Master Thesis, University of Bremen.
- Stepanaukas R and Sieracki ME. (2007). Matching phylogeny and metabolism in the uncultured marine bacteria, one cell at a time. *Proc Natl Acad Sci USA* **104**: 9052-9057.
- Suess E, Torres M, Bohrmann G, Collier RW, Greinert J, Linke P, Rehder G, Trehu A, Wallmann K, Winckler G, and Zuleger E. (1999). Gas hydrate destabilization: enhanced dewatering, benthic material turnover and large methane plumes at the Cascadia convergent margin. *Earth Planet Sci Lett* **170**: 1-15.
- Takano Y, Chikaraishi Y, Ogawa NO, Nomaki H, Morono Y, Inagaki F, Kitazato H, Hinrichs K-U, and Ohkouchi N. (2010). Sedimentary membrane lipids recycled by deep-sea benthic archaea. *Nature Geosci* **3**: 858-861.
- Teske A, Hinrichs K-U, Edgcomb V, de Vera Gomez A, Kysela D, Sylva SP, Sogin ML, and Jannasch HW. (2002). Microbial diversity of hydrothermal sediments in the Guaymas Basin: evidence for anaerobic methanotrophic communities. *Appl Environ Microbiol* **68**: 1994-2007.
- Thiel V, Peckmann J, Seifert R, Wehrung P, Reitner J, and Michaelis W. (1999). Highly isotopically depleted isoprenoids: molecular markers for ancient methane venting - occurrence and ecology. *Geochim Cosmochim Acta* **63**: 3959-3966.
- Tissot BP and Welte DH. (1984) *Petroleum formation and occurrence: a new approach to oil and gas exploration* 2nd ed. (Springer Verlag, Berlin).
- Treude T, Boetius A, Knittel K, Wallmann K, and Jørgensen BB. (2003). Anaerobic oxidation of methane above gas hydrates at Hydrate Ridge, NE Pacific Ocean. *Mar Ecol Prog Ser* **264**: 1-14.
- Treude T, Knittel K, Blumenberg M, Seifert R, and Boetius A. (2005). Subsurface microbial methanotrophic mats in the Black Sea. *Appl Environ Microbiol* **71**: 6375-6378.
- Valentine D. (2002). Biogeochemistry and microbial ecology of methane oxidation in anoxic environments: a review. *Ant Van Leeuw* **81**: 271-282.
- Von Damm KL, Edmond JM, Measures CI, and Grant B. (1985). Chemistry of submarine hydrothermal solutions at Guaymas Basin, Gulf of California. *Geochim Cosmochim Acta* **49**: 2221-2237.
- Wegener G, Shovitri M, Knittel K, Niemann H, Hovland M, and Boetius A. (2008). Biogeochemical processes and microbial diversity of the Gullfaks and Tommeliten methane seeps (Northern North Sea). *Biogeosciences* **5**: 1127-1144.
- Went FW. (1960). Organic matter in the atmosphere, and its possible relation to petroleum formation. *Proc Natl Acad Sci USA* **46**: 212-221.
- Whiticar M, J., Hovland M, Kastner M, and Sample J, C. (1995) in *Proceedings of the ODP, Scientific Results*, edited by B. Carson, G.K. Westbrook, R.J. Musgrave et al. (Ocean Drilling Program, College Station, TX), Vol. 146 (Pt. 1), pp. 484.
- Widdel F and Grundmann O. (2010) in *Handbook of hydrocarbon and lipid microbiology*, edited by K.N. Timmis, T. McGenity, J. R. van der Meer et al. (Springer Berlin Heidelberg), Vol. 2, pp. 909-924.
- Widdel F, Knittel K, and Galushko A. (2010) in *Handbook of hydrocarbon and lipid microbiology*, edited by K.N. Timmis, T. McGenity, J. R. van der Meer et al. (Springer Berlin Heidelberg), Vol. 3, pp. 1997-2021.

- Wilkes H and Schwarzbauer J. (2010) in *Handbook of hydrocarbon and lipid microbiology*, edited by K.N. Timmis, T. McGenity, J. R. van der Meer et al. (Springer Berlin Heidelberg), Vol. 1, pp. 5-48.
- Wilmes P and Bond PL. (2006). Metaproteomics: studying functional gene expression in microbial ecosystems. *Trends Microbiol* **14**: 92-97.
- Winderl C, Penning H, von Netzer F, Meckenstock RU, and Lueders T. (2010). DNA-SIP identifies sulfate-reducing *Clostridia* as important toluene degraders in tar-oil-contaminated aquifer sediment. *ISME J* **4**: 1314-1325.
- Yarza P, Ludwig W, Euzéby J, Amann R, Schleifer K-H, Glöckner FO, and Rosselló-Móra R. (2010). Update of the all-species living tree project based on 16S and 23S rRNA sequence analyses. *Syst Appl Microbiol* **33**: 291-299.
- Yu C-P and Chu K-H. (2005). A quantitative assay for linking microbial community function and structure of a naphthalene-degrading microbial consortium. *Environ Sci Technol* **39**: 9611-9619.
- Zelles L. (1999). Fatty acid patterns of phospholipids and lipopolysaccharides in the characterisation of microbial communities in soil: a review. *Biol Fertil Soils* **29**: 111-129.
- Zengler K, Heider J, Rosselló-Móra R, and Widdel F. (1999a). Phototrophic utilization of toluene under anoxic conditions by a new strain of *Blastochloris sulfoviridis*. *Arch Microbiol* **172**: 204-212.
- Zengler K, Richnow HH, Rosselló-Móra R, Michaelis W, and Widdel F. (1999b). Methane formation from long-chain alkanes by anaerobic microorganisms. *Nature* **401**: 266-269.

Acknowledgements

Thanks to...

Prof. Dr. Rudolf Amann, for giving me the opportunity to work as a doctoral student in the highly inspiring environment of the Molecular Ecology Group at the MPI in Bremen. Also, I thank you for giving me the opportunity to teach in the Microbial Diversity Course.

Dr. Katrin Knittel, for all your valuable support during my doctoral studies. I am very fortunate to have had you as my supervisor! Thank you for always being there, when I needed your advice. Thank you for teaching me in the field of molecular ecology and many other things. Also, thank you so much for supporting my ideas and projects. You always motivated me and gave me the feeling that I can make it. Thanks!

Prof. Dr. Heribert Cypionka, for introducing me to the fascinating world of marine microbiology as an undergraduate student. I will never forget my first practical course and all the following activities in your lab, which inspired me in such an outstanding way. Thank you so much for all your support also after I have left the ICBM. And above all, thank you for being my doctoral thesis committee member.

Prof. Dr. Ulrich Fischer, for being my thesis committee member.

Dr. Florin Musat, for being my committee member and for teaching me so much about the microbiology of hydrocarbon degraders. This work gained so much benefit from your great theoretical and methodological expertise.

Dr. Tillmann Lueders, for being my committee member. Also, thank you so much for teaching me SIP. You gave me the opportunity to work in your lab, when I needed your expertise right at the place. Thank you for many valuable discussions. I enjoyed my time in Munich so much, and thanks to your great group:

Frederick von Netzer, for all the fun in the lab.

Katrin Hörmann, for your help in the lab, and for showing me how to dress like a Bavarian.

Dr. Giovanni Pilloni, for answering all my questions.

Dr. Jana Seifert, for fruitful collaborations and meetings initiated by the DFG-project and beyond. Thank you for all your support for the SIP-project.

Florian Alexander Herbst, for Protein-SIP analysis of my challenging samples.

Nicole Rödiger, for all your help in the lab. Thank you for all your support during this thesis.

PD Dr. Bernhard Fuchs, Jörg Wulf, for advices and assistance with FACs.

Dr. Kyoko Kubo, for always being so kind and helpful.

Dr. Lars Schreiber, for teaching me multiplex PCR and providing several probes.

Dr. Marc Mußmann, for providing sediment samples and especially for your expertise with respect to single-cell genomic and NanoSIMS approaches.

Dr. Jörg Peplies, for NGS-pipeline analysis of 454-pyrosequences.

Dr. Cristina Moraru, for giving me the opportunity to teach in the Microbial Diversity Course.

Ramona Appel, for your valuable help in the Microbiology lab.

Dr. Ulrike Jaekel, for setting up the methanogenic enrichments with me and for providing pure and enrichment cultures.

Dr. Lubos Polerecky, for valuable discussions and introducing me the Look@NanoSIMS.

Dr. Alban Ramette, for teaching me numerous methods for statistical analysis.

Dr. Thomas Holler, Dr. Janine Felden, Dr. Gunter Wegener, for great times in the Microbiology lab, sediment samples, and all the information of thousands of additional samples. Thomas, thank you so much for reading this thesis and for helpful advises.

Prof. Dr. Antje Boetius, Prof. Dr. Andreas Teske, for providing so many samples from all over the oceans.

Cecilia Wentrup, Dr. Chia-I Huang, Dr. Jillian Petersen, Dr. Dennis Fink, Mario Schimak, Beate Kraft, for being the best office mates, colleagues, and friends.

Wiebke Rentzsch, Stephanie Boddien, and Alexander Makowka, for tens of thousands of CARD-FISH hybridizations and additional support in the lab.

All current and former members of the Molecular Ecology Group and all the other scientists I forgot to mention.

Micha, for your support and all the fun in every part of my live. Thank you so much for your patience, friendship, and your love.

My parents, for all your love and many more things that words cannot say.

Simon and Lena Kleindienst, for being great siblings, my best friends and soul mates.

Maike, Anna and all my other friends, for all the fun and continuous support.

Appendix

Table SIII.3: Proteins identified in the SIP-incubations. Protein IDs (protein group) contain the Uniprot Accession of the identified protein. If peptide identifications could be explained by different protein identifications, several proteins were grouped together, the first being the most probable one. Peptide Counts (all) contain the number of all peptides, which could be associated with this protein group, but are shared between groups. Peptide Counts (unique) contain all peptides, which were regarded as unique/specific for this protein group. If a protein group consists of several proteins, the number of peptides explained by the specific possible protein identification is given. The first accession explains all peptides belonging to this group. Protein Description contains the Uniprot protein description for the most probable protein identification.

Protein IDs	Peptide Counts (all)	Peptide Counts (unique)	Protein Description
<i>Protein identifications in the Amon MV butane sample</i>			
A8ZT73	2	2	Predicted phospho-2-dehydro-3-deoxyheptonate aldolase n=1 Tax= <i>Desulfococcus oleovorans</i> (strain DSM 6200 / Hxd3)
A8ZTP6	2	2	Glyceraldehyde-3-phosphate dehydrogenase, type I n=1 Tax= <i>Desulfococcus oleovorans</i> (strain DSM 6200 / Hxd3)
A8ZU48	11	3	60 kDa chaperonin n=1 Tax= <i>Desulfococcus oleovorans</i> (strain DSM 6200 / Hxd3)
A8ZUA1	8	3	ATP synthase subunit beta n=1 Tax= <i>Desulfococcus oleovorans</i> (strain DSM 6200 / Hxd3)
A9A067	3	2	CO dehydrogenase/acetyl-CoA synthase delta subunit n=1 Tax= <i>Desulfococcus oleovorans</i> (strain DSM 6200 / Hxd3)
B8FAG9	5	3	Methyl-viologen-reducing hydrogenase delta subunit n=1 Tax= <i>Desulfatibacillum alkenivorans</i> (strain AK-01)
B8FGE3	2	2	Ribosome-recycling factor n=1 Tax= <i>Desulfatibacillum alkenivorans</i> (strain AK-01)
B8FJ32	2	2	Phosphoribosylaminoimidazolecarboxamide formyltransferase n=1 Tax= <i>Desulfatibacillum alkenivorans</i> (strain AK-01)
B8FJ79	2	2	Acyl-CoA dehydrogenase domain protein n=1 Tax= <i>Desulfatibacillum alkenivorans</i> (strain AK-01)
B8FJC7	2	2	Acetyl-CoA acetyltransferase n=1 Tax= <i>Desulfatibacillum alkenivorans</i> (strain AK-01)
B8FM86	8	2	60 kDa chaperonin n=1 Tax= <i>Desulfatibacillum alkenivorans</i> (strain AK-01)
C0Q8U0	2	2	Putative uncharacterized protein n=1 Tax= <i>Desulfobacterium autotrophicum</i> (strain ATCC 43914 / DSM 3382 / HRM2)
C0QA19	5	3	CdhC n=1 Tax= <i>Desulfobacterium autotrophicum</i> (strain ATCC 43914 / DSM 3382 / HRM2)
C0QB00	2	2	PpaC n=1 Tax= <i>Desulfobacterium autotrophicum</i> (strain ATCC 43914 / DSM 3382 / HRM2)
C0QFU1	2	2	CspA n=1 Tax= <i>Desulfobacterium autotrophicum</i> (strain ATCC 43914 / DSM 3382 / HRM2)
C0QGH3	4	2	GdhA1 n=1 Tax= <i>Desulfobacterium autotrophicum</i> (strain ATCC 43914 / DSM 3382 / HRM2)
C0QHK6	2	2	QmoB n=1 Tax= <i>Desulfobacterium autotrophicum</i> (strain ATCC 43914 / DSM 3382 / HRM2)
C0QHU9	2	2	AapJ1 n=1 Tax= <i>Desulfobacterium autotrophicum</i> (strain ATCC 43914 / DSM 3382 / HRM2)
C0QKQ3	10	3	60 kDa chaperonin n=1 Tax= <i>Desulfobacterium autotrophicum</i> (strain ATCC 43914 / DSM 3382 / HRM2)
D1JF51	3	2	K(+)-insensitive pyrophosphate-energized proton pump n=1 Tax=uncultured archaeon
D1JIT0	5	5	Putative uncharacterized protein n=1 Tax=uncultured archaeon
D6Z3H3	2	2	Flagellin domain protein n=1 Tax= <i>Desulfurivibrio alkaliphilus</i> (strain DSM 19089 / UNIQEM U267 / AHT2)
D6Z4V3	7	2	ATP synthase subunit alpha n=1 Tax= <i>Desulfurivibrio alkaliphilus</i> (strain DSM 19089 / UNIQEM U267 / AHT2)
D6Z6P9	2	2	Sulfite reductase, dissimilatory-type beta subunit n=1 Tax= <i>Desulfurivibrio alkaliphilus</i> (strain DSM 19089 / UNIQEM U267 / AHT2)
E1Y9Y8	2	2	Protein hflC n=1 Tax=uncultured <i>Desulfobacterium</i> sp.
E1YAW7	7	4	Formate--tetrahydrofolate ligase n=1 Tax=uncultured <i>Desulfobacterium</i> sp.
E1YFJ9	2	2	3-isopropylmalate dehydrogenase n=1 Tax=uncultured <i>Desulfobacterium</i> sp.
E1YFV9	9	6	Putative uncharacterized protein n=1 Tax=uncultured <i>Desulfobacterium</i> sp.
E1YG97	2	2	50S ribosomal protein L7/L12 n=1 Tax=uncultured <i>Desulfobacterium</i> sp.
E1YHR5	2	2	Protein-export membrane protein secD n=1 Tax=uncultured <i>Desulfobacterium</i> sp.

Table SIII.3: continued

Protein IDs	Peptide Counts (all)	Peptide Counts (unique)	Protein Description
<i>Protein identifications in the Amon MV butane sample</i>			
E1YL47	6	2	Carbon monoxide dehydrogenase/acetyl-CoA synthase subunit alpha n=1 Tax=uncultured <i>Desulfobacterium</i> sp.
E1YLG8	10	2	ATP synthase subunit beta n=1 Tax=uncultured <i>Desulfobacterium</i> sp.
Q2LTG7	9	2	60 kDa chaperonin 2 n=1 Tax= <i>Syntrophus aciditrophicus</i> (strain SB)
Q2VP77	6	6	Formate dehydrogenase like protein, alpha chain n=1 Tax=uncultured archaeon
Q2VP78	8	8	Formate dehydrogenase like protein, beta chain n=1 Tax=uncultured archaeon
Q2VP80	8	8	Heterodisulfide reductase, alpha subunit n=1 Tax=uncultured archaeon
Q2VP82	10	10	Heterodisulfide reductase like protein, subunit A n=1 Tax=uncultured archaeon
Q2VP83	2	2	Heterodisulfide reductase subunit B n=1 Tax=uncultured archaeon
Q2VP84	2	2	Probable heterodisulfide reductase chain C n=1 Tax=uncultured archaeon
Q2Y4E0	9	9	Phosphate ABC transporter, phosphate-binding protein n=1 Tax=uncultured archaeon
Q2Y4Q6	2	2	Probable response regulator (CheY-like receiver domain and DNA-binding HTH domain) n=1 Tax=uncultured archaeon
Q31DM0	2	2	ATP synthase subunit beta n=1 Tax= <i>Thiomicrospira crunogena</i> (strain XCL-2)
Q648M4	5	5	F420H2 dehydrogenase subunit D (Fragment) n=1 Tax=uncultured archaeon GZfos37B2
Q648M5	2	2	F420H2 dehydrogenase subunit C n=1 Tax=uncultured archaeon GZfos37B2
Q648M6	2	2	F420H2 dehydrogenase subunit B n=1 Tax=uncultured archaeon GZfos37B2
Q648Y3	13	9	Methyl coenzyme M reductase subunit alpha n=2 Tax=environmental samples
Q648Y4	13	5	Methyl coenzyme M reductase subunit gamma n=2 Tax=environmental samples
Q648Y7	27	6	Methyl-coenzyme M reductase subunit beta n=2 Tax=environmental samples
Q64BJ1	25	4	Methyl coenzyme M reductase subunit beta n=1 Tax=uncultured archaeon GZfos27A8
Q64BK4	2	2	Sulfite reductase assimilatory-type n=1 Tax=uncultured archaeon GZfos27A8
Q64BZ9	2	2	Uncharacterized protein conserved in archaea n=2 Tax=environmental samples
Q64C60	7	7	N(5)N(10)-methenyltetrahydromethanopterin cyclohydrolase n=1 Tax=uncultured archaeon GZfos26B2
Q64C70	6	4	Methyl coenzyme M reductase subunit alpha n=1 Tax=uncultured archaeon GZfos26B2
Q64C71	11	3	Methyl coenzyme M reductase subunit gamma n=1 Tax=uncultured archaeon GZfos26B2
Q6AQ10	4	2	ATP synthase subunit beta n=1 Tax= <i>Desulfotalea psychrophila</i>
Q6ARV6	7	4	60 kDa chaperonin n=1 Tax= <i>Desulfotalea psychrophila</i>
A9A068; A0LLE1	5; 1	2; 0	CO dehydrogenase/acetyl-CoA synthase complex, beta subunit n=1 Tax= <i>Desulfococcus oleovorans</i> (strain DSM 6200 / Hxd3)
B8FGT4; Q2LR05	6; 2	2; 0	ATP synthase subunit beta n=1 Tax= <i>Desulfatibacillum alkenivorans</i> (strain AK-01)
B8FLB6; Q2LUL1	9; 1	3; 0	K(+)-insensitive pyrophosphate-energized proton pump n=1 Tax= <i>Desulfatibacillum alkenivorans</i> (strain AK-01)
E1YAG3; B8FDZ0	3; 1	3; 1	Glutamine synthetase n=1 Tax=uncultured <i>Desulfobacterium</i> sp.

Table SIII.3: continued

Protein IDs	Peptide Counts (all)	Peptide Counts (unique)	Protein Description
<i>Protein identifications in the Amon MV butane sample</i>			
E1YB73; Q5PS44	18; 2	8; 0	60 kDa chaperonin n=1 Tax=uncultured <i>Desulfobacterium</i> sp.
E1YLG6; Q2LQZ7	14; 2	8; 0	ATP synthase subunit alpha n=1 Tax=uncultured <i>Desulfobacterium</i> sp.
Q64BJ5; Q64B88	5; 1	5; 1	Coenzyme F420-reducing hydrogenase beta subunit n=1 Tax=uncultured archaeon GZfos27A8
Q64BP6; Q64BN2	4; 1	4; 1	Molybdenum formylmethanofuran dehydrogenase subunit (Fragment) n=1 Tax=uncultured archaeon GZfos27A8
A8ZWK4; E1YFW1; C0QKW1	5; 2; 1	3; 2; 1	Sulfate adenylyltransferase n=1 Tax= <i>Desulfococcus oleovorans</i> (strain DSM 6200 / Hxd3)
E1YC93; C0QB13; Q31JF1	8; 2; 1	6; 0; 0	Transcription termination factor Rho n=1 Tax=uncultured <i>Desulfobacterium</i> sp.
E1YL45; C0QAI7; A9A066	3; 1; 1	3; 1; 1	Putative uncharacterized protein n=1 Tax=uncultured <i>Desulfobacterium</i> sp.
Q31J32; A0LIA5; D6Z5M9; Q2LWW2	3; 1; 1; 1	3; 1; 1; 1	Glyceraldehyde-3-phosphate dehydrogenase n=1 Tax= <i>Thiomicrospira crumogena</i> (strain XCL-2)
B1AAN6; B8FME3; Q27RV6; Q6RCS6; Q93QV2; Q8VRR2 A9A0A5; B8FLC3	5; 2; 2; 2; 2; 1	3; 1; 1; 1; 1; 1	Dissimilatory sulfite reductase alpha subunit (Fragment) n=1 Tax=uncultured <i>Desulfobacteraceae bacterium</i>
A0LEA2; A8ZW56	2; 1	2; 1	Probable transaldolase n=1 Tax= <i>Syntrophobacter fumaroxidans</i> (strain DSM 10017 / MPOB)
A8ZVJ1; D6Z269	2; 1	2; 1	Malate dehydrogenase n=1 Tax= <i>Desulfococcus oleovorans</i> (strain DSM 6200 / Hxd3)
A8ZYD0; C0Q9B0	2; 1	2; 1	D-3-phosphoglycerate dehydrogenase n=1 Tax= <i>Desulfococcus oleovorans</i> (strain DSM 6200 / Hxd3)
C0QFH4; B8FA31	2; 1	2; 1	PstS3 n=1 Tax= <i>Desulfobacterium autotrophicum</i> (strain ATCC 43914 / DSM 3382 / HRM2)
Q6AJQ8; Q6AMN5	2; 1	2; 1	Probable flagellin (FliC) n=1 Tax= <i>Desulfotalea psychrophila</i>
A0LHD7; B8FJN2; A8ZTJ6	2; 1; 1	2; 1; 1	Nitrate reductase, gamma subunit n=1 Tax= <i>Syntrophobacter fumaroxidans</i> (strain DSM 10017 / MPOB)
B8FGU8; C0QJE8; A8ZZF0	2; 2; 1	2; 2; 1	AMP-dependent synthetase and ligase n=1 Tax= <i>Desulfatibacillum alkenivorans</i> (strain AK-01)
B8FLC2; A8ZXY9; E1YM39	2; 1; 1	2; 1; 1	D-3-phosphoglycerate dehydrogenase n=1 Tax= <i>Desulfatibacillum alkenivorans</i> (strain AK-01)
E1Y816; A8ZTQ4; B8FLE5	3; 2; 2	3; 2; 2	Bifunctional protein fold n=1 Tax=uncultured <i>Desulfobacterium</i> sp.
E1YCZ8; C0QJX2; A0LL46	2; 1; 1	2; 1; 1	Putative uncharacterized protein n=1 Tax=uncultured <i>Desulfobacterium</i> sp.
A6YCU7; Q8VRX5; Q8VRW3; A6YCT9	7; 5; 4; 2	2; 1; 0; 0	AprA (Fragment) n=1 Tax= <i>Desulfosarcina variabilis</i>
A8ZUU2; C0Q9Y7; B8FET7; C0Q9X5	2; 1; 1; 1	2; 1; 1; 1	Elongation factor Tu n=1 Tax= <i>Desulfococcus oleovorans</i> (strain DSM 6200 / Hxd3)
A8ZY46; A9A014; C0QL21; B8FC57	2; 2; 2; 1	2; 2; 2; 1	Acetoacetyl-CoA synthase n=1 Tax= <i>Desulfococcus oleovorans</i> (strain DSM 6200 / Hxd3)
A9ZRT0; A9ZRU5; A9ZRS5; A9ZRT5	2; 2; 1; 1	2; 2; 1; 1	Nitrogenase protein alpha chain n=1 Tax=uncultured archaeon
B8FHH8; Q2LXN9; A0LMP5; A0LMK3	2; 1; 1; 1	2; 1; 1; 1	Acetolactate synthase n=1 Tax= <i>Desulfatibacillum alkenivorans</i> (strain AK-01)
D1JID5; D1JF16; D1JFD7; D1JFF4	2; 2; 2; 2	2; 2; 2; 2	Thermosome, beta subunit n=1 Tax=uncultured archaeon
A8ZYQ2; E1Y8M3; D6Z0E1; C0QAU0; A0LFZ1	2; 2; 1; 1; 1	2; 2; 1; 1; 1	Putative uncharacterized protein n=1 Tax= <i>Desulfococcus oleovorans</i> (strain DSM 6200 / Hxd3)
E1YE68; B8FLW5; C0QLF7; E1Y9M2; A8ZRW8; A0LFF9; Q0W662	4; 4; 3; 3; 1; 1; 1	4; 4; 3; 3; 1; 1; 1	Pyruvate carboxylase subunit B n=1 Tax=uncultured <i>Desulfobacterium</i> sp.

Table SIII.3: continued

Protein IDs	Peptide Counts (all)	Peptide Counts (unique)	Protein Description
Protein identifications in the Amon MV butane sample			
A6YCW0; A6ZJR7; A6YCW2; D6Z3P1; A6YCX0; Q8VL01; Q8VRV2; A6YCW4	5; 5; 5; 4; 3; 2; 2; 1	2; 2; 2; 1; 1; 1; 1	AprA (Fragment) n=1 Tax= <i>Desulfobulbus propionicus</i> DSM 2032
Q5XQ95; Q64D58; Q647V3; Q64B47; Q649P7; Q64CB0; Q64DM9; Q6MZC4; Q64AM8	2; 2; 2; 2; 2; 2; 2; 2	2; 2; 2; 2; 2; 2; 2; 2	Proteasome subunit alpha n=1 Tax=uncultured archaeon GZfos26D8
D6Z5B9; Q2LUK2; A8ZXC0; B8FLH6; Q31IL3; A0LEW2; Q6ALY6; E1YEA8; C0QGV3; D1JA25; D1JG87	2; 2; 2; 2; 2; 1; 1; 1; 1; 1; 1	2; 2; 2; 2; 2; 1; 1; 1; 1; 1; 1	ATP-dependent chaperone ClpB n=1 Tax= <i>Desulfurivibrio alkaliphilus</i> (strain DSM 19089 / UNIQEM U267 / AHT2)
C0QD63; Q9K5B4; A8ZX94; Q8RKE5; O69400; B1PVU2; B1PVU4; Q8VRP9; O86971; O86975; Q5ZQR4; Q93EW2; Q5ZQN8; Q8VRS9; Q8VRP7; Q8VRP5; Q8GQI8; Q8VRN9; Q8VRP3; Q93EW0; Q8VRQ3; Q93KJ9	3; 3; 1	3; 3; 1	DsrB2 n=1 Tax= <i>Desulfobacterium autotrophicum</i> (strain ATCC 43914 / DSM 3382 / HRM2)
A9A069; C0QAX6; B8FJV7	4; 2; 1	2; 0; 0	Carbon-monoxide dehydrogenase, catalytic subunit n=1 Tax= <i>Desulfococcus oleovorans</i> (strain DSM 6200 / Hxd3)
B8FGU7; A8ZZJ0; A0LLR3	8; 5; 2	4; 2; 0	Formate--tetrahydrofolate ligase n=1 Tax= <i>Desulfatibacillum alkenivorans</i> (strain AK-01)
B8FGX7; C0QGV2; A0LMX6	4; 2; 1	4; 2; 1	Extracellular ligand-binding receptor n=1 Tax= <i>Desulfatibacillum alkenivorans</i> (strain AK-01)
A6YCU3; Q8VRX4; Q8VRV3; A6ZJR5	7; 4; 1; 1	2; 1; 0; 1	AprA (Fragment) n=1 Tax= <i>Desulfonema magnum</i>
Protein identifications in the Amon MV dodecane sample			
A0LEH2	8	1	A0LEH2 60 kDa chaperonin 1 n=1 Tax= <i>Syntrophobacter fumaroxidans</i> (strain DSM 10017 / MPOB)
A0LIH6	2	1	A0LIH6 Elongation factor Tu n=1 Tax= <i>Syntrophobacter fumaroxidans</i> (strain DSM 10017 / MPOB)
A0LLG0	5	2	A0LLG0 ATP synthase subunit alpha n=1 Tax= <i>Syntrophobacter fumaroxidans</i> (strain DSM 10017 / MPOB)
A0LML7	6	1	A0LML7 K(+)-insensitive pyrophosphate-energized proton pump n=1 Tax= <i>Syntrophobacter fumaroxidans</i> (strain DSM 10017 / MPOB)
A6YQC9	4	1	A6YQC9 AprA (Fragment) n=1 Tax= <i>Desulfobacter postgatei</i>
A6YCW6	3	1	A6YCW6 AprA (Fragment) n=1 Tax= <i>Desulfocapsa thiozymogenes</i>
A6YCW8	2	1	A6YCW8 AprA (Fragment) n=1 Tax= <i>Desulfofustis glycolicus</i>
A6ZJR1	4	1	A6ZJR1 AprA (Fragment) n=1 Tax= <i>Desulfotignum</i> sp. DSM 7120
A8ZTP6	2	2	A8ZTP6 Glyceraldehyde-3-phosphate dehydrogenase, type I n=1 Tax= <i>Desulfococcus oleovorans</i> (strain DSM 6200 / Hxd3)
A8ZUA1	9	3	A8ZUA1 ATP synthase subunit beta n=1 Tax= <i>Desulfococcus oleovorans</i> (strain DSM 6200 / Hxd3)

Table SIII.3: continued

Protein IDs	Peptide Counts (all)	Peptide Counts (unique)	Protein Description
<i>Protein identifications in the Amon MV dodecane sample</i>			
A8ZWK1	2	1	A8ZWK1 Heterodisulfide reductase, subunit A (HdrA) n=1 Tax= <i>Desulfococcus oleovorans</i> (strain DSM 6200 / Hxd3)
A8ZWK2	6	1	A8ZWK2 Methyl-viologen-reducing hydrogenase delta subunit n=1 Tax= <i>Desulfococcus oleovorans</i> (strain DSM 6200 / Hxd3)
A9A068	2	1	A9A068 CO dehydrogenase/acetyl-CoA synthase complex, beta subunit n=1 Tax= <i>Desulfococcus oleovorans</i> (strain DSM 6200 / Hxd3)
A9A069	3	1	A9A069 Carbon-monoxide dehydrogenase, catalytic subunit n=1 Tax= <i>Desulfococcus oleovorans</i> (strain DSM 6200 / Hxd3)
B8FAG9	4	2	B8FAG9 Methyl-viologen-reducing hydrogenase delta subunit n=1 Tax= <i>Desulfatibacillum alkenivorans</i> (strain AK-01)
B8FGT4	8	1	B8FGT4 ATP synthase subunit beta n=1 Tax= <i>Desulfatibacillum alkenivorans</i> (strain AK-01)
B8FGT6	6	1	B8FGT6 ATP synthase subunit alpha n=1 Tax= <i>Desulfatibacillum alkenivorans</i> (strain AK-01)
B8FJ32	2	2	B8FJ32 Phosphoribosylaminoimidazolecarboxamide formyltransferase n=1 Tax= <i>Desulfatibacillum alkenivorans</i> (strain AK-01)
B8FM86	8	2	B8FM86 60 kDa chaperonin n=1 Tax= <i>Desulfatibacillum alkenivorans</i> (strain AK-01)
C0Q978	6	2	C0Q978 ATP synthase subunit beta 2 n=1 Tax= <i>Desulfobacterium autotrophicum</i> (strain ATCC 43914 / DSM 3382 / HRM2)
C0Q980	3	1	C0Q980 ATP synthase subunit alpha 2 n=1 Tax= <i>Desulfobacterium autotrophicum</i> (strain ATCC 43914 / DSM 3382 / HRM2)
C0QAI9	5	3	C0QAI9 CdhC n=1 Tax= <i>Desulfobacterium autotrophicum</i> (strain ATCC 43914 / DSM 3382 / HRM2)
C0QB00	3	3	C0QB00 PpaC n=1 Tax= <i>Desulfobacterium autotrophicum</i> (strain ATCC 43914 / DSM 3382 / HRM2)
C0QBT0	3	3	C0QBT0 MalE n=1 Tax= <i>Desulfobacterium autotrophicum</i> (strain ATCC 43914 / DSM 3382 / HRM2)
C0QGH3	3	2	C0QGH3 GdhA1 n=1 Tax= <i>Desulfobacterium autotrophicum</i> (strain ATCC 43914 / DSM 3382 / HRM2)
C0QHK6	3	3	C0QHK6 QmoB n=1 Tax= <i>Desulfobacterium autotrophicum</i> (strain ATCC 43914 / DSM 3382 / HRM2)
D1JEQ1	2	2	D1JEQ1 Phosphoenolpyruvate carboxykinase n=1 Tax=uncultured archaeon
D1JF51	2	1	D1JF51 K(+)-insensitive pyrophosphate-energized proton pump n=1 Tax=uncultured archaeon
D1JIT0	4	4	D1JIT0 Putative uncharacterized protein n=1 Tax=uncultured archaeon
D6PYL1	2	1	D6PYL1 Methyl-coenzyme M reductase alpha subunit (Fragment) n=1 Tax=uncultured archaeon
D6Z3H3	2	2	D6Z3H3 Flagellin domain protein n=1 Tax= <i>Desulfurivibrio alkaliphilus</i> (strain DSM 19089 / UNIQEM U267 / AHT2)
D6Z3M4	2	1	D6Z3M4 Elongation factor Tu n=1 Tax= <i>Desulfurivibrio alkaliphilus</i> (strain DSM 19089 / UNIQEM U267 / AHT2)
D6Z3N9	2	1	D6Z3N9 Methyl-viologen-reducing hydrogenase delta subunit n=1 Tax= <i>Desulfurivibrio alkaliphilus</i> (strain DSM 19089 / UNIQEM U267 / AHT2)
D6Z4V3	6	1	D6Z4V3 ATP synthase subunit alpha n=1 Tax= <i>Desulfurivibrio alkaliphilus</i> (strain DSM 19089 / UNIQEM U267 / AHT2)

Table SIII.3: continued

Protein IDs	Peptide Counts (all)	Peptide Counts (unique)	Protein Description
<i>Protein identifications in the Amon MV dodecane sample</i>			
E1YAW7	4	1	E1YAW7 Formate--tetrahydrofolate ligase n=1 Tax=uncultured <i>Desulfobacterium</i> sp.
E1YB73	15	6	E1YB73 60 kDa chaperonin n=1 Tax=uncultured <i>Desulfobacterium</i> sp.
E1YC93	5	4	E1YC93 Transcription termination factor Rho n=1 Tax=uncultured <i>Desulfobacterium</i> sp.
E1YEA8	2	1	E1YEA8 Chaperone protein clpB n=1 Tax=uncultured <i>Desulfobacterium</i> sp.
E1YG91	3	1	E1YG91 Elongation factor Tu n=1 Tax=uncultured <i>Desulfobacterium</i> sp.
E1YKR8	2	2	E1YKR8 Putative uncharacterized protein n=1 Tax=uncultured <i>Desulfobacterium</i> sp.
E1YL48	4	2	E1YL48 Carbon monoxide dehydrogenase 1 n=1 Tax=uncultured <i>Desulfobacterium</i> sp.
E1YM45	4	1	E1YM45 K(+)-insensitive pyrophosphate-energized proton pump n=1 Tax=uncultured <i>Desulfobacterium</i> sp.
Q2ABQ9	2	1	Q2ABQ9 Methyl-coenzyme M reductase alpha subunit (Fragment) n=1 Tax=uncultured archaeon
Q2LPJ8	5	1	Q2LPJ8 60 kDa chaperonin 1 n=1 Tax= <i>Syntrophus aciditrophicus</i> (strain SB)
Q2VP77	13	13	Q2VP77 Formate dehydrogenase like protein, alpha chain n=1 Tax=uncultured archaeon
Q2VP78	6	6	Q2VP78 Formate dehydrogenase like protein, beta chain n=1 Tax=uncultured archaeon
Q2VP80	10	10	Q2VP80 Heterodisulfide reductase, alpha subunit n=1 Tax=uncultured archaeon
Q2VP82	10	10	Q2VP82 Heterodisulfide reductase like protein, subunit A n=1 Tax=uncultured archaeon
Q2VP83	3	3	Q2VP83 Heterodisulfide reductase subunit B n=1 Tax=uncultured archaeon
Q2VP85	3	3	Q2VP85 Iron-sulfur binding reductase n=1 Tax=uncultured archaeon
Q2Y4E0	7	7	Q2Y4E0 Phosphate ABC transporter, phosphate-binding protein n=1 Tax=uncultured archaeon
Q2Y4Q6	2	2	Q2Y4Q6 Probable response regulator (CheY-like receiver domain and DNA-binding HTH domain) n=1 Tax=uncultured archaeon
Q648M4	6	6	Q648M4 F420H2 dehydrogenase subunit D (Fragment) n=1 Tax=uncultured archaeon GZfos37B2
Q648M5	2	2	Q648M5 F420H2 dehydrogenase subunit C n=1 Tax=uncultured archaeon GZfos37B2
Q648M6	3	3	Q648M6 F420H2 dehydrogenase subunit B n=1 Tax=uncultured archaeon GZfos37B2
Q648Y3	9	8	Q648Y3 Methyl coenzyme M reductase subunit alpha n=2 Tax=environmental samples
Q648Y4	13	6	Q648Y4 Methyl coenzyme M reductase subunit gamma n=2 Tax=environmental samples
Q648Y7	25	7	Q648Y7 Methyl-coenzyme M reductase subunit beta n=2 Tax=environmental samples
Q64AJ9	2	2	Q64AJ9 Glutamine synthetase n=1 Tax=uncultured archaeon GZfos31B6
Q64BJ1	23	5	Q64BJ1 Methyl coenzyme M reductase subunit beta n=1 Tax=uncultured archaeon GZfos27A8
Q64C60	6	6	Q64C60 N(5)N(10)-methenyltetrahydromethanopterin cyclohydrolase n=1 Tax=uncultured archaeon GZfos26B2
Q64C70	6	5	Q64C70 Methyl coenzyme M reductase subunit alpha n=1 Tax=uncultured archaeon GZfos26B2
Q64C71	13	6	Q64C71 Methyl coenzyme M reductase subunit gamma n=1 Tax=uncultured archaeon GZfos26B2
Q64DF6	2	1	Q64DF6 Putative uncharacterized protein (Fragment) n=1 Tax=uncultured archaeon GZfos18F2

Table SIII.3: continued

Protein IDs	Peptide Counts (all)	Peptide Counts (unique)	Protein Description
<i>Protein identifications in the Amon MV dodecane sample</i>			
Q6AQ10	5	2	Q6AQ10 ATP synthase subunit beta n=1 Tax= <i>Desulfotalea psychrophila</i>
Q6AQ12	5	1	Q6AQ12 ATP synthase subunit alpha n=1 Tax= <i>Desulfotalea psychrophila</i>
Q6ARV6	6	2	Q6ARV6 60 kDa chaperonin n=1 Tax= <i>Desulfotalea psychrophila</i>
Q75ND0	3	1	Q75ND0 Methyl-coenzyme M reductase alpha subunit (Fragment) n=1 Tax=uncultured archaeon
Q8VRY9	4	1	Q8VRY9 Adenosine-5'-phosphosulfate reductase alpha subunit (Fragment) n=1 Tax= <i>Desulfobacter curvatus</i>
B8FAH0; Q6AP89	3; 1	2; 1	B8FAH0 Heterodisulfide reductase, subunit A (HdrA) n=1 Tax= <i>Desulfatibacillum alkenivorans</i> (strain AK-01)
A8ZU48; Q2LU42	10; 2	2; 0	A8ZU48 60 kDa chaperonin n=1 Tax= <i>Desulfococcus oleovorans</i> (strain DSM 6200 / Hxd3)
E1YLG6; Q2LQZ7; Q31DL8	12; 2; 1	6; 0; 0	E1YLG6 ATP synthase subunit alpha n=1 Tax=uncultured <i>Desulfobacterium</i> sp.
E1YLG8; Q2LR05; A0LLF8	10; 4; 3	1; 0; 0	E1YLG8 ATP synthase subunit beta n=1 Tax=uncultured <i>Desulfobacterium</i> sp.
A8ZWK4; C0QKW1; E1YFW1; A0LH38	3; 1; 1; 1	3; 1; 1; 1	A8ZWK4 Sulfate adenylyltransferase n=1 Tax= <i>Desulfococcus oleovorans</i> (strain DSM 6200 / Hxd3)
Q64BJ5; Q64B88	9; 1	9; 1	Q64BJ5 Coenzyme F420-reducing hydrogenase beta subunit n=1 Tax=uncultured archaeon GZfos27A8
Q64BP6; Q64BN2	5; 1	5; 1	Q64BP6 Molybdenum formylmethanofuran dehydrogenase subunit (Fragment) n=1 Tax=uncultured archaeon GZfos27A8
E1YFV6; A6YCR9	6; 1	1; 0	E1YFV6 Putative uncharacterized protein n=1 Tax=uncultured <i>Desulfobacterium</i> sp.
E1YFV9; Q6AP88	8; 1	4; 0	E1YFV9 Putative uncharacterized protein n=1 Tax=uncultured <i>Desulfobacterium</i> sp.
E1YAG3; B8FDZ0	3; 1	3; 1	E1YAG3 Glutamine synthetase n=1 Tax=uncultured <i>Desulfobacterium</i> sp.
C0QKQ3; Q5PS44	7; 2	1; 0	C0QKQ3 60 kDa chaperonin n=1 Tax= <i>Desulfobacterium autotrophicum</i> (strain ATCC 43914 / DSM 3382 / HRM2)
B8FGX7; C0QGV2	3; 1	3; 1	B8FGX7 Extracellular ligand-binding receptor n=1 Tax= <i>Desulfatibacillum alkenivorans</i> (strain AK-01)
B8FLB6; Q2LUL1	7; 1	3; 0	B8FLB6 K(+)-insensitive pyrophosphate-energized proton pump n=1 Tax= <i>Desulfatibacillum alkenivorans</i> (strain AK-01)
D6Z5V7; Q6AJB1	2; 1	1; 1	D6Z5V7 Glutamate dehydrogenase (NADP(+)) n=1 Tax= <i>Desulfurivibrio alkaliphilus</i> (strain DSM 19089 / UNIQEM U267 / AHT2)
D6Z6P5; B8FB52	3; 2	2; 1	D6Z6P5 Sulfate adenylyltransferase n=1 Tax= <i>Desulfurivibrio alkaliphilus</i> (strain DSM 19089 / UNIQEM U267 / AHT2)
E1YBM0; A0LFG2	2; 1	2; 1	E1YBM0 Uncharacterized protein AF_1420 n=1 Tax=uncultured <i>Desulfobacterium</i> sp.
C0QAX6; B8FJV7	3; 2	1; 1	C0QAX6 CdhA n=1 Tax= <i>Desulfobacterium autotrophicum</i> (strain ATCC 43914 / DSM 3382 / HRM2)
C0QFH4; B8FA31	2; 1	2; 1	C0QFH4 PstS3 n=1 Tax= <i>Desulfobacterium autotrophicum</i> (strain ATCC 43914 / DSM 3382 / HRM2)
E1YL47; B8FJV8	4; 2	2; 1	E1YL47 Carbon monoxide dehydrogenase/acetyl-CoA synthase subunit alpha n=1 Tax=uncultured <i>Desulfobacterium</i> sp.
Q6VVF3; Q2ABR5	2; 2	1; 1	Q6VVF3 Methyl-coenzyme M reductase subunit alpha (Fragment) n=1 Tax=uncultured archaeon
Q2LTG7; D6Z680	7; 6	1; 1	Q2LTG7 60 kDa chaperonin 2 n=1 Tax= <i>Syntrophus aciditrophicus</i> (strain SB)
A6YCU3; Q8VRX4; A6ZJR5	8; 6; 2	2; 1; 1	A6YCU3 AprA (Fragment) n=1 Tax= <i>Desulfonema magnum</i>
A6YCU9; Q8VRY0; A6YCU5	4; 4; 3	1; 1; 1	A6YCU9 AprA (Fragment) n=1 Tax= <i>Desulfospira joergensenii</i>

Table SIII.3: continued

Protein IDs	Peptide Counts (all)	Peptide Counts (unique)	Protein Description
<i>Protein identifications in the Amon MV dodecane sample</i>			
B8FGU7; A8ZZJ0; A0LLR3	6; 3; 2	3; 1; 0	B8FGU7 Formate--tetrahydrofolate ligase n=1 Tax= <i>Desulfatibacillum alkenivorans</i> (strain AK-01)
D6Z3P1; D2DHP1; A6YCV7	4; 2; 2	1; 1; 1	D6Z3P1 Adenylylsulfate reductase, alpha subunit n=1 Tax= <i>Desulfurivibrio alkaliphilus</i> (strain DSM 19089 / UNIQEM U267 / AHT2)
A9ZRT0; A9ZRU5; A9ZRS5; A9ZRT5	2; 2; 1; 1	2; 2; 1; 1	A9ZRT0 Nitrogenase protein alpha chain n=1 Tax=uncultured archaeon
B1AAN6; B8FME3; Q6RCS6; Q93QV2	4; 3; 3; 3	1; 1; 1; 1	B1AAN6 Dissimilatory sulfite reductase alpha subunit (Fragment) n=1 Tax=uncultured <i>Desulfobacteraceae</i> bacterium
B8FAH1; A6YCV7; A6YCS8; A6YCR3	9; 6; 3; 2	1; 0; 0; 0	B8FAH1 Adenylylsulfate reductase, alpha subunit n=1 Tax= <i>Desulfatibacillum alkenivorans</i> (strain AK-01)
A6YCU7; Q8VRX5; A6YCT9; Q8VRW3; Q8VRV3	7; 4; 3; 3; 2	2; 1; 0; 0; 0	A6YCU7 AprA (Fragment) n=1 Tax= <i>Desulfosarcina variabilis</i>
A8ZYQ2; E1Y8M3; D6Z0E1; C0QAU0; A0LFZ1	2; 2; 1; 1; 1	2; 2; 1; 1; 1	A8ZYQ2 Putative uncharacterized protein n=1 Tax= <i>Desulfococcus oleovorans</i> (strain DSM 6200 / Hxd3)
Q8VRP9; O86975; Q8VRP7; Q8VRN9; Q93KK0	2; 2; 2; 2; 1	1; 1; 1; 1; 1	Q8VRP9 Dissimilatory sulfite reductase beta subunit (Fragment) n=1 Tax= <i>Desulfobacter postgatei</i>
A8ZUU2; C0Q9Y7; B8FET7; Q2LQA3; Q6AP73; Q6AP86; C0Q9X5	4; 2; 2; 1; 1; 1; 1	2; 1; 0; 0; 0; 0; 1	A8ZUU2 Elongation factor Tu n=1 Tax= <i>Desulfococcus oleovorans</i> (strain DSM 6200 / Hxd3)
A0LIZ6; C0QB13; B8FEA4; Q31JF1; Q6AJM3; Q2LWV6; D6Z157; A8ZTL6	3; 3; 2; 2; 2; 2; 1; 1	2; 2; 1; 1; 1; 1; 1; 1	A0LIZ6 Transcription termination factor Rho n=1 Tax= <i>Syntrophobacter fumaroxidans</i> (strain DSM 10017 / MPOB)
A8ZXC0; D6Z5B9; Q2LUK2; B8FLH6; Q31IL3; A0LEW2; Q6ALY6; C0QGV3; D1JA25; D1JG87	3; 2; 2; 2; 2; 2; 1; 1; 1; 1; 1	2; 1; 1; 1; 1; 0; 1; 0; 1; 1	A8ZXC0 ATPase AAA-2 domain protein n=1 Tax= <i>Desulfococcus oleovorans</i> (strain DSM 6200 / Hxd3)
B8FAH2; A8ZWJ9; E1YFV5; A6YCU2; A6YCR6; A6YCT6; A6YCU6; C0QHK9; A6ZJR2; A6YCV6	3; 2; 2; 2; 2; 2; 2; 2; 1; 1; 1	3; 2; 2; 2; 2; 2; 2; 2; 1; 1; 1	B8FAH2 Adenylylsulfate reductase, beta subunit n=1 Tax= <i>Desulfatibacillum alkenivorans</i> (strain AK-01)
A6YCY1; Q8VRT7; A6YCY5; A6YCY7; A6YCX3; A6YCY8; A6YCY3; Q8VRT1; Q8VRT4; Q8VRV4; Q8VRT9; Q8VRV0; Q8VRU0; Q8VRV9	2; 2; 1; 1; 1; 1; 1; 1; 1; 1; 1; 1; 1; 1; 1	1; 1; 0; 0; 1; 0; 0; 0; 0; 0; 0; 0; 0; 1; 0	A6YCY1 AprA (Fragment) n=1 Tax= <i>Desulfomonile tiedjei</i> DSM 6799
B1PVU3; Q9K5B5; Q937M5; Q93NW1; Q8RKE6; Q9ACL3; Q8GQH9; Q8GQI1; Q8GQI3; Q8GQI5; Q5ZQP1; C9EI34; Q5ZQR7; Q8VRQ0; Q93EW3; Q5ZQR5; Q5ZQN9; Q8VRP8; Q93TS0; Q7X500; Q93KP5; Q93NV9	4; 2; 2; 2; 1; 1; 1; 1; 1; 1; 1; 1; 1; 1; 1; 1; 1; 1; 1; 1; 1; 1; 1	1; 0	B1PVU3 Dissimilatory sulfite reductase alpha subunit (Fragment) n=1 Tax=uncultured <i>Desulfobacteraceae</i> bacterium

Table SIII.3: continued

Protein IDs	Peptide Counts (all)	Peptide Counts (unique)	Protein Description
<i>Protein identifications in the Guaymas Basin butane sample</i>			
A8ZU48	9	4	A8ZU48 60 kDa chaperonin n=1 Tax= <i>Desulfococcus oleovorans</i> (strain DSM 6200 / Hxd3)
A8ZUA1	5	3	A8ZUA1 ATP synthase subunit beta n=1 Tax= <i>Desulfococcus oleovorans</i> (strain DSM 6200 / Hxd3)
B8FAG9	3	2	B8FAG9 Methyl-viologen-reducing hydrogenase delta subunit n=1 Tax= <i>Desulfatibacillum alkenivorans</i> (strain AK-01)
B8FE33	2	2	B8FE33 General secretory pathway protein E n=1 Tax= <i>Desulfatibacillum alkenivorans</i> (strain AK-01)
B8FJ32	2	2	B8FJ32 Phosphoribosylaminoimidazolecarboxamide formyltransferase n=1 Tax= <i>Desulfatibacillum alkenivorans</i> (strain AK-01)
B8FJ79	2	2	B8FJ79 Acyl-CoA dehydrogenase domain protein n=1 Tax= <i>Desulfatibacillum alkenivorans</i> (strain AK-01)
C0Q8U0	2	2	C0Q8U0 Putative uncharacterized protein n=1 Tax= <i>Desulfobacterium autotrophicum</i> (strain ATCC 43914 / DSM 3382 / HRM2)
C0Q978	3	2	C0Q978 ATP synthase subunit beta 2 n=1 Tax= <i>Desulfobacterium autotrophicum</i> (strain ATCC 43914 / DSM 3382 / HRM2)
C0QAI9	4	2	C0QAI9 CdhC n=1 Tax= <i>Desulfobacterium autotrophicum</i> (strain ATCC 43914 / DSM 3382 / HRM2)
C0QB00	2	2	C0QB00 PpaC n=1 Tax= <i>Desulfobacterium autotrophicum</i> (strain ATCC 43914 / DSM 3382 / HRM2)
C0QHK6	2	2	C0QHK6 QmoB n=1 Tax= <i>Desulfobacterium autotrophicum</i> (strain ATCC 43914 / DSM 3382 / HRM2)
C0QKQ3	8	3	C0QKQ3 60 kDa chaperonin n=1 Tax= <i>Desulfobacterium autotrophicum</i> (strain ATCC 43914 / DSM 3382 / HRM2)
D1JF51	3	2	D1JF51 K(+)-insensitive pyrophosphate-energized proton pump n=1 Tax=uncultured archaeon
D1JIT0	2	2	D1JIT0 Putative uncharacterized protein n=1 Tax=uncultured archaeon
D6Z3H3	2	2	D6Z3H3 Flagellin domain protein n=1 Tax= <i>Desulfurivibrio alkaliphilus</i> (strain DSM 19089 / UNIQEM U267 / AHT2)
E1YB73	13	7	E1YB73 60 kDa chaperonin n=1 Tax=uncultured <i>Desulfobacterium</i> sp.
E1YC93	2	2	E1YC93 Transcription termination factor Rho n=1 Tax=uncultured <i>Desulfobacterium</i> sp.
E1YFV9	3	2	E1YFV9 Putative uncharacterized protein n=1 Tax=uncultured <i>Desulfobacterium</i> sp.
E1YL47	5	2	E1YL47 Carbon monoxide dehydrogenase/acetyl-CoA synthase subunit alpha n=1 Tax=uncultured <i>Desulfobacterium</i> sp.
E1YLG6	11	6	E1YLG6 ATP synthase subunit alpha n=1 Tax=uncultured <i>Desulfobacterium</i> sp.
Q2VP77	2	2	Q2VP77 Formate dehydrogenase like protein, alpha chain n=1 Tax=uncultured archaeon
Q2VP78	4	4	Q2VP78 Formate dehydrogenase like protein, beta chain n=1 Tax=uncultured archaeon
Q2VP80	6	6	Q2VP80 Heterodisulfide reductase, alpha subunit n=1 Tax=uncultured archaeon
Q2VP82	3	3	Q2VP82 Heterodisulfide reductase like protein, subunit A n=1 Tax=uncultured archaeon
Q2Y4E0	7	7	Q2Y4E0 Phosphate ABC transporter, phosphate-binding protein n=1 Tax=uncultured archaeon
Q2Y4L6	2	2	Q2Y4L6 Putative uncharacterized protein n=1 Tax=uncultured archaeon
Q2Y4Q6	2	2	Q2Y4Q6 Probable response regulator (CheY-like receiver domain and DNA-binding HTH domain) n=1 Tax=uncultured archaeon
Q31DM0	2	2	Q31DM0 ATP synthase subunit beta n=1 Tax= <i>Thiomicrospira crumogena</i> (strain XCL-2)
Q31FJ5	2	2	Q31FJ5 OmpA/MotB family protein n=1 Tax= <i>Thiomicrospira crumogena</i> (strain XCL-2)
Q31I24	5	5	Q31I24 Thiosulfate-binding protein SoxY n=1 Tax= <i>Thiomicrospira crumogena</i> (strain XCL-2)

Table SIII.3: continued

Protein IDs	Peptide Counts (all)	Peptide Counts (unique)	Protein Description
<i>Protein identifications in the Guaymas Basin butane sample</i>			
Q31JN1	4	4	Q31JN1 Putative uncharacterized protein n=1 Tax= <i>Thiomicrospira crunogena</i> (strain XCL-2)
Q648G0	2	2	Q648G0 Putative uncharacterized protein n=1 Tax=uncultured archaeon GZfos3D4
Q648M4	2	2	Q648M4 F420H2 dehydrogenase subunit D (Fragment) n=1 Tax=uncultured archaeon GZfos37B2
Q648Y3	8	6	Q648Y3 Methyl coenzyme M reductase subunit alpha n=2 Tax=environmental samples
Q648Y4	7	3	Q648Y4 Methyl coenzyme M reductase subunit gamma n=2 Tax=environmental samples
Q648Y7	21	5	Q648Y7 Methyl-coenzyme M reductase subunit beta n=2 Tax=environmental samples
Q64BJ1	19	3	Q64BJ1 Methyl coenzyme M reductase subunit beta n=1 Tax=uncultured archaeon GZfos27A8
Q64C60	5	5	Q64C60 N(5)N(10)-methenyltetrahydromethanopterin cyclohydrolase n=1 Tax=uncultured archaeon GZfos26B2
Q64C70	3	2	Q64C70 Methyl coenzyme M reductase subunit alpha n=1 Tax=uncultured archaeon GZfos26B2
Q64CF0	4	2	Q64CF0 Putative uncharacterized protein n=1 Tax=uncultured archaeon GZfos23H9
Q6ARV6	4	2	Q6ARV6 60 kDa chaperonin n=1 Tax= <i>Desulfotalea</i> <i>psychrophila</i>
B8FGX7; C0QGV2	3; 1	3; 1	B8FGX7 Extracellular ligand-binding receptor n=1 Tax= <i>Desulfatibacillum alkenivorans</i> (strain AK-01)
E1YAG3; B8FDZ0	3; 1	3; 1	E1YAG3 Glutamine synthetase n=1 Tax=uncultured <i>Desulfobacterium</i> sp.
C0QFH4; B8FA31	2; 1	2; 1	C0QFH4 PstS3 n=1 Tax= <i>Desulfobacterium autotrophicum</i> (strain ATCC 43914 / DSM 3382 / HRM2)
A8ZXZ6; B8FLB6	8; 6	4; 4	A8ZXZ6 K(+)-insensitive pyrophosphate-energized proton pump n=1 Tax= <i>Desulfococcus oleovorans</i> (strain DSM 6200 / Hxd3)
E1YLG8; B8FGT4	6; 4	2; 2	E1YLG8 ATP synthase subunit beta n=1 Tax=uncultured <i>Desulfobacterium</i> sp.
Q31FM9; Q31FM8	12; 6	12; 6	Q31FM9 Flagellin n=1 Tax= <i>Thiomicrospira crunogena</i> (strain XCL-2)
Q64BP6; Q64BN2	2; 1	2; 1	Q64BP6 Molybdenum formylmethanofuran dehydrogenase subunit (Fragment) n=1 Tax=uncultured archaeon GZfos27A8
C0QIP7; E1YHN8; B8FMV8	2; 1; 1	2; 1; 1	C0QIP7 Pyruvate-flavodoxin oxidoreductase n=1 Tax= <i>Desulfobacterium autotrophicum</i> (strain ATCC 43914 / DSM 3382 / HRM2)
E1YCZ8; C0QJX2; A0LL46	2; 1; 1	2; 1; 1	E1YCZ8 Putative uncharacterized protein n=1 Tax=uncultured <i>Desulfobacterium</i> sp.
E1YL45; C0QAI7; A9A066	2; 1; 1	2; 1; 1	E1YL45 Putative uncharacterized protein n=1 Tax=uncultured <i>Desulfobacterium</i> sp.
Q2Y520; Q64D95; Q64CS3	3; 2; 2	3; 2; 2	Q2Y520 Thermosome subunit n=1 Tax=uncultured archaeon
Q64E03; Q64EA1; Q64D16	5; 5; 1	3; 3; 0	Q64E03 Methyl coenzyme M reductase subunit alpha n=2 Tax=environmental samples
Q6AN73; D6Z6P5; B8FB52	2; 1; 1	2; 1; 1	Q6AN73 Probable sulfate adenyltransferase n=1 Tax= <i>Desulfotalea psychrophila</i>
B8FGU7; A8ZZJ0; A0LLR3; Q64DF6	5; 3; 2; 2	2; 1; 0; 1	B8FGU7 Formate--tetrahydrofolate ligase n=1 Tax= <i>Desulfatibacillum alkenivorans</i> (strain AK-01)
A6YCU3; B8FAH1; A6YQC7; Q8VRX4; A6ZJR5	3; 2; 2; 2; 1	2; 1; 1; 1; 1	A6YCU3 AprA (Fragment) n=1 Tax= <i>Desulfonema magnum</i>
E1YDX7; B8FGS3; A8ZRW3; D6Z5B5; Q6AMQ3	3; 2; 1; 1; 1	2; 1; 0; 0; 0	E1YDX7 Chaperone protein dnaK n=1 Tax=uncultured <i>Desulfobacterium</i> sp.
D1JI94; Q649L2; Q64EC5; Q64A42; Q64E68; Q649Y4; Q648M3	3; 3; 3; 3; 3; 2; 2	3; 3; 3; 3; 3; 2; 2	D1JI94 Tetrahydromethanopterin S-methyltransferase, subunit H n=1 Tax=uncultured archaeon

Table III.3: continued

Protein IDs	Peptide Counts (all)	Peptide Counts (unique)	Protein Description
<i>Protein identifications in the Guaymas Basin dodecane sample</i>			
A8ZXZ6; B8FLB6	5; 4	2; 2	A8ZXZ6 K(+)-insensitive pyrophosphate-energized proton pump n=1 Tax= <i>Desulfococcus oleovorans</i> (strain DSM 6200 / Hxd3)
Q5XQ95; Q64D58; Q647V3; Q64B47; Q649P7; Q64CB0; Q64DM9; Q6MZC4; Q64AM8	2; 2; 2; 2; 2; 2; 2; 2; 2	2; 2; 2; 2; 2; 2; 2; 2	Q5XQ95 Proteasome subunit alpha n=1 Tax=uncultured archaeon GZfos26D8
Q648Y4; Q64C71	2; 2	2; 2	Q648Y4 Methyl coenzyme M reductase subunit gamma n=2 Tax=environmental samples
Q648Y7; Q64BJ1	7; 6	7; 6	Q648Y7 Methyl-coenzyme M reductase subunit beta n=2 Tax=environmental samples
Q649Z7; Q648C7; Q64D18; Q6MZD3; Q64AN5; Q64EF3; Q64EA3; Q64E05; D1JBK2; Q64CB9	2; 2; 2; 2; 2; 2; 2; 1; 1; 1	2; 2; 2; 2; 2; 2; 2; 1; 1; 1	Q649Z7 Methyl coenzyme M reductase subunit beta n=1 Tax=uncultured archaeon GZfos33H6
Q64CF0; D1JGR9; D1JBF2	3; 2; 1	3; 2; 1	Q64CF0 Putative uncharacterized protein n=1 Tax=uncultured archaeon GZfos23H9
Q64E03; Q64EA1; Q648C5; Q64D16 Q64EN9; D1JFA8	5; 5; 1; 1 2; 1	4; 4; 1; 1 2; 1	Q64E03 Methyl coenzyme M reductase subunit alpha n=2 Tax=environmental samples Q64EN9 Putative uncharacterized protein n=1 Tax=uncultured archaeon GZfos10C7
D1JI94; Q649L2; Q649Y4; Q64EC5; Q64A42; Q64E68; Q648M3	3; 3; 3; 3; 3; 2; 1	3; 3; 3; 3; 3; 2; 1	D1JI94 Tetrahydromethanopterin S-methyltransferase, subunit H n=1 Tax=uncultured archaeon
D1JID5; D1JF16; D1JFD7; D1JFF4	2; 1; 1; 1	2; 1; 1; 1	D1JID5 Thermosome, beta subunit n=1 Tax=uncultured archaeon
D6NIW8; B1PVU7; B6VHH8; Q6VVE7; Q5IEN1; A9ZRV3; Q5IEM9; D6NIU9; D6NIV8; D6NIV9; D6NIW0; D6NIW9; Q5IEN0; Q2ABR3; Q2ABQ4; A8KNR2; A8KNS7; C9DFT6; A8KNL6; A8KNU0; E5RQ44; E5RQ45; E5RQ47	2; 1	1; 0; 0; 0; 1; 0; 1; 1; 1; 1; 1; 1; 1; 0; 0; 1; 1; 1; 1; 1; 1; 1; 1	D6NIW8 Methyl coenzyme M reductase subunit A (Fragment) n=1 Tax=uncultured archaeon
D6Z4V1; B8FGT4; Q6AQ10; Q2LR05; A0LLF8	3; 2; 2; 2; 1	1; 0; 1; 0; 0	D6Z4V1 ATP synthase subunit beta n=1 Tax= <i>Desulfurivibrio alkaliphilus</i> (strain DSM 19089 / UNIQEM U267 / AHT2)
E1YLG8; A8ZUA1	3; 2	1; 1	E1YLG8 ATP synthase subunit beta n=1 Tax=uncultured <i>Desulfobacterium</i> sp.

Table SIII.4: Identified and labeled proteins and peptides in SIP-incubations. Protein IDs (protein group) contains the Uniprot Accession of the identified protein. If peptide identifications could be explained by different protein identifications, several proteins were grouped together, but the first is the most probable one. Majority Protein ID reduces the Protein IDs column to the most probable protein identifications. Assumed Function gives the function and Taxonomy the taxonomy given by Uniprot, both for the first protein accession. Labeled Peptides contains the peptide sequences found to be labeled with the relative isotope abundances (RIA) and labeling ratios (LR) at the different time points (T1, T2, T3).

Protein IDs	Majority Protein ID	Assumed Function	Taxonomy				
Labeled Peptides	RIA T1 (%)	RIA T2 (%)	RIA T3 (%)	LR T1	LR T2	LR T3	
<i>Identified labeled proteins and peptides in the Amon MV butane sample</i>							
A6YCU3;Q8VRX4;Q8VRV3;A6ZJR5	A6YCU3;Q8VRX4	adenylsulfate reductase subunit alpha	<i>Desulfonema magnum</i>				
	LALGEENILER	57.6		0.01			
	NDLMGLVR	51.3	50.9	0.08	0.07		
	IWTVEAHLR	50.8	53.0	0.10	0.17	0.22	
	SGAVAQGLSAINTYIGENTPDD	49.1	51.0	0.29	0.45	0.64	
	GPILMDTVTALAELGK	58.0	59.2	0.38	0.33		
	AVRDPEVEER		50.8		0.06	0.14	
A6YCU7;Q8VRX5;Q8VRW3;A6YCT9	A6YCU7;Q8VRX5;Q8VRW3	Adenosine-5'-phosphosulfate reductase alpha subunit	<i>Desulfobacteraceae</i>				
	VGAELTMMENR	48.5		0.05			
	EELVDLIYKPVR	52.2	54.3	0.25	0.36	0.67	
A8ZWK4;E1YFW1;C0QKW1	A8ZWK4	Sulfate adenyltransferase	<i>Desulfococcus oleovorans</i> (strain DSM 6200 / Hxd3)				
	ALLCTPLK	53.7	55.1	0.24	0.36	0.60	
	GLSEGTPIPDHFR	49.7	52.3	0.27	0.33	0.62	
C0QD63;Q9K5B4;A8ZX94;Q8RKE5;O69400;B1PVU2;B1PVU4;Q8VRP9;O86971;O86975;Q5ZQR4;Q93EW2;Q5ZQN8;Q8VRS9;Q8VRP7;Q8VRP5;Q8GQI8;Q8VRN9;Q8VRP3;Q93EW0;Q8VRQ3;Q93KJ9	C0QD63;Q9K5B4	Dissimilatory sulfite reductase subunit B	<i>Desulfobacteraceae</i>				
	VVVAFLPNEMPR	51.0	53.5	55.5	0.29	0.39	0.56
	A9A067	CO dehydrogenase/acetyl-CoA synthase delta subunit	<i>Desulfococcus oleovorans</i> (strain DSM 6200 / Hxd3)				
	VPSWLLIK	54.1	55.5	56.7	0.30	0.35	0.50
	A9A068	CO dehydrogenase/acetyl-CoA synthase complex, beta subur	<i>Desulfococcus oleovorans</i> (strain DSM 6200 / Hxd3)				
	EFQEDFEPILER	50.3	51.1	54.1	0.33	0.45	0.59
	E1YL47	CO dehydrogenase/acetyl-CoA synthase subunit alpha	uncultured <i>Desulfobacterium</i> sp. (N47)				
	FTTLAGVMGGGASSPGFVGHS	46.1	47.9	50.4	0.26	0.41	0.51
	GADLYCQMGGGK	47.1	46.8	49.2	0.50	0.58	0.61
A9A069;C0QAX6;B8FJV7	A9A069;C0QAX6	CO dehydrogenase, catalytic subunit	<i>Desulfobacteraceae</i>				
	ILLAATEVVK	55.4	56.9	58.9	0.16	0.28	0.49
	GVAGVVCNNAR		48.1			0.35	

Table SIII.4: continued

Protein IDs	Majority Protein ID	Assumed Function			Taxonomy		
	Labeled Peptides	RIA T1 (%)	RIA T2 (%)	RIA T3 (%)	LR T1	LR T2	LR T3
<i>Identified labeled proteins and peptides in the Amon MV butane sample</i>							
	C0QA19	bifunctional acetyl-CoA decarboxylase/synthase complex subunit			<i>Desulfobacterium autotrophicum</i> (strain ATCC 43914 / DSM		
	GVNDFVYK	48.9	50.5	54.7	0.27	0.53	0.66
	AAFEINPTGPNQPIEK	48.9	50.3	52.7	0.17	0.43	0.49
	FILGDGGLLR	52.6	53.4	55.2	0.23	0.43	0.56
	LIAFAAIQGGYK	52.4	53.7	56.6	0.27	0.33	0.56
	A8ZU48	60 kDa chaperonin			<i>Desulfococcus oleovorans</i> (strain DSM 6200 / Hxd3)		
	SWGSPVTK	47.0	49.0	50.9	0.26	0.31	0.38
	GYLSPYFVTDAEK	47.7	48.8	51.5	0.55	0.61	0.73
	B8FM86	60 kDa chaperonin			<i>Desulfatibacillum alkenivorans</i> (strain AK-01)		
	GYISPYFVTDSEK	48.9	50.5	54.7	0.27	0.53	0.66
E1YB73;Q5PS44	E1YB73	60 kDa chaperonin			uncultured <i>Desulfobacterium</i> sp. (N47)		
	ARVEDALNATR	45.0	47.7	51.2	0.20	0.25	0.29
	EGVITVEEAK	50.6	53.1	56.1	0.20	0.20	0.36
	EIELEDKFENMGAQMVK	48.7	50.7	56.5	0.25	0.31	0.38
	AAVEEGIVPGGVALVR	48.4	49.9	53.5	0.26	0.31	0.44
	AQIEETTSYDR	46.5		50.8	0.37		0.52
	AQIEETTSYDREK	46.8	48.9	51.8	0.48	0.53	0.60
	VGKEGVITVEEAK		52.9	54.7		0.11	0.21
	GIDKAIEVAVK		55.1	57.3		0.71	0.81
	Q2LTG7	60 kDa chaperonin			<i>Syntrophus aciditrophicus</i> (strain SB)		
	DLLPILEQIAK	55.4	58.2	60.3	0.24	0.43	0.45
	AQIDETTSYDR	45.2	47.5	50.7	0.52	0.65	0.75
	AQIDETTSYDREK	45.4	47.7	50.9	0.56	0.65	0.69
	Q6ARV6	60 kDa chaperonin			<i>Desulfotalea psychrophila</i>		
	EIAQVGTISANSDETIGNIIAEAI	52.8	54.2	57.4	0.57	0.64	0.77
E1YLG6;Q2LQZ7	E1YLG6	ATP synthase subunit alpha			uncultured <i>Desulfobacterium</i> sp. (N47)		
	VVSAVGEPIDGK	51.0		54.6	0.04		0.12
	VEMVAPGVIAR	49.2		54.2	0.09		0.16
	VELSETGVVLSVGDGIAR			54.2	0.11		
	STVAQVVSVLEK	50.9	53.2	56.0	0.30	0.45	0.66
	KSTVAQVVSVLEK			55.4			0.65
	E1YLG8	ATP synthase subunit beta			uncultured <i>Desulfobacterium</i> sp. (N47)		
	VIDLLVPFPR	51.7	55.1	57.6	0.01	0.03	0.08
	FTQAGSEVSALLGR	49.3	51.8	53.5	0.04	0.05	0.17
	MPSAVGYQPTLAVDLGELQER	49.9	51.9	54.4	0.06	0.06	0.24

Table SIII.4: continued

Protein IDs	Majority Protein ID Labeled Peptides	Assumed Function			Taxonomy		
		RIA T1 (%)	RIA T2 (%)	RIA T3 (%)	LR T1	LR T2	LR T3
<i>Identified labeled proteins and peptides in the Amon MV butane sample</i>							
	A8ZTP6	Glyceraldehyde-3-phosphate dehydrogenase, type I			<i>Desulfococcus oleovorans</i> (strain DSM 6200 / Hxd3)		
	AAALSMIPTTTGAAK			53.7			0.38
A8ZYD0;C0Q9B0	A8ZYD0;C0Q9B0	D-3-phosphoglycerate dehydrogenase			<i>Desulfobacteraceae</i>		
	SDYITHVPK	52.0	54.1	56.8	0.44	0.59	0.71
B8FLC2;A8ZXY9;E1YM39	B8FLC2;A8ZXY9;E1YM39	D-3-phosphoglycerate dehydrogenase			<i>Desulfobacteraceae</i>		
	AGIGLDNVDIPAATK		53.3	56.1		0.49	0.65
A8ZVJ1;D6Z269	A8ZVJ1;D6Z269	Malate dehydrogenase			<i>Desulfococcus oleovorans</i> (strain DSM 6200 / Hxd3);		
	VIGMAGVLSAR	49.2	51.3	53.9	0.16	0.35	0.53
A8ZY46;A9A014;C0QL21;B8F C57	A8ZY46;A9A014;C0QL21;B8F C57	Acetoacetyl-CoA synthase			<i>Desulfobacteraceae</i>		
	SDATLNPGGVR		50.5	51.8		0.19	0.26
	LNFAENLLR			54.6			0.29
E1YE68;B8FLW5;C0QLF7;E1 Y9M2;A8ZRW8;A0LFF9;Q0W 662	E1YE68;B8FLW5;C0QLF7;E1 Y9M2	Pyruvate carboxylase subunit			<i>Desulfobacteraceae</i>		
	TPFSMLLR			53.1			0.60
	E1YFJ9	3-isopropylmalate dehydrogenase			uncultured <i>Desulfobacterium</i> sp. (N47)		
	LYEGVETPIK	50.2	53.3	54.9	0.32	0.52	0.69
E1YC93;C0QB13;Q31JF1	E1YC93	Transcription termination factor Rho			uncultured <i>Desulfobacterium</i> sp. (N47)		
	GLIVSPPR	50.4	54.5	56.1	0.03	0.07	0.16
	ILSGGVDSNALQRPK	49.9		53.5	0.07		0.14
	VEAVNYEDPEIAR	47.4		53.9	0.41		0.65
	B8FAG9	Methyl-viologen-reducing hydrogenase delta subunit			<i>Desulfatibacillum alkenivorans</i> (strain AK-01)		
	TPGLSENFYK	49.4	51.2	54.8	0.34	0.44	0.62
B8FGU7;A8ZZJ0;A0LLR3	B8FGU7;A8ZZJ0	Formate--tetrahydrofolate ligase			<i>Desulfobacteraceae</i>		
	DVLIYSGAK	53.6	54.9	57.0	0.21	0.43	0.59
	YIEVTAITPTPLGEGK	52.5	54.9	57.4	0.23	0.42	0.61
	FSGLKPHVSVLTSTIR	49.4	52.3	54.7	0.24	0.39	0.62
	AGINPVVCINR	51.8	54.4	57.4	0.31	0.42	0.70
	E1YAW7	Formate tetrahydrofolate ligase			uncultured <i>Desulfobacterium</i> sp. (N47)		
	LDEITVAFDK			57.9			0.64
	RLDEITVAFDK	51.8	52.7	56.9	0.24	0.36	0.55
	GWTLPIRDVLIYSGAK	50.9	53.9	56.8	0.26	0.44	0.60

Table SIII.4: continued

Protein IDs	Majority Protein ID Labeled Peptides	Assumed Function RIA T1 (%)	RIA T2 (%)	RIA T3 (%)	Taxonomy LR T1	LR T2	LR T3
<i>Identified labeled proteins and peptides in the Amon MV butane sample</i>							
E1YL45;C0QAI7;A9A066	E1YL45	Methyltransferase			uncultured <i>Desulfobacterium</i> sp. (N47)		
	GMDYIDINLGPAK	51.3	54.2	58.3	0.15	0.27	0.49
	DPKPIQEEALFQK	50.9	50.7	55.1	0.20	0.34	0.52
	TLYSDSWLEV	45.5	49.5	52.4	0.30	0.41	0.52
	C0QHK6	heterodisulfide reductase subunit A			<i>Desulfobacterium autotrophicum</i> (strain ATCC 43914 / DSM		
	IAGQPGEFTVTFK	49.2	51.6	54.7	0.32	0.32	0.60
	ILVLGGGITGISAALDAAK	53.9		57.0	0.34		0.55
E1Y816;A8ZTQ4;B8FLE5	E1Y816;A8ZTQ4;B8FLE5	Bifunctional protein fold			<i>Desulfobacteraceae</i>		
	VLNAIDPDKDVDGFHPVNVGR	50.1	53.0	55.1	0.20	0.35	0.55
	AGVETSGAEVVVGR			53.9			0.54
B8FLB6;Q2LUL1	B8FLB6	K(+)-insensitive pyrophosphate-energized proton pump			<i>Desulfatibacillum alkenivorans</i> (strain AK-01)		
	KYIEDGHLGGK	51.9	54.2		0.14	0.31	
	YIEDGHLGGK	52.9	55.0		0.14	0.28	
	VSVIANVR	55.8	58.0	60.2	0.14	0.23	0.39
	AVTDPLDAVGNTTK	54.2	56.4	58.9	0.16	0.29	0.46
	LGGGIFTK	52.3	54.6	57.5	0.22	0.33	0.50
	VEAGIPEDDPR	50.7	53.1	55.5	0.26	0.41	0.55
	GADVADLVGK	49.5	51.6	54.4	0.26	0.43	0.59
<i>Identified labeled proteins and peptides in the Amon MV dodecane sample</i>							
A6YCU7;Q8VRX5;A6YCT9;Q8VRW3;Q8VRV3;A6YCU3;Q8VRX4		Adenosine-5'-phosphosulfate reductase alpha subunit			<i>Desulfobacteraceae</i>		
	TMMVACGGAVNIYQPR		60.9			0.09	
A6ZJR1		Adenosine-5'-phosphosulfate reductase alpha subunit			<i>Desulfotignum</i> sp. DSM 7120		
	YAPYGTAAALTPCLR		62.3			0.08	

Table SIII.4: continued

Protein IDs	Majority Protein ID Labeled Peptides	Assumed Function RIA T1 (%)	RIA T2 (%)	RIA T3 (%)	Taxonomy LR T1	LR T2	LR T3
<i>Identified labeled proteins and peptides in the Amon MV dodecane sample</i>							
B1PVU3;B1AAN6		Dissimilatory sulfite reductase alpha subunit			uncultured <i>Desulfobacterium</i> sp.		
	DWGPFDIQK		57.3			0.05	
C0QD63;Q9K5B4		Sulfite reductase, dissimilatory-type beta subunit			<i>Desulfobacteraceae</i>		
	VVVAFLPNEMPR		47.2			0.04	
B8FAH1;A6YCQ7;A6YCS8;A6YCR3;A6YCR1;Q8VRU1;A6YCU9;Q8VRY0;A6YCU5;Q8VRY9;A6YCQ9		Adenylylsulfate reductase, alpha subunit			<i>Desulfobacteraceae</i>		
	EDLIFDLGR		66.3			0.45	
	E1YFV6	Adenylylsulfate reductase, alpha subunit			<i>Desulfobacterium</i>		
	ATHEYGAGTATYYQTSSK	59.0	60.9		0.34	0.43	
B8FAH2;A8ZWJ9;E1YFV5;A6YCU2;A6YCR6;A6YCT6;A6YCU6		Adenylylsulfate reductase, beta subunit			<i>Desulfobacteraceae</i>		
	ICPTQAIIEVR	58.4	64.8	59.2	0.04	0.09	0.04
	AYNQEPDQCWECFSCVK		61.9			0.07	
C0QAI9;A9A068;E1YL47;B8FJV8		Carbon monoxide dehydrogenase / acetyl-CoA synthase subunit			<i>Desulfobacteraceae</i>		
	DIGVVLHAK	42.4	54.0		0.07	0.03	
E1YL47;B8FJV8		Carbon monoxide dehydrogenase/acetyl-CoA synthase subunit			<i>Desulfobacteraceae</i>		
	ASFEINPTGPNQPIEK	40.6	60.9		0.35	0.24	
	A8ZU48	60 kDa chaperonin			<i>Desulfococcus oleovorans</i> (strain DSM 6200 / Hxd3)		
	AQIEDTTSYDREK	61.3	63.4	57.7	0.83	0.94	0.73
	GYLSPYFVTDAEK	63.2	63.7		0.28	0.63	
	E1YB73	60 kDa chaperonin			uncultured <i>Desulfobacterium</i> sp.		
	LVAAGNNPMAIK	45.1	43.8		0.03	0.02	
	TSDMAGDGTATVTLAR	57.7	60.0		0.04	0.11	
	EGVITVEEAK	57.9	65.8	57.9	0.07	0.20	0.06
	AAVEEGIVPGGGVALVR	66.1	68.0	66.1	0.03	0.14	0.03
	AMLEDLAILTGGQVVSEDIGVF		58.2			0.12	

Table SIII.4: continued

Protein IDs	Majority Protein ID Labeled Peptides	Assumed Function RIA T1 (%)	RIA T2 (%)	RIA T3 (%)	Taxonomy LR T1	LR T2	LR T3
<i>Identified labeled proteins and peptides in the Amon MV dodecane sample</i>							
	Q6ARV6	60 kDa chaperonin			<i>Desulfotalea psychrophila</i>		
	DLLPVLEQVAK	69.4	71.5		0.37	0.68	
	A0LLG0	ATP synthase subunit alpha			<i>Syntrophobacter fumaroxidans</i> (strain DSM 10017 / MPOB)		
	VEVIAPGVIAR	67.2	68.5		0.12	0.46	
	E1YLG6	subunit alpha			<i>Desulfobacterium</i>		
	STVAQVVSVLEK	44.3	48.2		0.12	0.06	
	KVELSETGVVLSVGDGIAR		68.6			0.05	
	EAYPGDIFYNHSR		60.4			0.31	
	AEEISQIIK		69.1			0.06	
E1YLG8;Q2LR05;A0LLF8;A8 ZUA1;B8FGT4		ATP synthase subunit beta			<i>Desulfobacteraceae</i>		
	VIDLLVPFPR	63.1	66.6		0.02	0.05	
A8ZUA1;B8FGT4		ATP synthase subunit beta			<i>Desulfobacteraceae</i>		
	TIAMDVTDLVLR	56.3	60.0		0.40	0.59	
	C0QGH3	Glutamate dehydrogenase			<i>Desulfobacterium autotrophicum</i> (strain ATCC 43914 / DSM		
	IEMNSAIGPYK		64.2			0.11	
	FLAFEQVFK		66.2			0.15	
	B8FGU7	Formate--tetrahydrofolate ligase			<i>Desulfatibacillum alkenivorans</i> (strain AK-01)		
	FSGLKPHVSVLTSTIR		61.2			0.11	
	C0QHK6	Heterodisulfide reductase subunit A			<i>Desulfobacterium autotrophicum</i> (strain ATCC 43914 / DSM		
	TPGLQENFYK	61.7	66.9		0.24	0.33	0.00
A8ZUU2;C0Q9Y7;B8FET7;Q2 LQA3;Q6AP73;Q6AP86;E1YG 91;D6Z3M4;A0LIH6		Elongation factor Tu			<i>Desulfobacteraceae</i>		
	HYAHVDCPGHADYIK		60.0			0.07	
	B8FGX7	Extracellular ligand-binding receptor			<i>Desulfatibacillum alkenivorans</i> (strain AK-01)		
	IGINAPITGDIPK	63.7			0.05		
	AAVLYDVASDYPK	64.7	64.6		0.03	0.12	
	A0LML7	K(+)-insensitive pyrophosphate-energized proton pump			<i>Syntrophobacter fumaroxidans</i> (strain DSM 10017 / MPOB)		
	AAVTGDTVGDYPYKDTAGPAIN	38.6	58.9	54.1	0.24	0.23	0.22
	DTAGPAINPMIK	43.9			0.18		
	B8FLB6	K(+)-insensitive pyrophosphate-energized proton pump			<i>Desulfatibacillum alkenivorans</i> (strain AK-01)		
	VEAGIPEDDPR	48.3	62.6	58.8	0.21	0.25	0.20
	AAVTGDTVGDYPYK	51.7	59.1	53.0	0.06	0.36	0.24
	AVTDPLDAVGNTTK	54.1	60.2	53.3	0.54	0.65	0.48
	GADVGADLVGK	55.1	60.1	52.3	0.25	0.31	0.19
	AAVTGDTVGDYPYKDTAGPAV1	59.7	61.3		0.71	0.87	

Table SIII.4: continued

Protein IDs	Majority Protein ID Labeled Peptides	Assumed Function			Taxonomy		
		RIA T1 (%)	RIA T2 (%)	RIA T3 (%)	LR T1	LR T2	LR T3
<i>Identified labeled proteins and peptides in the Guaymas Basin butane sample</i>							
B8FAH2;A8ZJ9;E1YFV5;A6YCU2;A6YCR6;A6YCT6;A6YCU6;A6ZJR2;A6YCQ6							
	B8FAH2	Adenylylsulfate reductase, beta subunit			<i>Desulfobacteraceae</i>		
	DVLIYSGAK		63.8	62.4		0.91	0.85
	C0QA19	bifunctional acetyl-CoA decarboxylase/synthase complex subunit			<i>Desulfobacterium autotrophicum</i> (strain ATCC 43914 / DSM		
	FHQDFTK	46.1			0.22		
	FILGDGGLLR	52.2			0.24		
	AAFEINPTGPNQPIEK	52.7			0.22		
	FTTLAGVMGGGASSPGFVGHS	47.1			0.19		
C0QIP7;E1YHN8;B8FMV8	C0QIP7;E1YHN8;B8FMV8	Pyruvate-flavodoxin oxidoreductase			<i>Desulfobacteraceae</i>		
	GTAQNPDYFQGR	52.5			0.22		
	A8ZU48	60 kDa chaperonin			<i>Desulfococcus oleovorans</i> (strain DSM 6200 / Hxd3)		
	GYLSPYFVTDAEK	46.2	58.3	59.1	0.46	0.95	0.95
	SWGSPVTK	47.8	57.1		0.31	0.96	
	AAVEEVLPGGGVALVR	48.8	60.1	59.9	0.30	0.95	0.84
	GTLNVAVK	50.7	60.9		0.21	0.97	
	E1YB73	60 kDa chaperonin			<i>uncultured Desulfobacterium sp. (N47)</i>		
	ARVEDALNATR	46.5	56.4	56.4	0.05	0.89	0.77
	AQIEETSDYDREK	48.4	63.1		0.29	0.93	
	AAVEEVLPGGGVALVR	48.8	60.1		0.30	0.95	
	EGVITVEEAK	51.0	60.5	60.0	0.21	0.85	0.73
	TSDMAGDGTATVLR		54.2			0.92	
	VEDALNATR		57.5			0.84	
	E1YLG6	ATP synthase subunit alpha			<i>uncultured Desulfobacterium sp. (N47)</i>		
	STVAQVVSVEK	50.5			0.26		
	LDLAQYR		60.4	56.4		0.28	0.14
E1YLG8;B8FGT4	E1YLG8;B8FGT4	ATP synthase subunit beta			<i>Desulfobacteraceae</i>		
	FTQAGSEVSALLGR	47.6	58.6	58.1	0.05	0.73	0.38
	VIDLLVPFPR	52.7	63.3	63.4	0.02	0.76	0.76
E1YAG3;B8FDZ0	E1YAG3	Glutamine synthetase			<i>uncultured Desulfobacterium sp. (N47)</i>		
	LVPGEAPVNLAYSSR	47.4			0.03		

Table SIII.4: continued

Protein IDs	Majority Protein ID Labeled Peptides	Assumed Function			Taxonomy		
		RIA T1 (%)	RIA T2 (%)	RIA T3 (%)	LR T1	LR T2	LR T3
<i>Identified labeled proteins and peptides in the Guaymas Basin butane sample</i>							
E1YL45;C0QAI7;A9A066	E1YL45;C0QAI7;A9A066	Dihydropteroate synthase / Methyltransferase			<i>Desulfobacteraceae</i>		
	TLYSDSWLEV	46.8			0.35		
	GMDYIDINLGPAK	53.0			0.17		
B8FGU7;A8ZZJ0;A0LLR3;Q6 4DF6	B8FGU7;A8ZZJ0	Formate--tetrahydrofolate ligase			<i>Desulfobacteraceae</i>		
	DVLIYSGAK	52.8			0.15		
	AGINPVVCINR	53.0			0.24		
	NYNDEQLQR		55.4			0.63	
A8XZ6;B8FLB6	A8XZ6;B8FLB6	K(+)-insensitive pyrophosphate-energized proton pump			<i>Desulfobacteraceae</i>		
	AAVTGDTVGDYPYK	48.8	58.7	58.2	0.20	0.87	0.91
	GADVGADLVGK	49.9	60.2	59.8	0.25	0.89	0.90
	AAVTGDTVGDYPYKDTAGPAIN	50.6	60.3	58.7	0.19	0.95	0.97
	VEAGIPEDDPR	50.8	60.9	59.4	0.23	0.78	0.78
	DTAGPAINPMIK	52.8	62.5		0.21	0.94	
	LGGGIFTK	53.3	62.6	62.5	0.14	0.76	0.79
	AVTDPLDAVGNTTK	54.1	57.5	56.3	0.13	0.71	0.68
	VSVIANVR	56.0	61.7	63.9	0.09	0.02	0.80
<i>Identified labeled proteins and peptides in the Guaymas Basin dodecane sample</i>							
D6Z4V1;B8FGT4;Q6AQ10;E1 YLG8		ATP synthase subunit beta			<i>Desulfobacteraceae</i>		
	VIDLLVPFPR	66.00	63.20	63.90	0.34	0.36	0.52
A8XZ6;B8FLB6		K(+)-insensitive pyrophosphate-energized proton pump			<i>Desulfobacteraceae</i>		
	AAVTGDTVGDYPYK	57.70	57.30	58.40	0.24	0.57	0.49
	VEAGIPEDDPR	58.20	60.40	60.90	0.40	0.61	0.45
	AVTDPLDAVGNTTK	59.30	58.50	60.20	0.45	0.69	0.63
	GADVGADLVGK	60.30	58.90	61.00	0.22	0.56	0.46
	AAVTGDTVGDYPYKDTAGPAIN		61.60	61.90		0.38	0.71
	Q2LUL1	Putative K(+)-stimulated pyrophosphate-energized sodium p			<i>Syntrophus aciditrophicus</i> (strain SB)		
	AGVIGDTVGDPFK	57.70	56.00	55.10	0.47	0.70	0.67
E1YM45;A0LML7		K(+)-insensitive pyrophosphate-energized proton pump			<i>Syntrophobacter fumaroxidans</i> (strain DSM 10017 / MPOB)		
	AADVGADLVGK	56.40	57.10	56.00	0.43	0.65	0.58
	D1JF51	K(+)-insensitive pyrophosphate-energized proton pump			uncultured archaeon		
	AAVVGDTVGDPFK	54.70	56.00	55.10	0.47	0.70	0.67

Curriculum Vitae

Personal Information

Name: Sara Kleindienst
Date of birth: November 29th, 1982
Place of birth: Göttingen (Germany)

Education and Research Experiences

Sep 2008 - May 2012 Doctoral student in the Molecular Ecology Group of Prof. Dr. Rudolf Amann at the Max-Planck Institute for Marine Microbiology, Bremen (Germany) and student of the MARMIC graduate school (*International Max-Planck Research School of Marine Microbiology*)

Jul - Sep 2008 Research assistant in the Paleomicrobiology Group of Prof. Dr. Heribert Cypionka at the Institute for Chemistry and Biology of the Marine Environment (ICBM), Oldenburg (Germany)

Aug 2005 - Jan 2006 Student assistant in the Paleomicrobiology Group of Prof. Dr. Heribert Cypionka at the ICBM, Oldenburg (Germany)

Oct 2002 - Jun 2008 Diploma studies of Biology, Carl-von-Ossietzky University of Oldenburg (Germany) in the Paleomicrobiology Group of Prof. Dr. Heribert Cypionka at the ICBM, Oldenburg (Germany)

Cruise Participation

Apr - May 2008 RV Meteor M76/1 Cape Town (Rep. of South Africa) to Walvis Bay (Rep. of Namibia)

Fellowship and International Experience

Jun - Jul 2011 Research scholar from Marine Biological Laboratory (MBL) in Woods Hole, MA (United States), teaching assistance for “*Microbial Diversity*” Summer Course at MBL

Professional Presentations at Scientific Meetings and Conferences

S. Kleindienst, F. von Netzer, T. Lueders, A. Ramette, J. Peplies, R. Amann, F. Musat, and K. Knittel: “*Sulfate-reducing bacteria responsible for in situ hydrocarbon degradation at marine seeps*” (**Poster presentation**), International Society for Subsurface Microbiology (ISSM), Garmisch-Partenkirchen (Germany), Sep 2011

S. Kleindienst, F. von Netzer, T. Lueders, F. Musat, R. Amann, and K. Knittel: “*Active hydrocarbon-degrading sulfate-reducing bacteria at marine gas and oil seeps*” (**Oral presentation**), Association for General and Applied Microbiology (VAAM), Karlsruhe (Germany), Apr 2011

S. Kleindienst and K. Knittel: “*Distribution, activity, and function of sulfate-reducing bacteria in marine gas and oil seeps*” (**Oral presentation**), Annual meeting DFG - Priority Programme 1319: Biological transformations of hydrocarbons without oxygen - From the molecular to the global scale, Herrsching/München (Germany), Mar 2010

S. Kleindienst, F. Musat, R. Amann, and K. Knittel: “*In-situ analysis and stable-isotope probing of sulfate-reducing bacteria in hydrocarbon-rich sediments*” (**Poster presentation**), International Society for Microbial Ecology (ISME), Seattle, WA (United States), Aug 2010

S. Kleindienst and K. Knittel: “*Global search for hydrocarbon-degrading sulfate-reducing bacteria at marine gas and oil seeps*” (**Oral presentation**), Annual meeting DFG - Priority Programme 1319: Biological transformations of hydrocarbons without oxygen - From the molecular to the global scale, Machern/Leipzig (Germany), Mar 2010

S. Kleindienst, R. Amann, A. Boetius, and K. Knittel: “*Abundance and distribution of sulfate-reducing bacteria in hydrocarbon-rich sediments*” (**Poster presentation**), Gordon Research Conference: Applied & Environmental Microbiology - From Single Cells to the Environment, South Hadley, MA (United States), Jul 2009

S. Kleindienst, B. Orcutt, T. Treude, A. Boetius, R. Amann, and K. Knittel: “*Sulfate-reducing bacteria in hydrocarbon-rich sediments from the Gulf of Mexico*” (**Poster presentation**), Association for General and Applied Microbiology (VAAM), Bochum (Germany), Mar 2009

S. Kleindienst, J. Graue, B. Engelen, and H. Cypionka: “*Fermentation processes in tidal-flat sediments of the German Wadden Sea*” (**Poster presentation**), Association for General and Applied Microbiology (VAAM), Frankfurt (Germany), Mar 2008

Name: Sara Kleindienst

Ort, Datum: Bremen, 27.04.2012

Anschrift: Am Schlossgarten 4, 26122 Oldenburg.

ERKLÄRUNG

Hiermit erkläre ich, dass ich die Arbeit mit dem Titel:

Hydrocarbon-degrading sulfate-reducing bacteria in marine hydrocarbon seep sediments

selbstständig verfasst und geschrieben habe und außer den angegebenen Quellen keine weiteren Hilfsmittel verwendet habe.

Ebenfalls erkläre ich hiermit eidesstattlich, dass es sich bei den von mir abgegebenen Arbeiten um 3 identische Exemplare handelt.

.....
(Unterschrift)